Ocean Engineering & Oceanography 4

Zafarullah Nizamani

Environmental Load Factors and System Strength Evaluation of Offshore Jacket Platforms

Springer

Ocean Engineering & Oceanography

Volume 4

More information about this series at http://www.springer.com/series/10524

Zafarullah Nizamani

Environmental Load Factors and System Strength Evaluation of Offshore Jacket Platforms

Springer

Zafarullah Nizamani
Department of Environmental Engineering
Jalan University
Kampar
Malaysia

ISSN 2194-6396 ISSN 2194-640X (electronic)
Ocean Engineering & Oceanography
ISBN 978-3-319-15050-5 ISBN 978-3-319-15051-2 (eBook)
DOI 10.1007/978-3-319-15051-2

Library of Congress Control Number: 2014959854

Springer Cham Heidelberg New York Dordrecht London

Printed on acid-free paper

Springer International Publishing AG Switzerland is part of Springer Science+Business Media (www.springer.com)

For my family Mother, Father, Jamila and Shahzad

Preface

API (WSD) and ISO 19902 (LRFD) codes are being used nowadays for design of Jacket platforms all over the world. ISO code is a probabilistic code which takes into account the uncertainties of material and loads and thus enables economised designs. This advantage is not available for API code. The sustainable development of physical structures depend not only on reliability of structures but also on cost saving. ISO load factors are calibrated using Gulf of Mexico and North Sea environmental data. In this book, three offshore regions of Malaysia have been taken separately. The probabilistic uncertainty models for resistance and loads for local conditions are determined. Resistance uncertainty is evaluated using data collected from fabrication yard in Malaysia. Geometrical and material variations are statistically analysed from this data using probability distributions. Uncertainty model for nine component stresses and eleven joint stresses is analysed using MATLAB and statistical distributions. Environmental load uncertainty model included wave, wind and current parameters. The platform-specific and regional data is used for the analysis. The extreme distributions, i.e. Weibull and Gumbel are fitted for the analysis and their parameters are evaluated. SACS software is used to find the component stresses. Morrison Equation is used for application of wave load and BOMEL and Heideman's Equations are used to find the response from the stresses. 100-year loads are used to find the reliability. Seven code Equations are used to find the component reliability. The member selection for reliability analysis is based on diameter, thickness and slenderness ratios. The component reliability is found through FORM method of reliability using MATLAB code. For the target reliability API WSD code is used. Thus the environmental load factor which gives higher reliability than the target is selected. Codes define three types of Joints, K, T/Y and X in Jacket platforms. The environmental load factor is proposed using local geographic conditions. Though codes use component and joint-based environmental load factors only it is found necessary to include and check the system-based approach for the load factor also. ISO requires that to assess the strength of structure for extension of life, change in load or resistance of Jacket, 10,000-year load should be applied and Jacket strength evaluated. API and ISO code require that they should be checked against

probability of failure of 10^{-4}. In this text the probability of failure is determined and it is updated by applying the Bayesian updating technique.

This research is made at Universiti Teknologi PETRONAS (UTP) through its graduate assistantship scheme. Therefore my deep appreciation goes to the university without which it would not have been possible for me to do this research. I am thankful to Mr. Mohd Sapihie Ayob, Principal Engineer (Structural Mechanics) of PETRONAS Group Technical Solution, Technology & Engineering Division (PGTS), Malaysia for his support for a project related to this work. Many faculty staff and colleagues at Universiti Teknologi PETRONAS shared their knowledge and experience to complete this task. Without their help and sharing knowledge this work would not be as is shown in this final shape, such as Dr. Paul Frieze for useful discussions at initial stage of research. I am thankful for guidance on environmental load parameters from Dr. R.V. Ahilan and on structural reliability and FORM from Dr. Kaisheng Chen from Noble Denton. I am thankful to Mr. Bishwa Mohan Jha and Mr. Che Wahab from KENCANA HL Sdn Bhd who provided help to obtain onsite statistics of tubular members. I am also thankful to Dr. Hamid M.F.A., Scientige Sdn Bhd (on leave from Universiti Teknologi Malaysia). I am also thankful to my supervisors Dr. Narayanan S.P., V.J. Kurian and M.S. Liew for their guidance. I am especially thankful to my colleagues at UTP Mr. Cossa N.J. I would like to thank my other colleagues who were encouraging and supportive during this period of trial. I am also thankful for an open source code named as FERUM available through University of California, Berkeley.

November 2014 Zafarullah Nizamani

Contents

Symbols

A	Cross-sectional area, activity factor for Jacket
A_i	Variable area of tubular member, load uncertainty model
A_n	Nominal area of tubular member
a_1, a_2, a_3	Load coefficient
B_i	Resistance model uncertainty
C	Critical elastic buckling coefficient
$C_{m,y}$, $C_{m,z}$	Moment reduction factors corresponding to the member y and z axes
C_x	Elastic critical buckling coefficient
d	Water depth, Brace outside diameter, dead load ratio
D	Outside diameter of member, random dead load
D_l	Dead load, gravity load
E	Young's Modulus of elasticity
E_l	Environmental load
f_a	Absolute value of acting axial stress
f_b	Absolute value of acting resultant bending stress
f_c	Representative axial compressive strength
f_e	Smaller of Euler buckling strength in Y-Z directions
F_h	Absolute value of hoop compression stress
F_{hc}	Critical hoop stress
f_{he}	Representative elastic critical hoop buckling strength
f_{xe}	Representative elastic local buckling strength
FS	Factor of Safety
F_t	Allowable tensile stress
f_t	Representative axial tensile strength,
f_{ti}	Variable tensile strength
f_{tn}	Nominal tensile strength
F_y	Yield strength
F_{yi}	Random yield strength
F_{yn}	Nominal yield strength
$f_{e,y}$, $f_{e,z}$	Euler buckling strengths corresponding to member y and z axes
f_{xe}	Representative elastic buckling coefficient

f_{yb}	Brace yield strength
f_{yc}	Representative local buckling strength
f_{yc}	Yield strength of chord member or (0.8 of tensile strength)
fx(X)	Probability density function (PDF) of variable X at a value of x
G(x)	Performance/Limit state function. G(x) = 0, Limit state surface with respect to design value of x
g	Acceleration due to gravity, gap between braces
H	Maximum wave height
H_d	Design wave height
H_{max}	Maximum wave height
$H_{max(des)}$	Design wave height (100 year)
H_R	Wave height which gives RSR of 1.0
H_{var}	Random wave height
I	Moment of Inertia of cross-section
ICSF	Implicit code safety factor
K	Effective length factor
K_y, K_z	Effective length factor for y and z directions
L	Wave length or Component span, random live load
L_l	Live Load
l	Unbraced length, live load ratio
L_y, L_z	Un braced lengths in y and z directions
M	Bending moment due to factored actions
M_a	Allowable capacity for brace bending moment
M_c	Bending force in chord member
MF	Material factor
M_p	Plastic moment strength of chord
M_{uj}	Joint Bending Moment
M_y	Elastic yield moment
N	Total number of simulation
N_f	Number of failures
n	Platform life in years
n_p	Average number of people on Jacket
P	Return period probability
p	Annual probability that the event will not occur
P_a	Allowable capacity for brace axial load
P_c	Axial force in chord member
P_d	Gravity load proportion
P_f	Probability of failure
Pf_n	Target probability of failure
P_s	Probability of survival
P_w	Environmental load proportion
P_{uf}	Updated probability of failure
P_{uj}	Joint Axial Strength
P_y	Yield strength of chord, Axial strength due to yielding, $P_y = A \times f_y$

P_{ult}	Ultimate load
Q	Load
$\bar{Q}$	Mean load
Q_e	100 year design load
Q_l	Large value of Q
Q_i	Nominal load
Q_f	Chord force factor, base shear (damaged state)
Q_u	Strength factor
R	Resistance effect
$\bar{R}$	Mean resistance
R_l	Low value of resistance R
R_n	Nominal resistance
R_{ult}	Ultimate resistance of Jacket
r	Radius of Gyration $r = \sqrt{I/A}$
SR	System redundancy
T	Chord wall thickness
t	Wall thickness of member, brace wall thickness
t_l	Design life of Jacket
S	Strength given by code Equation
Tapp	Apparent wave period
Tp	Peak period
Tz	Mean zero-crossing period and is assumed to equal to Tp/1.4
u	Current speed
V_c	Current speed
v_r	COV of resistance
V_{pf}	COV of failure probability
v_q	COV of load
Var (x)	Variance of x
v	Poisson's ratio = 0.3
W	Load effects, random environmental load
w	Environmental load ratio
W_e	Environmental load ratio
W_f	Warning factor for sudden failure
x*	Design point
X	Random variable
X_m	Resistance model uncertainty
X_w	Load model uncertainty
z	Safety margin
Z	Theoretical value of plastic section modulus of component
Z_e	Elastic section modulus, $Z_e = \frac{\pi}{64}[D^4 - (D-2t)^4]/(D/2)$
Z_P	Plastic section modulus, $Z_P = \frac{1}{6}\left[D^3 - (D-2t)^3\right]$
γ_D	Dead load factor
γ_d	Gravity load factor
γ_L	Live load factor

γ_R	Resistance factor
γ_W	Environmental load factor
$\emptyset$	Material strength safety factor
γ_i	Load factor
$\gamma_{R,t}$	Partial resistance factor for axial tensile strength ($\gamma_{R,t} = 1.05$)
μ	Mean
μ_g	Mean of limit state function
μ_Q	Mean load
μ_R	Mean resistance
μ_s	Social criteria factor
σ	Standard deviation
σ_b	Bending stress due to forces from factored actions; when $M > M_y$, σ_b is to be considered as an equivalent elastic bending stress $\sigma_b = M/Z_e$
$\sigma_{b,y}$, $\sigma_{b,z}$	$\sigma_{b,y}$ = Bending stress about member y-axis or z-axis (in plane) due to forces from factored actions
σ_c	Axial compressive stress due to forces from factored actions
σ_g	Standard deviation of limit state function
σ_h	Hoop stress due to forces from factored hydrostatic pressure
σ_Q	Stand deviation of load
σ_R	Stand deviation of resistance
σ_t	Axial tensile stress due to forces from factored actions
σ_{ti}	Variable tensile stress
σ_{tn}	Nominal tensile stress
γ_c	Compression resistance factor
γ_d	Gravity load factor
γ_w	Environmental load factor
$\gamma_{R,b}$	Partial resistance factor for bending strength, $\gamma_{R,b} = 1.05$
$\gamma_{R,c}$	Partial resistance factor for axial compressive strength, $\gamma_{R,c} = 1.18$
γ_{Rq}	Yield strength factor (1.05)
λ	Column slenderness parameter
λ_{ult}	Factor which increases until collapse
θ	Angle between brace and chord
β	Reliability index
Φ	Cumulative distribution function for the standard normal variables

Abbrevations

AASHTO	American Association of State Highway and Transportation Officials
ACI	American Concrete Institute
AISC	American Institute of Steel Construction
API RP2A (WSD)	American Petroleum Institute-Recommended Practice (Working Stress Design)
API RP2A (LRFD)	American Petroleum Institute-Recommended Practice (Load and Resistance Factor Design)
BOMEL	Company name
CDF	Cumulative Distribution Function
COV	Coefficient of Variation
DNV	Det Norske Veritas (Norwegian Certifying Authority)
DSF	Damaged Strength Factor
FERUM	Compiler for FORM Method of Reliability
FORM	First Order Reliability Method
GOM	Gulf of Mexico
H_{max}	Maximum wave height
IPB	In-Plane Bending
ISO 19902	International Standard Organization code for (Petroleum and natural gas industries—Fixed steel offshore structures)
ISO LRFD (MS)	Environmental load factor from this research (Malaysian study)
LRFD	Load and Resistance Factor Design
LSD	Limit State Design
MC	Mean Coefficient
MCS	Monte Carlo Simulation
MS	Malaysian Study (This Research)
M–S	March–September
NE	North East
N–M	November–March
NPD	Norwegian Petroleum Directorate

NS	North Sea
NW	North West
OPB	Out Plane Bending
PAFA	Company name
PDF	Probability Density Function
PF	Probability of Failure
PMO	Peninsular Malaysia Operation
PTS	PETRONAS Technical Standard
RSR	Reserve Strength Ratio
S	South
SACS	Structural Analysis Computer Software
SBO	Sabah Operation
SF	Safety Factor
SKO1	Sarawak Operation (Platform No. 1)
SKO2	Sarawak Operation (Platform No. 2-Fixed at Mud line)
SKO2a	Sarawak Operation (Platform No. 2 with Pile Soil Foundation)
SNS-NNS	Southern North Sea, Northern North Sea
SP	Statistical Parameters
SW	South West
UPF	Updated Probability of Failure
VC	Variation Coefficient
We/G	Environmental Load to Gravity Load Ratio
WSD	Working Stress Design

Chapter 1
Introduction

Abstract Jacket platform acts as base for overall structure which is used to extract hydrocarbon from oceans. They are generally suitable for shallow and intermediate waters with a depth of (<150 m), but they have been built for depths like 529 m such as Bullwinkle by Shell in Gulf of Mexico. Structural design methodology of civil engineering design codes has changed from allowable stress design to limit state (load and resistance factor) design. Codes for structural design go through changing process, and whenever a new finding is reported and verified, it is incorporated in the code.

1.1 Design Codes of Practice for Jacket Platforms

API RP2A Working Stress Design (WSD) forms the basis of offshore steel Jacket platform design all over the world and has proved to be accepted design standard since it was first issued in 1969 [1]. WSD is a factor of safety-based code which is derived from WSD theory and reduces the ultimate resistance strength to allowable stress for safe design. In WSD, minimum resistance results from test results of yield strength and for load from past experience; thus, safety factor was inherent in these codes though not apparent. Since the loads/resistances are varying, the assumptions used in WSD design process, i.e. a single factor of safety for all load combinations, cannot maintain a constant level of structural safety [2]. WSD method uses safety factors without taking into consideration the uncertainties, and it assumes that all variables are deterministic. Thus, safety of platform is achieved by WSD through the use of a factor of safety against the inherent uncertainties of load and resistance. For allowable stress design, safety of structure is achieved by the use of a safety factor against the uncertainties of load using some arbitrary experience and judgment like 1/3 decrease for allowable stresses. This method provides no knowledge about effects of various random variable parameters on the safety of Jacket platform.

Z. Nizamani, *Environmental Load Factors and System Strength Evaluation of Offshore Jacket Platforms*, Ocean Engineering & Oceanography 4,
DOI 10.1007/978-3-319-15051-2_1

WSD and LRFD codes have prominent differences. WSD and LRFD codes differ essentially in that load and resistance factor design (LRFD) uses more factors of safety which produces more uniform safety levels [1, 3]. The WSD considers the uncertainties related to the load and resistance by providing safety factor using judgement and reduction of yield strength to allowable strength. LRFD has the provision to deal with the uncertainties and variations coming from the load and resistance by using random variable statistics. Jacket platforms have to face crucial loading effects, which require proper estimation of loads and design. To cover this aspect, WSD is found to be uneconomical as no consideration is given for uncertainties and LRFD as efficient due to consideration of randomness of uncertainties. In modern-day structural design, LRFD codes have replaced WSD codes like AISC, API, ACI and AASHTO. American Petroleum Institute (API) Working stress method is now being replaced by a more robust and logical, limit state design, a probability-based method as other codes have already shifted to LRFD. It has been accepted worldwide that LRFD method is not only more reliable but also allows the environmental load factors, to be established by use of geographical conditions/locations [1, 4–8]. LRFD method is being utilised nowadays for the further development of research-based design codes. The LRFD codes of practice are component and joint reliability-based design standards. LRFD is considered better representative of the situation on the ground, with actual variations taken into consideration. It has safety factors on both load and resistance side of limit state equations. This represents uncertainty more realistically during the design practice as compared to WSD method.

The probabilistic codes for limit state design take into account the uncertainties of material and load. LRFD code has safety factors which take into consideration load and resistance uncertainties separately. LRFD code provides safety factors for load, i.e. dead, live and environmental load separately. For resistance, tension, compression, bending, shear and hydrostatic stresses are provided with resistance factors separately. With the use of probability distributions, the determination of effects of random variable can be quantified more robustly. LRFD provides higher and more consistent safety levels. Jacket platform is optimised to achieve maximum reliability by using minimum material [9]. Load and resistance factors are derived so that the structure designed by means of the planned provisions will be at the predefined target level [10]. The advantage of this method is that the latest knowledge can be incorporated into the code, whereas this was not possible for working stress method. LRFD results in uniform component and joint safety indices than WSD, for wide range of water depths, loads and platform configurations. It results in lighter Jackets for cases when environmental load-to-gravity load ratio is low (shallow water depths, static loading). Heavier Jackets will result where environmental load to gravity load is higher and load and resistance uncertainties are high (deep water and dynamic loadings) [2].

1.2 Geographic Region of Offshore Malaysia

Physics of ocean wave influences the Jacket design load, and its influence varies for different regions of the world [11]. There are about 250 Jacket platforms currently operating in offshore Malaysia, and any research on the reliability of Jacket platforms will be very much useful for the oil and gas industry. The main offshore regions in Malaysia have been classified in this book as Peninsular Malaysia Operation (PMO), Sabah Operation (SBO) and Sarawak Operation (SKO). Malaysia lies within 7°N from equator which is considered to be safe against extreme storms. Using local geographical and fabrication uncertainties, this work proposes the modified environmental load factors for components and joints.

API and ISO code use Gulf of Mexico (GOM) and North Sea (NS), geographical environmental parameters for calibration with severe environmental conditions. When this code is used for design of Jacket platforms in less severe environment, the design becomes uneconomical. API RP2A WSD is the design code in practice for design of offshore Jacket platforms in Malaysia. PETRONAS Technical Standards (PTS) provide necessary input with regard to metocean parameters for offshore Malaysia [12]. Therefore, a design environment criterion for platforms in South East Asia is taken by use of GOM loading criteria, and thus, there is amplification of 60 % during platform design due to scarcity of data [13]. High environmental load factors used in this region, due to short lead time between discovery of hydrocarbon and platform design, can result in waste of economic resources. Due to these factors, it is extremely essential that actual environmental load factors should be ascertained for this region using component, joint and system reliability. The critical part in structural design of members is assigning the properly evaluated environmental load and resistance factors. The motivation for the present book has come from the need to establish the load factors for Jacket platforms in Malaysia keeping in view the local environmental and fabrication consideration. Such factors can contribute for ISO 19901 and 19902 regional annex for Malaysia in particular and offshore industry in general for the efficient design of Jacket platforms in offshore Malaysia. There is a great need not only to analyse metocean data but also to check the environmental load factor. To evaluate the component and joint environmental load factors for Malaysia, we have to find seven types of component stresses and four types of joint stresses specified by API and ISO codes. The cost of Jacket could be saved by 15 % if change of location-dependent LRFD load factors is applied [14] in Java Sea where Jackets are not dominated by wave loads but by gravity loads. In the light of above facts, it becomes very essential to research on extreme environmental load factor for Jacket platforms in offshore Malaysia region. Offshore industry of Malaysia follows the load factors calibrated for GOM and NS which are considerably higher for this region due to mild weather conditions of Malaysia. It is clear that different regions have different environmental loads and the same can be evaluated for offshore Malaysia. Environmental load factors data for six geographical regions are shown in Table 1.1. The table clearly shows that the load factors differ according to their environmental loading conditions [15].

Table 1.1 Environmental load factors [1, 14, 15]

Region	Load factor
Gulf of Mexico	1.35
Central and South North Sea	1.18
Northern North Sea	1.25
NW Australia	1.36
Indonesia	1.0
Mediterranean Sea	1.30

1.3 Uncertainty

Effective utilisation of component, joint and overall system of Jacket platform is achieved by taking into consideration the uncertainty of material and load. The randomness with respect to load and uncertainty in structural material requires stochastic/probabilistic methods for analysis. The design uncertainties need to be taken into consideration, when dealing with a balance between safety of structures, purpose and its cost as shown in Fig. 1.1. The sustainable development of physical structures depends not only on reliability of structures but also on cost saving. An efficient design of a structure needs a balance between material and risk cost [16].

1.3.1 Uncertainty of Resistance

Uncertainties in capacity or member strength occur due to material or geometric variability. Material uncertainties are used to measure statistical spread, evaluated by using the data from fabrication yard and mill test reports. This is due to limitation in engineering theories to predict the component and system response and capacity. The load and resistance model uncertainties lead us to a safety factor which can cater for these uncertainties and thus a safe structure. Factor of safety is used for these uncertainties and provide the increased safety margins against future structural damage or deterioration [17] or an addition of scope of work. The limit state defines the failure or safe region for the member; the failure can be a

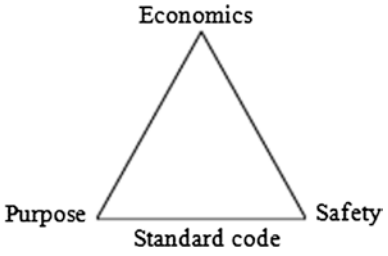

Fig. 1.1 Benefits of standard codes

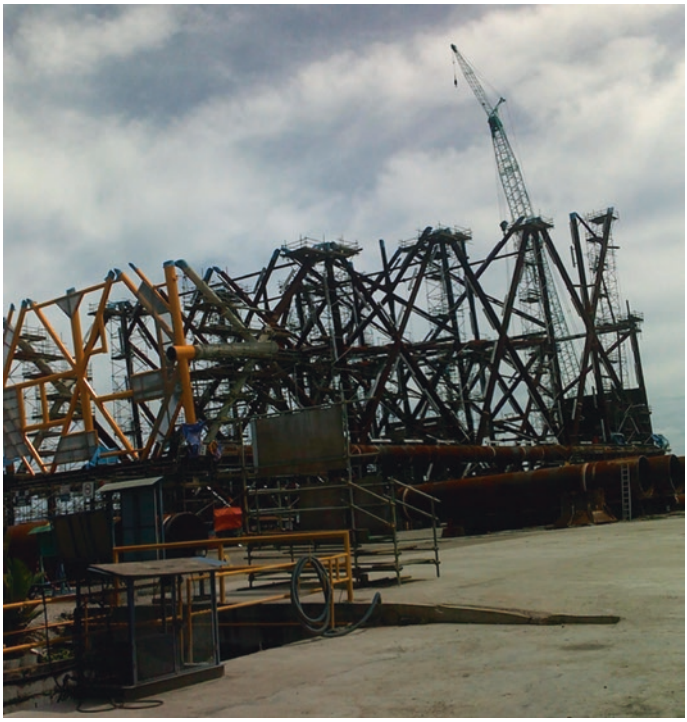

Fig. 1.2 Jacket platform under fabrication at a yard in Malaysia

single or combined failure mode like compression or compression plus bending. These models of limit state are also prone to uncertainty [18]. A component fails when it is not capable of resisting the loads and the failure occurs due to yielding, deflection or buckling. Component failure occurs due to failure of one member like braces and legs. In case of joints, the failure modes may be axial, in-plane bending or out-plane bending. Statistics for resistance include the characteristics of material and geometrical properties. In this book, variability in resistance parameters is evaluated through fitting of it by use of probability distribution. The data for resistance is collected from offshore fabrication yard, and for environmental loads, the data available from specific platforms design are used. Figure 1.2 shows a Jacket under construction at a fabrication yard.

1.4 Uncertainty of Loads

The characteristics of structural design are dependent on load uncertainties which are more specifically related to environmental loads. Platforms are designed to resist three kinds of loads to which they are subjected, namely (a) environmental

loads, i.e. wave, currents and wind, (b) dead loads, i.e. weight of structure, and (c) live loads, i.e. weight of consumable supplies and fluids in pipes and tanks. Proper evaluation of metocean parameters is still being investigated in GOM and NS, so that their prediction can be made effectively. The metocean data used in GOM and NS have still large coefficient of variation (COV). The metocean data bank in Malaysia is still in its infancy. ISO 19901 does not provide any information with regard to variables of environmental load parameters for South China Sea. The code proposes that data should be collected by each country itself. In this book, statistical parameters (mean, standard deviation, COV, etc.) are obtained for geometrical and material properties. Statistical parameters for environmental loads, i.e. wind, wave and current, are also evaluated. Statistical modelling of load and resistance with their respective distribution parameters is developed from the data and compared with data produced by experts in this area of specialisation.

1.5 Structural Safety and Reliability

Structural safety requires that required strength (R) should be greater than the design loads (Q). Structural reliability analysis is made by use of theory of limit state or failure state. Freudenthal is considered the first researcher who came up with statistical approach using structural reliability analysis for design of structures [19]. The reliability-based structures are designed so that their reliability is always higher than the target reliability, i.e. minimum specified by the well-established standards. The reliabilities are found for working stress method (implicit reliability) as well as LRFD method. Using reliability-based methods, safety indices are computed for the ultimate limit state. This will be used as a base for evaluation of load factors for this region. Using FORM reliability analysis, the reliability index is determined for component, joint and overall system, which is used for determination of the environmental load factors.

1.5.1 Environmental Load Factor for Component and Joint

The safety factors play major role for avoiding a case of failure of Jacket platform. Component and joint reliability is used to find environmental load and resistance factors for Jacket platform. ISO 19902 code specifies the environmental load and resistance factors for the component and joint using GOM and NS calibration. Environmental load factors are determined using characteristic values of the random variables. At present, the environmental load factors being used by API and ISO are calibrated for extreme environments such as in GOM and NS. The load factors have been evaluated in GOM, NS and work on establishing metocean parameters is still in progress in this area, as more data become available [20]. These are the areas of hurricanes (typhoons in Pacific Ocean) and severe winter storms, respectively. The uncertainties of load and resistance considered are by use

Table 1.2 Load factors used for calculating the internal forces [4]

Governing conditions	Partial action factors		
	γD	γL	γW
Operating	1.3	1.3	1.0
Extreme	1.1	1.1	1.35

of the local conditions of these regions. Though many studies have been conducted on the efficiency of different codes with regard to the load factors, still work is under progress in many parts of world [20]. In GOM, Graff et al. [5] showed that 19 %, i.e. 5,500 tons, would be saved on total weight of Jacket of 27,800 tons of steel. Thomas and Snell found reduction of weight of Jacket by 0.75 % at one particular level by using LRFD method in NS [21]. They need to be more representative for the regions of less severe environment such as offshore Malaysia. The resistance factors established by API and ISO are dependent on load factors. If environmental load factors are changed, the resistance factor is checked using new load factors. The semi-probabilistic codes, API LRFD and ISO 19902, have environmental load and resistance factors as shown in Table 1.2. This is the reason for the probabilistic evaluation of environmental loads recently in China and Indonesia [14, 22] to check the influence of LRFD code.

The load and resistance factors in LRFD need to be checked for site-specific conditions due to change of geography and material fabrications. Thus, LRFD method brings out regional differences in variation to design for extreme and operating conditions. This is more relevant in case of offshore structures where the environmental loads are much varying in nature and are most of the times not normally distributed. This results in variability of loads and affects the structural reliability, measured by reliability index (β). To cater for the requirements for other regions of the world, it is necessary to develop local factors considering their own geographical environment. The justification for finding environmental load factors for Jacket platforms for Malaysia can be attributed to the following reasons. The main justification came from the ISO 19900-1 which says that for each geographic region, environmental load factor should be evaluated specifically for that region. ISO 19902 clause A.9.9.3.3 reports that "for structures with the same geometrical and structural properties, harmonisation in safety levels (as are in GOM), hence requires location dependent partial action factors". Environmental load factors have been determined for GOM, Northern NS, Southern NS, Central NS, China, Mediterranean Sea, Australia and Gulf of Guinea, and they should be determined for regional environmental conditions [1, 11, 23, 24]. The work in two regions of Jawa and Makassar (Indonesia) has also been reported [14]. In China, Duan et al. [25] have done research on developing combinations of environmental load factors for China. Sakrit [26] has done reliability analysis of Jacket platforms in Gulf of Thailand using onshore data. The work on reliability index for Jacket platforms is reported in PMO region of Malaysia [27, 28]. There is a need for an extensive study covering all the three regions of Malaysia to determine the environmental load factors for components, joints and system. Therefore, it is high time that this issue should be looked into for offshore Malaysia.

1.5.2 System Reliability and Environmental Load Factor

Jacket platforms are designed as per component and joint-based design codes, and the end product is structural system [18]. The component and joint reliability cannot be optimised without taking into account the overall impact on the system reliability. For system reliability, this book covers four platforms which are analysed using pushover analysis and depending upon the base shear, Reserve Strength Ratios (RSR) are determined. The system environmental load factor should be less than that achieved for component and joint due to the ductile behaviour of Jacket which redistributes the stresses in nearby components if a member fails.

1.6 Bayesian Updating of Probability of Failure

Due to change of load and resistance conditions due to usage requirements at the site or when extension of service life is being considered, probability of failure of Jacket is evaluated as per ISO guidelines. To check the extension of life and reassessment, ISO and API require Jacket should be checked against a wave and current load of 10,000 year return period and probability of failure should be determined at this load. For the reassessment purpose, the probability of failure is updated by using the Bayesian updating. There is a need to update this probability of failure considering probability of survival using Bayesian updating. The change of loading and resistance conditions and need for extension of life of Jacket currently require checking for probability of failure of 10^{-4}. This method considers only failure probabilities, and thus, if a Jacket cannot take a load of this magnitude, restrengthening is required which may incur huge cost. If probability of survival is also included in this analysis, the restrengthening may not even be required. Offshore industry practice for reassessment of Jacket is by finding probability of failure of Jacket using ISO and API code requirement. An extrapolated 10^4 years environmental load is applied, and probability of failure is calculated. If this probability of failure gives a return period less than 10,000 years, modifications or restrengthening of Jacket is required. This method can be improved if not only probability of failure is considered but also probability of survival is taken into consideration. When both are combined, the probability of failure decreases considerably at higher loads [29]. The application of Bayes theorem has only recently been finding application for reliability analysis. Bayesian updating of probability of failure on Jacket platforms in this region has never been conducted, and there is a need to conduct this research to avoid costly modifications. If we could include results not only from probability of failure but also from probability of survival, then a difference is seen in reduction of probability of failure and which have been recommended by researchers [29].

Bayesian updating has been suggested by Ang, Nowak and many other authors [30, 31]. This is a useful tool where low probability of failure is of importance. It considers probability of failure by taking into consideration probability of

survival. Its benefit for Jacket platforms has been highlighted in a work in NS [29]. Bay's theorem is very useful for updating of probability of failure using probability of survival. When we apply the environmental load on Jacket platform, the responses can be determined. Using these responses, the probability of failure could be evaluated. If this load is higher than what ISO code recommends, and if the Jacket can still survive, this information could be used to find updated probability of failure. Most of Jacket platforms in Malaysia have already completed their design life or will soon be completing. The reassessment will be required for extension of life, and ISO code requires a load with a return period of 10^4 should be applied and Jacket strength evaluated. Only probability of failure is considered in present-day assessment which may show that Jacket cannot take a required load. If Bayes theorem for updating of probability of failure is applied for the same Jackets, it gives us reduced probability of failure at higher loads, and thus, modification work can be avoided. This is done for all four platforms. Then, Bayesian updating technique is used, in which first Jacket is preloaded to find the minimum RSR values. This load which gives minimum RSR is used to find the updated probability of failure. This is made for intact and damaged members of Jacket.

1.7 Outline of the Chapters

Chapter 2 deals with discussion on past works done in this area of research. Chapter 3 shows methods applied for the preparation of this book. Chapter 4 deals with statistical analysis of uncertainty of resistance variables. Resistance uncertainty of geometric and material variables for Jacket platforms is determined, and this is not available in this region. Resistance model uncertainty is also not reported in this region before. ISO uncertainty mathematical models are used to find the model uncertainty of component and joint stresses. Uncertainty of structural characteristics of steel (geometry and material properties), i.e. material resistance, is also determined. Chapter 5 deals with load variables. The site-specific load data for three regions are used to model the load uncertainty variables which have not been reported in previous studies. The reduction in environmental load means a significant reduction of loads which can contribute in the reduction of cost of construction. It discusses the statistical features of uncertainty of load. Determination of probability distributions and their parameters for environmental loads has been explained. Uncertainty in environmental load is used to find the statistical properties. Chapter 6 deals with numerical analysis of code equations for Jacket component. Chapter 7 deals with the determination of environmental load using component reliability analysis. Probabilistic models for reliability are developed which are used for reliability analysis. Methods used to find the reliability index in this thesis like FORM and Monte Carlo are discussed. Members are selected using diameter, thickness and slenderness ratios. In this chapter, component reliability is evaluated for primary members of Jacket, i.e. leg, horizontal

brace at periphery, horizontal diagonal and diagonal brace members under seven different types of stresses. The environmental load factor is determined using component reliability for four platforms. Chapter 8 deals with determination of environmental load using joint reliability analysis using FORM method of reliability. Joints are selected using chord and brace diameter ratios. For joint reliability K-, T/Y- and X-joints are analysed for axial tension, axial compression, in-plane bending and out-plane bending stresses. The environmental load factor is determined using joint reliability for four platforms. Chapter 9 deals with environmental load factors using system reliability. RSR is used to find the system reliability and the system-based environmental load factor. Probability of failure is determined for Jacket platform as per design load and at return period of 10^4-year load. Results of this book can form the basis for proposed changes in the provisions of structural design for environmental load factors for this region. Chapter 10 contains Bayesian updating of probability of failure using probability of survival. Bayesian updating is used to find probability of failure along with probability of survival at much higher loads for intact and damaged members. Chapter 11 concludes the book with summary of results achieved. At the end, recommendations are made for the future research in this area of specialisation.

References

1. Theophanatos, A., Cazzulo, R., Berranger, I., Ornaghi, L., Wittengerg, L.: Adaptation of API RP2A-LRFD to the Mediterranean Sea. Presented at the Offshore Technology Conference, OTC 6932, Houston (1992)
2. Lloyd, J.R., Karsan, D.I.: Development of a reliability-Based alternative to API RP2A. Presented at the Offshore Technology Conference, OTC 5882, Houston (1988)
3. Mangiavacchi, A., Rodenbusch, G., Radford, A., Wisch, D.: API offshore structures standards: RP 2A and much more. Presented at the Offshore Technology Conference, OTC 17697, Houston (2005)
4. ISO19902.: International Standard Organization 19902 (2007)
5. Graff, J.W., Tromans, P.S., Efthymiou, M.: The reliability of offshore structures and its dependence on design code and environment. Presented at the Offshore Technology Conference, OTC 7382, Houston (1994)
6. Turner, R.C., Ellinas, C.P., Thomas, G.A.N.: Towards the worldwide calibration of API RP2A-LRFD. In: Offshore Technology Conference, OTC 6930, Houston (1992)
7. Theophanatos, A., Wickham, A.H.S. : Modelling of environmental loading for adaptation of API RP 2A-load and resistance factor design in UK offshore structural design practice. In: Proceedings of Institution of Civil Engineers, pp. 195–204 (1993)
8. Turner, R.C.: Partial safety factor calibration for North Sea adaptation of API RP2A-LRFD. Presented at the Institution of Civil Engineers (1993)
9. Phani, R.A.: robust estimation of reliability in the presence of multiple failure modes. Doctor of Philosophy, Mechanical and Materials Engineering, Wright State University (2006)
10. Nowak, A.S.: Calibration of LRFD bridge code. J. Struct. Eng. **121**(8), 1245–1251 (1995)
11. Snell R.O., Wisch, D.J.: ISO 19900 series: offshore structures standards. In: Offshore Technology Conference, OTC *19605*, Houston (2008)
12. PTS (ed.): PETRONAS Technical Standard Malaysia: PETRONAS (2010)

13. French, S., Seeto, J., Dominish, P.G.: Structural integrity assessment and life extension of platforms in Australia and Southeast Asia. Presented at the BOSS (1992)
14. Pradnyana, G., Surahman, A., Dasbi, S.: Review on the regional annex of ISO-13819 standard for planning, designing, and constructing fixed offshore platforms in Indonesia. Presented at the sixth AEESEAP Triennial Conference Kuta, Bali, Indonesia (2000)
15. Moses, F., Stahl, B.: Calibration issues in development of ISO standards for fixed steel offshore structures. J. OMAE Trans. ASME **122**(1), 52–56 (2000)
16. Moses, F.: Reliability based design of offshore structures. Presented at the American Petroleum Institute (1981)
17. Wisch, D.J.: Fixed Steel Standard: IS0 & API Developments—IS0 TC 671SC 7NVG 3. Presented at the Offshore Technology Conference, OTC 8423, Houston (1997)
18. Wisch, D.J.: API offshore structures standards: changing times. Presented at the Offshore Technology Conference, OTC 19606, Houston (2008)
19. Wang, W.: Structural system reliability: a study of several important issues. Doctor of Philosophy, The Johns Hopkins (1994)
20. DNV, TA&R: Comparison of API, ISO, and NORSOK offshore structural standards, Bureau of ocean energy management, regulation, and enforcement, Washington, D.C. (2012)
21. Thomas G.A.N., Snell, R.O.: Application of API RP2A-LRFD to a north sea platform structure. In: Offshore Technology Conference OTC 6931, Houston (1992)
22. Jin, W., Hu, Q., Shen, Z., Shi, Z.: Reliability-based load and resistance factors design for offshore jacket platforms in the Bohai bay: calibration on target reliability index. China Ocean Eng. **23**(1), 15–26 (2009)
23. Birades, M., Cornell, C.A., Ledoigt, B.: Load factor calibration for the Gulf of Guinea adaptation of APIRP2A-LRFD. In: Behaviour of Offshore Structures, London (2003)
24. BOMEL(b): System-based calibration of North West European annex environmental load factors for the ISO fixed steel offshore structures code 19902 (2003)
25. Duan, Z.D., Zhou, D.C., Ou, J.P.: Calibration of LRFD format for steel jacket offshore platform in China offshore area (1): statistical parameters of load and resistances. China Ocean Eng. **20**(1), 1–14 (2005)
26. Sakrit, C.: Safety and reliability of a fixed offshore platform in the gulf of Thailand. MSc, Offshore Technology and Management, AIT, Bangkok (2010)
27. Leng D.C.: A reliability analysis of Malaysia jacket platform. Master of Science, UTM (2005)
28. Tan, C.: A numerical analysis of fixed offshore structure subjected to environmental loading in Malaysian water. Master of Science, Faculty of Mechanical Engineering, UTM (2005)
29. Gerhard, E.: Assessment of existing offshore structures for life extension. Doctor of Philosophy, Department of Mechanical and Structural Engineering and Material Science, University of Stavanger, Stavanger, Norway (2005)
30. Ang A.H., Tang, W.H.: Probability concepts in engineering, vol. 1 (2007)
31. Nowak, A.S., Collins, K.: Reliability of structures, 2nd edn. CRC Press, Taylor & Francis Group (2013)

Chapter 2
Past Developments

Abstract Offshore platforms are only 65 years old and are fairly new compared to other types of civil engineering structures. The first steel platform was installed in Gulf of Mexico (GOM) in 1947. In this chapter, brief overview of the past work done in this area is outlined. American Petroleum Institute (API) was the first to publish the code for offshore Jacket platforms, namely API RP2A WSD in 1969. API LRFD was published in 1993 with errata in 2003 and has not yet been revised. ISO 19902 was published in 2007 and is the most updated LRFD code available for steel Jacket platform design today.

2.1 Design Codes of Practice for Jacket Platforms

API WSD code has been updated throughout these years until recently an erratum was issued for 21st edition in March, 2008. It was followed by DNV in Norway and separate guidelines for United Kingdom. Canada and Australia published their own codes for offshore platform design. LRFD format of code is a probability-based code. For API RP2A LRFD code development, the target reliability was set against API WSD. The target reliability for a probabilistic code is by using the reliability of platforms designed by existing codes, personal judgement and the safety requirement. The hydrocarbon exploring companies such as Shell and PETRONAS have developed their own technical standards with respect to geographically specific regions [1, 2]. These standards refer to API RP2A WSD or ISO 19902 for the detailed design and assessment. API WSD is still in practice in most parts of the world due to non-availability of regional environmental load factors presented in ISO 19902.

Structural design codes provide a set of minimum technical guideline for satisfactory design. They also provide a path for research findings to create their way into practice of this field [3]. The LRFD method treats the load according to their types and the loads dominated by environment are treated appropriately.

Z. Nizamani, *Environmental Load Factors and System Strength Evaluation of Offshore Jacket Platforms*, Ocean Engineering & Oceanography 4,
DOI 10.1007/978-3-319-15051-2_2

2.1.1 API RP2A-WSD

API WSD uses safety factor which is same for all types of loads, whereas API LRFD and ISO use different factors based on each type of stresses. WSD code safety factors have been found empirically [4]. In WSD, allowable stresses are either expressed implicitly as a fraction of yield stress or buckling stress or by applying a safety factor on critical buckling stress [5]. WSD strength of component or joint can be evaluated by using Eq. (2.1),

$$\frac{R}{\mathrm{FS}} \geq D_l + L_l + E_l \tag{2.1}$$

where R = resistance effect, FS = factor of safety, D_l = dead load, L_l = live load and E_l = environmental load. WSD method has safety factor provided only to the resistance of the material without considering the uncertainties related to the loads as shown in Eq. (2.2),

$$Q < \text{Ø}R \tag{2.2}$$

where Q = load and Ø = material strength safety factor, and it covers the randomness of material and load. This safety factor theory assume the concept that probability distributions of Q and R exist but not known [6]. Thus, a large value of load $Q = Q_1$ is taken and low value of resistance $R = R_1$ is taken (allowable yield strength is less than the specified yield strength of steel), the factor of safety takes into consideration the uncertainties as shown in Eq. (2.3),

$$\mathrm{FS} = R_1/Q_1 \tag{2.3}$$

where R_1 and Q_1 are resistance and load typical values. If $Q_1 < R_1$ i.e. if load is smaller than resistance, structure is safe but if $Q_1 > R_1$, then it means failure of structure. So, to avoid any damage to structure, safety factor is provided in advance at design stage.

In working stress, design resistance is divided by a factor of safety but LRFD takes into consideration the inherent natural uncertainties in applied action and resistance of components [7]. Due to this discrepancy, LRFD method of design has been introduced to replace WSD. In the limit state design, these uncertainties of load and resistance are considered more realistically by using reliability analysis methods. The drawbacks of WSD code have been outlined as it is excessively conservative and did not provide engineer any insight of degree of risk or design safety of Jacket [8]. It has no risk balanced capabilities, and there is little justification for safety factors. Bilal reports that uncertainty using deterministic factors of safety could lead to inconsistent reliability levels and may produce over design. WSD does not provide insights into the effects of individual uncertainties and real safety margins [9]. The main disadvantages of deterministic measure are shown below:

(i) Structural model uncertainty
(ii) Uncertainty of external loads
(iii) Human error

2.1.2 API RP2A-LRFD/ISO 19902

The first code using limit state design using probabilistic analysis was formulated by Canada for cold formed steel members in 1974 [10]. Denmark and Norwegian Certifying Authority, DNV was the first to introduce the limit state design code for Jacket platform which was published in 1977 [7, 11–13]. In 1993, API RP2A-LRFD was published and it has been updated by ISO 19900 series of codes for offshore structures. In this method, resistance and load are factored using uncertainty. This type of design is described as balanced design as it provides a balanced allocation of resources [14]. LRFD provides a safe and economically efficient way of designing Jackets to different environmental load conditions. It is also able to incorporate regional and geographical conditions in the design. Instead of factor of safety, load and resistance factors are used. In LRFD, the load combination equation is shown in Eq. (2.4),

$$\text{Ø}R_n \geq \gamma_D D_1 + \gamma_L L_l + \gamma_w E_l \tag{2.4}$$

where, R_n = nominal resistance, γ_D = dead load factor, D_l = Nominal dead load, γ_L = live load factor, L_l = Nominal live load, γ_w = environmental load factor, E_l = Nominal environmental load (100-year extreme). LRFD format can be represented in more general way in Eq. (2.5),

$$\text{Ø}R = \sum_{i=1}^{n} \gamma_i Q_i \tag{2.5}$$

where R = characteristic/nominal value of resistance, Q_i = characteristic or nominal value of load, Ø = resistance factor (for uncertainty in stress), γ_i = load factor (for uncertainty in load), n = number/type of load components (Gravity load and environmental load).

2.1.3 Benefits of Limit State Design Code

LRFD approach provides logical thinking while designing the structures, i.e. it considers the uncertainties of resistance and load. Semi-probabilistic approach simplifies the design process. Safety factor calculation remains deterministic one, but load and resistance factors are established depending on the requirement of structures whose reliability is chosen in advance. Nominal load and resistance values can be same in WSD and LRFD codes. LRFD code use factors which are chosen taking into consideration uncertainty in relation to action and resistance, i.e. spread of values and insufficient data. We can derive resistance and load factors using probabilistic methods design criteria. Factors are adjusted with a uniform degree of reliability to all structural elements in a given class of structure [6]. For instance, each type of stress can be dealt accordingly like axial compression or axial tension. Furthermore, as more test data on variables become available, these factors can be modified as per the updated statistical parameters of random variables.

Dead, live and environmental loads are treated separately using probabilistic methods and each type of load is taken after making statistical analysis. These factors can be increased in case of structures which are at high risk like nuclear power plants or offshore structures but can be decreased for low-risk structures. WSD uses same factors for both types of structures. The benefits of LRFD can be outlined below:

(i) It gives superior consistency in the reliability of offshore Jacket platforms.
(ii) LRFD has efficient utilisation of materials compared to factor of safety design method, i.e. WSD.
(iii) Randomness and uncertainties can be taken care off more specifically.
(iv) Platforms can be designed as per the actual requirements of operator, i.e. specific for certain location, type and life span.
(v) This is by use of logical interpretation of new research.
(vi) Since deck is designed using AISC (2005) which is reliability-based design code, it is logical that Jacket should also be designed using LRFD code.
(vii) LRFD provides incentives for research with regard to uncertainties, which take part for determination of partial load factors.

2.1.4 Safety Factor

Any structure designed and built with latest knowledge cannot claim to be free from chance of failure. The safety factor is used to give allowance for variation of material and load uncertainties of Jacket platforms. Optimal safety margin for design of Jacket may be observed as problem which involves trade-off between cost and acceptable failure probability [15]. It is a known fact that design involves many uncertainties which are not clear at the time of design. Thus, the structural engineer uses probabilistic reasoning for design of structure. The selection process of partial safety factors is called code calibration [16]. The calibration of safety factor is done in such a way that large safety factor is provided in presence of large uncertainties, whereas small safety factor is provided in small uncertainties. Code developers assume certain values for basic parameters, which are expected to cover for the uncertainties involved with the material properties during the entire life of the structure. By the use of these uncertainties, the model equations are developed which contain some factors. These are called factors of safety in WSD and load and resistance factors in limit state design and provide a high level of assurance that the structure will perform satisfactorily. This is defined as ratio of expected strength of response of Jacket to expected applied loads [17].

Despite all these safety factors, due to some unforeseen load condition, some member resistance problem may cause the failure of structure [6]. Structural failures demonstrate that however the design is considered safe still accident happen. Offshore accidents cause not only loss of lives but also produce economic losses and environmental catastrophe.

Fig. 2.1 Jacket platform under fabrication at a yard

2.2 Geographic Region of Offshore Malaysia

Brunei in 1929 became the first country in South East Asia to produce hydrocarbons [18]. In 1992, there were 65 number of platforms in Baram delta Sarawak and 120 in rest of Malaysia [18]. For offshore Malaysia, Baram delta is the biggest and has platforms with integrated drilling, production and quarters facilities [18]. Figure 2.1 shows platform under fabrication at a yard.

2.2.1 History of Offshore Oil Production

The ever increasing demand for oil and gas has forced engineers to go for offshore exploration, specifically during the energy crises of 1970s. Prior to 1947 offshore Jacket model for most of offshore operations were used to be wooden piled decks, connected to shores through trestles [19]. In 1947, Kerr Mcgee-Phillips-Stanolind group used 22 piles to support a drilling deck in Gulf of Mexico in 6.1 m water depth opened a new chapter in marine soil operations. Jacket piles were driven through vertical legs and acted as anchors. Today Jacket platforms in water depth of more than 300 m are built to withstand the huge forces of nature such as hurricanes and typhoons [20]. The demand for more hydrocarbons has forced us to go

into ever deeper ocean waters with hostile environment for exploration and production. Nowadays, offshore structures taller than the Eiffel tower are designed to withstand extremely rare waves of more than 30 m high, collision with ships, scour at mud line, earthquakes or other environmental hazards [21].

The work for finding load and resistance factors for different offshore regions has made much progress such as North Sea, Mediterranean Sea, Canada, Australia, South China Sea, Bohai Sea and Gulf of Guinea. API RP2A LRFD has been adopted for use in the North Sea, UK sector after an initial transition period during which appropriate load factors were developed. Large majority of platforms installed in the UK sector after 1995 were also designed using the LRFD format in preference to the WSD [13, 22]. The effect of load variables is significant in different regions of world depending on geography. Specifically, the regions near equator, where climate is mild and there is less chance of rare events occurring significantly.

2.2.2 Jacket Platform Design in Malaysia

In Malaysia, API RP2A WSD is used by offshore design and fabrication industry along with PETRONAS technical standard (PTS), for local environmental load parameters. Soon ISO 19902 code will be used to design the Jackets platform with an environmental load factor of 1.35. The application of environmental load factors which is optimised for GOM offshore region and materials may be not be reasonable for Malaysian waters [23]. The calibration of load factor has never been done so far in this region.

2.3 Uncertainty

Load and resistance are considered as random variables. The main uncertainties deal with the tolerance to which structural members are built and the loads and environmental conditions to which they will be exposed throughout their life [21]. This variation is stated by the probability distribution function and their correlation function if it is considered. In this book, random variables are treated as independent and no correlation is taken into consideration. Figure 2.2 shows the types of uncertainty used for reliability analysis.

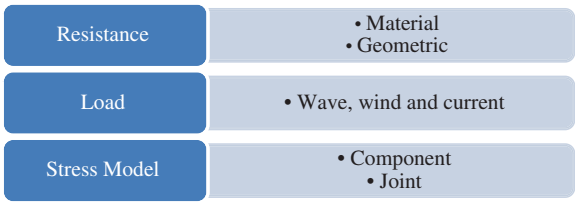

Fig. 2.2 Types of uncertainties

2.3.1 Uncertainty of Loads and Resistance

Structural design depends on uncertainties which come from environmental loads and resistance of material. The geographical variation of environmental load is so much that ISO 19902 has reported that due to uncertainty of load and resistance load factors should be ascertained in each region separately. Structural design assumes load and resistance which are random in nature. The case of offshore Jacket platforms needs special importance, because it deals with loads which are not simple random variable. Environmental loads are not like live loads acting on land-based structure but are more severe due to unpredictable weather conditions. This environmental load can act with unexpected severity on offshore structures. The resistance can also be reduced due to sudden damage to Jacket. Thus, probabilistic techniques are required for estimating the design loads and resistance. This book highlights the reliability analysis of Jackets and significance of different structural and load variables including their respective uncertainties influencing the safety of Jackets.

2.3.2 Basic Uncertainty

Uncertainty modelling is the first important step for the reliability analysis for the Jacket platforms. Parameters of modelling of uncertainty are mean (central tendency), variance (dispersion about the mean) and probability distribution functions [24]. Structural reliability is based on the theory of probability and its treatment to different uncertainties whose role is dominant as far as behaviour of structure is concerned. These uncertainties, if not treated properly, may cause failure, collapse or damage to structure which may become unserviceable and threat to environment. These problems can only be solved by introducing the probability to account for the risks involved in the uncertain design of offshore Jacket platforms. Uncertainties are dealt with by taking into consideration random variable parameters of load and resistance. The reliability analysis is significantly dependent and very susceptible to uncertainty modelling [25].

Structural analysis calculations of offshore platforms are also subject to uncertainties. Uncertainties are analysed by using how much basic information is available about that random variable parameter [26]. Modelling uncertainties are introduced by all physical models used to predict the load effects and the structural response [27]. The results are geometric and material variability. Equation (2.6) defines the risk and probability of failure of structure. Probabilistic calculation techniques enable these uncertainties to be taken into account. They provide a probability that it will resist the load, (probability that it will not resist the load, known as the failure probability of the member) which characterises its reliability.

$$\text{Risk} = 1 - \text{Reliability} \tag{2.6}$$

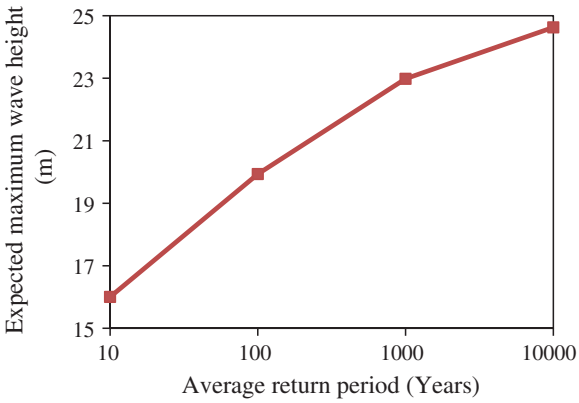

Fig. 2.3 Exceedance probability curve for wave height in GOM [107]

Jacket will fail if the strength is less than the applied load and probability of failure is shown by Eq. (2.7),

$$P_f = \text{Resistance(strength)} < \text{Load} \tag{2.7}$$

Uncertainty reflects lack of information which could be on the load side or on resistance side [28]. Uncertainties deal with how much load we shall consider for design (loading) and how much load a structure can withstand (resistances). We do not know how big are the largest waves the Jacket will be exposed to throughout the expected design life of the Jacket. This will depend on the geographic location and the design life of Jacket. For instance, in GOM, chances of rare event occurring within expected design life will be higher than in Malaysia. This extreme and rare wave height for design is assumed to occur once every 100 years thus it has a probability of 0.01 of occurrence in a given year. Figure 2.3 shows the exceedance probability curve for wave height at GOM site up to 10,000 years.

Probabilistic calibration is done to find safety factors in a balanced manner. This takes into consideration the sources of uncertainty in environmental loads and material resistance [29]. Failure of structures has shown us that it is impossible to build a risk-free structure. This is due to the nature of extreme environmental loads and uncertainty in material, fabrication, construction, human error and structural analysis of Jacket platforms [30]. Failure of ocean structures has huge impact on oil industry. Such failures have catastrophic effect on the industry. The notable ones are Alexander Kielland (Norway-1980), Ocean ranger (Canada-1985), Piper Alpha (North Sea, UK 1988) Petrobras-36 (Brazil 2001), Deepwater horizon (USA 2011). The failure mode of above five structures was fatigue, buoyancy control system failure, natural gas fire, buoyancy control system failure and explosion and fire, respectively.

2.3.3 Sources of Uncertainty

Uncertainty determination depends on computational tools. This enables the determination of analytical results by determining the component and joint safety,

subjected to the uncertain variable loads and resistances during design [26]. There are many sources of uncertainty which are defined below.

2.3.3.1 Natural

This comes from randomness of loads and material resistance and is difficult to control. An example is the tsunami which hit Japan in 2011. Natural and inbuilt randomness of environmental loads and earthquake, which are acting on the structure such as wave, wind and current contain uncertainty of time, period, interval magnitude and parameters (height and direction). The Jacket may be exposed to 100-year wave height during its service life. Deterministic calculations verify that each member of the structure can withstand the hundred-year wave. The material uncertainty includes yield strength, ductility and elongation. These can be due to operating, i.e. fatigue or extreme environmental, i.e. storm or extreme natural calamity, i.e. earthquake [26].

2.3.3.2 Statistical Uncertainty

This type of uncertainty is related to statistical modelling of distribution of the random parameters [14, 18]. If the number of data points is increased, this type of uncertainty is reduced.

2.3.3.3 Human Mistakes

This type of uncertainty depends on knowledge of person designing the structure, construction and operation of the structure such as piper alpha disaster in 1988 caused by communication gap between platform operators. Statistical analysis of failure shows that 90 % of these failures are due to human errors [10].

2.3.4 Parameters of Uncertainty

Variability of member resistance and environmental load parameters can be found through collection of data and fitting of it using probability distribution. Statistical parameters (mean, standard deviation, coefficient of variation, etc.) can be obtained for the random variables.

2.3.4.1 Random Variables

For structural design, it is extremely important to evaluate the probability of failure and safety levels of a Jacket, especially in the event when variables are random. The variables used for reliability analysis for Jacket platforms are geometric, material properties and loads are not considered as deterministic [31]. The structural

safety is shown by two independent properties, i.e. load effect forces (moments, axial, and shear forces) acting on the structure or its components due to applied forces and strength or resistance, both are random variables. In the case of load effects, these are the forces caused by man, material and nature, and for the case of resistance these are due to the mechanical and geometrical properties of material.

2.3.4.2 Bias

Bias is defined as a ratio of actual capacity to calculated capacity [32]. It is also defined as mean value over nominal value. It will always be there for geometric variables. For resistance variables, mean bias is found by average of measured values against the actual test results or dimension provided by design engineer. If mean value is not equal to 1.0, it shows that it has a bias in the model [33]. Some risk of bias of the analysis will be there always when using computational models, which can define safe and unsafe platforms [34].

2.3.4.3 Return Period

API and ISO objectives report that offshore structures should have ability to withstand the 100-year storm load. The environmental loads acting on the structure are random variables. This makes the reliable estimation of offshore loads for their design life difficult. Random nature of offshore environment can only be estimated by taking into consideration return period of probabilistic models of environmental loads. For Jacket design, it is 100 years and for reassessment and life extension, it is 10,000 years. In North Sea with 100-year wave, the 10-year return period of current has been used as further explained in Chap. 3.

2.3.4.4 Distribution Types

Type of distributions for random variables is an important factor for reliability analysis. For rare events, the extreme types of distributions are used and for geometric and material resistance, commonly normal or lognormal distributions are reported in texts. Distribution and their parameters are compulsory tools for level III reliability which is explained in Chap. 7.

2.3.5 Types of Resistance Uncertainty

2.3.5.1 Geometrical and Material

This uncertainty relates to the randomness due to geometrical and material variations. This is related to straightness, diameter, thickness, length, yield strength,

elongation and tensile strength. In previous study, diameter, thickness, young's modulus and yield strength variables are considered for material uncertainty [4]. This type of uncertainty can be dealt properly with the application of controlled manufacturing and fabrication by using international standards and quality control. Many researchers have been working on resistance uncertainty, such as [30, 35–37]. Material properties used for assessment should be estimated using actual material properties of existing structures [38]. Still present day, there are minor but important variations remain between characteristic values mentioned on structural drawings and fabricated Jacket components placed at site as shown in Chap. 3.

2.3.5.2 Physical Stress Model

Model uncertainty is due to deviation of material strengths, from component or joint stress biases, with respect to actual strength acquired from tests results [29]. This type of uncertainty accounts for possible deviation of model assumptions of the resistance of a given section from the actual resistance of geometrical properties. The load model may also show variation due to natural variation in loads. This type of uncertainty is related to shortage of knowledge, information or unavailability of software. These can be reduced by applying the more detailed methods [14]. Norwegian Design regulation requires, "Design loading effects and design resistances should be computed by using deterministic computational models". These models shall aim at giving expected average values without introducing any increase or reduction in safety. The uncertainty of the computational models is being included in the partial coefficients [34]. Table 2.1 shows the stress model uncertainty considered in this research.

Table 2.2 shows the model uncertainty (X_m) from Mediterranean Sea. It should be remembered that it depends on API RP 2A WSD 18th Ed. There have been large changes in API RP 2A 21st Ed. published in 2008 particularly for joint models.

Table 2.1 Uncertainties in model predictions

Component		Joint
Tension	Tension and bending	Tension
Compression column buckling	Compression (column buckling) and bending	Compression
Compression local buckling	Compression (local buckling) and bending	In-plane bending
Shear	Tension and bending and hydrostatic pressure	Out-plane bending
Bending	Compression (column buckling), bending and hydrostatic pressure	
Hydrostatic	Compression (Local buckling) and hydrostatic pressure	

Table 2.2 Model uncertainty for Mediterranean Sea using API WSD 18 ED [85]

Tubular member		X_m	COV
Tension and bending		1.093	0.058
Compression (column buckling) and bending		1.075	0.053
Compression (local buckling) and bending		1.222	0.064
Hydrostatic		0.99	0.095
Tension and bending and hydrostatic pressure		1.018	0.106
Compression (local buckling) and hydrostatic pressure		1.082	0.104
Joints			
K	Tension/compression	1.32	0.028
	IPB	1.185	0.183
	OPB	1.113	0.179
T/Y	Tension	2.207	0.401
	Compression	1.306	0.291
	IPB	1.296	0.328
	OPB	1.388	0.354
X	Tension	2.159	0.546
	Compression	1.145	0.144
	IPB	1.595	0.250
	OPB	1.147	0.250

2.4 Resistance Uncertainty-Background Study

ISO 19902 Clause 7.7.4 requires that the test/measured data should be validated by simulation for the resistance of material taking into account the structural behaviour variability of material [39]. DNV report 30.6 recommends that for resistance model, normal distribution should be considered for the reliability analysis of Jacket platforms [33]. The difference between strength and load variable is highlighted by the fact that strength variable is considered unsuitable if its value is less than the mean value as it may cause failure. For model equations, the mean value should be greater than 1.0 which shows the conservativeness of code equations and usually normal distribution is assumed for it [40]. The load variable is unsuitable, if it is greater than its mean value which can cause failure. Previous studies on resistance of material have been made by many authors [12, 16, 35, 41–43]. Currently no information is available about any similar study conducted in Malaysia.

Structural design strength depends on characteristic values of basic random variables of resistance. The behaviour of these variables of strength may vary in such a way that they become unsafe at any time throughout design life. Structure can fail if the characteristic value of load exceeds the characteristic

Table 2.3 Resistance uncertainties for jacket platforms

Types of resistance uncertainty	Example
Material uncertainty	Yield strength, modulus of elasticity, elongation, tensile strength
Geometric uncertainty	Diameter, thickness
Fatigue uncertainty	Degradation of material
Corrosion uncertainty	Degradation of material

load carrying capability. Uncertainty determination depends on computational tools available at hand. This enables correct analysis by determining the component safety, subjected to the uncertain variable loads and resistances during design [26]. Generally, load tends to increase with time, whereas resistance tends to decreases with time. Thus, uncertainty of load and resistance increases with time [46]. Ellingwood [44] says that the result of uncertainty is risk, which is defined as "the product of the probability of failure and costs associated with failure of structure" [45]. High probability of failure means low reliability thus cost of failure will be high. These problems can only be solved by introducing the probability into account for the risks involved for the uncertain design of offshore Jacket platforms.

The strength of Jacket depends on the variability of its components from which the member is built. The primary members of Jacket are piles, legs, horizontal periphery braces, horizontal internal braces and vertical diagonal braces. Jacket members are in seven different types of stresses, and joints are in four types of stresses. Code provides equations to find these stresses of resistance of random variables from which members are fabricated. Table 2.3 shows the uncertainties related to offshore Jacket platforms. In this book, material and geometric uncertainties are discussed, due to their relevance to ultimate limit state design, which is the most significant limit state design as compared to other types of limit states.

The probability of failure can be updated if changes in COV are known, i.e. after the design of Jacket members or joints. This is possible after the material tests results or actual geometrical properties statistical analysis. For instance at design stage, the COV taken was 0.15 but when actual material test report was issued and it becomes known that the actual COV was 0.1. Using the reliability analysis, new probability of failure can be determined [28]. In this book, fatigue and corrosion uncertainty are not discussed further.

2.4.1 Material Uncertainty

Materials like steel have variability due to construction practices. The basic strength or resistance uncertainty includes yield strength, elastic modulus (Young's modulus). ISO takes yield strength distribution for North Sea as lognormal. Bias

of 1.127 and standard deviation of 0.057 was achieved in one study [43]. Duan [12] takes yield strength distribution for China as normal, with a bias of 1.0 and COV of 0.05 was achieved.

2.4.2 Characteristic Resistance

Characteristic resistance should have low probability of being exceeded at any specified design life of Jacket. It is defined as that value below which not more than 5 % of the test results of large number of test would fall [46] or it is 0.05 fractile of a lower end of normal distributions [47, 48]. Characteristic strength should be equal to guaranteed yield strength but shall not exceed 0.8 times the guaranteed tensile strength [34] or minimum of upper yield strength. Characteristic values of geometric quantity are the dimensions specified by the design engineer [47].

2.4.3 Geometric Uncertainty

The structure can fail due to resistance failure from variation in dimension and fabrication errors. The geometrical uncertainties include diameter, thickness and length and effective length factor. ISO reports following results for statistical properties of geometry of tubular members [43]. Normal distribution was taken for diameter, thickness, length and effective length factor for leg and brace. Mean bias of 1.0 and COV of 0.0025 was achieved for diameter. Mean bias of 1.0 and COV of (0.004 + 0.25/T) was achieved for thickness. Mean bias of 1.0 and COV of 0.0025 was achieved for length. Mean bias of 1.1 and standard deviation of 0.0935 was achieved for effective length factor for leg member. For braces, the mean bias was achieved as 0.875 and COV of 0.097. Further details can be found in Chap. 4.

2.4.4 Resistance Model Uncertainty

The modelling uncertainty is predicted from the ISO code equations. Seven component stresses and four joint stresses for each joint type are modelled for resistance. The uncertainty model for resistance (X_m) is shown by Eq. (2.8),

$$X_m = \frac{\text{Actual Resistance}}{\text{Predicted Resistance}} \tag{2.8}$$

This model uncertainty depends on the statistical parameters for basic variables, i.e. diameter, thickness, yield strength and modulus of elasticity. The detailed results from literature are shown in Chap. 4.

2.4.4.1 Single Stresses

The variation of model uncertainty for single stress has been reported by ISO and BOMEL [39, 43]. Mean bias for tensile strength was achieved as 1.0 with standard deviation of 0.0. For column buckling strength, from experimental tests results it was found to be with a bias of 1.057, COV of 0.041 and standard deviation of 0.043. For local buckling, mean bias was 1.065, COV of 0.068 and standard deviation of 0.073. For bending, the experimental bias was reported to be 1.109, COV was 0.085 and standard deviation was 0.094. The experimental bias for hoop buckling was found to be 1.142, COV was 0.124 and standard deviation was 0.1416.

2.4.4.2 Double Stresses

The variation of model uncertainty for two combined stresses has been reported by ISO and BOMEL [39, 43]. For tension and bending, the bias was found to be 1.109 and standard deviation was 0.094. For compression and bending, the experimental bias for compression (local buckling) and bending was found to be 1.246, COV was 0.067 and standard deviation of 0.084. For compression (column buckling), mean bias was 1.03, COV was 0.082 and standard deviation was 0.084.

2.4.4.3 Three Stresses

The variation of model uncertainty for three combined stresses has been reported by ISO and BOMEL [39, 43, 49]. For tension, bending and hydrostatic pressure, the experimental bias for axial tension, bending and hydrostatic pressure was found to be 1.075, COV was 0.098 and standard deviation was 0.105. For compression, bending and hydrostatic pressure, the experimental bias for compression (short column), bending and hydrostatic pressure was found to be 1.199 and COV was 0.134 and standard deviation was 0.161. The experimental bias for compression (long column), bending and hydrostatic pressure was found to be 1.197, COV was 0.091 and standard deviation was 0.109.

2.4.5 Critical Review of Resistance Uncertainty

Safety and risk are associated concepts though different in character, i.e. risk is quantifiable but safety is not, it is something to be achieved or assured [50]. The safety of Jacket platforms can be assured within risk management by considering the hazards to which they are subjected. It is emphasised by ISO code that resistance modelling has to be done for each geographic region. ISO and China studies report that the geometrical variables are normally distributed. The yield strength distribution was found to be lognormal for ISO in North Sea but Det Norske

Veritas (DNV) in one of its reports takes it as Normal. Study made in China reported it to be normal as will be shown in Chap. 4. The difference in variables is not much high, as is expected due to quality control on fabrication and manufacture of materials nowadays. Literature on resistance uncertainty is not available in Malaysia and therefore this issue will be dealt in this book. The influence of yield strength and model uncertainty on reliability analysis is emphasised by many researchers working in this area of study.

2.5 Load Uncertainty

The variability of load is considered random in nature and during reliability analysis, probability distribution and its parameters are used instead of a deterministic value. Proper estimation of load is the most important step for the design of structure. Sustainable development requires structural robustness of Jacket platforms against extreme environmental events. Environmental load uncertainty considered safe during design of a Jacket platform may become unsafe during one hurricane event in GOM. This was experienced during hurricane Ivan in 2004. Reliability analysis of Jacket platforms requires load models should be the probability distribution based due to random nature of loads.

Extreme value distributions, i.e. Fretchet, Weibull and Gumbel, are three theoretical distributions which are commonly applied to model load uncertainty parameters [51]. These distributions are formulated for the maximum, of an infinite number of events. It is easy to apply them as they represent the maximum load intensity to capture the tail characteristics of these distributions. Many researchers have assumed Weibull distribution for environmental load uncertainty for their study [52–54].

2.5.1 Load Uncertainty Parameters

There are two basic approaches to find the environmental load factor parameters, i.e. energy spectral density and statistical analysis method [55]. In this book, the second approach is adopted.

2.5.1.1 Characteristic Load

Characteristic value is taken as the most probable extreme value with a specified return period. The characteristic value of environmental load for extreme conditions is defined as the most probable largest value in a period of 100 years [34]. The nominal value is the value of random variable which has a probability of not being exceeded during reference period of 100 years as prescribed by ISO 19902. It is the maximum value corresponding to load effect with a standard probability

of exceedance. It is the fractile in upper end of normally distributed function of load [48]. Primary environmental loads for fixed Jackets include waves, wind and currents but most of time waves produce the dominating load effect [34, 56].

2.5.1.2 Return Period Probability

Return period probability is shown in Eq. (2.9),

$$P = 1 - p^n \tag{2.9}$$

where n = platform life in years (30 years), p = annual probability that the event will not occur. Probability of occurrence of an event in 100 years is given by,

$$1/100 = 0.01$$

A return period of 100 years means an annual probability of occurrence of 0.01 or probability of non-occurrence of 0.99

$$P = 1 - (0.99)^{30} = 0.26 \text{ or } 26\,\%$$

The results show that probability that it will experience at least one event with a return period of 100 years during its life is 26 %.

2.5.2 Statistical Data Uncertainty for Environmental Load

Environmental loads vary significantly due to uncertainty of wind, wave and current. Environmental loads are highly variable and the Jacket may fail from overloading effects as they sometime may produce loading effect which is more than the design loads. The COV of extreme environmental loading for North Sea is 65 % and GOM is 77 % [57]. The intense tropical cyclones (typhoons) in the Pacific Ocean create governing extreme conditions in these areas. Storm is termed as three phase progress of severe sea involving a development, a peak and decay phase as shown in Fig. 2.4. The total duration may be between 12 and 39 h of sea state, characterised by development phase, i.e. growth (0–18) h, a peak duration of 3 h (18–21) and subsequent decay phase duration of 21–39 h, i.e. 18 h [58–60].

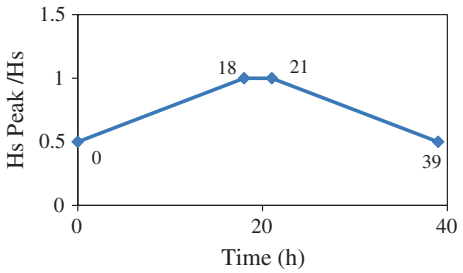

Fig. 2.4 Development of storm growth, peak and decay [59, 60]

The wave is the dominant load here along with gravity loads. The effects of any load which are less than 10 % of the effects of any other type of load may be ignored like wind loads [61].

The extrapolation of probabilistic models depends on distribution functions plotted in straight ascending lines. The wind speed, wave height, time period and current speed are plotted against the return period. Straight line is fitted to the plotted data and it is extended beyond the available data to acquire the estimation of extreme values for the desired return periods. This straight line which fits to the data may be subject to some errors on uncertainty of extrapolation [53]. The errors can only be decreased by increasing the data points with extended time period.

2.5.2.1 Collection of Data

ISO code points out that the statistics of long-term estimation of metocean parameters requires that the individual number of storms used for the statistical analysis must be statistically independent. Wave height taken at hourly rate depends on the wave height of the previous hour. Thus, situation of independence of wave is not achieved. To produce independent data points, only numbers of storms are considered for the statistical analysis. Collection of data for wave height is made in two steps:

(i) Long-term statistics uses the highest significant wave height and its associated period. The data are taken from storm data. It is taken for average of 20 min time periods and recorded after 3 h intervals.
(ii) Short-term statistics uses expected amplitude of highest wave. Such an extreme sea state is estimated, from assumption of linearity. Thus, the higher peaks are taken as Rayleigh distributed.

2.5.2.2 Weibull Distribution

Weibull 2-parameter distribution is an extreme value distribution. It is used to capture the variability of rare event which may occur once during the return period. The variable x has the CDF as shown in Eq. (2.10),

$$F(x; a, b) = 1 - \exp\left[-\left(\frac{x}{a}\right)^b\right] \tag{2.10}$$

Parameters a = scale and b = shape, $Fx(a, b)$ = Cumulative Distribution Function (CDF) of variables a, b. Their linear form can be shown by taking the natural logs twice of CDF of Eq. (2.9) in $x_{(i)}$, Eq. (2.11) [62] which shows that,

$$\ln\left\{-\ln\left[1 - F\left(x_{(i)}\right)\right]\right\} = -b\ln(a) + b\ln\left(x_{(i)}\right) \tag{2.11}$$

The plotting of $\ln\left\{-\ln\left[1 - F\left(x_{(i)}\right)\right]\right\}$ against the data $x_{(i)}$ results in a straight line, if the data came from Weibull distribution. The parameter "a" is found from

intercept and "b" by slope of straight line. The slope corresponds to shape and intercept to scale parameters. Scale parameters are used for the model "F" on the measurement axis by using its scale. This parameters show the horizontal stretching or contracting of the model "F". They are shown always in the following form as "a" in $\frac{x-b}{a}$. The shape parameter determines the basic shape of function "F", gives a measure of dispersion. This parameter does not relate to x in a set arrangement common to all models "F" [62].

2.5.2.3 Gumbel Distribution

The Gumbel distribution variable x has the CDF as shown in Eq. (2.12),

$$F(x; c, d) = \exp\left\{-\exp\left[-\frac{x-c}{d}\right]\right\} \tag{2.12}$$

Parameters c = location and d = scale. Their linear form can be shown by taking the natural logs twice of CDF as shown in Eq. (2.13) in $x_{(i)}$, [62]

$$-\ln\left\{-\ln\left[F\left(x_{(i)}\right)\right]\right\} = -d(\mathrm{c}) + d\left(x_{(i)}\right) \tag{2.13}$$

The plotting of $-\ln\left\{-\ln\left[F\left(x_{(i)}\right)\right]\right\}$ against the data $x_{(i)}$ results in a straight line, if the data came from Gumbel distribution. The parameter "d" is found from intercept and "c" by slope of straight line. The slope corresponds to location and intercept to scale parameters. Location parameters locate the model F on its measurement axis. They are identified by their relation to x in the function "F", i.e. $(x - c)$ in (2.12). Scale parameters scale the model "F" on the measurement axis. This parameter shows the horizontal stretching or contracting of the model "F" [62].

2.5.2.4 Wave

The primary parameter in the classification of sea states is the wave height, which is calculated from peak to trough. The actual selection of design wave height, to be used for specific platforms deign, is a matter of engineering knowledge and judgement. Jacket platforms are inherently more sensitive to waves than current and winds [54, 63, 64]. This is due to peak response always occurs at the time of maximum wave height [63, 65]. During a conventionally short time period of 20 min for a sea state to be regarded as statistically stationary, the most important measure is significant wave height, which is a average wave height of highest one-third of the waves. Only wave parameters are taken into consideration for calibration of environmental load factor for API RP 2A LRFD. Mean bias and COV was set up as 0.70 and 37 % [39]. This was same as for wind, therefore only wave was considered for reliability analysis. Weibull distribution fits well with significant wave height [66]. Design wave height is obtained by multiplying the significant wave height by a factor in range of 1.8–2.0 [67].

2.5.2.5 Current

Currents can play significant role in total forces acting on Jacket platform. Current refers to motion of water which arises from sources other than surface waves. Tidal currents arise from astronomical forces and wind-drift currents arise from drag of local wind on water surface [68]. When extreme waves along with superimposed current occur in same direction, velocities from both can combine and produce large wave pressure [23]. Independence of wave should be assumed because there is no reason to believe that extreme wave will occur at the same time as extreme current [4]. The maximum wave height and maximum current occurred only once simultaneously out of 38 storms in North Sea [69].

This current load may never reach the probability of failure of 10^{-1} in the region of Malaysia. During storm conditions, current give rise to horizontal structural forces equal to 10 % of the wave-induced forces [70]. Even in Norwegian continental shelf, current load experienced is not higher than 10-year load with yearly probability of exceedance of 10^{-1} [71]. That is the reason why ISO code considers 1–5 years time period for operational conditions for South China Sea instead of 1 year as is considered for Gulf of Mexico or North Sea. In North Sea, the current speed used for design of offshore Jacket platform is of 10 year maximum with associated 100-year design wave [72].

2.5.2.6 Wind

During storm conditions, wind could have significant effect on design of Jacket platforms and it can induce large forces on exposed parts. The effect of wind force depends on size and shape of structural members and on wind speed. Wind force arises from viscous drag of air on component and from difference in pressure on windward and leeward sides [67]. For Jacket platforms, wind load can be modelled as deterministic quantity [73, 74]. Wind force is small part, i.e. less than 5–10 % of wave force [64, 75]. Wind is measured at 10-m reference height. Wind influences the build up of waves which can take significant time, i.e. many hours. This shows that the short-term variations of wind speed and sea elevation may be considered independently [29]. Wind is responsible for generation of surface waves [76]. Bias and COV for wind was found to be as 0.78 and 37 %. This was almost same as wave parameters [39]. Wind was assumed to be 2 parameters Weibull distribution for northern North Sea [77].

2.5.2.7 Environmental Load Modelling Uncertainty

Environmental load model uncertainty was taken as normal distribution with COV of 0.15 and mean bias value of 1.09 [43].

2.5.3 Critical Analysis of Load Uncertainty

The gravity loads and environmental loads both are random variables. The gravity load statistics have been taken from literature in this book. Gravity loads are taken as normal and environmental load are selected as Weibull and Gumbel but Weibull is preferred choice of engineers. The load uncertainty has large COV which influences the probability of failure significantly as will be shown in Chap. 7. The data collection is very important for reducing this uncertainty. Therefore, if this uncertainty is to be reduced, then more accurate data collection method should be applied.

2.6 Environmental Load Modelling of Jacket Response

The environmental load model is necessary for the development of load factor using reliability index. Total wave force on platform equals to square of wave height [78]. In this book, the responses of Jacket (strength of components) in terms of basic applied loads which govern its behaviour are modelled. This can be represented by stochastic processes or random variables. For the FORM analysis, it is necessary to use random variable formulations [79]. Different methods for finding the response of offshore Jackets subjected to random ocean forces have been widely published [4, 16, 80–82] and two are shown below. Methods suggested by SHELL for development of load factors for ISO are shown in Eq. (2.14) [43, 83, 84].

$$W = aH_{\max}^2 + bH_{\max} + cV_{\mathrm{c}}^2 + dV_{\mathrm{c}} + e \tag{2.14}$$

where W = Load effects, $H_{\max}$ = variable annual maximum wave height, V_c = variable current speed, coefficients of a, b, c, d and e are found from curve fit tool of MATLAB. Another method is proposed by Heidman which is shown by Eq. (2.15) [20],

$$W = a_1(H_{\max} + a_2 v_c)^{a_3} \tag{2.15}$$

Coefficients of a_1, a_2 and a_3 are found from curve fit tool of MATLAB, $H_{\max}$ = maximum wave height and v_c = current speed. Here a_1 factor depends on the size of load area of Jacket [14].

2.6.1 Environmental Load Uncertainty Model

The environmental load model uncertainty (X_w) was used in development of API LRFD and ISO codes. ISO and BOMEL take it as normal distribution with mean bias of 1.09 and COV of 0.18 [43].

2.6.2 Dead Load

ISO categorises the dead load into 2 classes. Permanent load action, G_1, includes self-weight of structure and associated equipment. This is self-weight part of gravity load. Permanent load action, G_2, represents the self-weight of equipment and other objects that remain constant for long periods of time, but which can change from one mode of operation to another. It is treated as normal random variable. The statistical parameters of bias (mean over nominal) are taken from ISO code. The distribution was considered as normal with mean bias of 1.0 and COV of 0.06 [39, 64, 85–88]. In South China Sea, mean bias is 1.0 and COV of 0.08 which is reported in literature [86, 88].

2.6.3 Live Load

It is the permanently mounted variable load Q_1 and variable action, Q_2, represents the short duration action. The distribution is considered as normal with mean bias of 1.0 and COV of 0.1. These values are used for calibration of Jacket platforms in GOM and North Sea [85, 39]. The same values are used for calibration of load and resistance factor design for platforms in China [88] but mean bias of 1.0 and COV of 0.14 is suggested by [86].

2.7 Structural Reliability

Risk and safety are two intertwined words. For Jacket platforms, safety can be achieved by management of hazards produced by rare events of wave, wind and currents. Material strength of tubular components and joints plays significant role against risk. After treating the uncertainty of resistance and load, the issue of structural reliability is dealt with for three areas, i.e. component, joint and system. Reliability is defined as an ability, to achieve a desired purpose of platform under operational and extreme conditions, for its designed life. Structural reliability concept consists of structural safety and resistance, serviceability, durability and robustness [38]. Performance of a platform is measured in terms of reliability index or return period (probability of failure). Calibration of North Sea and GOM LRFD code development has used six Jacket platforms [89, 90]. Structural reliability can be found for time-dependent or independent reliability analysis. In this book, time independent reliability is considered.

Before probability-based codes were developed, structural codes contained safety criteria using allowable stress method. Structural system was assumed to act always elastically and inelastic behaviour was never assumed. The risk was catered by reducing the yield strength of member. Actual loads were calculated first and then members were selected so that the allowable member strength remained below certain limit like 66 % of yield strength. Thus, a factor of safety of 2/3 was

always there in the member for extreme load combinations. Code developers use this factor using judgement. Reliability analysis methods using probability and statistics, started to gain importance since 1960 under the patronage of CA Cornell, NC Lind and H.S. Ang. It was Cornell who in 1969 proposed second moment reliability index method [91] which was further developed by Hasofer and Lind, who gave a proper format to invariant reliability index [14, 92]. Rackwitz and Fiessler gave an efficient numerical procedure for finding the reliability index by using non-normal probability distributions. Rosenblueth and Turkstra gave load combinations. Moses helped in the development of API LRFD for Jacket platforms on which ISO 19902 code is based [16, 41, 93]. Der Kiuregian developed FERUM software for reliability analysis [94] which uses FORM reliability analysis method.

For normal distribution, the characteristic value used to be taken as 1.645 times standard deviation, i.e. an upper value and a lower value for load and resistance as shown in Eqs. (2.16 and 2.17). On load and resistance curve, the characteristic value is the 0.95 fractile for load and 0.05 for resistance. This shows that on load side 95 % of design load will lie below this value. On resistance side only 5 % values will be below the design strength. Equations (2.16 and 2.17) show the load and resistance characteristic values.

$$\text{Characteristic load} = \mu + 1.645\,\sigma \tag{2.16}$$

$$\text{Characteristic resistance} = \mu - 1.645\,\sigma \tag{2.17}$$

where μ = mean of normal distribution and σ = Standard deviation of normal distribution. It is possible to relate the number of standard deviations to probability of occurrence. One standard deviation both side of mean relates to 67 % of probability of occurrence and two standard deviations equals to 95 % [95].

2.7.1 Reliability Levels

Levels are characterised by amount of information about the problem is provided or it is determined by how many random variable parameters are being used. If characteristic values are used then it is called level I. If standard deviation and coefficient of correlation are also used then it is termed as level II, and if cumulative distribution function is also used then it is level III [14]. If engineering economic analysis is involved then it is level IV.

2.7.2 Parameters of Structural Reliability

2.7.2.1 Limit State

When a structure exceeds a particular limit and the Jacket is unable to perform as desired, then at that particular limit it is said that limit state has reached. If that

limit state is exceeded then the Jacket is considered unsafe. Conditions separating satisfactory and unsatisfactory states of structure are known as limit state [38]. There are four categories of limit state. The ultimate limit state is concerned with collapse of structure or component and it is necessary that it must have extremely low probability of failure. This limit state is concerned with maximum load carrying capacity of Jacket [48]. The structure must be able to withstand actions and influences occurring during construction and anticipated use in this limit state [38]. The serviceability limit state is related to interruption of normal use of that Jacket, this includes large deflection, excessive vibration, cracks, etc. Structure must remain fit for use under expected conditions of serviceability limit state conditions [38]. Fatigue limit state is due to cyclic loading and governs for operational conditions. Accidental limit state is used in consideration of accidental loads. It should maintain integrity and performance of Jacket from local damage or flooding [48].

2.7.2.2 Reliability Index

Reliability is a measure of probability of failure of structural member. It is the probability that system will carry out its intended purpose for certain period of time under conditions defined by limit state. This is a truth that it is practically not possible to make a member which does not fail for any kind of load. There will always be some chance or probability that the uncertain load will become large or resistance will be smaller than estimated, which will cause the member failure. It depends on what risks or reliability index value, the related industry is ready to take. For example, if the risks are high, as in offshore industry, higher reliability index or safety index is required but this increases the cost of structure. If risk is low, lower reliability index may also be accepted as in some cases of non-important structures. Table 2.4 shows that as probability of failure decreases the reliability index increases. The same can be shown graphically in Fig. 2.5 that shows the reliability index (β) against probability of failure (P_f). Where (β) can be found through Microsoft Excel function, using Eq. (2.18),

$$\beta = \text{NORMSINV}(P_f) \tag{2.18}$$

Table 2.4 Probability of failure and reliability index relationship [29]

β	Pf	Return period
1.28	1×10^{-1}	1 in 100
2.33	1×10^{-2}	1 in 100
3.09	1×10^{-3}	1 in 1,000
3.72	2×10^{-4}	1 in 5,000
4.26	1×10^{-4}	1 in 10,000
4.75	1×10^{-6}	1 in 1,000,000
5.20	1×10^{-7}	1 in 10,000,000

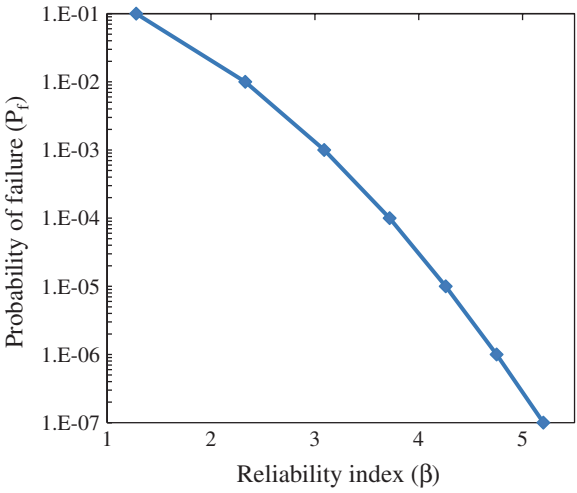

Fig. 2.5 Relationship between safety index and probability of failure [29]

2.7.2.3 Probability of Failure

Risk is defined by probability of occurrence of unfavourable event. There is no risk-free design. Risk depends on degree of overlap of load and resistance probability density curves [8]. Optimised design is reached when increase in initial cost is balanced by decrease in expected failure consequence cost [8]. Reliability model defines load and resistance as probabilistic random variables. It is referred as unsatisfactory performance of components particular performance criteria. Platforms in North Sea are designed for a ductility requirement of 10^{-4}/year with a possible annual failure probability of collapse of 10^{-5}, Efthymiou calls this could be 10^{-7} [96]. Annual failure probability is considered for structures where human life is of concern. Where material cost is of importance, design life of structure is considered for failure probability [39, 97]. The preferred safety level for engineering structures is by using loss of life probability due to structural failure. Individual accepted risk is by use of death due to failure of structure and in developed countries it is 10^{-4}/year [98].

In reliability-based design, an engineer is allowed to select a probability of failure which is proportionate with the failure consequences. This makes design engineer to decide what probability of failure he shall take for a particular Jacket. Thus by this concept, component or joint can be utilised to full capacity, thus making an economical Jacket such as unmanned Jackets [8]. Structure cannot be designed with 100 % surety that it will sustain all types of loads forever, i.e. there is no zero risk structural design. If higher safety margins are provided then the load and resistance curves will move further apart thus it will reduce the probability of failure but it will not totally remove load and resistance overlap [8].

The structural failure is shown as Eq. (2.19)

$$P_f = P(R < Q) \tag{2.19}$$

where P_f = probability of failure and P = probability. Thus, probability of survival can be shown by Eq. (2.20),

$$P_s = 1 - p_f \tag{2.20}$$

where P_s = probability of survival.

2.7.2.4 Target Reliability

Target reliability for offshore platforms depends on either reliability of platforms designed as per the old code like API WSD or on probability of failure acceptable to society. In this book, probability of failure is determined by assessing the effects of wave and current loading which are the most severe loading criteria for design of offshore platforms. Target reliability is required for calibration, in order to make sure that certain safety levels are maintained. It is minimum annual average reliability shown as a maximum failure probability for a given safety class, consequence, category and failure types, provided by the codes of practice for Jacket design. For setting a value, it requires some exercise of engineering judgement [99]. Target reliability is different for manned and unmanned Jacket platforms. For manned platforms, decision is made by required probability of failure, due to environmental loading. It should be small as compared to other high consequences and major risks such as fire, explosions and blowouts [100]. There is agreement among researchers that if annual probability of failure due to some cause is less than 1 in 10,000, then it is small in relation to major risks [100]. Assuming that in North Sea during 30 year, there are 250 platforms, now platform years will be $(30 \times 250) = 7{,}500$ platform years. Expected number of failures over 30 years period is then P(a) $\times$ 7,500, [P(a) = annual probability of failure]. Most probable outcome will be zero failures if [P(a) $\times$ 7,500 < 0.5], which leads P(a) < 1 in 15,000 [100].

DNV reports acceptable annual target reliability for redundant Jackets as 3.09 or probability of failure of 10^{-4} [33]. Many researchers have proposed target code of API WSD/API LRFD RP 2A/ISO 19902, for selection of target safety index. Separate partial factors are used for load effect types (axial, bending force, hydrostatic, etc.) [85]. For Ekofisk area, in North Sea, target annual probability of failure is 5×10^{-4} (design should make sure a 2,000-year return period of collapse limit state) [101]. This target failure probability of 1/2,000 per year is chosen as it is consistent with API guidelines for design of new platforms [101]. DNV provides the values for safety index and probability of failure used by the codes. Table 2.5 shows the target reliability for North Sea Jackets.

Table 2.5 Indicative target reliability [120]

Limit state	Annual	Lifetime
Ultimate limit state	3.8	4.7
Fatigue limit state	1.5–3.8	–
Serviceability limit state	1.5	3.0

Table 2.6 Probability of failure recommended for NS jackets [120]

Conditions	P_f
Severe consequence, i.e. (potential fatalities or significant environmental damage)	4^{-4}
Only economic consequences are involved	1^{-3}

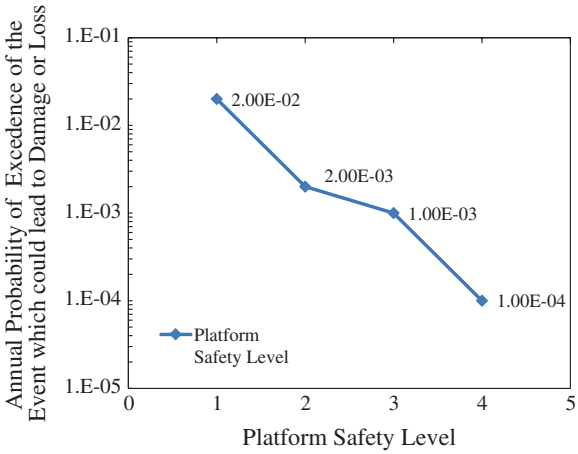

Fig. 2.6 Acceptance criteria for ductile jacket platform at different safety levels [96]

In order to apply reliability methods, it is necessary to find components failure function, uncertainty model, probability calculation method and target safety levels [102]. Table 2.6 shows the target reliability in shape of P_f using consequence of failure of fatalities or economic reasons.

Figure 2.6 shows acceptance criteria for target reliability of Jacket platforms at different safety levels. 1×10^{-4} is used for manned platforms, 1×10^{-3} is used for unmanned platform (high consequence), 2×10^{-3} unmanned platform (low consequence) and 2×10^{-2} closed down platform (ready for removal).

2.7.3 Review of Structural Reliability Methods

There are basically two types of reliability analysis methods, i.e. simulation and analytical. The major example for simulation method is Monte Carlo simulation. Monte Carlo simulation is easy to use, robust and accurate by using large number of samples, though it requires large number of analysis for achieving the good quality approximation of low probability of failure. The problem with this simulation technique is that it produces noisy approximation of probability. Analytical methods include moment-based methods such as First Order Reliability Method [44]. Cornell in 1969 proposed reliability method, i.e. Mean Value First Order Second Moment [103]. It was in 1974 when Hasofer and Lind proposed reliability index using FORM method.

2.7.3.1 First Order Second Moment (FOSM) Method

Probabilistic calibration is done to find safety factors in a balanced manner. It takes into consideration the sources of uncertainty in environmental load and material resistance [29]. This is a level II reliability method. In this, safety is measured by the first and second moments like mean and standard deviation. The method was proposed by Cornell using theory of reliability measurement in 1967 [14]. The safety index depends on mean μ and standard deviation σ which are expressed in Eq. (2.21).

$$\beta = \frac{\mu}{\sigma} \tag{2.21}$$

where β = reliability index, μ = mean (used to express the central tendency for a random variable in a distribution curve), σ = standard deviation (dispersion of random variable). This means that safety index is the distance in terms of standard deviations. It lies between origin and mean values of margin of safety in distribution curve [14]. Probabilistic calculation techniques enable these uncertainties to be taken into account. Probability distributions characterise the uncertainties associated with mean load ($\bar{Q}$) and mean resistance ($\bar{R}$). It is expected that safety factors calibrated for drag-dominated wave loads will be conservative for inertia-dominated load [29]. Equation 2.22 shows the ratio expressed as lognormal distribution. If the coefficients of variation of resistance (v_r) and load (v_q) are less than 30 %, the safety index can be calculated by [89],

$$\beta = \text{Ln}\,(\bar{R}/\bar{Q})/\sqrt{v_r^2 + v_q^2} \tag{2.22}$$

where, $\bar{R}$ = mean resistance, $\bar{Q}$ = mean load, v_r = COV of resistance v_q = COV of load.

2.7.3.2 First Order Reliability Method (FORM)

FORM reliability method has been used for reliability analysis of Jackets by many researchers [36, 40, 42]. This is the most significant tool available to find reliability index and widely being followed nowadays to find reliability. The FORM solution provides geometrical interpretation of reliability index as the distance between origin and design point in standard normal space [32]. The first step is to transform the basic variables which may not be normally distributed into the space of standard normal variables. Thus, it is transformation of limit state surface from given space of basic variables to a corresponding limit state surface in standard normal space. Design point is the point on limit state surface which is nearest to origin and is found by optimisation process. This is taken as the most likely failure point. Here, limit state surface in standard normal space is approximated by a tangent plane at the design point.

2.7.3.3 Simulation Techniques Like Monte Carlo Simulation (MCS)

Monte Carlo simulation is another method used to find probability of failure and reliability index. This is an alternative or complementary tool for estimation of probability of failure [32]. Rubinstein in 1981 was the pioneer of Monte Carlo simulation method. It generates large number of random variable (x) samples through the use of random number generator. If the limit state function is implicit, the computation requires large number of simulations for exact function evaluation. Accuracy in this technique depends on number of simulations [97]. The sample values of random variables generated are extremely large and number of failures is counted. Thus, capacity of computer required to do the analysis is used to be high. The probability of failure can be evaluated by Monte Carlo simulation as shown in Eq. (2.23),

$$P_f = \frac{N_f}{N} \tag{2.23}$$

where N_f = number of failures, N = total number of simulation. COV of failure probability (V_{pf}) can be evaluated by Eq. (2.24),

$$V_{pf} = \frac{1}{\sqrt{P_{f \times N}}} \tag{2.24}$$

However, there are few problems with this method. In this method, approximation of performance function is used to reduce the computational cost. Random sampling used in this method produces inaccuracy in the results [26]. It is because the random numbers generated by the random number generators, which are produced in clusters and not uniformly distributed over the whole design space, may repeat again. The other problem in this method is that estimated probability of failure depends on sample numbers used for simulation. Therefore, if lower order failure probabilities are required, the sample numbers needed are higher which increases the cost of computation [26].

2.8 Component Reliability and Previous Work

Component failure occurs due to formation of plastic hinge, member buckling, joint failure due to fatigue cracking or brittle fracture [103]. Component reliability for Jacket platforms has been determined by researchers such as [27, 38, 40, 42, 79, 104]. The work on component reliability has been done in many regions of world including GOM, North Sea, China, Mediterranean Sea and Gulf of Guinea. Failure probability of each component depends on the magnitude of the stresses and corresponding strengths. Strength of tubular component is function of mechanical properties of material, yield strength and dimensional properties. Only the uncertainties in yield strength are of major importance in governing the failure

probabilities of tubular legs and brace components [78]. This is due to the fact that leg members have low slenderness ratio. Failure is governed by yield stress and reliability of component can be increased by using steel with high mean yield strength [78]. Jacket design depends on elastic skeletal frame analysis. Distribution of stresses is found when it is subjected to design environmental loads.

Individual component stresses are evaluated to make sure that no elements fail against the governing criteria [105]. This type of failure is related to stresses which are produced in members like compression (buckling local or global), bending due to yielding of material and hydrostatic. PAFA reports that gravity load dominates the leg members but environmental load dominates the design of brace members [106]. For buckling, governing design condition is in place extreme environmental condition. This condition is valid for majority of structural components in offshore platforms. Most frequent components found in Jacket platform are tubular members under combined compression and bending with ratio of compression to bending stresses being generally high [107].

2.8.1 Component Reliability Index-critical Review

Codes of practice for Jacket design, API WSD and ISO 19902 are both component and joint-based design codes. Component reliability for Jacket platforms in North Sea was made for ISO code development by BOMEL [42]. Environmental load factor for extreme conditions achieved for North Sea was 1.25. For consistency with GOM calibration, environmental load factor of 1.35 was retained for ISO code. Environmental load factor for component proposed for Mediterranean Sea is 1.30 [38]. Therefore, it is high time to evaluate the load factor for offshore Malaysia.

2.9 Resistance Factor

Resistance of tubular members is multiplied by resistance factor which represents the uncertainty related to prediction of failure mechanism [108]. Resistance factor depends on type of resistance, i.e. tension and bending can be predicted more accurately as compared to column buckling. Therefore, ISO resistance factor for tension and bending is 1.05 but for compression it is 1.18.

2.10 Joint Reliability and Previous Work

Joint reliability has been determined by researchers such as in GOM, North Sea, China, Mediterranean Sea and Gulf of Guinea [38, 40, 42, 109–111]. For Jackets, the joints are connected by primary members called chords usually with larger diameter

compared to secondary members called braces. In tubular Jacket frame, intersections between main members (chord) and secondary members (brace) are welded together and are called tubular joints [112]. Chord and brace members undergo combined stresses. This is due to hydrostatic pressure and bending moment which arise due to wave and current forces and from load distribution at the nodal points [5]. Joints are the most critical part of truss structure like Jacket. The work on modelling of joint stresses is still very active. With respect to API code, 21st edition published in 2000, the errata published in API 2008 contain many changes in joint design equations.

Out of all three types of joints K, T/Y and X, the X-type is the most preferred one due to its ductile nature. Capacity and redundancy for ductile redistribution of stresses for an X-braced joint contributes to the reserve strength of structural system which may not be the case for K-Joints. X Joint imparts significant ductility, mobilises alternative load paths and gives high frame capacity. Thus, ductile behaviour of X braces at failure and brittle behaviour of K-braced frames suggest that different acceptance criteria may be appropriate for redistribution of forces for structural system [105]. That is, the reason that X-braced frames are more in new Jackets as compared to old Jackets.

2.10.1 Joint Reliability Index-critical Review

Joint reliability for Jacket platforms has been done for ISO code development by BOMEL. Joint environmental load factor for extreme conditions achieved for North Sea is 1.25 [42]. For consistency with GOM, load factor of 1.35 is retained in ISO code. In Mediterranean Sea, joint environmental load factor proposed is 1.20 [38].

2.11 Reliability and Environmental Load Factor

Bilal [9] reports that primary factors affecting the evaluation of load factor are characterisation of failure modes (limit states), assessing implicit reliability levels in existing design code, i.e. API WSD and assigning the target reliability. Target reliability selection depends on calibration of existing code by judgement. Calibration is process of finding reliability levels in components and joints designed using API WSD code [9]. The safety factor in working stress design is evaluated arbitrarily using experience and judgement of designers. Loads are factored on the basis of load uncertainties, i.e. the environmental loads have larger safety factor as compared to gravity loads [108]. The design load action is found from characteristic load multiplied by a load coefficient γ. Characteristic loads are same for ultimate and serviceability limit states and only their load coefficients differ. Serviceability limit state takes γ_w value as 1.0 while for ultimate limit state, ISO and API takes γ_w as 1.35 for environmental loads [33]. In structural engineering, useful function of reliability analysis has been precise in the development of

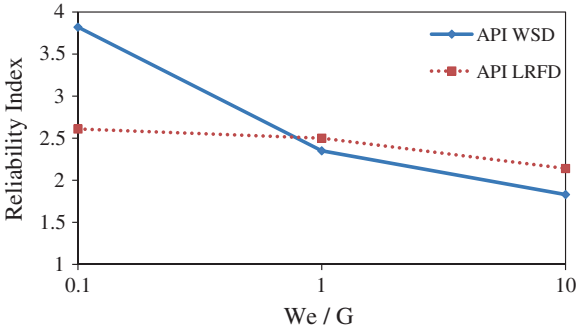

Fig. 2.7 Variation of We/G ratio with reliability index for axial tension [7]

structural codes where the end product has been an optimised set of partial factors [78]. In load and resistance factor design, uncertainties are considered objectively by performing reliability analysis taking characteristic values of statistical variables. The environmental load factor can be decided by using target reliability as shown in Fig. 2.7. Here target reliability is shown by API WSD and ISO gives us the reliability of new code. The new code reliability index at We/G ratio of 1.0 gives higher reliability as compared to API WSD. This higher reliability will give us the required load factor, as this will contain higher reliability than API WSD which has already proved its robustness.

The safety index for LRFD was lower for low environmental to gravity loads ratios and higher for high environmental to gravity load ratios [88]. Theophanatos has proposed environmental load factors for Mediterranean Sea using variation of Reliability Index with Varying W_e/G [38].

2.11.1 Code Calibration

There are various methods used for code calibration such as judgement, fitting, optimisation, or combination of these. Code calibration for ISO is a method to determine the target reliability by decision making or optimisation of the load factors or resistance factors [113]. Optimisation process is used when it is to be enforced for common level of specific designed structures to that particular target reliability. The target reliability should be selected so that structures designed as per the design codes are homogeneous and independent of material and loading (operational and extreme) conditions [87].

2.12 Nonlinear Collapse Analysis

Progressive collapse is a feature of structural system rather than of an individual component. Structural codes specified element design, without giving consideration to assembly of multi-element structures, till “Ronan Point” disaster in 1968.

Structural collapse brought the consideration of problem of progressive collapse commonly referred as “domino effect” [98]. For ultimate limit state, during linear elastic analysis, strength of structure is considered up to first yield. Due to residual stresses, local yielding may occur for loading less than ultimate limit state condition [114]. Ductility of steel makes it possible to redistribute the stresses which make it possible to face some yielding. Structural failure can be explained as full development of yield mechanism. Soreide reports that nonlinear collapse analysis of maximum load criteria simulates the real behaviour of structure during collapse [114]. The allowable stresses are not taken as they used to be in linear elastic analysis but a ratio of design load to collapse strength of structure is evaluated. The work on nonlinear collapse analysis for Jacket platforms has been conducted by [89, 114–117]. This is currently most popular method of analysis for structural system strength in the presence of extreme loads. Chakrabarti reports that for a Jacket with nonlinear analysis will always give near to or lower than the collapse load compared to linear elastic analysis [114]. Structural Analysis and Computer Systems (SACS) software is used for Jacket analysis in this book. SACS uses its collapse analysis module for nonlinear analysis of Jacket.

2.13 System Reliability and Reserve Strength Ratio (RSR)

System reliability of Jackets in North Sea and GOM has been studied by many researchers [70, 117–119]. The comparison of system and component reliability provides a measure of effect of redundancy in reliability index [79]. For system reliability assessment, it is important to evaluate the likelihood of system failure following first component failure [46]. Structural system reliability has been defined as series and parallel. It is a complex approach for evaluating the system strength in case of nonlinear analytical behaviour. An approximate method has been proposed for Jacket system analysis in North Sea [82]. The structure’s model is developed directly as a system and nonlinear analysis and failure modes are evaluated directly [89]. It is important for economic exploitation of hydrocarbon reserves, from new and old Jackets to understand and realistically predict the ultimate response of the Jacket [105]. One clear progress from elastic design to inelastic design is considered to be evolution towards more efficient steel structure design by using system strength evaluation [115]. Failure of a structure is said to be global collapse, i.e. load exceeding the ultimate capacity of the Jacket [120]. System reliability starts with a single member failure but it causes the failure of whole structure. Reliability of Jacket platform depends on performance of components but it is governed by structural system [7]. Reliability of system is a product of individual member reliabilities. System reliability is taken higher than component reliability or system probability of failure is taken lower as compared to component probability of failure [121]. The uncertainties in the Jacket loading model are assumed due to wave height for system reliability. The wave period and current speed are taken as deterministic functions of the wave height [73].

If the Jacket has survived the extreme wave loading without any damage, the uncertainty about the strength should be updated and reduced [70]. This will be checked during application of Bayesian updating. The preloading of Jacket at a load level with probability of exceedance of 10^{-5} or less will prove the safety of platform against similar loading conditions if ever to arise. It is very essential to develop a methodology for optimisation of loads and resistance. RSR is the ratio of maximum tolerable load as per nonlinear analysis and characteristic design load. The RSR should be determined in all directions and the lowest RSR should be taken as Jacket's RSR [114]. Out of all directions, minimum RSR is used to find the reliability as ISO code is looking for optimised Jacket. The most important RSR value is the lowest, which is related to the weakest direction or extreme environmental loading [82]. Graff and BOMEL have given the methodology for finding RSR by considering structural system [82, 122] using North Sea Jacket platforms. RSR against different We/G ratios for North Sea platform has been calibrated previously [82]. With increasing We/G values, RSR is decreasing and high load factor gives high RSR values.

2.13.1 Previous Work on System Reliability and Load Factors

The environmental load factor for North Sea has been proposed by BOMEL by use of system reliability [82]. System environmental load factor of 1.25 is achieved for North Sea Jackets. The environmental load factor of 1.35 is suggested due to consistency with GOM. The target probability of failure is set as 3×10^{-5} proposed by Efthymiou [82] for system reliability as reported by BOMEL. Environmental load factor adopted by ISO are evaluated based on the probability of failure of 3×10^{-5} [82]. The reliability index lies in range of 2.5–5.0, which is higher than component reliability index, i.e. 2.5–3.5 of these platforms as suggested also by Moan [121]. The reliability index against load factor is evaluated for platforms in North Sea for three We/G ratios [82]. The load factor selected here is 1.25 by using notional target reliability of 4.0. Load factor is determined at the point where We/G line crosses the target reliability. This is due to the reason that the target reliability is the required safety level. Therefore, once this is achieved, the load factor will be considered as safe as per the new code.

2.13.2 System-based Environmental Load Factor-Critical Review

During design phase, the lead time is so small that actual site-specific data on environmental load and material are not available with design engineer. Therefore,

once Jacket is installed, its probability of failure is evaluated. The API and ISO codes require that system strength should be checked against environmental load of 10,000 years return period. Jacket platforms are designed using component and joint reliability. Environmental load factor for system only shows the redundancy of Jacket, and it is not used during design of Jacket. System-based environmental load factor for Jacket has been evaluated by BOMEL [82]. System strength is evaluated by using collapse analysis of Jacket, base shear, wave and current loads. System environmental load factor shows the redundancy available in Jacket.

2.14 Assessment of Jacket

ISO and API codes require that Jacket should be assessed and monitored for any damages throughout its life. Before Jacket reaches the end of its design life, it is assessed whether it can withstand a load of 10,000-year wave return period as per the guidelines of ISO and API. This is a very important step before extension of service life is decided for Jacket. The cost of new Jacket design, fabrication and installation is quite huge. Thus, extension of life of Jacket will save a lot of money for the operator.

2.14.1 Bayesian Updating and Probability of Failure

Reassessment of Jacket platforms requires that platform must sustain a load of 10,000 years. Jacket failure due to structural design flaw was 10 % of all accidents in offshore industry worldwide [123]. Jacket platforms are designed with limited data available during design phase. This leads to uncertainty for future loads and resistances. The mathematical modelling of the structural design also becomes uncertain in the presence of random uncertainty of load and resistance. The information gathered after the installation of Jacket is used to extrapolate the extreme environmental event for wave height, wind and current speed. This is where probabilistic design comes into account. Codes of practice for Jacket platforms recommend notional failure probability to assess the effects of variable loads or strength problems. The updating of probability of failure with additional information collected on material and load can be used in many engineering applications. There could be variations in loading pattern or material problems arising due to severe environmental weather effects from ocean environment after certain time of existence of Jacket under water. It can be due to change of loading pattern, subsidence of Jacket, development of cracks, degradation due to fatigue or any other reason such as marine growth [114]. These observations at site can be used to update the probability of failure of Jacket by using the Bayesian method of updating. This will give us foresight about the ductile strength of the Jacket. Frieze et al. [79] used it for updating RSR for finding bias in push over analysis.

Bayes' theorem is used in cases when combined knowledge of statistical and judgmental information is available for updating probabilities through observed outcomes [124]. This theorem calculates the probability of occurrence of event "A", which depends on other mutually exclusive and collectively exhaustive event "B", given that event "B" has already occurred [125]. When additional information has become available about an existing Jacket, the knowledge implicit in that information may be used to improve the prior estimate of structural probability of failure [43]. Assessment of existing structure becomes real when damages are observed, use of platform is expected to be changed, deviations from project descriptions are observed, the lifetime is up to extension beyond what is planned and inspection schedules are planned to be revised [126]. Bayesian updating procedures allow the updating of probability for modelling uncertainty parameters and structural global response [127]. Bays theorem uses rational approach for incorporating the prior information or judgment into prediction of future behaviour of structures [128].

Bay's updating is calculated using Monte Carlo simulation. The updating probability of failure for Jacket platforms in North Sea has also been done [114]. Here, the updated probability of failure decreases with increasing of wave height. This is due to the reason that updating depends on both probability of failure and probability of survival results.

2.14.2 Damaged Structural Members

ISO 19902 clearly allows for existing Jackets to be accepted, with limited damage to individual components, provided that reserve strength against overall system failure and deformation remain acceptable [85]. Nonlinear collapse analysis approach is used by removing Jacket members and collapse capacity of damaged members is evaluated by Eq. (2.25) [116]. In this book, minimum RSR values are looked into along with Bayesian updating of probability of failure are discussed in Chap. 10.

$$\text{Damaged Strength Ratio} = \frac{\text{Design load}}{\text{Ultimate collapse capacity}} \tag{2.25}$$

2.14.3 Critical Review of Updating of Probability of Failure

The updating of probability of failure using Bayesian approach has been recommended by [15, 43, 129]. Updating of probability of failure using Bayesian technique has been adopted for Jacket platforms in Norway, for Jacket platform, this is used by [70, 102, 117–119]. This method can be used when the design life approaches its end and Jacket is required to be re-evaluated for its strength and extension of Jacket design life.

2.15 Summary

The critical analysis of this chapter shows that this topic is extremely important for the hydrocarbon industry of offshore Malaysia. If economics are to be considered as primary importance then this book will play some role in future developments of Jacket platform design in offshore Malaysia. The uncertainty models for resistance have never been evaluated in this region. The importance of reliability-based environmental load factor for component, joint and system shows that it should be evaluated. The updating of probability of failure also shows its importance with regard to extension of life of Jackets in Malaysia and for some cases like damaged members. For South China Sea, its use has not been reported in the literature.

References

1. Shell: Sarawak-Shell, design of fixed offshore structures (10.1) (2005)
2. PTS: PETRONAS Technical Standard, ed. PETRONAS, Malaysia (2010)
3. Ellingwood, B.R.: LRFD: implementing structural reliability in professional practice. Eng. Struct. **22**(2), 106–115 (2000)
4. Birades, M., Cornell, C.A., Ledoigt, B.: Load factor calibration for the gulf of guinea adaptation of APIRP2A-LRFD. In: Behaviour of Offshore Structures, London (2003)
5. AME: Buckling of offshore structures: assessment of code limitations', Offshore Technology Report, OTO 97049 (Advance mechanics & engineering), Health Safety Executive, UK (1997)
6. Galambos, T.V.: Load factor design of steel buildings. AISC Eng. J. (1972)
7. Ferguson, M.C.: A Comparative Study Using API RP2A-LRFD. Presented at the offshore technology conference, OTC 6308, Houston (1990)
8. Brand, P.R., Whitney, W.S., Lewis, D.B.: Load and resistance factor design case histories. presented at the offshore technology conference, OTC, 7937, Houston (1995)
9. Bilal, M.A.: Development of Reliability-Based Load and Resistance Factor Design (LRFD) Methods for Piping. ASME, New York (2007)
10. Madsen, H.O.: Integrity and Reliability of Offshore Structures. Veritas Research, Norway (1987)
11. Mangiavacchi, A., Rodenbusch, G., Radford, A., Wisch, D.: API offshore structures standards: RP 2A and much more. Presented at the offshore technology conference, OTC, 17697, Houston (2005)
12. Duan, Z.D., Zhou, D.C., Ou, J.P.: Calibration of LRFD format for steel jacket offshore platform in China offshore area (1): statistical parameters of load and resistances. China Ocean Eng. **20**(1), 1–14 (2005)
13. Raaij, K.V.: Dynamic behaviour of Jackets exposed to wave-in-deck forces, Doctor of Philosophy (DR. ING.), Department of Mechanical & Structural Engineering & Materials Science, University of Stavanger, Norway (2005)
14. Guenard, Y.F.: Application of structural system reliability analysis to offshore structures, Doctor of Philosophy, Civil Engineering, Stanford University (1984)
15. Ang, A.H., Tang, W.H.: Probability Concepts in Engineering, vol. 1. Wiley, New York (2007)
16. Moses, F.: Application of reliability to formulation of fixed offshore design codes. Presented at the marine structural reliability symposium (1995)

17. Choi, S.K., Grandhi, R.V., Canfield, R.A.: Reliability-Based Structural Design. Springer, London (2007)
18. French, S., Seeto, J., Dominish, P.G.: Structural integrity assessment and life extension of platforms in Australia and Southeast Asia. Presented at the BOSS (1992)
19. Wisch, D.J.: Fixed steel offshore structure design-past, present and future. In: Offshore Technologi Conference, OTC, 8822, Houston (1998)
20. Aagaard, P.M., Besse, C.P.: A review of the offshore environment-25 years of progress. J. Pet. Technol. **25**, 1355–1360 (1973). Society of Petroleum Engineering
21. Baecher, G.B., Christian, J.T.: Reliability and Statistics in Geotechnical Engineering. Wiley, New York (2003)
22. Wisch DJ: API offshore structures standards: changing times. Presented at the offshore technology conference, OTC 19606, Houston (2008)
23. Thomas, R., Wartelle, R., Griff, C.L.: Fixed platform design for South East Asia, Society of Petroleum Engineering (1976)
24. Bilal, M.A., Haldar, A.: Practical structural reliability techniques. J. Struct. Eng. **110**(8), 1707–1724 (1984)
25. Marley, M., Etterdal, B, Grigorian, H: Structural Reliability Assessment of Ekofisk Jacket Under Extreme Loading. Presented at the Offshore Technology Conference, OTC 13190, Houston (2001)
26. Phani, R.A.: Robust estimation of reliability in the presence of multiple failure modes, Doctor of Philosophy, Mechanical and Materials Engineering, Wright State University (2006)
27. Guenard,Y., Goyet, J., Remy, B., Labeyrie, J.: Structural Safety Evaluation of Steel Jacket Platforms. Presented at the marine structural reliability symposium, Virgenia (1987)
28. Anthony, P.P., Paul, K.Y., Paul, R.C.: Effect of Design, Fabrication and Installation on the Structural Reliability of Offshore Platforms. Presented at the Offshore Technology Conference, OTC 3026, Houston (1977)
29. Moses, F.: Reliability Based Design of Offshore Structures. Presented at the American Petroleum Institute (1981)
30. Chakrabarty, B., Bhar, A.: Sensitivity Analysis in Structural Reliability of Marine Structures. Presented at the 3rd international ASRANet Colloquium, Glasgow, UK (2006)
31. ENERGO: Reliability vs. consequences of failure for API RP 2A fixed platforms using API bulletin 2INT-MET (2009)
32. DNV: Classification note 30.6 structural reliability analysis of marine structures (1992)
33. Holland, I.: Norwegian regulations for design of offshore structures. Presented at the offshore technology conference, OTC 2863 (1977)
34. Frieze, P.A., Hsu, T.M., Loh, J.T., Lotsberg: Back ground to draft ISO provisions on intact and damaged members, BOSS (1997)
35. Shama, M.A.: Marine structural safety and economy. Presented at the society of naval architecture and marine engineers, USA (1991)
36. Hassan, Z.: Calibration of deterministic parameters for reassessment of offshore platforms in the Arabian Gulf using reliability based methods, Doctor of Philosophy, Mechanical engineering University of Western Australia (2008)
37. Gulvanessian, H., Calgaro, J.A., Holicky, M.: Designers' Guide to EN 1990 Eurocode: Basis of Structural Design. Thomas Telford, UK (2002)
38. Theophanatos, A, Cazzulo, R., Berranger, I., Ornaghi, L., Wittengerg, L.: Adaptation of API RP2A-LRFD to the Mediterranean Sea. Presented at the Offshore Technology Conference, OTC 6932, Houston (1992)
39. JCSS: Joint Committee on Structural Safety (JCSS) Model Code (2001)
40. Moses, F., Stahl, B.: Calibration issues in development of ISO standards for fixed steel offshore structures. J. OMAE Trans. ASME **122**(1), 52–56 (2000)
41. Hess, P.E., Bruchman, D, Assakkaf, I.A., Ayyub, B.M.: Uncertainties in Material Strength, Geometric and Load Variables. Presented at the American Society of Naval Engineers (2002)

42. BOMEL: Component Based Calibration of North Western European Annex Environmental Load Factors for the ISO Fixed Steel Offshore Structures Code 19902 (2003)
43. Melchers, R.E.: Structural Reliability Analysis and Prediction, 2nd edn. Wiley, New York (2002)
44. Ellingwood, B.R.: Probability-based codified design: past accomplishments and future challenges. Struct. Saf. **13**(3), 159–176 (1994)
45. Billington, C.J., Tebbett, I.F.: The basis for new design formula of grouted jacket to pile connections. Presented at the offshore technology conference, OTC3788, Houston (1980)
46. ISO-2394: General Principles on reliability for structures, ISO-2394. In: ISO (1998)
47. DNV: Design of offshore steel structures, general (LRFD) method. In: DNV-OS-C101 (2008)
48. BOMEL: Comparison of tubular member strength provisions in codes and standards (2001)
49. Elms, D.: Safety Concepts and Risk Management, Structural Safety and its Quality Assurance: ASCE (2005)
50. Kunda, J.: Load Modelling, Structural Safety and its Quality Assurance, ASCE (2005)
51. Sorensen, J.D., Sterndorff, M. J.: Stochastic model for loads on offshore structures from wave, wind, current and water elevation. Presented at the structural safety and reliability (2001)
52. Petrauskas, C., Aagaard, P.M.: Extrapolation of historical storm data for estimating design-wave heights. In: Society of Petroleum Engineers (1971)
53. Bitner-Gregersen, E.M., Cramer, E.H.: Uncertainties of load characteristics and fatigue damage of ships structures. Mar. Struct. **8**(2), 97–117 (1995)
54. Chakrabarti, S.K.: Hydrodynamics of Offshore Structures. WIT Press, UK (1987)
55. Tromans, P.S., Forristall, G.Z.: What is appropriate wind gust averaging period for extreme force calculations? Presented at the offshore technology conference, OTC 8908, Houston (1998)
56. Thomas, G.A.N., Snell, R.O.: Application of API RP2A-LRFD to a North Sea platform structure. In: Offshore Technology Conference OTC 6931, Houston (1992)
57. Graff, J.W., Tromans, P.S., Efthymiou, M.: The reliability of offshore structures and its dependence on design code and environment. Presented at the offshore technology conference, OTC 7382, Houston (1994)
58. Tromans, P.: Extreme Environmental Load Statistics in UK waters (2001)
59. Driver, D.B., Borgman, L.E., Bole, J.B.: Typhoon wind, wave and current directionality in the South China Sea. Presented at the offshore technology conference, OTC 7416, Houston (1994)
60. Turkstra, C.J.: Design Load Combination Factors, Structural Safety Series (1985)
61. Bury, K.: Statistical Distributions in Engineering. University of Cambridge, Cambridge (1999)
62. Tromans, P.S., Vanderschuren, L.: Response Based design conditions in the North Sea: application of a new method. Presented at the offshore technology conference, OTC 7683, Houston (1995)
63. API: American Petroleum Institute RP2A (WSD) (2008)
64. Wen, Y.K., Banaon, H.: Development of environmental combination design criteria for fixed platforms in the Gulf of Mexico. Presented at the offshore technology conference, OTC6540, Houston (1991)
65. Grant, C.K., Dyer, R.C., Leggett, I.M.: Development of a new metocean design basis for the NW shelf of Europe. Presented at the offshore technology conference, OTC 7685, Houston (1995)
66. Jahns, H.O., Wheeler, J.D.: Long-Term Wave Probabilities Based on Hindcasting of Severe Storms. Presented at the Society of Petroleum Engineers 3934 (1973)
67. Surrey: A review of reliability considerations for fixed offshore platforms, Surrey University, Offshore Technology Report-OTO 2000 037, Health and Safety Executive, UK, Offshore Technology Report-OTO 2000 037, Health and Safety Executive, UK (2000)

68. Heideman, J.C., Hagen, O., Cooper, C., Dahl, F.E.: Joint probability of extreme waves and currents on Norwegian Shelf. J. Waterw. Port Coast. Ocean Eng. **115**, 534–546 (1989)
69. Dawson, T.H.: Offshore Structural Engineering. Prentice-Hall Inc, New Jersey (1993)
70. Gerhard, E., Sorensen, J.D., Langen, I.: Updating of structural failure probability based on experienced wave loading. Presented at the international offshore and polar engineering conference, Honolulu, Hawaii, USA (2003)
71. Gudmestad, O.T., Moe, G.: Hydrodynamic coefficients for calculation of hydrodynamic loads on offshore truss structures. Mar. Struct. **9**(8), 745–758 (1996)
72. Gierlinski, J.T., Yarmier, E.: Integrity of fixed offshore structures: a case study using RASOS software. In: 12th international conference on offshore mechanics and arctic engineering (OMAE), Glasgow (1993)
73. Sigurdsson, G.,Skallerud, B., Skjong, R., Amdahl, J.: Probabilistic collapse analysis of Jackets. Presented at the OMAE, Houston (1994)
74. Petrauskas, C., Botelho, D.L.R., Krieger, W.F., Griffin, J.J.: A Reliability Model for Offshore Platforms and its Application to ST151"H" & "K" Platforms During Hurricane Andrew (1992)
75. Fugro: Wind and wave frequency distributions for sites around the British Isles, (Fugro-GEOS) Offshore Technology Report 2001/030, Health and Safety Executive, UK (2001)
76. Johannessen, K., Meling, T.S., Haver, S.: Joint distribution for wind and waves in the northern north sea. Int. J. Offshore Polar Eng. **12**(1), 1–8 (2002)
77. Bea, R.: Selection of environmental criteria for offshore platform design. J. Petrol. Technol. SPE **4452**(26), 1–206 (1974)
78. Baker, M.J., Ramachandran, K.: Reliability analysis as a tool in the design of fixed offshore platforms. The Integrity of Offshore Structures. Proc. 2nd International Symposium, July 1981. Applied Science Publishers, Glasgow (1981)
79. Frieze, P.A., Morandi, A.C., Birkinshaw, M., Smith, D., Dixon, A.T.: Fixed and jack-up platforms: basis for reliability assessment. Mar. Struct. **10**(2), 263–284 (1997)
80. Renolds, B.F., Trench, D.J., Pinna, R.: On the relationship between platform topology, topside weight and structural reliability under storm overload. J. Constr. Steel Res. **63**(8), 1016–1023 (2007)
81. Stahl, B., Aune, S., Gebara, J.M., Cornell, C.A.: Acceptance criteria for offshore platforms. J. Offshore Mech. Arct. Eng. **122**(3), 153–156 (1998)
82. BOMEL: System-based calibration of North West European annex environmental load factors for the ISO fixed steel offshore structures code 19902 (2003)
83. Efthymiou, M., Graaf, G.W., Tromans, P.S., Hines, I.M.: Reliability based criteria for fixed steel offshore platforms. J. Offshore Mech. Arct. Eng. OMAE **119**(2), 120–124 (1997)
84. Jin, W., Hu, Q., Shen, Z., Shi, Z.: Reliability-based load and resistance factors design for offshore Jacket platforms in the Bohai bay: calibration on target reliability index. China Ocean Eng. **23**(1), 15–26 (2009)
85. ISO19902: International Standard Organization 19902, (2007)
86. API: American Petroleum Institute RP2A LRFD (2003)
87. Zhou, D.C., Duan, Z.D., OU, J.P.: Calibration of LRFD for steel jacket offshore platform in china offshore area (2); load, resistance and load combination factors. China Ocean Eng. **20**(2), 199–212 (2006)
88. Lloyd, J.R., Karsan, D.I.: Development of a reliability-based alternative to API RP2A. Presented at the offshore technology conference, OTC 5882, Houston (1988)
89. Skallerud, B., Amdahl, J.: Nonlinear Analysis of Offshore Structures. Research Studies Press LTD, Baldock (2002)
90. Xiaoming, Y.: Reliability and Durability based Design Sensitivity Analysis and Optimization, Doctor of Philosophy, Mechanical Engineering, The University of Iowa (1996)
91. Nowak, A.S., Raymond, J.T.: Reliability-based design criteria for timber bridges in Ontario. Candian J. Civ. Eng. **13**(1), 1–7 (1986)
92. Moses, F., Larrabee, R.D.: Calibration of the draft RP2A-LRFD for fixed platforms. In: Offshore technology conference, OTC 5699 (1988)

93. Mattrand, C., Bourinet, J.M, Dubourg, V: A Review of Recent Features and Improvements Added to Ferum Software, Safety, Reliability and Risk of Structures, Infrastructures and Engineering Systems (2010)
94. Allen, M.T., Nowak, A.S., Bathurst, R.J.: Calibration to determine load and resistance factors for geotechnical and structural design, Transportation Research Board, Washington D.C (2005)
95. Gudmestad, O.T.: Challenges in requalification and rehabilitation of offshore platforms-on the experience and developments of a norwegian operator. J. Offshore Mech. Arct. Eng. **122**(1), 3–6 (1999)
96. Sigurdsson,G.: Guidelines for offshore structural reliability analysis: application to jacket platforms, DNV report no. 95–3203 (1996)
97. Chapter 5. Probabilistic design tools and applications [Online]
98. Furnes, O., Sele, A.: Offshore structures-implementation of reliability. In: Extreme Loads Response Symposium, Integrity of offshore structures, Society of Naval Architects and Marine Engineers (1982)
99. Efthymiou, M., Graham, C.G.: Environmental loading on fixed offshore platforms. Soc. Underwater Technol. **26**, 293–320 (1990)
100. Manuel, L., Schmucker, D.G., Cornell, C.A., Carballo, J.E.: A reliability-based design format for jacket platforms under wave loads. Mar. Struct. **11**(10), 413–428 (1998)
101. Eurocode: Euro Code 1 (1993)
102. Faber, M.H.: Basics of structural reliability (2002)
103. Gierlinski, J.T.: Reliability analysis system for offshore structures, *RASOS*: BOSS 92 (1992)
104. Onoufriou, T., Forbes, V.J.: Developments in structural system reliability assessments of fixed steel offshore platforms. Reliab. Eng. Syst. Saf. **71**(2), 189–199 (2001)
105. Bolt, H.M.: Results from large scale ultimate strength tests of K-braced jacket frame structures. Presented at the offshore technology conference, OTC 7783, Houston (1995)
106. PAFA: Implications for the assessment of existing fixed steel structures of proposed ISO 13819-2 member strength formulations, PAFA consulting engineers for Health Safety and Executive, UK (2000)
107. Johansen, N.J.T.: Partial safety factors and characteristics values for combined extreme wind and wave load effects. J. Solar Energy Eng. ASME **127**(2), 242–252 (2005)
108. Theophanatos, A., Wickham, A.H.S.: Modelling of environmental loading for adaptation of API RP 2A-Load and Resistance Factor Design in UK offshore structural design practice. In: Proceedings of Institution of Civil Engineers, pp. 195–204 (1993)
109. Turner, R.C.: Partial safety factor calibration for North Sea adaptation of API RP2A-LRFD. Presented at the Institution of Civil Engineers (1993)
110. Karsan, D.I., Marshall, P.W., Pecknold, D.A., Mohr, W.C., Bucknell, J.: The new API RP2A, 22nd edition tubular joint design practice. In: Offshore technology conference, OTC 17236, Houston, USA (2005)
111. Pecknold, D., Marshall, P.W., Bucknell, J.: New API RP2A tubular joint strength design provisions. In: Offshore technology conference, OTC 17310, Houston, USA (2005)
112. Thandavamoorthy, T.S.: Finite element modelling of the behaviour of internally ring stiffened T-Joints of offshore platforms. J. Offshore Mech. Arct. Eng. OMAE 131(4) (2002)
113. Rackwitz, R., Streicher, H.: Optimization and target reliabilities. Presented at the JCSS Workshop on Reliability Based Code Calibration, Zurich, Switzerland (2002)
114. Gerhard, E.: Assessment of existing offshore structures for life extension, Doctor of Philosophy, Department of Mechanical and Structural Engineering and Material Science, University of Stavanger, Stavanger, Norway (2005)
115. Hellan, Ø., Moan, T., Drange, S.O.: Use of nonlinear pushover analyses in ultimate limit state design and integrity assessment of Jacket structures. Presented at the Behaviour of Offshore Structures Conference, Massachusetts (1994)
116. Hellan, Ø.: Nonlinear Pushover and Cyclic Analysis in Ultimate Limit State Design and Reassessment of Tubular Steel Offshore Structures. Norwegian Institute of Technology, University in Trondheim, Norway (1995)

117. Dalane, J.I.: System reliability in design and maintenance of fixed offshore structures. Norwegian Institute of Technology, University in Trondheim, Norway (1993)
118. Bea, R.: Developments in the assessment and requalification of offshore platforms. Presented at the offshore technology conference, OTC 7138, Houston (1993)
119. DNV2018: Guidelines for Offshore Structural Reliability Analysis-General, appendix B (1995)
120. Mark, M., Birger, E., Henrik, G.: Structural reliability assessment of Ekofisk jacket under extreme loading. In: Offshore technology conference, OTC 13190, Houston (2001)
121. Moan, T.: Target Levels for Structural Reliability and Risk Analysis of Offshore Structures, Risk and Reliability in Marine Technology. AA Balkema, Rotterdam (1998)
122. Graaf, V.D., Efthymiou, J.W., Tromans, P.S.: Implied reliability levels for RP 2A-LRFD from studies of north sea platforms. Presented at the society for underwater technology international conference, London (1993)
123. Kvitrud, A., Ersdal, G., Leonardsen, R.L.: On the risk of structural failure on norwegian offshore installations. Presented at the proceedings of ISOPE 2001, 11th international offshore and polar engineering conference, Stavanger, Norway (2001)
124. Nowak, A.S., Collins, K.: Reliability of Structures, 2nd edn. CRC Press, Taylor & Francis Group, USA (2013)
125. Haldar, A.M.: Probability Reliability and Statistical Methods in Engineering Design. Wiley, New York (2000)
126. Ditlevsen, H.O.: Structural Reliability Methods. Wiley, New York (2007)
127. Fatemeh, J., Iervolino, L., Manfredi, G.: Structural modeling uncertainties and their influence on seismic assessment of existing RC structures. Struct. Saf. **32**(3), 220–228 (2010)
128. Enright, M., Frangopol, D.: Condition prediction of deteriorating concrete bridges using bayesian updating. J. Struct. Eng. **126**(10), 1118–1125 (1999)
129. Puskar, F.J., Ku, A.P., Sheppard, R.E.: Hurricane Lili's impact on fixed platforms and calibration of platform performance to API RP2A. Presented at the offshore technology conference, OTC 16802, Huston (2004)

Chapter 3
Research Applications

Abstract Probabilistic models are defined for uncertainty, variability and probability distribution functions. These depend on measured data and statistical procedures. After defining basic variables, which have influence on failure of components, joints and system, failure functions are defined for each one of these in the form of ultimate limit state equation. Finally, system strength is evaluated at design and extrapolated higher load.

3.1 Introduction

The reliability theory has evolved from the structural, aerospace and manufacturing industries. This approach considers uncertainty of load and resistance and uses judgement in dealing with the structural problems. It provides a way of quantifying those uncertainties and a way to handle them consistently [1]. There are four types of uncertainties in structural engineering, namely aleatory (inherent/physical randomness), epistemic (statistical/lack of knowledge), model-related and human error-based. The physical randomness is always present in our nature, such as wind, wave and current. This inherent randomness is most difficult to forecast. Epistemic uncertainty relates to small number of available data to analyse such as yield strength, diameter and thickness of member. This could be improved by the increase of data sets. Model uncertainties are due to our lack of understanding and simplification of the equation provided by codes for calculating the stresses/forces in the component. Human error uncertainty depends on knowledge of person designing, constructing and operating the Jacket.

The necessary tools for calibration of LRFD are statistics of random variable, i.e. mean value, standard deviation (SD) and distribution patterns [2]. We need data for analysis of statistical parameters and probability distribution patterns of material (resistance) and environmental load. Ultimate limit state is used where human life is involved. It also corresponds with maximum load carrying capacity [3]. First-order reliability method (FORM) is used to evaluate P_f, for component, joint and system. Environmental load factors γw are found so that the factored

Z. Nizamani, *Environmental Load Factors and System Strength Evaluation of Offshore Jacket Platforms*, Ocean Engineering & Oceanography 4,
DOI 10.1007/978-3-319-15051-2_3

load has a predetermined probability of being exceeded [4]. Bayesian updating is used to update probability of failure using Monte Carlo simulation with intact and damaged Jacket model.

3.2 Resistance Uncertainty for Jacket Platforms in Malaysia

The uncertainty in resistance variable plays a major part in safety, performance and structural behaviour of tubular members. These uncertainties can make variations in resistance that will lead ultimately to significant effect on the reliability analysis of Jacket platforms. The actual strength is always random in nature and it tends to show its behaviour in random way. To measure the uncertainty for reliability analysis, we need to define the basic variables involved in the limit state equation. These variables are defined by probability/cumulative density function along with other statistical properties such as mean bias, SD and COV. In this book, basic random variables are analysed first and their statistical parameters were determined. Then, the basic stresses using ISO 19902 code equations are simulated and their statistical parameters are determined. Once this random behaviour is understood, it makes the task of designer much easier due to reduced uncertainty of material. This book assumes that reliable models of uncertainty can be developed, using limited amount of data. These uncertainty models are used to find the reliability of components, joints and systems using ultimate strength limit state design.

For reassessment of existing platforms, we need to define the actual uncertainties of the material and environmental loads acting at the site. Material uncertainties may change after some time due to degradation of material especially from fatigue and corrosion environment, but here, this degradation is not considered. These uncertainties become most important if we want to find probability of failure for operational conditions. Finally, recommendations are made for the statistical characteristics of the random variables to be used for the reliability analysis for ultimate limit state design of Jacket platforms in offshore Malaysia.

3.2.1 Collection of Data for Resistance Parameters

The statistical data for resistance depend on material test report and field measurements at the ISO certified fabrication yard in Malaysia, and those data are used for statistical modelling. The collected data came from Jackets which are under construction at the yard. Field data collected include the geometrical parameters, i.e. diameter and thickness. The material properties depend on mill test reports for 6 Jacket platforms. The details of these platforms are provided in Table 3.1 covering all three regions of Malaysia.

Thickness of tubular members is obtained through direct measurement of tubular members available at the site and dimensional drawings available at the yard. Diameter

Table 3.1 Details of selected platforms for resistance uncertainty

Platform	Location	Height (m)	Fabrication year	No. of legs	Material source
A	PM	73.40	2009	4	Japan
B	PM	72.00	2009	4	Japan
C	PM	60.40	2007	4	Japan
D	Sarawak	56.70	2005	4	Japan
E	Sarawak	53.60	2008	4	Japan
F	Sabah	55.20	2009	3	Japan

variability is obtained using as-built drawings. Material strength variation is analysed from test reports available with the fabricator. Water depth of platforms varied between 53 and 74 m which is the representative water depth for Jacket platforms in Malaysia. All these platforms are designed and fabricated as per API RP2A WSD code 21st edition, which is the code used for finding the target reliability in this research. These platforms are three- and four-legged. The common platforms in this region have four, six and eight legs. The source material for these platforms is from Japan.

In total, 72 mill tests' results are used to measure the variability of material properties of tubular members. For geometric variability, 260 specimens are taken for leg diameter, 113 for brace diameter and 26 for thickness variation. Table 3.2 and Fig. 3.1 show the data available at fabrication yard for yield strength variability and diameter variability. Diameter is recorded at four diagonal places in tubular member and its average is used as measured value. Its design value is already mentioned in fabrication drawings. Thus, a bias of one member is recorded. All

Table 3.2 Variability of material properties as shown in as mill test report

Mechanical test		
Yield stress (MPa)	Tensile strength (MPa)	Elongation (%)
319	475	31
308	471	24
320	475	28
318	471	31
357	505	26

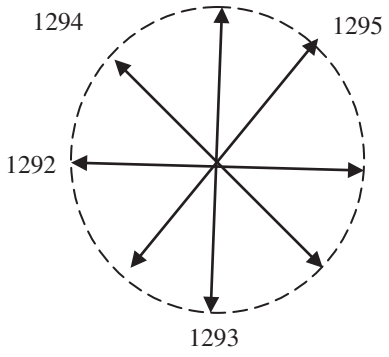

Fig. 3.1 Variability of diameter

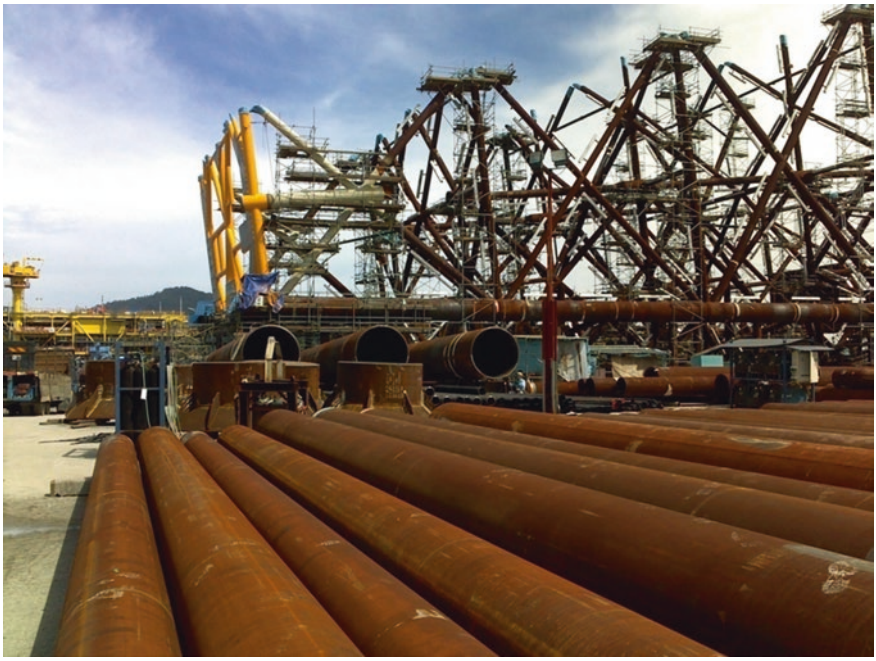

Fig. 3.2 Fabrication yard in Malaysia

bias values of diameter are then put in Easy Fit software to get the mean coefficient and variation coefficient. Figure 3.2 shows a Jacket under construction along with its components at the fabrication yard.

3.2.2 Statistical Analysis of Geometric and Material Variables

This uncertainty relates to the randomness due to geometrical and material variations. They come from diameter of leg and brace, thickness of leg and brace and yield strength. Though this type of uncertainty can be dealt with properly, with the application of quality control using international standards, still there remains some uncertainty. These are defined as errors which are covered by fabrication tolerance limit. These variations, between characteristic values mentioned on structural drawings and fabricated component, are due to geometric uncertainty. For instance in the case of diameter, there are four values measured at 90° angle from one another. The average of these four values are taken as measured mean and divided by the characteristic value. The characteristic value is mentioned on the structural drawings. The mean bias of diameter and thickness is calculated by Eq. (3.1),

$$\text{Mean bias} = \frac{\text{Measured (average)}}{\text{Nominal/mean}} \tag{3.1}$$

The benefit of this method is that mean bias of any diameter value can be ascertained easily. It is obtained by multiplying any nominal value of variable by its mean bias. The mean bias values are then statistically analysed, and respective distributions are reported for all variables. Tubular members are further divided into leg and brace members. Brace thickness increases as we go down towards mud level [5]. Joint angle is another variable to be used for joint reliability. COV shows the variability in the model. For reliability analysis on resistance model, we must be sure that 95 % values taken by the design engineer are higher than that value of actual resistance. Mill test reports are used to find the statistical properties of yield and tensile strength of the tubular members. As per ISO requirement, the ratio of yield to ultimate tensile strength is shown in Eq. (3.2) [6] which should be less than 0.85.

$$\frac{\text{Yield Strength}}{\text{Ultimate Tensile Strength}} = \frac{355}{490} = 0.724 < 0.85 \tag{3.2}$$

All variables are assumed to be independently distributed. The data are analysed by using three goodness-of-fit tests which are Kolmogrov–Smirnov, Anderson–Darling and chi-square tests, and the best fit is reported. The distribution types, bias and COV for materials found are used for the reliability analysis of component and joints.

3.2.2.1 Resistance Variables Taken from Previous Studies

There are three other resistance variable parameters, i.e. length (L) of tubular member, effective length factor (K) and Young's modulus (E). The mean bias and SDs and distribution types are shown in Table 3.3.

3.2.3 Component and Joint Stress Model Uncertainty

The ISO code equation is used for determining statistical modelling uncertainty of stresses as shown in Fig. 3.3. High amount of random data is produced using Monte Carlo Simulation. The uncertainty related to prediction of resistance model variability can be calculated using simulation techniques. Monte Carlo simulation

Table 3.3 Statistical parameters of random variables [7, 8]

Random variable parameters	Distribution	Mean bias	Standard deviation
Length (L)	Normal	1.0	0.0025
Effective length factor K (leg)	Normal	1.1	0.0935
Effective length factor K (brace)	Normal	0.875	0.097
Young's modulus of elasticity (E)	Normal	1.0	0.05

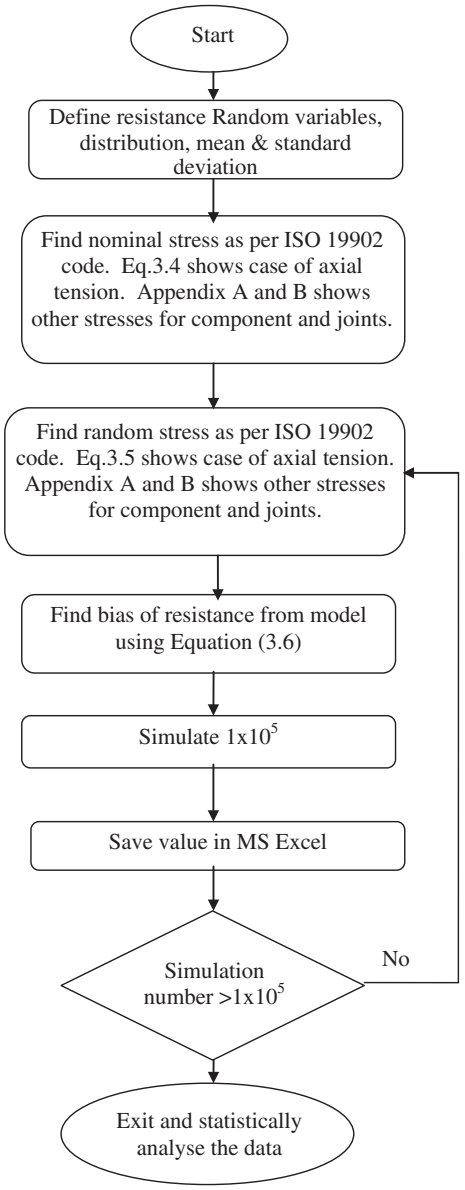

Fig. 3.3 Flow chart for determining resistance model uncertainty

is used to generate long simulated data by MATLAB code. In this case, data of 1×10^5 simulations are generated using statistical parameters of random variables, giving reliable outcome without any experiments. Data generated by this simulation are used to find distribution and its parameters. This type of simulation is used when resources are limited and experiments are not possible or extremely

difficult to do. The uncertainty variables as mentioned in Sect. 3.2.2 are used to find model uncertainty X_m for nine different stresses for components and four types of stresses for K-, T/Y- and X-joints for Jacket platforms.

3.2.3.1 Case Study: Axial Tension Model Uncertainty

In this book model, variability of axial tension stress using ISO code is explained. ISO axial tension stress can be found by Eq. (3.3),

$$\sigma_{\mathrm{t}} = f_t \times A \tag{3.3}$$

where σ_{t} = tensile stress, f_{t} = tensile strength, A = area of tubular member. Two main steps are used to find the simulated statistical parameters of the stress of components under axial tension as shown below:

1. Define the nominal values which are used by actual stress model, i.e. Fyn, Dn and Tn. Thus, in our first part, all input values used will be nominal and deterministic as shown in Eq. (3.4),

$$\sigma_{\mathrm{tn}} = f_{\mathrm{tn}} \times A_{\mathrm{n}} \tag{3.4}$$

   where σ_{tn} = nominal tensile stress, f_{tn} = nominal tensile strength, A_n = nominal area of tubular member

2. Define the variable values which are used by member or joint stress model, i.e. Fyi, Di and Ti. The biases of mean and SDs are defined as variables along with their probability distributions. Thus, Eq. (3.5) contains input variables containing distribution and its parameters. The output will also be variable, changing each time when analysed.

$$\sigma_{\mathrm{ti}} = f_{\mathrm{ti}} \times A_i \tag{3.5}$$

   where σ_{ti} = variable tensile stress, f_{ti} = variable tensile strength and A_i = variable area of tubular member. The limit state equation for resistance bias using Monte Carlo simulation is shown by Eq. (3.6)

$$\text{Resistance Bias} = \frac{\sigma_{\mathrm{tn}}}{\sigma_{\mathrm{ti}}} \tag{3.6}$$

σ_{tn} = nominal stress and σ_{ti} = varying stress
The resistance biases will change each time analysis is made due to variable denominator in Eq. (3.6) which gave mean bias of axial tension model stresses. Now there are 10^5 simulations which produced as many resistance values due to different variable strengths. These values are statistically analysed using Easy Fit software. The statistical parameters are taken using best model fit using statistical test result. This model stress uncertainty evaluation is done for nine component stresses and eleven joint stresses. The importance of model uncertainty variable can be seen from sensitivity study as shown in Table 7.4.

3.3 Load Uncertainty for Offshore Jacket Platforms in Malaysia

For load uncertainty, the random variables are wave, wind and current. The nature of environmental load is probabilistic, and we need to ascertain the randomness of the load. Two-parameter Weibull and Gumbel distributions are used for the analysis to find the best fit. The authentic available data are in shape of 1-, 10-, 50- and 100-year return periods. Parameters of distribution are determined first, which are used to find mean and SD. From this uncertainty, variables are extrapolated up to 10,000 years which is specified by ISO 19902 and API RP2A for extension of life of existing platforms. Finally, the data are compared with data from Gulf of Mexico (GOM), northern North Sea (NNS), southern North Sea (SNS) and central North Sea (CNS).

3.3.1 ISO and Metocean Criteria

Metocean design conditions are extremely important for the design of platform. ISO 19900-1 recommends three methods of considering the parameters for design [9]. For the North Sea, widely used method to obtain design wave height has involved fitting cumulative distributions to the significant wave heights of successive 3-h storm sea state. It is common to neglect both the correlation between consecutive sea states and uncertainty in the extreme environmental load. Through distributions, 100-year return period wave is estimated. Norwegian Petroleum Directorate (NPD) uses a combination of a wave along with annual probability of exceedance of 10^{-2} and current with an annual probability of exceedance of 10^{-1}. Research for waters outside Europe, USA and Australia proposes that considering joint probability for the environmental load parameters reduces the design loads on drag-dominated Jacket platforms by 10–40 % [9]. This book considers drag wave-dominated Jackets because that is the case for steel offshore Jackets for hydrocarbon drilling in Malaysia.

3.3.1.1 Method 1

In this method, 100-year return period wave height with associated wave period, wind and current speeds are taken into consideration. This is suitable for the Jackets where environmental action is dominated by waves. In this method, we need associated current with wave. ISO directs that this wave and current should be from same storm conditions, such types of data are not available till yet. This makes Method 1 not possible.

3.3.1.2 Method 2

In this method, 100-year wave height and wave period along with the 100-year wind speed and the 100-year current speed are taken into consideration. They should be evaluated by extrapolation of the individual environmental parameters considered independently. When joint probability information for environmental conditions is not available, a conservative estimate of environmental load can be found. Sum of 100-year environmental actions caused by independent extreme values of wind speed, wave height and period and current speed are used. This is using assumption that they act simultaneously and in the same direction. Environmental variables are estimated from return period of 100 years, using measured or hind cast time series extending over a period of 5-year record. The 100-year wind, wave and current maximum values are assumed to occur at the same time and in the same direction. For Jacket platform, this design load will be much more severe and extreme than the true 100-year load [9].

3.3.1.3 Method 3

Any combination of wave height, period, wind and current speed which results in: (a) the global extreme environmental action on the structure with a return period of 100 years, (b) a relevant global response of the structure which could be base shear or overturning moment with a return period of 100 years. This method uses associated current speed, wind speed, wave height and significant structural response effects. Directional effects of environmental load parameters and water depth variation from tide and surge are required to be considered.

Thus Method 3 is the preferred method by ISO 19901, but due to lack of appropriate data, this method could not be used. Since the correlation between wind, wave and current cannot be established due to lack of data, Method 2 is adopted.

3.3.2 Environmental Load Uncertainty Parameters

Three parameters of environmental load acting on Jacket platforms are considered here, i.e. significant wave height (Hs), wind speed and surface current speed in three regions of offshore Malaysia. Four platforms are taken for analysis representing three regions of Malaysia, i.e. one from Peninsular Malaysia (PMO), one from Sabah (SBO) and two from Sarawak (SKO1 and SKO2). To find the effect on load uncertainty, the data available for nearby platforms from same region are included in the analysis.

Table 3.4 Water depths ranges for platforms in Malaysia

Location	Water depth (m)	
	Minimum	Maximum
PMO	60.0	79.2
SBO	36.9	59.1
SKO	46.0	95.0

3.3.2.1 Climate

The load produced by extreme storm is important for the calculation of the design load for offshore Jacket platforms. The load is produced by combination of waves, currents and wind, though waves are generally the dominant factor [10]. The type of weather in offshore Malaysia is half-yearly. North-east (NE) monsoon from November to March months and half-year-long south-west (SW) monsoon from May to September, the months of October and April are counted as transitional intra-monsoon period. The direction of wind is north-east towards Peninsular Malaysia and north-east to north-west towards Sabah and Sarawak region in NE monsoon period. In SW monsoon, the wind direction is south–south-west. But NE monsoon is more extreme, i.e. wave height and wind speed are higher. Table 3.4 shows the water depth variations in the region which is quite large.

3.3.2.2 Design Wave

The South China Sea is the largest sea in the north-west Pacific. It connects to the outside seas through the straits of Taiwan, Luzon, Mindoru, Para Barke, Banka, Gaspar, Karimata and Malaka. This book considers only offshore Malaysia region. Significant wave height is the dominant metocean variable [11]. Present-day design methods depend on unidirectional or long-crested waves, where all energy comes from a single direction. Real sea waves are multidirectional where it is considered that energy comes from many directions simultaneously. The use of unidirectional waves is regarded as conservative factor in design [12]. The direction of wave is NE and NW from November to March monsoon period and S–SW from May to September monsoon period in this region [13]. Wave direction becomes unstable (without any clear prevailing direction) during transition period. The highest significant wave in deepwater South China Sea, during tropical cyclone, is reported as high as 9.5 m [13]. Table 3.5 shows the maximum wave height in three regions, the data are taken from four platforms which are used for reliability analysis. Wave heights used are the highest in their respective regions.

Table 3.6 shows the relationship between maximum wave height and significant wave height. Ratio lies in between 1.86 and 2.05. In GOM the ratio was 1.93, but ISO gave 1.76 with water depth of 300 m [14].

Table 3.5 Maximum and critical values of significant wave height

Location	Design wave (H_{max}) with return period of 100 years		Platform specific H_{max}
	Minimum (m)	Maximum (m)	(m)
PMO	4.6	10.9	10.9
SBO	2.3	7.7	7.7
SKO1	3.0	9.9	9.9
SKO2	4.7	11.7	11.7

Table 3.6 Ratio of H_{max} /H_s for platforms in offshore Malaysia and GOM

Area	H_s (m)	H_{max} (m)	H_{max}/H_s
PMO	5.3	10.9	2.05
SBO	4.3	7.7	1.79
SKO1	5.2	9.9	1.90
SKO2	6.3	11.7	1.86
GOM (300 m water depth)	14.6	25.8	1.76 (ISO)

Table 3.7 Current at surface level (maximum/critical directions)

Location	Current at surface with return period of 100 years		
	Minimum (m/s)	Maximum (m/s)	Platform specific (m/s)
PMO	0.68	1.50	1.47
SBO	0.66	2.23	0.94
SKO1	0.40	1.80	1.05
SKO2	0.40	1.80	1.2

3.3.2.3 Current

Stronger currents flow in December and in August near Peninsular Malaysia, but they are not as strong as they are near Sabah and Sarawak [13]. 1/7 power law is used to find current at different depths [10, 11]. Table 3.7 shows the comparison between three regions for minimum and maximum currents at critical directions. The current values used in this book are not highest from the given region, but those have not much effect on overall reliability as explained in Sect. 3.3.1.

3.3.2.4 Wind

In South China Sea, waves are mainly controlled by the wind field [13]. The wind speed is measured at 10 m above sea level. Strong sustained winds produce severe sea states and both wind and wave loads are high in the event of storm. In open sea

Table 3.8 Variation of wind speed in platform at specific locations

Location	3-s gust with 100-year return period	
	Minimum (m/s)	Maximum (m/s)
PMO	29	55
SBO	24	50
SKO1	22	50
SKO2	22	50

waters, the long-term variations of wind speed and sea elevation are highly correlated in the storm event [15]. Wind produces large drag forces on offshore Jacket platforms. Most often, the wind load does not dominate over the wave load in the extreme design conditions [16]. For the Jackets, the wind generates a little part, of the order of 10 %, of the sum of extreme load and ISO code reports that sustained wind speed should be used to compute the extreme global load for the design of Jacket [16]. ISO prefers 10-min mean for global design of the structure and 3-s gust for design of component. Table 3.8 shows the maximum values prevalent at the specific platforms.

3.3.3 Geographical Data for Environmental Load Parameters for Offshore Malaysia

There are 20 data sets from PMO region, 11 from SBO region and 22 from SKO region. Available data is in shape of 1, 10, 50 and 100 years. Here, 10- and 100-year data are taken for analysis. 10-year data are taken because it is more representative of operating conditions of Malaysia. 100-year data are taken as it was maximum processed data available which is required of ISO and API codes for Jacket design. This formed the basis for the statistical analysis of environmental load parameters.

3.3.4 Statistical Analysis of Environmental Load Parameters

Probability distribution for a random variable shows the uncertainty of the given variable. Many authors have taken extreme value distributions for the wind, wave and current parameters. For extreme conditions, Weibull and Gumbel distributions are the most important distributions as these can capture and predict well the rare tail end events. The reliability analysis results are sensitive to tail of probability distribution. Thus, choice of distribution type is always significant and resistance is most of time normally distributed [17]. The bias and COV of environmental loads in different regions of the world are shown in Table 3.9.

Table 3.9 Environmental load parameters (wind, wave and current) [2, 18, 19]

Region	BIAS	SD	COV
GOM	0.750	0.216	0.288
Central North Sea	0.861	0.192	0.222
Northern North Sea	0.877	0.165	0.188
NW Australia	0.780	0.257	0.33
China	0.827	0.142	0.172

3.3.4.1 Extrapolation of Wave, Wind and Current

Cumulative distribution functions for Weibull and Gumbel distribution are evaluated using the linear model. Two points are used for curve fitting for extrapolation. With two load parameters and their corresponding CDF values of distribution, a linear fit is made in Microsoft Excel. Using linear equation, along with CDF of 1,000 and 10,000 years, the corresponding values are determined for load parameter. For example, the linear fit for wave height of one platform at PMO is shown as $0.577\ x + 4.418$. In this text, x is the value of corresponding CDF values. This model is used to find the extrapolated value for wave heights, wind and current speed for 1,000- and 10,000-year return periods as will be shown in Chap. 5.

3.3.5 Weibull Distribution

In this text, extreme distribution of Type 2 Weibull distribution is used. This type is used when rare events are of interest.

3.3.5.1 Extrapolation of Significant Wave Height (Weibull Distribution): Case Study of PMO Platform

Linear extrapolation of Weibull distribution is used. The probability of exceedance and CDF values as per Weibull are shown in Table 3.10. For PMO metocean reports gave 10- and 100-year significant wave heights as 4.9 and 5.3 m, respectively. The linear equations for 10- and 100-year values are shown in Eqs. (3.7 and 3.8) [20].

$$\ln\left\{-\ln\left[1 - F\left(x_{(i)}\right)\right]\right\} = \ln - \{\ln(1 - 0.9)\} = 0.834 \tag{3.7}$$

$$\ln\left\{-\ln\left[1 - F\left(x_{(i)}\right)\right]\right\} = \ln - \{\ln(1 - 0.99)\} = 1.527 \tag{3.8}$$

Thus, 10- and 100-year values of wave height are plotted at vertical axis against CDF of 0.834 and 1.527 on horizontal axis. The trend line equation is plotted for these two values. Now with trend line equation and CDF of 1,000 and

Table 3.10 Cumulative distribution function (CDF)—Weibull distributions

Return period	Probability of exceedance	CDF—Weibull
10	$\left[1-\left(\frac{10}{100}\right)\right]=0.9$	0.834032
100	$\left[1-\left(\frac{1}{100}\right)\right]=0.09$	1.52718
1,000	$\left[1-\left(\frac{1}{1000}\right)\right]=0.999$	1.932645
10,000	$\left[1-\left(\frac{1}{10000}\right)\right]=0.9999$	2.2203

10,000 years available, the corresponding wave heights are extrapolated. The same method is adopted for wind and current extrapolation. The parameters of Weibull distributions are evaluated as below:

3.3.5.2 Weibull Shape Factor

The shape factor for Weibull distribution is evaluated for one case study here.

$$\begin{aligned}\text{Ln}(x) &= \text{Ln}\ (4.9) = 1.589\\ \text{CDF}\ (10-100) &= 0.834-1.527=-0.693\\ 1.589-\text{Ln}\ (5.3) &= -0.078\\ \text{Shape factor}\ (b) &= \frac{-0.693}{-0.078}=8.8\end{aligned}$$

3.3.5.3 Weibull Scale Factor

$$\begin{aligned}\text{Ln}(8.8) &= 2.17\\ 8.8\times 1.589 &= 14.0\\ 0.834-14 &= -13.20\\ -13.20/(-8.8) &= 1.49\\ \text{Scale factor}\ (a) &= \text{Exp}(1.49)=4.46\end{aligned}$$

3.3.5.4 Weibull Mean

Using these parameters mean value is evaluated as shown in Eq. (3.9), [21]

$$\text{Mean}\ (\mu)=a\times\Gamma\left(1+\frac{1}{b}\right) \tag{3.9}$$

where Γ = gamma function

$$1+\frac{1}{8.8}=1.11$$

Now Microsoft Excel gamma function is given by:

$$\text{Exp(Gamma Ln (1.11))} = 0.946$$
$$\text{Mean} = 4.46 \times 0.946 = 4.22$$

3.3.5.5 Weibull Standard Deviation

Now parameter of SD is found as shown in Eq. (3.10), [21]

$$\text{Standard deviation } (\sigma) = a\left[\Gamma\left(1+\frac{2}{b}\right) - \Gamma^2\left(1+\frac{1}{b}\right)\right]^{1/2} \tag{3.10}$$

$$1+\frac{2}{8.8} = 1.22$$
$$\text{Exp(Gamma Ln (1.22))} = 0.911$$
$$(0.946)^2 = 0.895$$
$$\text{Standard deviation} = 4.46 \times (0.911 - 0.895)^{0.5} = 0.57$$

3.3.6 Gumbel Distribution

3.3.6.1 Extrapolation of Significant Wave Height (Gumbel Distribution): Case Study of PMO Platform

For platforms in PMO region, 10- and 100-year significant wave heights as shown in metocean reports are 4.9 and 5.3 m. The probability of exceedance as per Gumbel is shown in Table 3.11. Linear model of Gumbel distribution is given for 10 and 100 years in Eqs. (3.11) and (3.12) [20].

$$-\ln\left\{-\ln\left[F\left(x_{(i)}\right)\right]\right\} = -\ln\{-[\ln(0.9)]\} = 2.25 \tag{3.11}$$

$$-\ln\left\{-\ln\left[F\left(x_{(i)}\right)\right]\right\} = -\ln\{-[\ln(0.99)]\} = 4.60 \tag{3.12}$$

Thus, 10- and 100-year values of wave height are plotted at vertical axis against CDF of 2.25 and 4.60 on horizontal axis. The trend line equation is

Table 3.11 Cumulative distribution function (CDF)—Gumbel distributions

Return period	Probability of exceedance	CDF—Gumbel
10	$\left[1-\left(\frac{10}{100}\right)\right] = 0.9$	2.250367
100	$\left[1-\left(\frac{1}{100}\right)\right] = 0.99$	4.600149
1,000	$\left[1-\left(\frac{1}{1000}\right)\right] = 0.999$	6.907255
10,000	$\left[1-\left(\frac{1}{10000}\right)\right] = 0.9999$	9.21029

plotted for these two values. Now with trend line equation and CDF of 1,000 and 10,000 years available, the corresponding wave heights are extrapolated. The same method is adopted for wind and current extrapolation using Gumbel extrapolation.

3.3.6.2 Gumbel Scale Parameter

$$2.25 - 4.6 = -2.349$$
$$4.9 - 5.3 = -0.4$$
$$\text{Scale factor}\,(d) = \frac{-2.349}{-0.4} = 5.87$$

3.3.6.3 Gumbel Location Parameter

$$5.87 \times 4.9 = 28.785$$
$$2.25 - 28.78 = -26.53$$
$$\text{Location factor}\,(c) = \frac{-26.53}{-5.87} = 4.52$$

3.3.6.4 Gumbel Mean

Using location and scale factors parameters, the mean is evaluated by using Eq. (3.13).

$$\begin{aligned} \text{Mean}\,(\mu) &= c + \left(\frac{0.57722}{d}\right) \\ \text{Mean}\,(\mu) &= 4.52 + \frac{0.57722}{5.87} = 4.62 \end{aligned} \tag{3.13}$$

3.3.6.5 Gumbel Standard Deviation

Using location and scale parameters, SD is found from Eq. (3.14).

$$\begin{aligned} \text{Standard Deviation}\ (\sigma) &= \frac{\pi}{d\sqrt{6}} \\ \text{Standard Deviation}\ (\sigma) &= \frac{\pi}{5.87\sqrt{6}} = 0.218 \end{aligned} \tag{3.14}$$

When both distributions are analysed, it is found that Gumbel gave higher mean values as shown in Chap. 4. Therefore, Weibull distribution is found to be best fit and thus selected.

Table 3.12 Weibull distribution parameters from three different regions

	Parameter	10 year	100 year	Scale	Shape
PMO	H_{max} (m/s)	9.6	10.8	8.33	5.89
	Tp (s)	10.3	10.8	9.73	14.62
	Current (m/s)	0.98	1.10	0.85	6.00
SBO	H_{max} (m/s)	6.8	7.7	5.86	5.58
	Tp (s)	10.6	11.0	18.71	10.14
	Current (m/s)	0.78	0.94	0.62	3.71
SKO1	H_{max} (m/s)	5.5	9.2	2.96	1.35
	Tp (s)	9.7	11	8.34	5.51
	Current (m/s)	0.96	1.05	0.86	7.73
SKO2	H_{max} (m/s)	10.4	11.7	9.03	5.89
	Tp (s)	10.9	11.4	10.33	15.46
	Current (m/s)	1.05	1.20	0.89	5.19

3.3.7 Environmental Load for SACS

Table 3.12 contains the platform-specific load parameters for selection of input values for finding the environmental load for component and joint reliability. Table 3.12 shows the basic values used for conversion into random input for load parameters in SACS. Using these values along with Weibull distribution, 50 random values are generated for wave, current and time period using MATLAB. These 50 random load values are used to get 50 stresses from SACS output file for each component and joint. The corresponding 50 component and joint output stresses are produced by SACS analysis using Morison equation. These are converted to load model using curve fit tool of MATLAB.

3.3.7.1 SACS Modelling of Jacket

To get environmental load effect for the reliability analysis, 50 stress values for wave, time period and current are found. For statistics of environmental load, it is necessary to make component and joint stresses dimensionless, which is acquired by dividing it by 100-year characteristic values [11]. Therefore, the output of applied stresses from SACS is normalised before being used for curve fitting tool of MATLAB. Figure 3.4 shows the normalised stresses and curve fit equation results. The input for surface fitting is wave height, current and normalised stress values. It can be seen from Fig. 3.4 that vertical axis is the normalised joint stresses for one joint. The horizontal axis is the output from curve fit model containing same wave height and current for which stress is achieved.

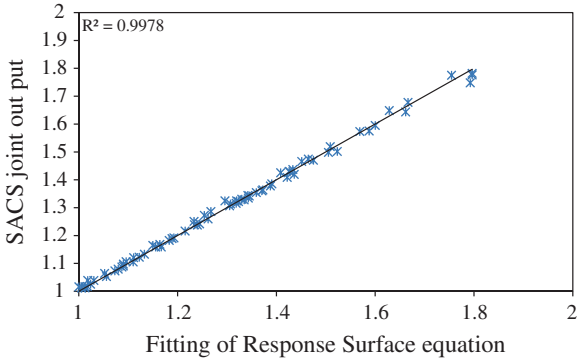

Fig. 3.4 Surface fitting validation for SBO platform

3.4 Structural Reliability

When randomness of material or load is low, a deterministic model can be used. In cases when random uncertainty is high, stochastic models containing statistical properties should be used [22]. Safety margin between load and resistance is indicated by limit state in Eqs. (3.15) and (3.16),

$$g = R - Q \leq 0 \tag{3.15}$$

where $g =$ Limit state function

$$g = R/Q \leq 1 \tag{3.16}$$

Probability of failure is given by Eq. (3.17),

$$P_{\mathrm{f}} = P(g < Q) \tag{3.17}$$

Here, $(g < 0)$ indicates failure region, $g > 0$ safe region and $g = 0$ failure surface; mean of limit state function is shown as Eq. (3.18),

$$\mu_{\mathrm{g}} = \mu_R - \mu_Q \tag{3.18}$$

where $\mu_R =$ mean resistance and $\mu_Q =$ mean load

SD of limit state function is shown by Eq. (3.19),

$$\sigma_g = \sqrt{\sigma_R^2 + \sigma_Q^2} \tag{3.19}$$

where $\sigma_R =$ SD of resistance, $\sigma_Q =$ SD of load. Reliability index can be found as shown in Eq. (3.20) which is a level II reliability method,

$$\beta = \frac{\mu_g}{\sigma_g} \text{ or } \frac{\mu_R - \mu_Q}{\sqrt{\sigma_R^2 + \sigma_Q^2}} \tag{3.20}$$

Common stochastic methods for reliability analysis are simulation techniques like Monte Carlo or moment-based techniques like FORM. This book does not take into consideration of time variant variables, i.e. fatigue and corrosion. FORM and Monte Carlo simulation methods of reliability are used for time invariant random variables [3]. These methods vary with respect to accuracy, required input data, computational effort and reliability can be used as professional criteria for the choice of load and resistance factors [23].

3.4.1 Form

Here, random variables are defined by first moment (mean), second moment (coefficient of variation) and type of distribution. Approximating of limit state function is evaluated by reliability-based algorithms like FOSM and FORM.

3.4.1.1 First-order Second Moment Method (FOSM)

It is defined by mean value first-order second moment method (MVFOSM). First order means first-order expansion of transfer equation. The main variables are mean and SD only, and no distribution is needed. Taylor series expansion is used for the expansion of equation depending on mean value. Considering that our variables are independently distributed, approximate limit state function at mean value is given by Eq. (3.21) [22],

$$\tilde{g}(X) \approx g(\mu_x) + \nabla g(\mu_x)^T \left(X_\mathrm{i} - \mu_{x_i}\right) \tag{3.21}$$

$\mu_x = \left(\mu_{x_1}, \mu_{x_2} \ldots \mu_{x_n}\right)^T$, $\nabla g(\mu_x)$ is the gradient of g evaluated at μ_x as shown in Eq. (3.22)

$$\nabla g(\mu_x) = \left[\frac{\partial_\mathrm{g}(\mu_x)}{\partial_{x_1}}, \frac{\partial_\mathrm{g}(\mu_x)}{\partial_{x_2}}, \ldots . . \frac{\partial_g(\mu_x)}{\partial_{x_n}}^T\right] \tag{3.22}$$

The mean value of limit state function is $\tilde{g}(X)$ as shown in Eq. (3.23):

$$\mu_{\tilde{g}} \approx E\{g(\mu_x)\} = g(\mu_x) \tag{3.23}$$

Since then $\mathrm{Var}\left[g(\mu_x)\right] = 0$ and $\mathrm{Var}\, \nabla g(\mu_x) = 0$

The SD value of limit state function is $\tilde{g}(X)$ as shown in Eqs. (3.24) and (3.25),

$$\sigma_{\tilde{g}} = \sqrt{\mathrm{Var}\tilde{g}(X)} = \sqrt{\left[\nabla g(\mu_x)^T\right]^2 \mathrm{Var}(X)} \tag{3.24}$$

$$= \left[\sum_{i=1}^{n} \left(\frac{\partial_g(\mu_x)}{\partial_{xi}}\right)^2 \sigma_{xi}^2\right]^{1/2} \tag{3.25}$$

The reliability index is given by Eq. (3.26),

$$\beta = \frac{\mu_{\tilde{g}}}{\sigma_{\tilde{g}}} \tag{3.26}$$

If the limit state equation is linear, this will become same as Eq. (3.20). In case when limit state function becomes nonlinear, then approximation is made here by taking the actual limit state function at mean value, thus making it linear. Thus, Eq. (3.26) is named as MVFOSM for evaluating reliability index. Here, random variables used are mean (first moment) and variance (second moment). There are two drawbacks found in this method. In case of high nonlinearity, this method is not suitable. This method fails to be invariant with different mathematical equal equations of same question.

3.4.1.2 Hasofer and Lind Reliability Index

The above method was improved by Hasofer and Lind (HL), and thus, better results are possible for nonlinear cases. Difference between HL and MVFOSM is that this method takes design point (most probable point) as the approximation of limit state function instead of mean value. This method uses iterations to converge. This method also takes distribution into considerations for finding the reliability index. HL method proposes linear mapping of basic variables into a set of normalised and independent variables (u_i) [22]. The standard normalised random variables for resistance and load are shown in Eq. (3.27),

$$\widehat{R} = \frac{R - \mu_R}{\sigma_R}, \widehat{Q} = \frac{Q - \mu_Q}{\sigma_Q} \tag{3.27}$$

where μ_R andμ_Q = mean values of resistance and load, σ_R and σ_Q = SD of resistance and load. Transformation from limit state surface of $g(R, Q)$ in original coordinate system into standard normal coordinate system $\left(\widehat{R}, \widehat{Q}\right)$ is shown in Eq. (3.28),

$$\widehat{g}\left(\widehat{R}, \widehat{Q}\right) = \widehat{R}\sigma_R - \widehat{Q}\sigma_Q + \left(\mu_R - \mu_Q\right) = 0 \tag{3.28}$$

The shortest distance from origin $\left(\widehat{R}, \widehat{Q}\right)$ in normal coordinate system to failure surface of $\widehat{g}\left(\widehat{R}, \widehat{Q}\right)$ is equal to reliability index, i.e. $\beta = \widehat{O}P^*$. Failure surface for independent and normally distributed variables for nonlinear function is shown in Eq. (3.29),

$$g(X) = g(x_1 x_1 \cdots x_n)^T \tag{3.29}$$

Variables are transformed into standard forms by Eq. (3.30),

$$u_i = \frac{x_i - \mu_{x_i}}{\sigma_{x_i}} \tag{3.30}$$

where μ_{x_i} and σ_{x_i} are the mean and SD of x_i. The mean and SD of standard normal distribution are 0, 1. Thus, reliability index is shortest distance from origin to failure surface, given by Eq. (3.31),

$$\beta = \min\left(U^T U\right)^{1/2} \tag{3.31}$$

There are certain limitations in this method, i.e. in some cases, there is a problem of non-convergence. But the main issue still remained, that is, it considered only normal distributed random variables.

3.4.1.3 Hasofer–Lind (HL) and Rackwitz–Fiessler (RF) Methods

This is extension of HL method and the only difference is that it can take non-normal distribution for finding the reliability index. Non-normal distributed variable is transformed into normal space. Using this method, FORM model by use of FERUM is adopted in this book. FERUM is developed in MATLAB and is an open source compiler available from University of California, Berkley [24]. FERUM is used in this book for component, joint and system reliability analysis.

3.4.2 Monte Carlo Simulations for Determination of Probability of Failure

This method is used when random behaviour is evaluated by sampling techniques. MCS uses randomly generated sampling sets for uncertain random variables of load and resistance. This is used to find approximate probability of some event, which is the result of a series of probabilistic processes [22]. Following steps are followed here in this method: (1) type of probability distribution function is selected for the particular random variable, (2) samples are generated by probability density function, (3) limit state function is defined, (4) Using simulation the response is evaluated. This method is used to find probability of failure and for updating of probability of failure using Bayesian updating technique. Probability of failure in Monte Carlo simulation is shown by Eq. (3.22)

$$\text{Probability of Failure } (P_\text{f}) = \frac{\text{Number of failures}}{\text{Total numbuer of simulations}} \tag{3.32}$$

The Eq. (3.33) gives the return period of load, using probability of failure,

$$\text{Return Period} = \frac{1}{P_\text{f}} \tag{3.33}$$

Monte Carlo simulation uses randomly generated samples as per their probability distributions. Probability of failure is achieved by solving Eq. (3.32) for large number of times. It is a ratio of number of samples (failed), i.e. in unsafe region divided by total number of samples of random variable, i.e. simulations. The accuracy of this technique depends on number of simulations used in the analysis. The number of simulations used in this text is fixed at 1×10^7. For each simulation, there is new wave height and new model uncertainty factor for load and resistance. The platform will fail if the load effect (Q) exceeds the resistance of the member (R). The reliability index can be found by Eq. (3.34):

$$\beta = \Phi^{-1}(P_\text{f}) \tag{3.34}$$

where Φ^{-1} = inverse standard normal distribution. Probability of failure can be found by Eq. (3.35),

$$P_\text{f} = 1 - \Phi(\beta) \tag{3.35}$$

Φ = Cumulative distribution function for the standardised normal variable.

3.4.3 Selection of Jacket Platforms for Reliability Analysis

Offshore Malaysia has three regions and Jacket platforms are selected to represent each region. Two platforms are from Sarawak, one from Sabah and one from Peninsular Malaysia. These platforms are designed as per API RP2A-WSD 21st edition. SACS software is used for static linear and nonlinear analyses. The availability of the original SACS model of the platform is compulsory for the calibration. This is because the designed structure has already proved its strength and it could be used for target reliability. The load models used in the original SACS model are necessary for this analysis. The characteristics for selection of platform depend on, i.e. varying number of legs and different water depths. Table 3.13 and Figs. 3.5, 3.6, 3.7 and 3.8 show the details of the platforms selected for the reliability analysis. Their water depth varies from 42 to 95 m which represents the range of depths of platforms in offshore Malaysia.

These Jackets are checked for material and geometrical variability, load effect ratios (axial to bending to hydrostatic) and load type ratios (dead to live to environmental). Load capacities are calculated for the components, joints and overall system. Table 3.14 shows a case study showing the benefits of using mean coefficient and variation coefficient to convert into any required value of mean and SD.

Table 3.13 Details of selected platforms for reliability analysis

Platform location	Water depth (m)	Installation year	No. of legs	Design wave height (m)
PMO	61.00	2006	4	10.8
SBO	42.80	2007	6	7.7
SKO1	72.40	2003	4	9.9
SKO2	94.8	2008	4	11.7

Fig. 3.5 Jacket platform at PMO

3.4.4 SACS Analysis

SACS is three-dimensional space frame software for analysis of Jackets for all loading conditions, i.e. dead, live and environmental loads, i.e. wind, wave, current. Environmental loads are applied horizontally on the platform. Wind acts

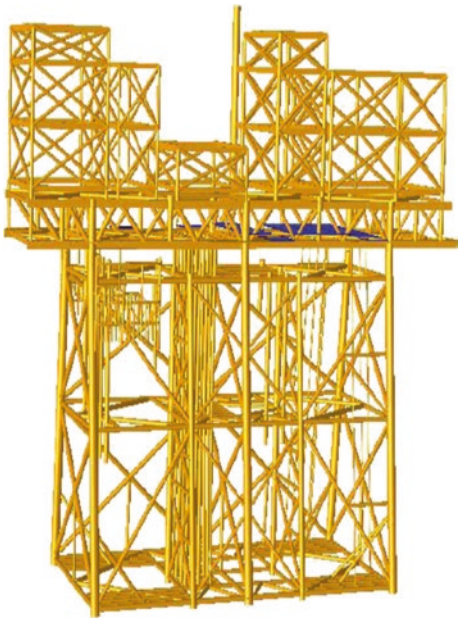

Fig. 3.6 Jacket platform at SBO

Fig. 3.7 Jacket platform at SKO (SKO1)

Fig. 3.8 Jacket platform at SKO (SKO2)

mainly on topside, and wave and current act on the Jacket members. Wave and current forces on the members are calculated using Morison equation. SACS analysis is used to find the component stresses, joint stresses and system base shear at design loads and at higher loads.

3.4.5 Load Ratios

Jacket platform is divided into different levels, and representative members and joints are selected from Jacket. Major gravity loads are supported by legs and braces in vertical plane, while horizontal loads (which are variable) are supported by

Table 3.14 Random variable used to find the reliability index

Factor	Distribution	Initial value	MC	VC	Mean used	SD
Fy	Normal	340	1.230	0.050	418.200	17.000
D	Normal	610	1.001	0.0014	610.610	0.854
T	Normal	25	1.024	0.016	25.600	0.400
d	Normal	610	0.9993	0.0018	609.573	1.098
t	Normal	16	1.024	0.016	16.384	0.256
Angle	Normal	90	1.000	0.050	89.709	4.238
Dead load	Normal	1.0	1.000	0.060	1.000	0.060
Live load	Normal	1.0	1.000	0.100	1.000	0.100
Xm (tension)	Normal	1.26	1.260	0.050	1.260	0.063
Wave height	Weibull	2.59	2.590	1.060	2.590	1.060
Current	Weibull	0.81	0.810	0.120	0.810	0.120
Xw	Normal	1.0	1.000	0.150	1.000	0.150

Table 3.15 Dead, live and environmental load ratios

W_e/G	0.1	0.25	0.5	1.0	2.5	5.0	10	25	50
Dead load (d) (70 % of G)	0.64	0.56	0.47	0.35	0.20	0.12	0.06	0.03	0.01
Live load (l) (30 % of G)	0.27	0.24	0.20	0.15	0.09	0.05	0.03	0.01	0.01
Environmental load (w)	0.09	0.20	0.33	0.50	0.71	0.83	0.91	0.96	0.98
Unity check ($d + l + w = 1$)	1.00	1.00	1.00	1.00	1.00	1.00	1.00	1.00	1.00

horizontal braces [25]. Loads acting on Jacket vary in their influence. Shallow water Jackets are dominated by gravity load and deepwater Jackets are dominated by environmental load (γw). The dead, live and environmental load ratios for Jackets are shown in Table 3.15. Gravity load consists dead and live loads. It is reported that on Jacket platform, 70 % of gravity load is dead and 30 % is live load [7]. Load proportions are used to represent the variability of load under which a Jacket can undergo at site. Load ratios are derived from total load which is equated to 1.0. Case study of evaluating of load ratio is given in Appendix D. For GOM, load ratios used are in range of 0.3–40, and for North Sea, it was between 0.3 and 12 [19]. Ratios used for Mediterranean Sea has been 0.3–12 for extreme conditions and 0.2–0.6 for operating conditions [26]. In this text, load ratios 0.1–50 are considered for reliability analysis.

3.4.6 Soil Conditions Effect on Component and Joint

The effect of fixing of Jacket at mud level or providing the effective pile foundations at mud level is different for component and joint cases and overall system. In this text, one platform from Sarawak (SKO2a) is used with pile foundation and SKO2 is fixed at mud level for analysis. Tables 3.16, 3.17 and 3.18 show the

Table 3.16 Load coefficients for K-joint

K-joint						
	Stress type	a_1	a_2	a_3	a_4	a_5
K-SKO2	Axial	0.01218	−0.07960	0.10520	−0.06624	0.259
	IPB	0.01652	−0.13650	−0.00648	0.02542	0.388
	OPB	0.05543	−0.91780	−0.02879	0.25140	4.008
K-SKO2a	Axial	0.01216	−0.07914	0.10680	−0.06986	0.258
	IPB	0.01646	−0.13590	−0.00541	0.02542	0.387
	OPB	0.05322	−0.87510	0.005137	0.20830	3.815

Table 3.17 Load coefficients for T/Y-joint

T/Y-joint						
	Stress type	a_1	a_2	a_3	a_4	a_5
T/Y-SKO2	Axial	−0.00407	0.22560	0.2013	−0.4439	−0.3101
	IPB	0.003423	0.02700	0.1224	0.1545	−0.1315
	OPB	0.02387	−0.32660	−0.2178	0.2196	1.5990
T/Y-SKO2a	Axial	−0.00350	0.23100	0.1322	−0.3425	−0.3347
	IPB	0.003422	0.02697	0.1221	0.1550	−0.1314
	OPB	0.02020	−0.26460	−0.1344	0.1385	1.3360

Table 3.18 Load coefficients for X-joint

X-joint						
	Stress type	a_1	a_2	a_3	a_4	a_5
X-SKO2	Axial	0.006135	−0.00264	0.1172	0.02035	0.04043
	IPB	0.002713	0.03073	0.1204	0.19250	−0.15200
	OPB	0.004213	0.009521	0.1619	0.08998	0.01732
X-SKO2a	Axial	0.00613	−0.002620	0.1171	0.02093	0.04001
	IPB	0.002765	0.029820	0.1221	0.19050	−0.14840
	OPB	0.004303	0.008561	0.1582	0.09002	0.01726

coefficients achieved for both cases for SKO2 and SKO2a platform using response fitting. The results show that there is not much difference in coefficients which gave minor difference in reliability index. Therefore, reliability analysis is not performed for component and joint of SKO2a platform. For system reliability, the coefficients are slightly different, and thus, it is evaluated calculated in Chap. 10.

3.5 Component Reliability

Jacket platform is divided into different bays. Members are selected from their location, diameter to thickness variation and slenderness ratio. The primary members are leg and brace. Brace members are further divided into horizontal

Table 3.19 Geometry groups for component reliability analysis

Type of component	Bay	Outer diameter (mm)	Wall thickness (mm)	Length (mm)
Horizontal diagonal	Mid	813	15	3,000
	Mid	813	25	21,200
Horizontal brace periphery	Mid	813	15	7,700
	Mid	813	15	9,500
Leg	Bottom	1,650	25	13,100
	Bottom	1,200	20	5,000
Vertical diagonal	Top	762	30	7,820
	Top	914	20	18,521

periphery, horizontal diagonal and vertical diagonal. Seven component stresses are analysed for each member. For combined stresses, the limit state equation contained combination ratios for each type of stress. Table 3.19 shows component grouped for one platform and selected for reliability analysis. Similarly, different groups are selected from other regions. Figure 3.9 shows the flow chart of the methodology to evaluate component and joint reliability.

3.5.1 Single Stresses Case Study: Axial Tension

Code equation for axial tension provided by ISO and API WSD is shown by Eqs. (3.36) and (3.37), respectively.

$$\sigma_t \leq \frac{f_t}{\gamma_{R,t}} \tag{3.36}$$

where $\gamma_{R,t}$ = resistance factor, σ_t = tensile stress and f_t = tensile strength

$$F_t = 0.6F_y \tag{3.37}$$

where F_t = allowable tensile stress and F_y = yield strength. Reliability analysis provides strength of component using ISO code Eq. (3.38),

$$R = f_{yi} \times A_i \times X_m \tag{3.38}$$

where f_{yi} = random yield strength, A_i = random area of tubular member and X_m = model uncertainty. To find the applied stress, reliability analysis for loading purpose will include Eqs. (3.39) and (3.40) for API WSD and ISO, respectively,

$$S = f_{yn} \times A_n \tag{3.39}$$

where f_{yn} = nominal yield strength and A_n = nominal tubular area

$$S = 0.6 \times F_{yn} \times A_n \tag{3.40}$$

where S = strength given by code equation. Application of load ratios for reliability analysis is given by Eq. (3.41),

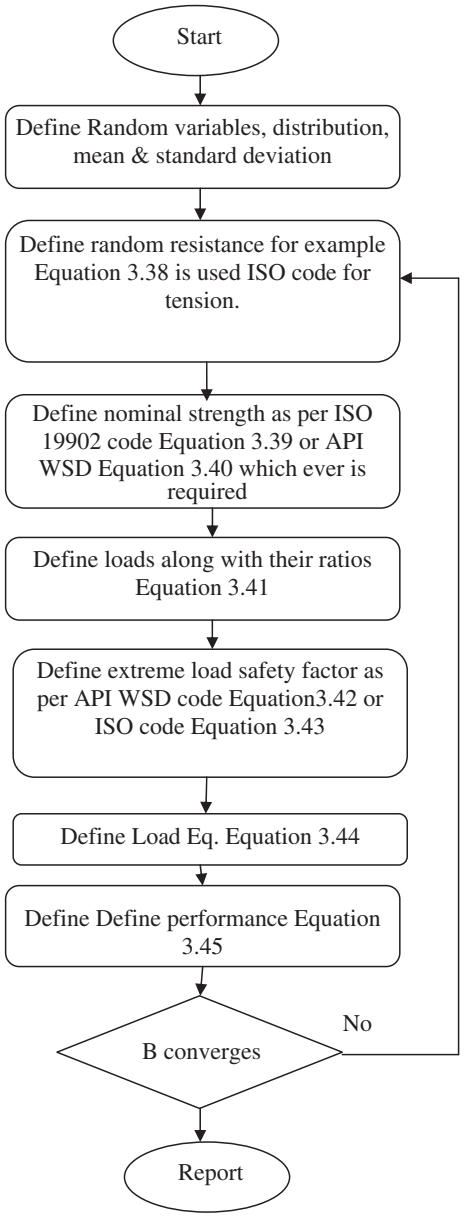

Fig. 3.9 Flow chart for component and joint reliability

$$L_r = dD + lL + wW/X_w \tag{3.41}$$

where d, l and w are the dead, live and environmental load ratios shown in Table 3.15 and D, L and W are the variable uncertain random dead, live and environmental load and X_w = environmental load uncertainty model. In this text, it is

taken from study which was conducted for ISO [7]. Normal distribution is considered with mean of 1.0 and SD of 0.15. Parameters of random variables are defined separately in FERUM. The main part of calibration is that we want a component or joint which is fully utilised we need to define factor of safety as per the code. Factor of safety in API WSD for extreme conditions is shown by Eq. (3.42)

$$\text{FS(API WSD)} = \frac{4}{3 \times 1.67} \tag{3.42}$$

The factor of safety in ISO 19902 for extreme conditions is given by Eq. (3.43)

$$\text{FS(ISO)} = \frac{(1/1.05) \times (D + L + W/X_w)}{(1.1D + 1.1L + (1.35 \times W/X_w))} \tag{3.43}$$

where FS = factor of safety, 1.05, 1.1 and 1.35 are tensile resistance, gravity load and environmental load factors. The actual load applied by API or ISO can be shown as Eq. (3.44),

$$L = S \times L_r \times \text{FS} \tag{3.44}$$

The limit state equation becomes, as shown in Eq. (3.45),

$$g = R - L \tag{3.45}$$

Same procedure is adopted for all other types of stresses to find the reliability.

3.6 Joint Reliability

There are three types of joints identified by the codes, i.e. K, T/Y and X. They are defined by the way loads act on the joint and geometry of the joint. There are four types of stresses tension, compression, in-plane bending and out-plane bending for each joint. The process flow for reliability adopted is same as explained earlier. Table 3.20 shows the groups of geometry considered for reliability from one platform. Similarly, different groups of joints are selected from Jacket from other regions of offshore Malaysia.

Table 3.20 Geometry groups for joint reliability analysis

Type of joint	Chord diameter (mm)	Chord thickness (mm)	Brace diameter (mm)	Brace thickness (mm)	Brace angle (°)
K	1,200	40	914	25	90
	813	30	813	25	55
T/Y	711	30	457	25	83
	1,200	40	711	15	90
X	813	15	711	12	42
	1,200	50	813	30	90

3.6.1 Target Reliability

When Jacket platform designed as per existing code has proved its strength and reliability, it is considered safe to take the reliabilities of that platform as our target reliability. In theory, it is said that it should consider minimisation of cost of construction, maintenance cost and consequence of failure. Target reliability for components and joints is set as per API WSD reliability, and reliability achieved by ISO is compared with WSD. For practical purpose, calibration of factor of safety of new code is done against reliability of in-service Jackets designed. Jackets designed as per the old code are taken as target reliability. In this text for each case, ISO and WSD reliabilities are found out separately and then compared to find the environmental load factor. Component target reliability for Jacket legs and braces is set at 3.85 and 3.88 for North Sea [27].

3.7 Environmental Load Factor

When API WSD designed platforms have already survived certain amount of time in rough weather, they have established their robustness in design. Now we can take their reliability as safe against failure, and the reliability index higher than API WSD can be taken as safe as API WSD. The reliability found using ISO 19902 and API WSD code is plotted together. Reliability index is determined with different load factors as per ISO code. When the ISO reliability index crossed the target reliability (higher reliability than available reliability), it is taken as the load factor for that member, joint or overall platform.

3.8 Resistance Factor

Environmental load factor achieved for components and joints is used to find resistance factor for component stresses. This is necessary so that ISO resistance factors could be assessed and evaluated with new load factors proposed for this region. Two types of stresses are checked here which are axial tension and compression using FORM method.

3.9 System Reliability-Based Environmental Loads

Probability of failure for Jacket platform is determined by increasing the wave heights for 10,000-year return period and higher. Wave height is increased so that effect of wave on deck could also be ascertained. The effect of load and resistance

model uncertainty and RSR on probability of failure/return period is evaluated. Failure of platform in eight directions is initiated by compression buckling of primary components of Jackets, i.e. horizontal and vertical diagonal brace, leg and piles. In this text, maximum wave height is increased, which increased the applied wave load and corresponding base shear of platform is obtained.

Regression analysis is used to find the coefficients for response surface equation by converting the wave and current forces into environmental load model by the use of curve fit tool. Probabilities of failure, return periods, safety indices and their COV are obtained against an RSR of 1.5–2.5. For system reliability analysis, target probability of failure is taken from previous studies. SACS collapse module is used for nonlinear analysis of the platform. MATLAB code is used for FORM analysis to find reliability index. Fatigue wear and tear is considered negligible, and fatigue limit state is not checked against failure. The system reliability for critical direction is taken as 4.46 in North Sea. The probability of failure at system level should be about an order of magnitude smaller than at component level [27].

3.9.1 SACS Collapse Module

SACS software has collapse module used for nonlinear analysis. This module has its parallel in SESAME software named USFOS. This module includes member buckling with eight or more hinge points. It also includes evaluation of joint failure due to excessive strain causing strain hardening as well as residual stresses. This module includes collapse view which shows progress of failure, gradual plastification and finally collapse mechanism.

It requires main input file to be established before this model is formulated. The primary file is used to define geometry, material and loading properties. The load is defined along with different combinations of operating and extreme conditions. Extreme loading conditions are used for collapse analysis. One difference between linear and nonlinear analysis in SACS module is the defining of loading conditions. Dead, live and dead loads are combined for loading conditions in linear analysis, but for collapse analysis, loads are separately defined. First of all, linear analysis is run with all load combinations in eight directions, i.e. at each 45°, if Jacket is four, six or eight legs. The combination and direction which gives maximum base shear is selected for collapse analysis.

The next step is the formulation of collapse module which includes following ten steps defined as follows.

1. Maximum iterations per load increment
2. Number of member segments
3. Maximum number of member iterations
4. Define deflection tolerance
5. Rotation tolerance
6. Member deflection tolerance

7. Strain hardening ratio
8. Maximum ductility allowed
9. Load type, number of its increments, start and end load factor. For instance,

   Load type = dead load,

   Number of its increments = 5

   Start load factor = 0

   End load factor = 1

   $$\text{Load increment} = \frac{\text{End factor} - \text{Begin factor}}{\text{Number of increments}}$$

   Each time load will be increased by 1/5 = 0.2 times the actual load, until it reaches to 1.0; this is for dead and live load, but end load factor for environmental load is put beyond 1.0. This is due to the fact that environmental load is increased until collapse failure of Jacket occurs.
10. Defining member groups which are not to be analysed in this module such as pipes and conductors.

3.9.2 Collapse Analysis of Jacket

Working stress design (WSD) is considered linear elastic behaviour of platforms for determination of loads and resistance. Ductility is measured in RSR, which is the main criterion for ultimate strength of platforms. Ultimate capacity of platform can be determined by using nonlinear static pushover analysis. In this approach, first of all gravity loads, i.e. dead and live, are applied, followed by increase of environmental loads till failure occurs. Resistance at collapse is represented by Eq. (3.46) which provides the pushover strength of member [28],

$$R_{\text{ult}} = \lambda_{\text{ult}} E \tag{3.46}$$

where R_{ult} = ultimate resistance of platform, λ_{ult} = factor which is increased until collapse, E = modulus of elasticity

Design codes provide check against ultimate strength as shown in Eq. (3.47):

$$\frac{R_{\text{ultimate}}}{\gamma_R} \geq \gamma_d D_l + \gamma_w E_l \tag{3.47}$$

where γ_R = resistance factor, γ_d = gravity load factor, γ_w = environmental load factor, D_l = gravity load, environmental load. The minimum requirement for safe structure from pushover analysis is given by Eq. (3.48),

$$\lambda_{\text{ult}} \geq \gamma_R \times \gamma_w \tag{3.48}$$

$\lambda_{\text{ult}} \geq 1.18 \times 1.35 = 1.59$ (ISO for compression failure)
The minimum RSR is recommended by ISO and API, i.e. 1.58 as per API RP 2A WSD and 1.85 for ISO 19902 codes for high consequence and manned platforms.

The minimum RSR range considered in this text is in the range of 1.5–2.5 which is considered as reasonable [29]. Here in this analysis, wave load is increased and corresponding RSR is found. The main objective is to find wave height which will give RSR of 1.0 considered as fully optimised Jacket.

3.9.3 SACS Load Model

Once this collapse module is defined in SACS, pushover analysis is conducted to find reserve strength ratio of Jacket. The load sequence followed in this analysis is as follows: (1) all dead load, (2) all live load and (3) environmental load is increased until failure is reached. At each load increment, base shear is recorded; the first important information to be noted is base shear at 100-year environmental load, second is when first member fails, and the last is when Jacket collapses completely.

3.9.4 SACS Jacket Model for Pushover Analysis

Platform SACS geometry models are not changed, and only load models are changed which is necessary to check the effects of overloading. Table 3.21 gives details of the platforms used for system reliability analysis. Water depth and topside height varies with respect to each region. Jacket length given in this text covers from bottom of mud line to the top of leg. Design wave is the maximum wave height for that particular platform site for 100-year extreme conditions. Free board for each platform also varied from 10.5 to 16.5 m. The height of topside, excluding helipad deck, is shown in Table 3.21.

Pushover analysis depends on nonlinear collapse analysis of SACS module. RSR depends on ultimate strength divided by characteristic design load (100-year extreme load). In this analysis, gravity and environmental loads are increased from a factor of 0 to 1 in load step of 0.1 and the environmental load is then increased beyond one (which is 100-year extreme load) until the collapse of a member/system.

Table 3.21 Basic details of Jackets considered for system analysis

Region (platform)	Jacket length (m)	Water depth (m)	Design wave height (m)	Free board (m)	Topside height (m)
PMO	78.2	61.7	10.8	16.5	25.7
SBO	53.3	42.8	7.7	10.5	30.5
SKO1	85.7	72.3	9.9	16.5	26.9
SKO2	107.9	94.8	11.7	13.1	21.0

RSR is calculated when first member failed; this is due to the fact that this member has lowest RSR value as per WSD code. We need optimally designed structure for environmental load for Jackets designed as per ISO code, which requires that member should be checked with minimum RSR. Jackets used for reliability have four and six legs, and therefore, environmental load in eight directions is used to find the minimum RSR. Maximum design wave is used from all directions. The range of values for RSR depending on failure load to characteristic load, i.e. 100-year design load, is achieved as 2.0–4.9. For consistency, the range of RSR is fixed at 1.50–2.25. Higher values of RSR represented extra safety in Jacket platform, and therefore, they are not used.

3.9.5 Wave and Current Loads in Malaysia

Platform analysis is made for different wave heights keeping current values constant for one wave height. This is required to find the wave height which would give minimum value of RSR of 1.0 and variability for curve fit is evaluated at this RSR. This is a case of severe environmental load condition for Jacket platforms. Current velocities vary at different heights above mud level in linear stretching profile as proposed by API WSD and ISO 19902 codes. There are three current values, i.e. near mud level, at mid-level and at surface level. Current speed is fixed for a given wave height.

For platform at PMO region, the wave heights increased in steps of 10.8, 11.3, 11.9, 12.4, 13.0, 13.5, 16.0 and 19.0 m. Design current velocities for 100-year storm conditions at different water depths are 0.57, 1.0 and 1.1 m/s at 1 m above mud level, mid-water and at surface level, respectively. Thus, for instance, when a wave of 10.8 m height is analysed, each current speed is used separately for eight directions. Thus, 24 analyses are made for each wave height and there are 192 SACS analysis for the given platform. For platform at SBO region, wave heights considered are 7.7, 8.1, 8.5, 8.9, 9.2, 9.6, 11.6, 13.9, 16.2 and 18.1 m. The 100-year current velocities are 0.68, 0.86 and 0.94 m/s at 1 m above mud level, mid-water and at surface level, respectively. Thus, 240 SACS analyses are made for this platform. For platform SKO1 at SKO region, wave heights considered are 9.9, 10.4, 10.9, 11.4, 11.9, 12.4, 15, 17.5, 20 and 22.5 m. The 100-year current velocities are 0.68, 0.95 and 1.05 m/s at 1 m above mud level, mid-water and at surface level, respectively. Thus, 240 SACS analyses are made for this platform. For platform SKO2 at SKO region, wave heights considered are 11.7, 12.3, 12.9, 13.5, 14, 14.6, 17.6, 20.5 and 23.4 m. The 100-year current velocities are 0.55, 0.95 and 1.20 m/s at 1 m above mud level, mid-water and at surface level, respectively. Thus, 216 SACS analyses are made for this platform. Same number of separate analysis is made for SKO2a platform to get its response coefficients. Wave height properties in shape of base shear are shown in Chap. 10 and Appendix E.

3.9.6 Curve Fitting

The curve fitting for the platforms is made using MATLAB curve fit tool. The custom polynomial equation for wave and current is defined to get the parametric values for the given coefficients. Response surface fit proposed by Heidman and Efthymiou in Eq. (2.15) as shown by Gerhard is used to get the load effects from Jacket base shear and wave heights [30]. The coefficients are derived using the least mean square method. Data are analysed at 95 % confidence level and coefficient of variance, i.e. R^2 value of above 0.90.

3.9.7 Safety Factor for Jacket System: API WSD and ISO 19902

Figure 3.10 shows the flow chart to evaluate the system reliability index. In this text, a relationship is established between API WSD RSR and ISO RSR. This depends on safety factors available with both codes. These safety factors are apparent as well as inherent. Therefore, both are highlighted and effects of change of code are explained. The methodology adopted in this text is used for calibration of ISO code [31]. Design capacity of component in ISO code is given by Eq. (3.49),

$$\frac{R}{\gamma_c} \leq (\gamma_d \times P_d + \gamma_w \times P_w) \tag{3.49}$$

where P_d = gravity load proportion, P_w = environmental load proportion, γ_c = compression resistance factor, γ_d gravity load factor and γ_w environmental load factor. There is a relationship between WSD and ISO RSR. The RSR for ISO code could be found from Eq. (3.50),

$$\text{RSR}_{\text{ISO}} = \text{MOS}_{\text{ISO}} \times \text{MF} \times \text{ICSF} \times \text{SR} \times P_d P_{\text{wISO}} \tag{3.50}$$

Material factor (MF) depends on the yield strength. In this text, it is achieved to be 1.23; making consistency with ISO code, it is fixed as 1.15 to be on the lower side. Here, it is taken from ISO code, i.e. for grade 345 MPa, it has been reported that average material strength is higher by 15 % [32]. System redundancy (SR) depends on platform-specific values as shown in Chap. 9. The ultimate load can be found using Eq. (3.51),

$$P_{\text{ult}} = (\gamma_d \times P_d + \gamma_w \times P_w) \times M_F \times \text{ICSF} \tag{3.51}$$

The ISO RSR could be shown as Eq. (3.52); this will be used in limit state Eq. (3.57),

$$RS\acute{R} = \text{ICSF} \times \text{MF} \times \text{SR} \tag{3.52}$$

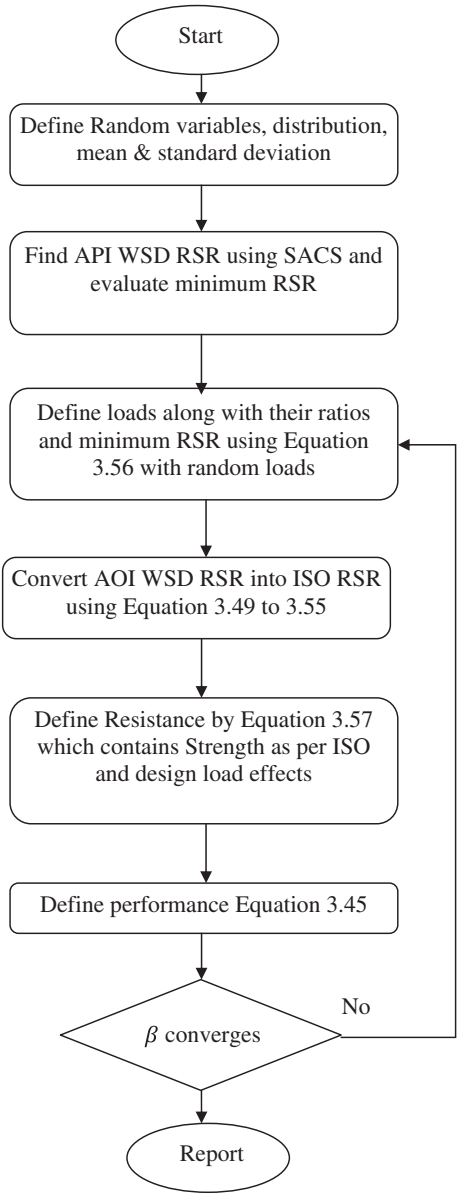

Fig. 3.10 Flow chart for system reliability

RSR values are also selected using platform-specific values as shown in Tables 9.2–9.6. P_d/P_w ratio varies here ranging from 0.1 to 20. The load factor is calibrated as per P_d/P_w ratio of 1.0 which is considered reasonable as per the conditions of offshore [7]. Implicit code safety factor (ICSF) is the difference between applied stresses and strength provided by code Eq. (3.53).

$$\text{ICSF} = \frac{\text{RSR}_{\text{WSD}}}{\left(P_d/P_w\right) \times \text{SR} \times \text{MF} \times \text{MOS}_{\text{WSD}}} \tag{3.53}$$

Safety margin (MOS_{WSD}) is set as reported by code, i.e. for extreme conditions, there should be one-third increase in the required stresses. Therefore, in this text, it is fixed as 1.32 which is also suggested by [30, 31]. For ISO, this safety factor is provided by Eq. (3.54),

$$\text{MOS}_{\text{ISO}} = \left(\frac{\gamma_d \times P_d + \gamma_w \times P_w}{P_d + P_w}\right)\gamma_c \tag{3.54}$$

ISO gravity and environmental load which are used in limit state equation can be shown in Eq. (3.55),

$$P_d P_{\text{wISO}} = 1 + \left[1 - \left\{\frac{1}{(\text{MOS}_{\text{ISO}} \times \text{MF} \times \text{ICSF})}\right\}\right] \times \frac{P_d}{P_w} \tag{3.55}$$

3.9.8 Limit State Function for System Environmental Loading

The limit state function for load and resistance for system reliability is shown by Eqs. (3.56) and (3.57):

$$\text{load} = \text{RSR}_{\text{WSD}} \times \left[Dd + Ll + w\left(\frac{a_1(H_{\max} + a_2 V_c)^{a_3}}{X_w}\right)\right] \tag{3.56}$$

where $w =$ environmental load ratio

$$\text{Resistance} = a_1\left(H_{\max(des)} + a_2 V_c\right)^{a_3} \times MOS_{\text{ISO}} \times P_d P_{\text{wISO}} \times RS\acute{R} \times X_w \tag{3.57}$$

$H_{\max(\text{des})} =$ Design wave height.

3.9.9 Target System Probability of Failure

Notional target failure probability is determined by using Eqs. (3.58) and (3.59) [33]. Equation 3.59 is also used by CIRIA Report 63 [34],

$$Pf_n = 10^{-4} \times \mu_s \times t_l \times n_{\text{p}}^{-1} \tag{3.58}$$

where $t_l =$ design life of structure, i.e. 30 years (PTS manual), $n_{\text{p}} =$ average number of people at/near platform $= 70$, $\mu_s =$ social criteria factor (for offshore structures) $= 5.0$

$$Pf_n = 10^{-5} \times A \times W_{\text{f}}^{-1} \times t_l \times n_{\text{p}}^{-1/2} \tag{3.59}$$

where A = activity factor (for offshore structures) = 10.0, W_f = warning factor for sudden failure = 1.0

Failure probability is found to be 2.14×10^{-3} and 3.58×10^{-3} from Eqs. (3.58) and (3.59), respectively. Efthymiou reports probability of failure of 10^{-4} (reliability index = 4.0). Therefore, in this text, Melchers target reliability of 3.58 and Efthymiou target reliability 4.0 are used.

3.10 System-Based Environmental Load Factor

System reliability-based environmental load factors for offshore Malaysia are determined using calibration of API WSD design code [30, 31]. The given method establishes the relationship between RSR and environmental load factors. The RSR achieved depends on API WSD design code. Therefore, it is first converted to RSR ISO code as shown in Sect. 3.9.5. Redesign as per ISO code is not selected due to following facts: the actual design is API WSD which has proved its strength and reliability at site. Besides, API WSD has been in changing process. The erratum was published only in 2008 which incorporates the latest changes of ISO code. The RSR depends on inherent and apparent factors of safety of codes along with redundancy in system. The structural reliability is determined with respect to varying W_e/G ratios and different RSR values within practical range. Therefore, lower values of RSR are used in this analysis as they would give optimally designed Jackets. The main aim depended on safety level of WSD and economy of ISO code which makes maximum use of utilisation of member.

3.11 Assessment of Jacket Platform

There are many uncertain parameters used in Jacket design. The complete safety of Jacket cannot be guaranteed. Future loading conditions, inability at design stage to accurately get data for material resistance, the simplified code equations used to predict the load behaviour, and errors and omissions due to human factors [35]. This makes the reliability check even more necessary after the completion of Jacket platform. Design life of Jacket platform in Malaysia is fixed as 30 years. Even before reaching that age, due to the requirements from insurance and other governmental institutions, the assessment is made mandatory after 3–5 years. Therefore, once in operation, it becomes necessary to get its probability of failure updated using latest resistance and load conditions. In this book, probability of failure is found first at design load, and then, it is determined for a return period load of 10,000 years. This is increased to higher values of wave height as explained in Sect. 3.9.3. Monte Carlo simulations are used to find the probability of failure for all the platforms.

3.11.1 Uncertainty Model for Resistance and Load

Load model uncertainty, which predicts extreme environmental conditions and transforms the storm condition wave to an individual wave height, is shown by Eq. (3.60),

$$L = A_i \times a_1 (H_{\text{var}} + a_1 \times V_c)^{a_3} \tag{3.60}$$

where H_{var} = random wave height. Resistance model uncertainty is shown by Eq. (3.61),

$$R = B_i \times \text{RSR} \times a_1 (H_{\max} + a_1 \times V_c)^{a_3} \tag{3.61}$$

where A_i, B_i are load and resistance model uncertainty parameters and are shown in Table 3.22. The resistance model uncertainty parameters, i.e. mean is 1.0 and coefficient of variation (COV) is 0.1 [31], and the COV used by DNV are in range of 0.05–0.1. DNV gives conservative values, and therefore, Efthymiou' recommended values are taken. For load model uncertainty, Haver [29] has given COV of 0.15. RSR values considered are in between 1.5 and 2.5.

Thus, limit state function can be shown by Eq. (3.62),

$$g = B_i \times \text{RSR} \times a_1 (H_{\max} + a_1 \times V_c)^{a_3} - A_i \times a_1 (H_{\text{var}} + a_1 \times V_c)^{a_3} \tag{3.62}$$

where H_{var} = varying wave height as per Weibull distribution parameters. Figure 3.11 shows the flow chart to evaluate probability of failure of Jacket using design load.

3.11.2 Bayesian Updating of Probability of Failure-Intact Structure

The Jacket platform is overloaded with increase in wave height till an RSR value of 1.0 is reached and the corresponding wave is recorded. Using this experience acquired from the Jacket analysis, we are confident enough that the platform will be safe against a wave height which produces an RSR of 1.0. This new wave height is used to find the survival probability of platform (P_s), as shown in Eq. (3.63),

$$P_s = \frac{\text{Number of Survival}}{\text{Total Number of Simulations}} \tag{3.63}$$

Table 3.22 Uncertainty factors used for limit state equation [29]

Factor	Description	Distribution parameters
A_i	Load model uncertainty	Normal distribution $\mu = 1.0, \sigma = 0.15$
B_i	Resistance model uncertainty	Normal distribution $\mu = 1.0, \sigma = 0.10$

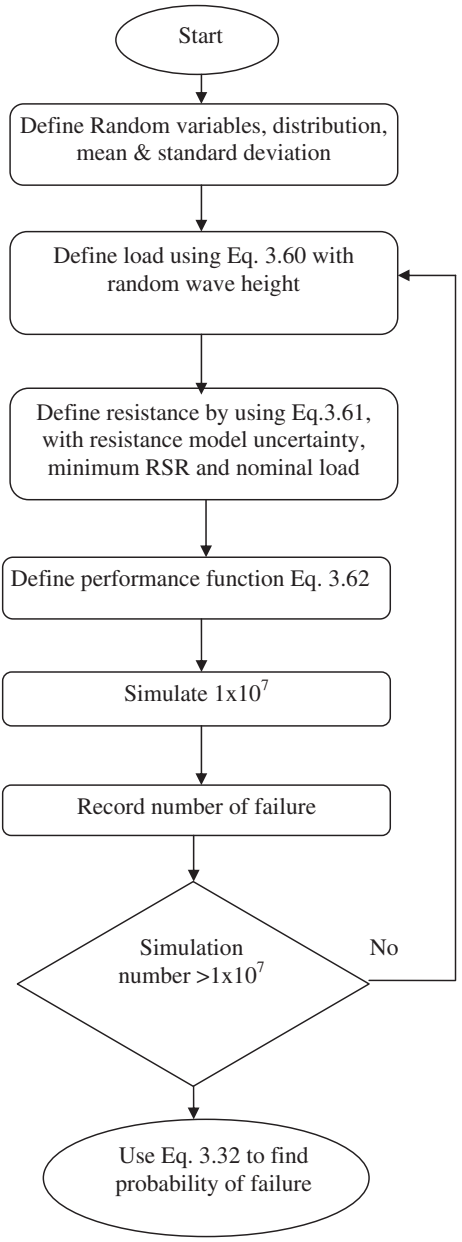

Fig. 3.11 Flow chart for finding probability of failure

When P_f is evaluated given that P_s is also known, then we can find the updated probability of failure (P_{uf}) using Eq. (3.64). Failure probability has already been found using Eq. (3.32). The new updated probability of failure is given by Eq. (3.64),

$$P_{\text{uf}} = P(g < 0 | S > 0) \tag{3.64}$$

where $P(g < 0)$ = probability of failure of limit state function and $P(S > 0)$ = probability of survival of limit state function

Thus, updated probability of failure (P_{uf}) can be shown by Eqs. (3.65) and (3.66),

$$P_{\text{uf}} = \frac{P\left[g(x) < 0 \cap S > 0\right]}{P[S > 0]} \tag{3.65}$$

$$P_{\text{Uf}} = P(g|S)P(S) \tag{3.66}$$

Survival limit state function is given by Eq. (3.67),

$$g = B_i \times \text{RSR x } a_1 \times (H_{\text{d}} + a_2 \times V_c)^{a_3} - A_i * a_1 * (H_R + a_2 \times V_c)^{a_3} \tag{3.67}$$

where H_{d} = design wave height and H_R = wave height when RSR = 1.0

Figure 3.12 shows the flow chart to update probability of failure using Bayesian updating technique.

3.11.3 Bayesian Updating of Probability of Failure-Damaged Structure

The knowledge of increased wave load effect is used to find the Bayesian updated failure probability. When some Jacket members fail, the overall capacity of Jacket could be reduced. This assumption is used by removing three members one by one from each Jacket. At each member failure, corresponding base shear is evaluated and its strength is determined as shown in Chap. 10. Damaged strength factor is given in Eq. 3.68. This reduced capacity is used to find updated probability of failure. The capacity is reduced about 50 % in case of three member failures. As this is not acceptable, the probability of failure is determined for two member failures.

$$\text{DSF} = \frac{Q_f}{Q_e} \tag{3.68}$$

where Q_f = base shear (damaged state) and Q_e = 100-year design load.

3.12 Summary

In this chapter, uncertainty models developed for resistance and load are explained. The extreme distribution models of Weibull and Gumbel are outlined with respective mathematical modelling. Structural reliability methods of FORM and Monte Carlo simulation are presented. Typical ISO and API reliability limit state equation for tension are discussed for uncertainty modelling and reliability

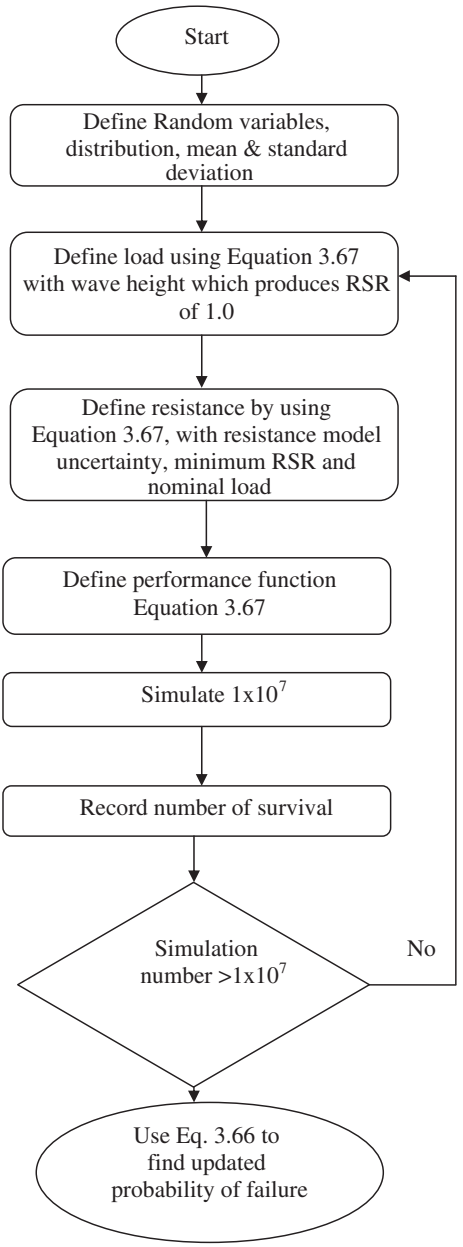

Fig. 3.12 Flow chart for Bayesian updating of probability of failure

analysis. Environmental load factor determination for Jacket platform is discussed using component and joint and system reliability analysis. Jacket assessment for 10,000 years and higher return period load is discussed. Lastly, Bayesian updating is explained which is a necessary tool for updating the probability of failure.

References

1. Baecher, G.B., Christian, J.T.: Reliability and Statistics in Geotechnical Engineering, Wiley (2003). ISBN: 978-0-471-49833-9
2. Duan, Z.D., Zhou, D.C., Ou, J.P.: Calibration of LRFD format for steel jacket offshore platform in China offshore area (1): statistical parameters of load and resistances. China Ocean Eng. **20**(1), 1–14 (2005)
3. ISO 2394: General principles on reliability for structures (1998)
4. Nowak, A.S.: Calibration of LRFD bridge code. J. Struct. Eng. **121**(8), 1245–1251 (1995)
5. Bolt, H.M., Billington, C.J., Ward, J.K.: Results from large-scale ultimate load tests on tubular jacket frame structures. Presented at the Offshore Technology Conference, OTC 7451, Houston (1994)
6. Frieze, P.A., Hsu, T.M., Loh, J.T., Lotsberg, I.: Back ground to draft ISO provisions on intact and damaged members, BOSS (1997)
7. BOMEL: Component based calibration of North Western European annex environmental load factors for the ISO fixed steel offshore structures code 19902 (2003)
8. AME: API RP2A-LRFD—Its consequences for and adaptation to north Sea offshore design practice. Advanced Mechanics and Engineering, Ltd. for Health Safety Executive, UK (1991)
9. Petroleum and natural gas industries: Specific Requirements for Offshore Structures—Part 1: Metocean Design and Operating Considerations (2005)
10. Tromans, P.S., Vanderschuren, L.: Response based design conditions in the north sea: application of a new method. Presented at the Offshore Technology Conference, OTC 7683, Houston (1995)
11. Tromans, P.: Extreme environmental load statistics in UK waters. Offshore Technology Report, HSE, 2000/066 (2001)
12. Standing, R.G.: The Sensitivity of Structure Load and Responses to Environmental Modelling, in Advances in Underwater Technology. Modelling the Offshore Environment, Society of Underwater Technology, Ocean Science and Offshore Engineering (1987)
13. Yiquan, Q., Zhizu, Z., Ping, S.: Extreme wind, wave and current in deep water of South China Sea. Int. J. Offshore Polar Eng. **20**(1), 18–23 (2010)
14. Bea, R.: Gulf of Mexico hurricane wave heights. J. Pet. Technol. 27(9), 1–160 (1975) (SPE 5317)
15. Johansen, N.J.T.: Partial safety factors and characteristics values for combined extreme wind and wave load effects. J. Solar Energy Eng. ASME **127**(2), 242–252 (2005)
16. Tromans P.S., Forristall, G.Z.: What is appropriate wind gust averaging period for extreme force calculations? Presented at the Offshore Technology Conference, OTC 8908, Houston (1998)
17. DNV: Classification note 30.6 structural reliability analysis of marine structures (1992)
18. Moses, F., Stahl, B.: Calibration issues in development of ISO standards for fixed steel offshore structures. J. OMAE Trans. ASME **122**(1), 52–56 (2000)
19. Turner, R.C., Ellinas, C.P., Thomas, G.A.N.: Worldwide calibration of API RP2A-LRFD. J. Waterw. Port Coast. Ocean Eng. **120**(5), 11 (1992)
20. Bury, K.: Statistical distributions in engineering: University of Cambridge (1999)
21. Monahan, A.H.: The probability distribution of sea surface wind speeds. Part I: theory and seawinds observations. J. Clim. **19**(4), 497–520 (2006)
22. Choi, S.K., Grandhi, R.V., Canfield, R.A.: Reliability-Based Structural Design. Springer, London (2007)
23. Nowak, A.S., Maria, M.S.: Structural reliability as applied to highway bridges. Struct. Eng. Mater. **2**(2), 218–224 (2000). (Wiley)
24. Bourinet, J.M.: FERUM 4.1 user's guide (online) (2010)
25. Zhou, D.C., Duan, Z.D., OU, J.P.: Calibration of LRFD for steel jacket offshore platform in China offshore area (2); load, resistance and load combination factors. China Ocean Eng. **20**(2), 199–212 (2006)

26. Theophanatos, A. Cazzulo, R. Berranger, I. Ornaghi, L., Wittengerg, L.: Adaptation of API RP2A-LRFD to the Mediterranean Sea. Presented at the Offshore Technology Conference, OTC 6932, Houston (1992)
27. Morandi, A.C., Frieze, P.A., Birkinshaw, M., Smith, D., Dixon, A.T.: Jack-up and jacket platforms: a comparison of system strength and reliability. Marine Struct. **12**(4), 311–325 (1999)
28. Skallerud, B., Amdahl, J.: Nonlinear Analysis of Offshore Structures. Research Studies Press LTD (2002)
29. Gerhard, E., Sorensen, J.D., Langen, I.: Updating of structural failure probability based on experienced wave loading. Presented at the International Offshore and Polar Engineering Conference Honolulu, Hawaii, USA (2003)
30. Gerhard, E.: Assessment of existing offshore structures for life extension. Doctor of Philosophy, Department of Mechanical and Structural Engineering and Material Science, University of Stavanger, Stavanger, Norway (2005)
31. BOMEL: System-based calibration of North West European annex environmental load factors for the ISO fixed steel offshore structures code 19902 (2003)
32. Graaf, V.D., Efthymiou, J.W., Tromans, P.S.: Implied reliability levels for RP 2A-LRFD from studies of north sea platforms. Presented at the Society for Underwater Technology International Conference, London (1993)
33. Melchers, R.E.: Structural Reliability Analysis and Prediction, 2nd edn. Wiley, UK (2002)
34. Gifford, W.D.: Risk analysis and the acceptable probability of failure risk analysis (2004)
35. Bilal, M.A., Haldar, A.: Practical structural reliability techniques. J. Struct. Eng. 110(8), 1707–1724 (1984)

Chapter 4
Uncertainty Modelling of Resistance

Abstract Resistance or strength parameters in LRFD are taken as random variables. Uncertainty modelling is the most important step for reliability analysis. The random variables are analysed, and range of type of distributions, mean values and standard deviations are discussed.

4.1 Introduction

This chapter deals with statistical data analysis for strength variables. The resulting estimates of reliability significantly rely on and are very sensitive to uncertainty modelling [1]. This chapter deals with basic resistance uncertainty of geometric and material properties and ISO component and joint stresses model resistance. The statistical parameters for model resistance are found by using Monte Carlo simulations for component and joint resistance. Easy Fit statistical software is used to analyse and find the probability distributions for resistance variables.

4.2 Resistance Uncertainty

The work on resistance variations has been done on onshore and offshore structures in different parts of the world. In this text, an effort is made to analyse the data as per existing conditions in Malaysia which is required as per ISO 19902 requirement. There are three steps for this analysis. The first one is to collect the data on random variables. The second step is to make statistical analysis of basic random variables used for design equations of tubular members and joints. The last step is to use these resistance random variables in ISO 19902 code equations and get the parameters for the stress uncertainty models which are faced by Jackets. Nine random stresses are modelled using ISO 19902 code for component

Z. Nizamani, *Environmental Load Factors and System Strength Evaluation of Offshore Jacket Platforms*, Ocean Engineering & Oceanography 4,
DOI 10.1007/978-3-319-15051-2_4

Fig. 4.1 Tubular member for variability analysis

and four for each type of K-, T/Y- and X-joint. After the analysis, it is compared with other similar studies made in different offshore regions. Figures 4.1 and 4.2 are analysed for uncertainty analysis.

4.3 Statistical Properties of Fundamental Variable for Resistance

The basic variables of resistance are geometry and material, i.e. thickness, diameter, yield strength and modulus of elasticity. It is reported that reliability index depends on geometry and material strength for Jacket platforms [2]. The results from this book are compared with studies in ISO 19902 code, GOM, North Sea and China. In this text, resistance uncertainty bias is used for statistical analysis. Bias is defined as ratio of actual characteristic value to assumed characteristic value [3]. Probability density function (PDF) shows the frequency of occurrence of certain parameters. This could be a normal distribution with perfectly parabolic

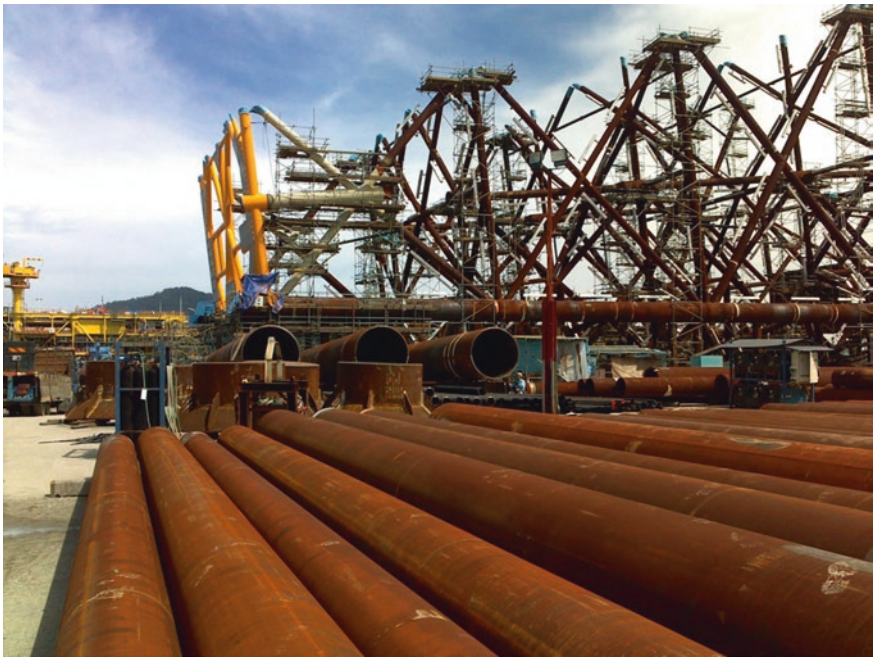

Fig. 4.2 Jacket platform at site

curve. Here, central tendency will be more, and likely occurrence will be at the middle of parabola.

4.3.1 Geometric Properties

The uncertainties for geometric properties are the diameter and thickness for legs and braces. These are the basic variables for the reliability analysis. Samples collected for thickness variations are 26, for leg diameter 260 and for brace diameters 113. Measured samples for angles are 85 obtained from as-built drawings. Geometrical design and fabrication nowadays are well controlled due to ISO quality control standards. The variations measured are very low for geometrical variables. That is the main reason that distribution is also normally distributed. Figure 4.3 shows the plan of Jacket at a bay with position of horizontal braces and legs. The chord–braces angles, however, accurately they may be connected, still show some variations. Table 4.1 shows the difference in design and actual values for angle at one bay of Jacket. This difference is actually covered by tolerance limit provided for each variable by the design codes.

Analysed data is shown in Table 4.2 and Figs. 4.4, 4.5, 4.6 and 4.7. Statistical analysis is used to find the parameters of distribution and PDF by using

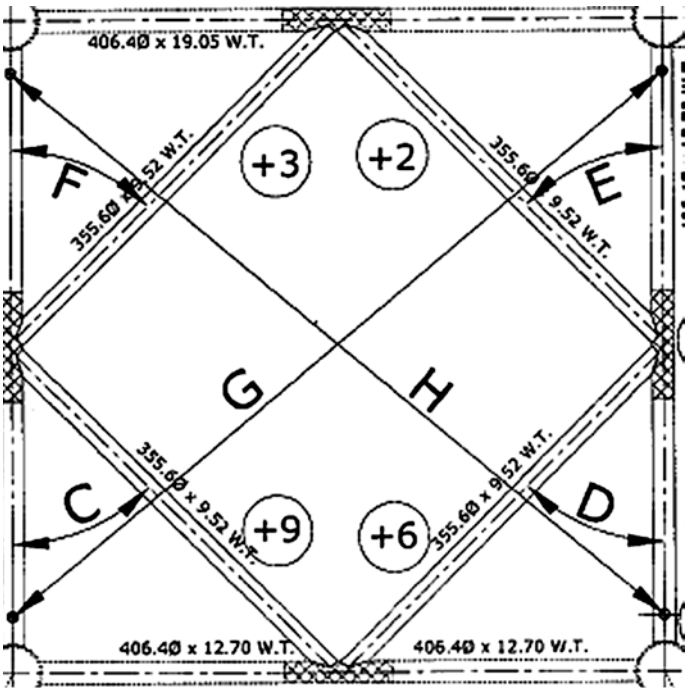

Fig. 4.3 Angle variations

Table 4.1 Angle variations measured using Fig. 4.3

Location	Design value	Actual	Deviation	Tolerance
C	45°	45.0013	+0.0013	5°
D	45°	44.8958	−0.1042	5°
E	45°	44.8852	−0.1148	5°
F	45°	44.6777	−0.3223	5°

goodness-of-fit tests. Distributions are fitted, and the best fit is reported. The results show that the best fit is achieved with normal distribution. Though lognormal curve is also very close to normal but depending on Anderson–Darling and Kolmogorov–Smirnov test results best fit is proposed. Here, Weibull distribution came at third place during the applied statistical tests. These three distributions are evaluated out of many others due to recommendation by ISO code [4]. The best distribution fit achieved for China, North Sea (DNV) code and ISO 19902 is also normal. The values matched the results from China, North Sea and GOM. The variation coefficient is very small for diameter and angle except wall thickness which has relatively higher variations. This trend is also present in GOM, North Sea and China. Variation in diameter of legs and braces is presented separately; this is done due to difference in leg and brace diameter variations. Angle variation from other sources is not available for comparison.

Table 4.2 Statistical variation in geometry of tubular component and joints

Type of variability	Statistical parameter	MS		Duan [5]	ISO (BOMEL) [6]	Adams [7]
		Leg > 1,000 mm	Brace < 1,000 mm	China	ISO	GOM
Diameter (mm)	Distribution	Normal	Normal	Normal	–	Normal
	MC	1.001	0.9993	1.0	1.005	1.0
	VC	0.0014	0.0018	0.0025	0.001	0.0025
Wall thickness (mm)	Distribution	Normal	Normal	Normal	–	Normal
	MC	1.024		1.0	1.0	1.0
	VC	0.016		0.015–0.050	0.0024 + 0.25/T	0.021
Angle	Normal	–		–	–	–
	MC	0.999		–	–	–
	VC	0.00281		–	–	–

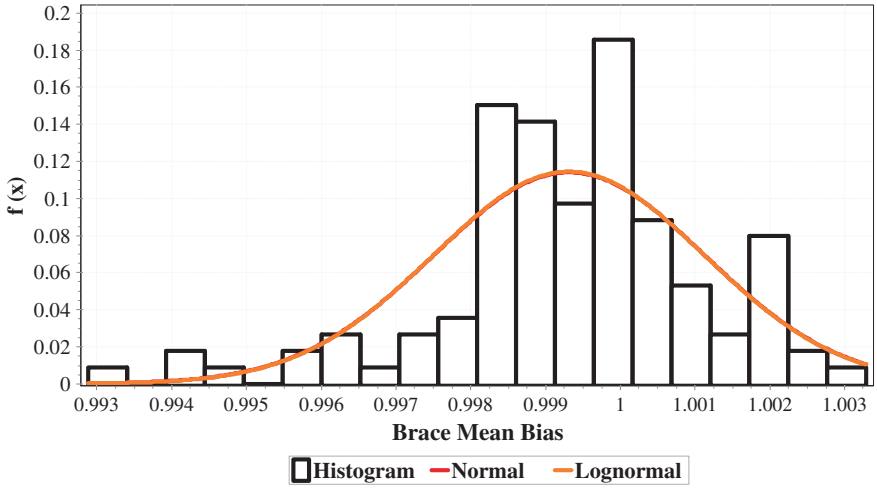

Fig. 4.4 Probability density function for brace diameter <1,000 mm

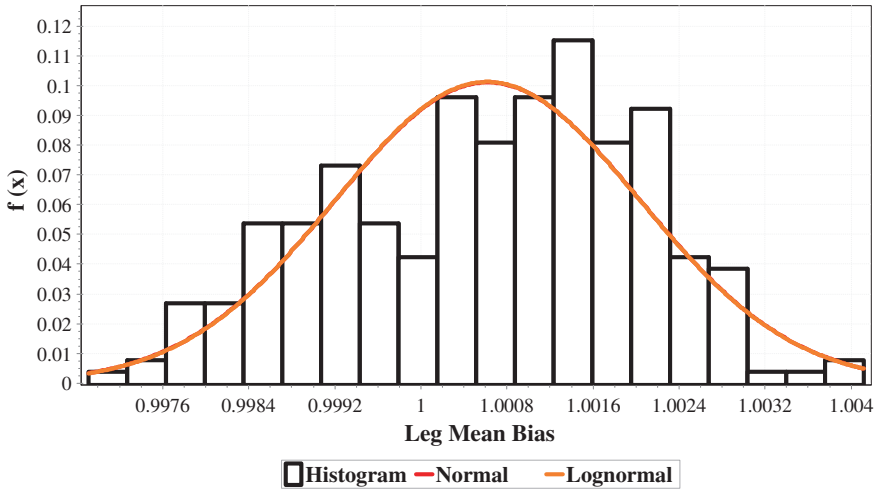

Fig. 4.5 probability density function for leg diameter >1,000 mm

4.3.2 Material Properties

It is always assumed that the lower tail of material strength distribution is of important for the evaluation of reliability [8]. Material property uncertainties considered are yield strength, tensile strength and elongation. Table 4.3 and Figs. 4.8, 4.9 and 4.10 show the statistical parameters and PDF. The sample size for yield

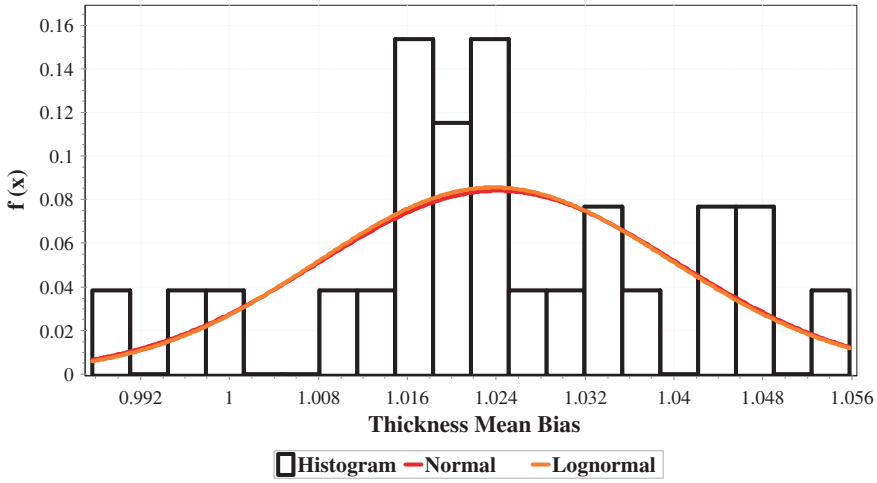

Fig. 4.6 Probability density function for thickness variation

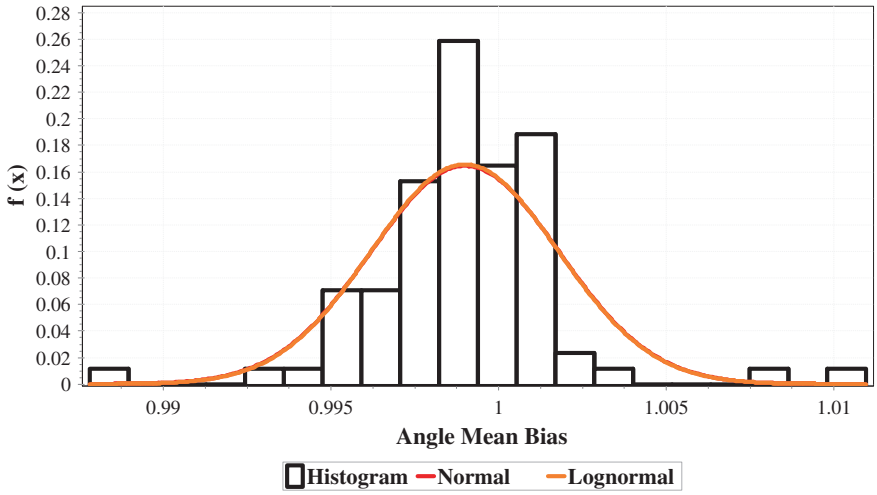

Fig. 4.7 Probability density function for angle variation

strength obtained from mill certificates are 72 with nominal yield strength of 340, 345 and 355 MPa. Three distributions are fitted, and the best fit is reported as per goodness-of-fit tests. The analysis shows that the collected data fit with the normal distribution though lognormal is very close and Weibull came at third place. The results achieved in China report normal distribution and from North Sea, DNV Code and ISO 19902 reported Lognormal, though DNV in another study [9] recommended normal distribution for material strength variable.

For tensile strength, sample size is 72, and mill tests reported characteristic strength of 490 MPa. The best fit is found to be normal distribution; other

Table 4.3 Statistical variation in yield strength

Type of variability	Statistical parameter	MS	Duan [5]	ISO (BOMEL) [6]	Adams [7]
Yield strength	Distribution	Normal	Normal	Log-normal	Log-normal
	MC	1.230	1.12	1.13	1.02–1.09
	VC	0.050	0.05	0.06	–
Tensile strength	Distribution	Normal	–	–	–
	MC	1.123	–	–	–
	VC	0.039	–	–	–
Elongation	Distribution	Normal	–	–	–
	MC	1.520	–	–	–
	VC	0.090	–	–	–

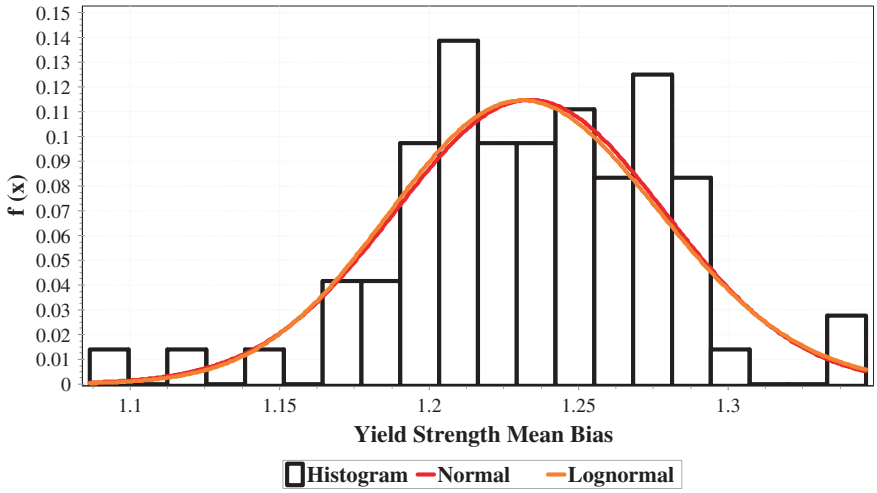

Fig. 4.8 probability density function for yield strength

parameters are mean bias 1.123 and COV 0.039. For elongation, sample size is 70, and characteristic value of 18–20 % is reported in mill certificates. After analysis, the distribution as per goodness-of-fit test is found to be normal, with mean bias of 1.52 and COV of 0.09.

4.4 Probabilistic Model Stresses Used in ISO Code 19902

Once basic random variables results are available and it is easy to find resistance model uncertainties using ISO 19902 model stress equations. The model uncertainty (x_m) is determined so that it could be used for reliability analysis of Jacket platforms in offshore Malaysia.

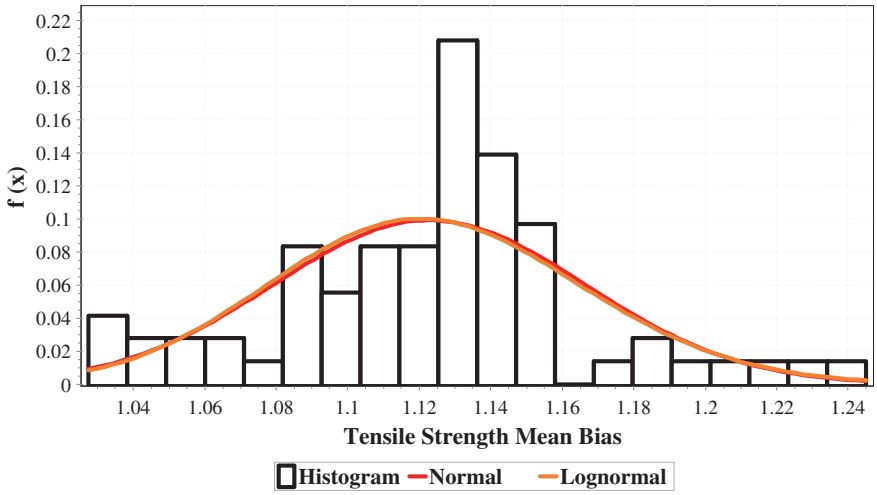

Fig. 4.9 Probability density function for tensile strength

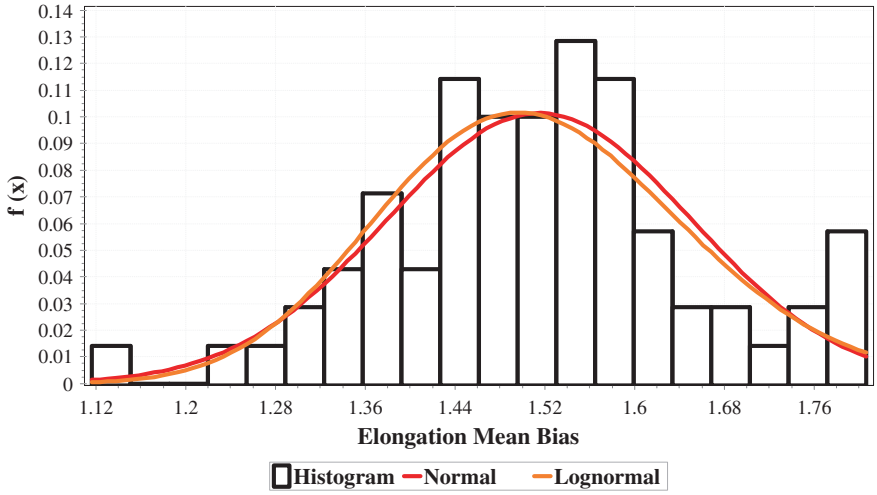

Fig. 4.10 probability density function for elongation

4.4.1 Component Stresses

API RP2A WSD and ISO 19902 code of practice identify nine types of stresses which Jacket members undergo during operating and storm loading conditions. Monte Carlo simulation is used to find stress variability as it is difficult to find the variability using test modelling. Simulated sample size is fixed at 1×10^5, and the

nominal f_y used is 345 MPa. Probability distribution curve again showed that the difference in normal and lognormal is very small as compared to Weibull. The best fit is normal for all types of component stresses.

4.4.1.1 Single Stresses

ISO 19902 and API RP2A code identify member stresses, in which Jacket platform undergoes during operation. Table 4.4 and Figs. 4.11, 4.12, 4.13, 4.14, 4.15 and 4.16 show the statistical properties and PDF for single stress. Parameters of distribution for geometric and material properties used in the given equation are normal. The law of probability says that combined distributions will give the result of normal distribution. BOMEL shows the data reported for North Sea which is incorporated in ISO code. Duan et al. [5] show data analysis for China LRFD. The report of MSL depends on experimental results from tubular members. Result shows minor variation in mean coefficients. The range of mean coefficients is in between 1.13 and 1.26 here, except for hydrostatic where it is 1.59. The given range for ISO is 1.0–1.14, and for China, it is 1.16–1.32. The variation coefficient is in between 0.05 and 0.16. For ISO, it is between 0.0 and 0.14, and for China, it is 0.07–0.12.

4.4.1.2 Two Stresses

Table 4.5 and Figs. 4.17, 4.18 and 4.19 show the uncertainty model for the combined two stress code equations. In this text, the mean values achieved are 1.19 to 1.27. For ISO code, the same are in range of 1.03–1.25 which is not much different from the results presented in this book. The standard deviation achieved here is in range of 0.047–0.050. The same achieved for ISO code is 0.083–0.094, which shows more variation in the results. This is due to difference in basic random variables used by ISO code. Other reasons such as improved quality of material and fabrication standards introduced in the manufacturing industries in recent years may also have reduced the variability here. Due to these reasons, uncertainties are reduced, with less variability in material and in geometry of tubular members. MSL and BOMEL 2001 studies showed similar trend as is shown in this text.

4.4.1.3 Three Stresses

Table 4.6 and Figs. 4.20, 4.21 and 4.22 show the uncertainty model for the given ISO code equations. The mean biases achieved in this text are 1.27–1.30, and the same for ISO is in the range of 1.08–1.20. This shows that mean values are higher by small margin as compared to ISO code. The standard deviation is 0.05, and for ISO, it is 0.11–0.16 which is higher than this book, showing higher variation in ISO data. MSL

Table 4.4 Resistance model uncertainty for single stress

Types of stresses	SP	MS	ISO (BOMEL) [6]	Duan [5]	MSL [10]		BOMEL 2001 [11]	Moses, 1995 [12]
					ISO, 2000	WSD, 2000		
Tension	MC	1.26	1.0	1.19	–	–	–	–
	VC	0.05	0.0	0.07	–	–	–	–
Column buckling	MC	1.26	1.05	1.16	1.26	1.16	1.06	1.19
	VC	0.05	0.04	0.12	0.06	0.08	0.05	0.12
Local buckling	MC	1.24	1.07	1.23	1.26	1.40	1.07	–
	VC	0.05	0.07	0.10	0.09	0.08	0.07	–
Bending	MC	1.13	1.11	1.32	1.16	1.43	1.11	1.26
	VC	0.05	0.09	0.11	0.09	0.12	0.10	0.11
Shear	MC	1.26	1.0	1.19	–	–	–	–
	VC	0.05	0.05	0.08	–	–	–	–
Hydrostatic	MC	1.59	1.14	–	1.43	1.85	1.14	1.05
	VC	0.16	0.14	–	0.12	0.12	0.12	0.11–0.15

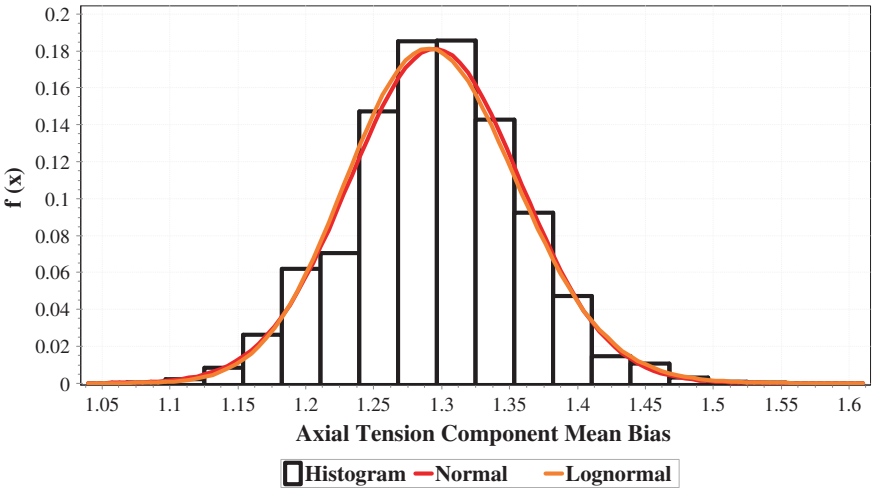

Fig. 4.11 Probability density function for tension

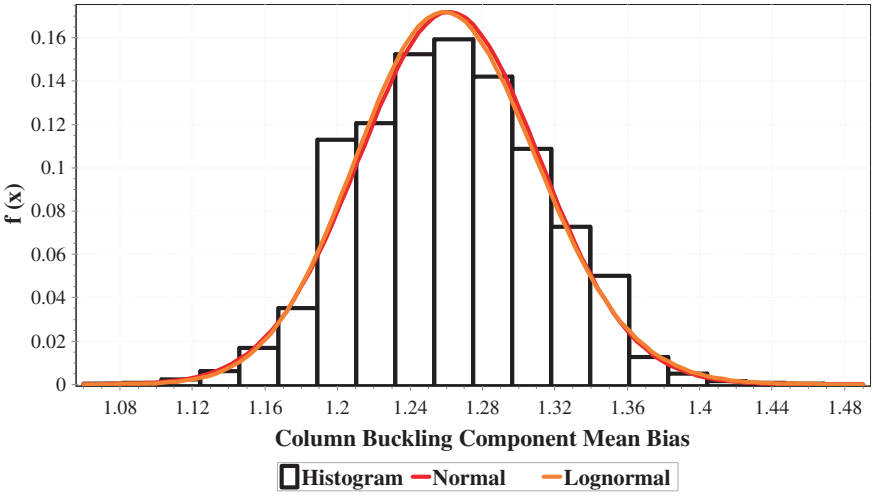

Fig. 4.12 Probability density function for column buckling

and BOMEL 2001 showed similar trend. The variability in this text is less than as reported in literature. Thus, with less uncertainty, higher reliability can be achieved.

4.4.2 Joint Stresses

There are three types of joints, i.e. K-, Y/T- and X joints used in Jacket platform as defined by codes of practice. Offshore Jacket design codes identify four types of stresses under which each joint is subjected at site. Probability distribution curve

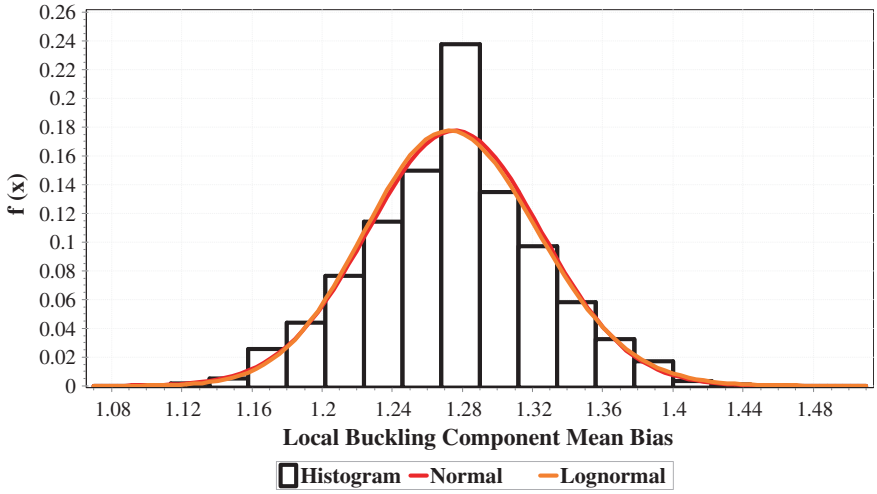

Fig. 4.13 Probability density function for local buckling

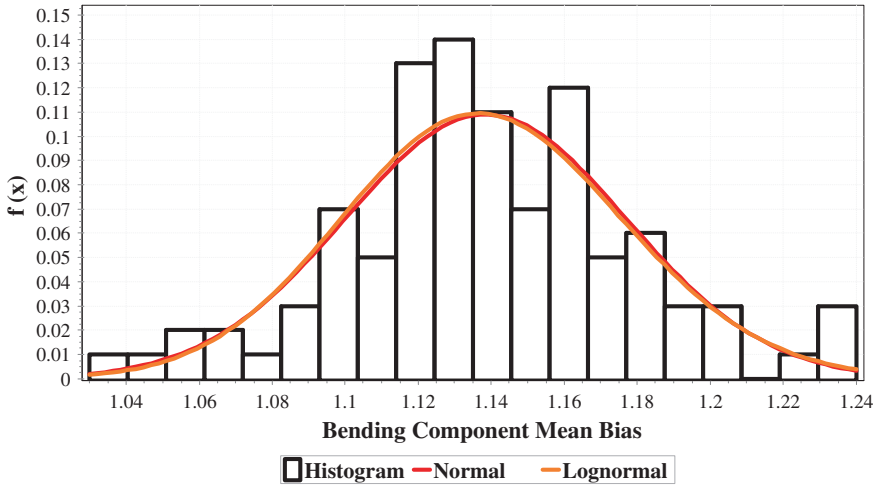

Fig. 4.14 Probability density function for bending

again showed that the difference in normal and lognormal is very small as compared to Weibull. The best fit is normal for all types of joints and for all stresses. The variability in this text is less than as reported in literature. With less uncertainty, higher reliability can be achieved.

4.4.2.1 K-Joint

Table 4.7 and Figs. 4.23, 4.24 and 4.25 show the uncertainty model for K-joint stress equations. ISO gives same equation in case of K-joint for compression

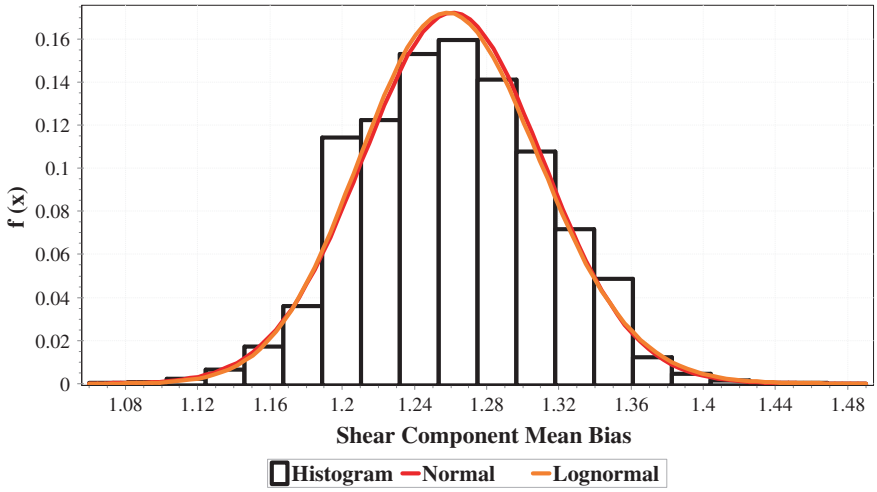

Fig. 4.15 Probability density function for shear

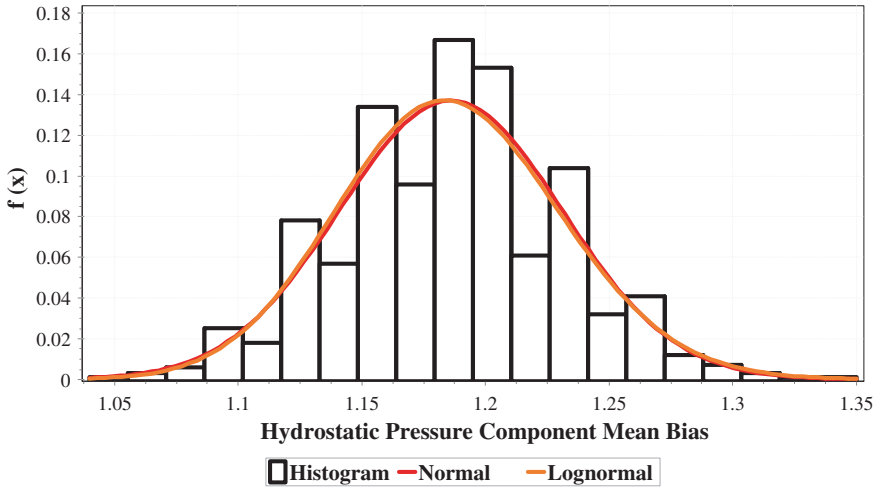

Fig. 4.16 PDF for hydrostatic pressure (hoop buckling)

Table 4.5 Resistance model uncertainty for combined two stresses

Types of stresses	SP	MS	ISO (BOMEL) [6]	MSL, 2000 [10]			BOMEL, 2001 [11]
				ISO	LRFD	WSD	
TB	MC	1.19	1.11	–	–	–	–
	VC	0.05	0.10	–	–	–	–
CB (column buckling)	MC	1.27	1.03	1.14	1.15	1.15	1.03
	VC	0.05	0.08	0.10	0.10	0.09	0.08
CB (local buckling)	MC	1.23	1.25	1.41	1.43	1.61	1.25
	VC	0.05	0.08	0.06	0.05	0.11	0.08

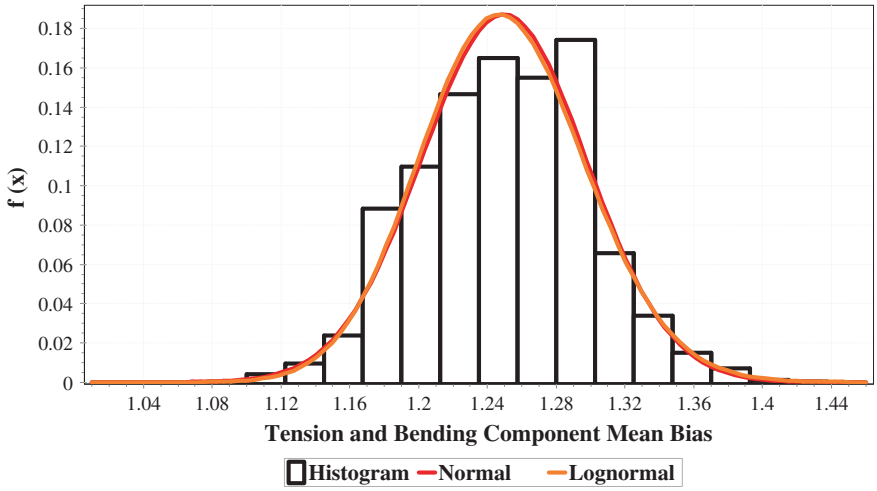

Fig. 4.17 Probability density function for tension and bending

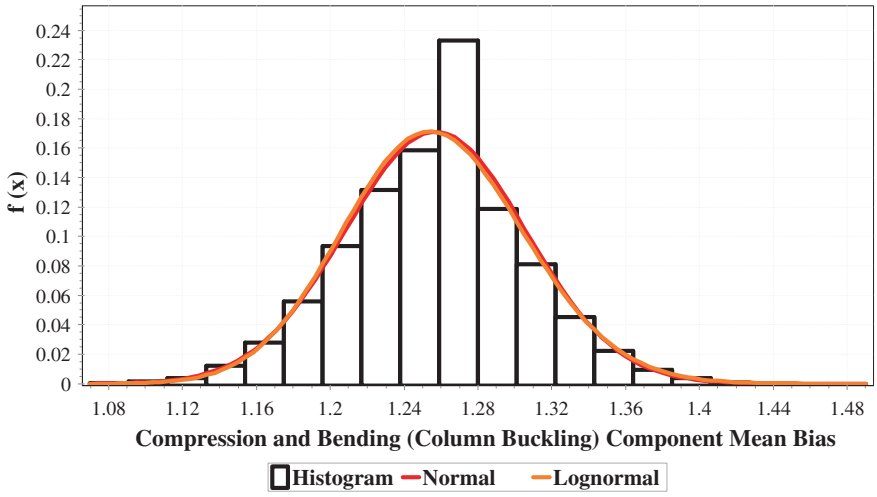

Fig. 4.18 PDF for compression and bending (column buckling)

and tension. The mean bias achieved in this text is 1.27–1.29 for all four types of stresses. The same for ISO is in the range of 1.22–1.24 which depends on actual test results reported by MSL. This shows that mean values here are higher by small margin as compared to ISO code. The standard deviation in this text is 0.10, and for ISO, it is 0.13–0.18 which is higher than the values given in this text, showing higher variation in ISO data.

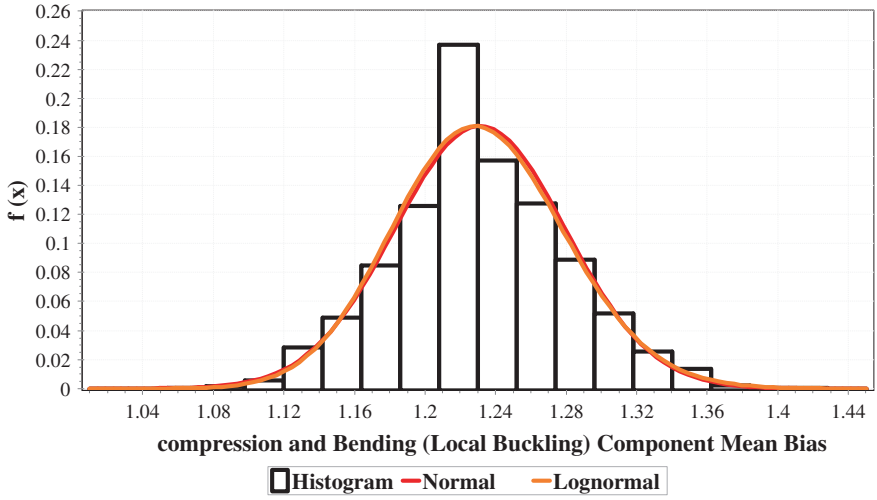

Fig. 4.19 PDF for compression and bending (local buckling)

Table 4.6 Resistance model uncertainty under combined three stresses

Types of stresses	SP	MS	ISO (BOMEL) [6]	MSL,2000 [10]			BOMEL, 2001 [11]
				ISO	LRFD	WSD	
TBH	MC	1.27	1.08	–	–	–	–
	VC	0.05	0.11	–	–	–	–
CBH (column buckling)	MC	1.28	1.20	1.33	1.29	1.43	1.25
	VC	0.05	0.11	0.16	0.12	0.20	0.14
CBH (local buckling)	MC	1.30	1.20	1.35	1.36	1.63	1.25
	VC	0.05	0.16	0.19	0.13	0.19	0.14

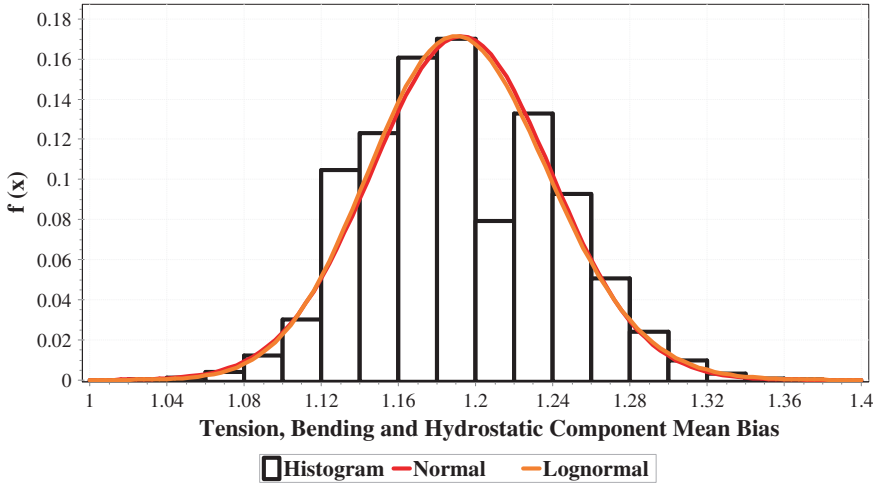

Fig. 4.20 PDF for tension, bending and hydrostatic pressure

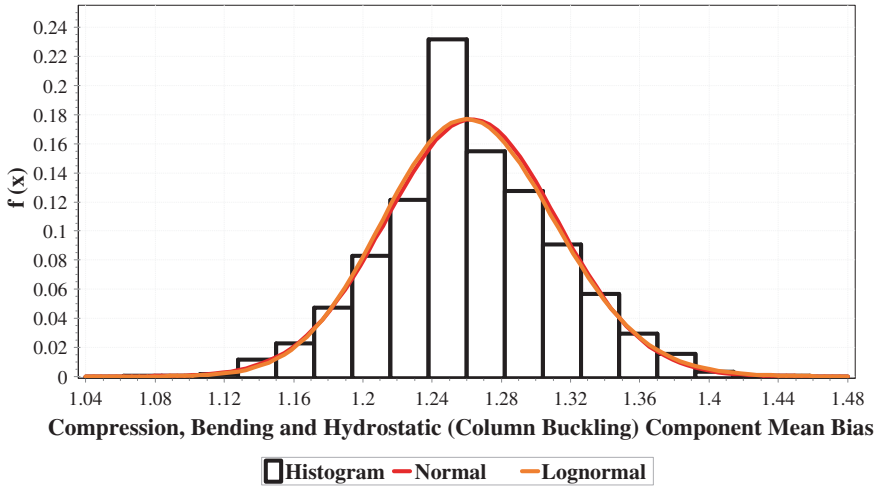

Fig. 4.21 PDF for compression, bending and hydrostatic pressure (column buckling)

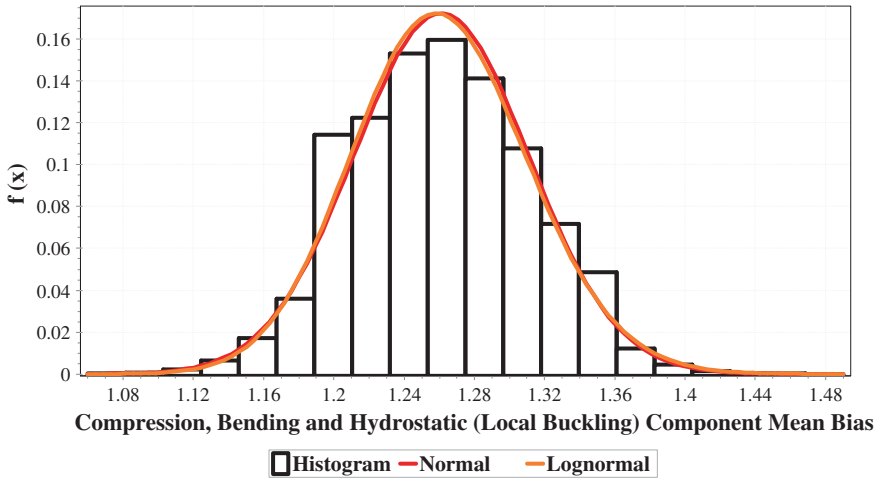

Fig. 4.22 PDF for compression, bending and hydrostatic pressure (local buckling)

Table 4.7 Resistance model uncertainties of K-joint

Types of stresses	SP	MS	Duan [5]	ISO (BOMEL) [6]	Ferguson [13]	MSL [10]	
						ISO (LRFD)	API (WSD)
Tension/ compression	MC	1.29	1.58	1.23	1.22	1.23	1.7
	VC	0.10	0.23	0.17	0.1	0.17	0.15
IPB	MC	1.27	1.31	1.24	1.29	1.24	1.64
	VC	0.10	0.21	0.13	0.14	0.13	0.15
OPB	MC	1.27	1.14	1.22	1.23	1.22	1.48
	VC	0.10	0.26	0.18	0.16	0.18	0.20

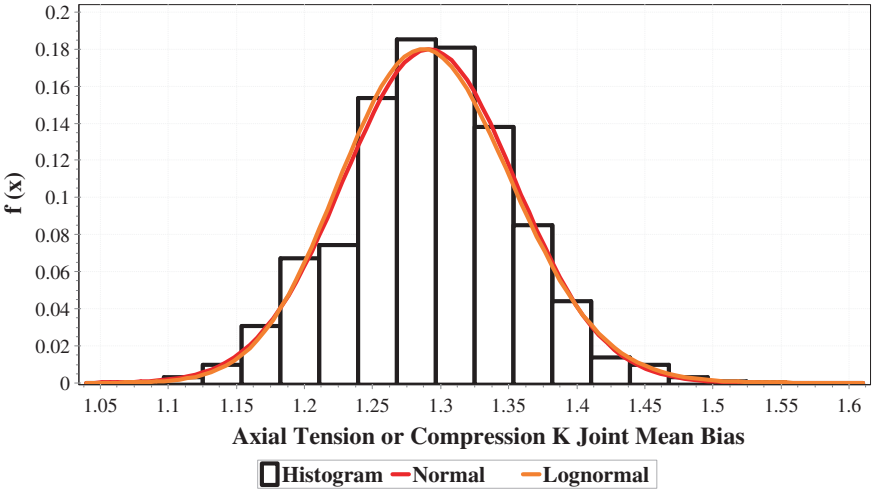

Fig. 4.23 Probability density function for K-joint tension/compression

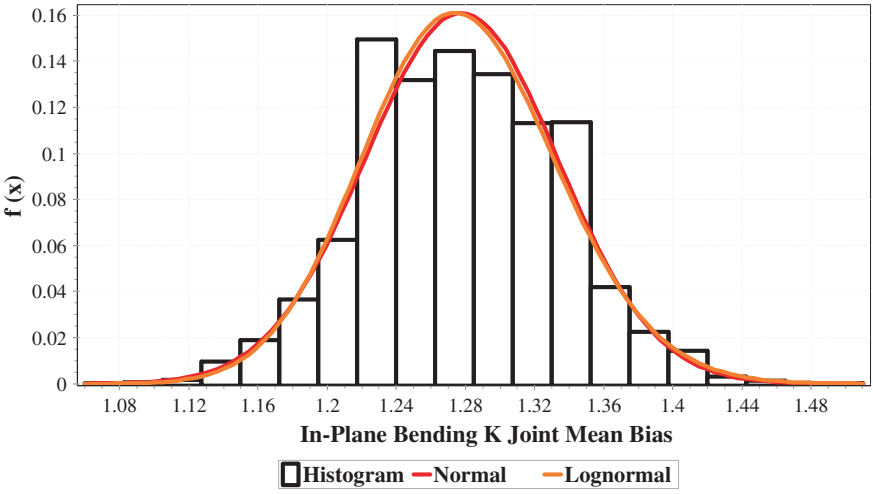

Fig. 4.24 Probability density function for K-joint IPB

4.4.2.2 T/Y-Joint

Table 4.8 and Figs. 4.26, 4.27, 4.28 and 4.29 shows the uncertainty model for T/Y-joint stress equation. The mean bias achieved here is 1.27–1.30 for all four types of stresses, and the same for ISO is in the range of 1.21–1.71. The standard deviation in this text is 0.10, and for ISO, it is 0.13–0.41 which is higher than the values presented here, showing higher variation in ISO data.

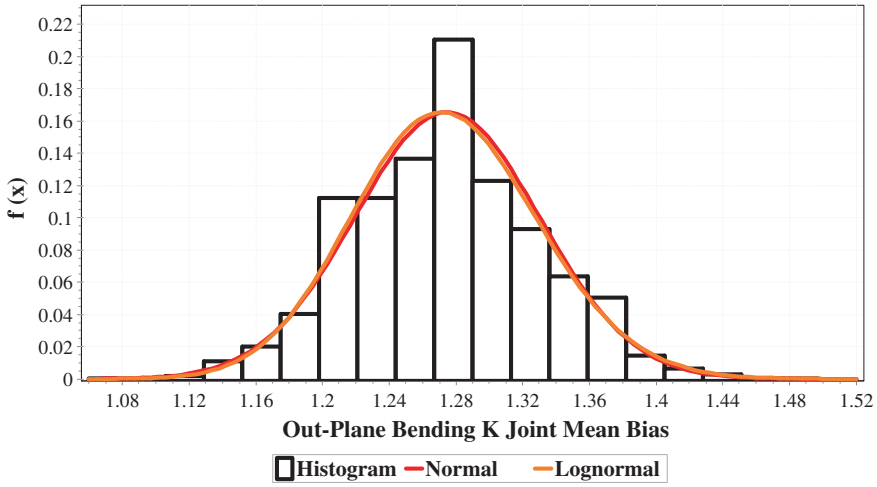

Fig. 4.25 Probability density function for K-joint OPB

Table 4.8 Resistance model uncertainties of T/Y-joint strength

Types of stresses	SP	MS	Duan [5]	ISO (BOMEL) [6]	Ferguson [13]	MSL [10]	
						LRFD	WSD
Tension	MC	1.30	1.53	1.71	1.48	1.70	2.3
	VC	0.10	0.28	0.41	0.43	0.40	0.74
Compression	MC	1.30	1.28	1.27	1.12	1.30	1.4
	VC	0.10	0.21	0.17	0.09	0.16	0.20
IPB	MC	1.28	1.31	1.21	1.29	1.21	1.66
	VC	0.10	0.21	0.13	0.14	0.12	0.25
OPB	MC	1.27	1.14	1.27	1.23	1.27	1.46
	VC	0.10	0.26	0.15	0.16	0.14	0.25

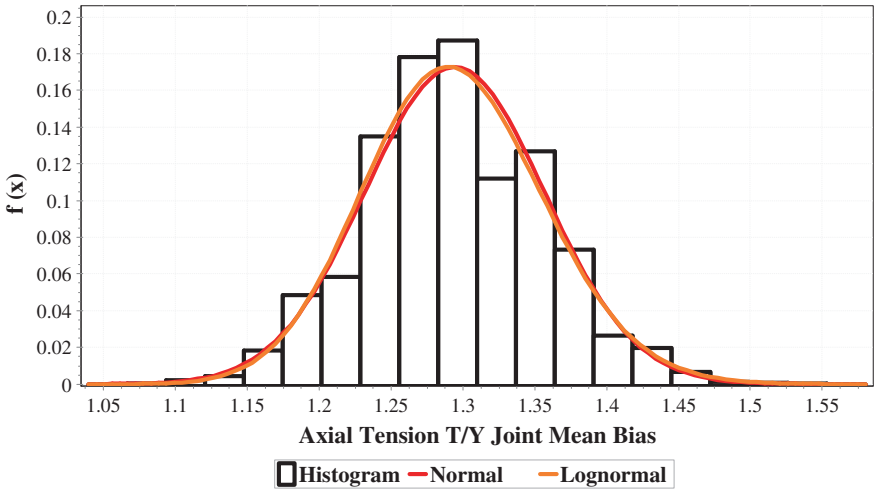

Fig. 4.26 Probability density function for T/Y-joint axial tension

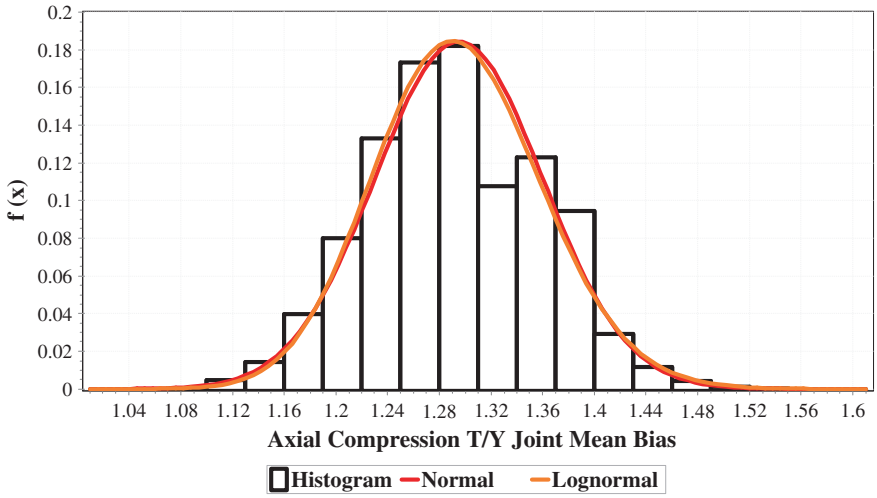

Fig. 4.27 Probability density function for T/Y-joint axial compression

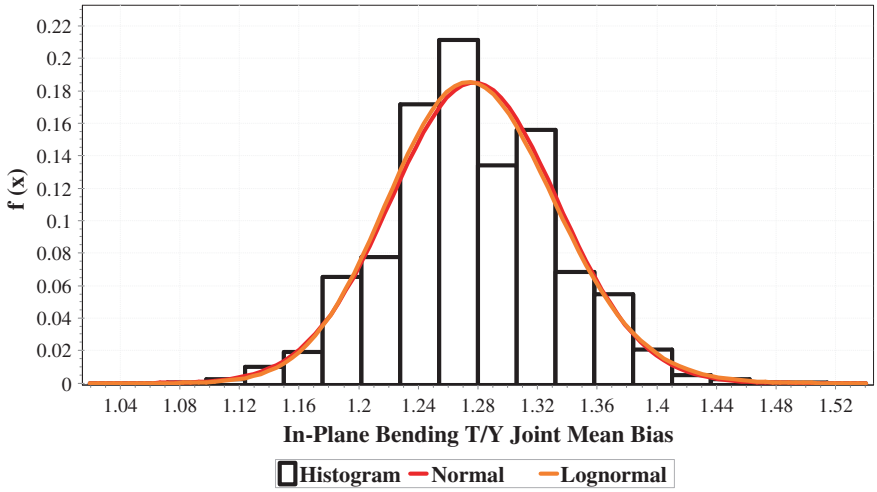

Fig. 4.28 Probability density function for T/Y-joint IPB

4.4.2.3 X-Joint

Table 4.9 and Figs. 4.30, 4.31, 4.32 and 4.33 show the uncertainty model for X-joint stress equation. The mean bias achieved here is 1.24–1.28 for all four types of stresses, and the same for ISO is in the range of 1.14–1.40. The standard deviation is 0.04–0.068, and for ISO, it is 0.06–0.25 which is higher than as given in this book, showing higher variation in ISO data.

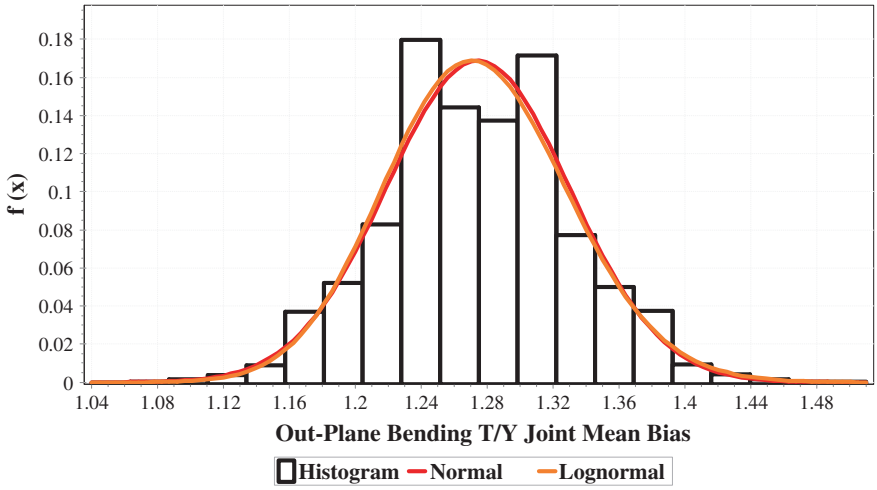

Fig. 4.29 Probability density function for T/Y-joint OPB

Table 4.9 Resistance model uncertainties of X-joint strength

Types of stresses	SP	MS	Duan [5]	ISO (BOMEL) [6]	MSL [10]	
					ISO(LRFD)	API (WSD)
Tension	MC	1.24	1.68	1.40	1.4	2.0
	VC	0.04	0.18	0.27	0.25	0.96
Compression	MC	1.29	1.2	1.17	1.2	1.4
	VC	0.07	0.16	0.11	0.10	0.13
IPB	MC	1.28	1.31	1.24	1.23	1.76
	VC	0.06	0.21	0.09	0.09	0.28
OPB	MC	1.28	1.14	1.14	1.13	1.47
	VC	0.06	0.26	0.07	0.06	0.11

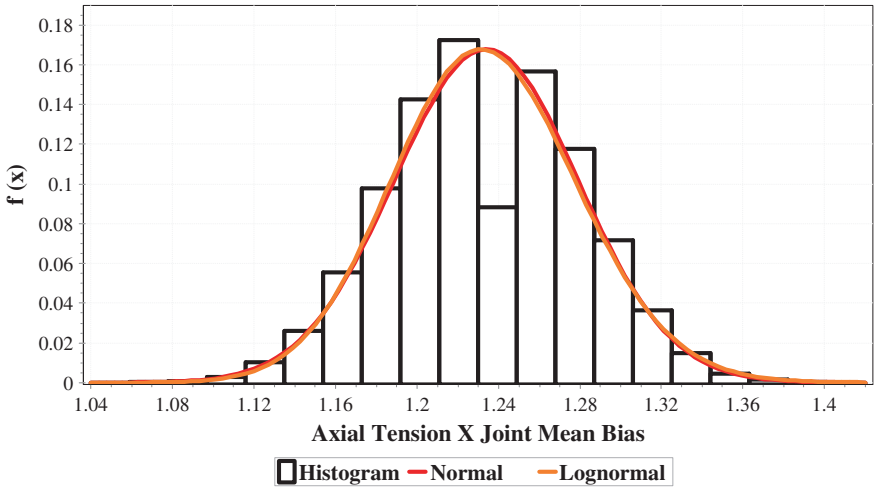

Fig. 4.30 Probability density function for X-joint axial tension

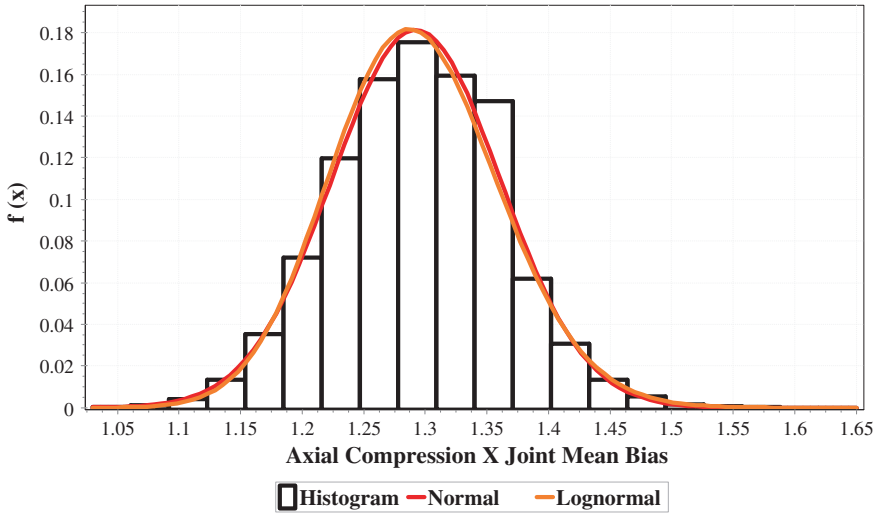

Fig. 4.31 Probability density function for X-joint axial compression

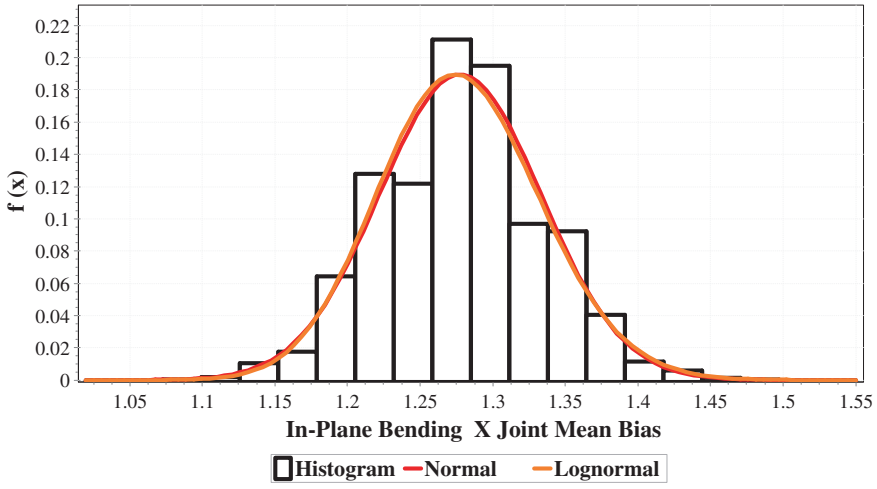

Fig. 4.32 Probability density function for X-joint IPB

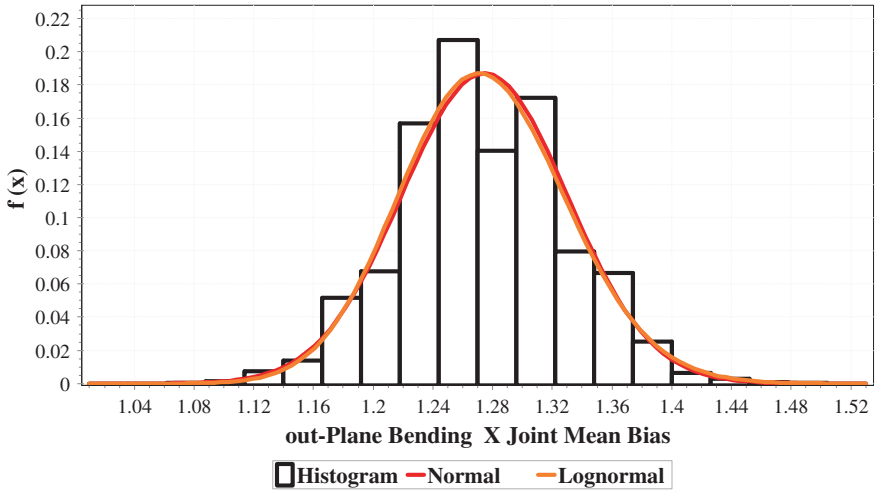

Fig. 4.33 Probability density function for X-joint OPB

4.5 Summary

To develop reliability models, we need to identify the variability in actual tubular members and model stress equations used by ISO code. The actual strength of tubular member varies from the characteristic/nominal strength. This is due to the variation in basic variables such as material strength and dimensional properties, i.e. yield strength, elastic modulus, diameter and thickness. The resistance of Jacket reduces with time period due to effects of ocean environment. This problem is catered by providing certain safety factor while designing the Jacket. The bias and COV evaluated, on the basis of data base of actual data, reflected that geometry and material variability existed in Malaysia as is expected which is also reported in GOM, North Sea and China. Following are the main conclusions from this chapter.

1. Uncertain basic variables, i.e. thickness, diameter, yield strength, tensile strength, elongation and angle, are modelled depend on actual variability in the material available in Malaysia. The standard deviation and mean bias and COV are evaluated, and the reported values show similarity between this book and the studies conducted in GOM, North Sea and China. This book shows less variability in basic parameters of resistance uncertainty.
2. Nine ISO code stress equations for component and eleven for joints are statistically modelled for evaluating model uncertainty. The model equations recommended by ISO code are used to find the variability of model uncertainty. The uncertainty models achieved are compared with models developed for ISO 19902 and in China. The variation in this book is less than that reported in literature. Using this variability in the reliability model, the offshore Malaysia Jacket will have higher reliability. The results from this research are used for reliability analysis of components and joints using ultimate limit state design of Jacket platforms in Malaysia.

References

1. Marley, M., Etterdal, B., Grigorian, H.: Structural reliability assessment of Ekofisk Jacket under extreme loading, presented at the Offshore Technology Conference, OTC 13190, Houston (2001)
2. Ingebrigtsen, T., Loset, O., Nielsen, S.G.: Fatigue design and overall safety of grouted pile sleeve connections, in Offshore technology conference, OTC 6344, Houston (1990)
3. Johansen, N.J.T.: Partial safety factors and characteristics values for combined extreme wind and wave load effects. J. Solar Energy Eng. ASME **127**(2), 242–252 (2005)
4. ISO-2394: General principles on reliability for structures, ISO (1998)
5. Duan, Z.D., Zhou, D.C., Ou, J.P.: Calibration of LRFD format for steel jacket offshore platform in china offshore area (1): statistical parameters of load and resistances. China Ocean Eng. **20**(1), 1–14 (2005)
6. BOMEL(a): Component based calibration of North Western European annex environmental load factors for the ISO fixed steel offshore structures code 19902 (2003)
7. Adams, A.J., Warren, A.V.R., Masson, P.C.: On the development of reliability-based design rules for casing collapse, SPE 48331 (1998)
8. Niels, J., Peter, H., Sten, F.: Calibration of Partial Safety Factors For Extreme Loads in Wind Turbines, European Wind Energy Conference and Exhibition, Spain (2003)
9. DNV: Classification Note 30.6 "Structural Reliability Analysis of Marine Structures" (1992)
10. MSL: Load factor calibration for ISO 13819 regional annex: component resistance, Offshore Technology Report, 2000/072, Health and Safety Executive, UK (2000)
11. BOMEL: Comparison of tubular member strength provisions in codes and standards (2001)
12. Moses, F.: Application of reliability to formulation of fixed offshore design codes Presented at the marine structural reliability symposium (1995)
13. Ferguson, M.C.: A comparative study using API RP2A-LRFD Presented at the offshore technology conference, OTC 6308, Houston (1990)

Chapter 5
Uncertainty Modelling of Load

Abstract This chapter deals with statistical data analysis for load variables. The random variables are analysed with statistical distributions evaluated. The parameters of load distributions like mean and standard deviations are determined. An extrapolation up to 1,000 years of return period is made using Weibull and Gumbel distributions along with their parameters.

5.1 Introduction

Environmental load parameters, i.e. wind, wave and current, are considered as random variables. For load, it uses the database record, offshore Malaysia industry. Microsoft Excel is used to do the regression analysis for extrapolation of extreme event for sea state parameters, i.e. wind, wave and current. The extrapolation is made to acquire data for higher return periods. Least square fitting method is used to find cumulative distribution function.

5.2 Load Factor and Uncertainty

Uncertainty of random variable plays a significant role for the determination of reliability index. Load factor is suitable and appropriate means of finding the reliability of structures to meet local geographical requirements [1]. Load factors are produced by code calibration using reliability analysis. The basic input to the reliability analysis for environmental load factors for Jacket platforms is statistical parameters of environmental load [1, 2].

Z. Nizamani, *Environmental Load Factors and System Strength Evaluation of Offshore Jacket Platforms*, Ocean Engineering & Oceanography 4,
DOI 10.1007/978-3-319-15051-2_5

5.3 Load Uncertainty

Environmental load uncertainty is much higher than the capacity of Jacket or resistance uncertainty [3]. Loads acting on offshore platforms act in different directions. The gravity loads act vertically downwards, whereas environmental loads (wind, wave and current) act horizontally. For the design of Jacket, we need to know the maximum environmental loads ever to act on the structure. This maximum load which can occur at any time during the entire service life of Jacket is the most critical variable to be taken into account during design. ISO and API codes require 100-year extreme conditions of wave for the design of Jacket platforms. One sudden event may even exceed this condition and can reach up to extreme waves of 10,000-year return period. For instance, waves in Gulf of Mexico (GOM) during hurricane Evan are reported to have reached heights of 10,000-year return period. For the platforms designed for return period of 100 years, this makes the task of design engineer very difficult.

Due to these conditions, it is necessary to find the reliability of Jacket component and joint, depending on the design environmental conditions, and for system, the applied load is 10,000 years as recommended by ISO 19902. To find the reliability index, we need to have distribution parameters for the random variables for environmental loads, i.e. wave, wind and current. Therefore, first of all, distribution parameters are found using Weibull two-parameter and Gumbel distributions. Secondly, the linear model of these distributions is used for extrapolation of data corresponding to 10,000-year return period; then, the parameters of distributions are found. Design criteria for environmental loads are inherently uncertain for the design of Jacket platforms due to variability of climate. The main design parameters for Jacket platforms depend on statistical characteristics of wave, wind and current.

The metocean record from existing platform sites in Malaysia shows that there have been typhoons occurring in this region. The basic cause for this weather condition is strong wind surges in south-east of PMO region. This phenomenon is always prevailing during north-east monsoon months of November–March. Waves generated by typhoons can cause widespread damage on Jacket platforms.

Weibull distribution is taken for the wave, wind and current in North Sea [4]. Many authors have used Weibull distribution in preference to Gumbel distribution for environmental load parameters ranging from GOM, North Sea and Arabian Gulf [1, 5–8]. Statistics of extreme value is acquired through design wave which is depends on extrapolation of historical storm value data. The record period is usually very short as compared to the return period selected for probability of exceedance. This recorded period ranges 5–20 years, which makes extrapolation of data extremely important.

5.4 Wave and Current Directionality for Offshore Malaysia

The South China Sea is the largest semi-enclosed marginal sea in the north-west Pacific and connects to the outside seas through the Taiwan Strait, Luzon Strait, Mindoru Strait, Para Barke Strait, Banka Strait, Gaspar Strait, Karimata Strait and

Malaka Strait. The climate of this region is primarily well known for two main weather systems: monsoons and tropical cyclones. The prevalent directions of wave and current from the recorded data for the three regions of Malaysia are discussed in this text. Environmental loads on platforms consist of wind, current, wave, earthquake, snow, ice and movement of earth. This includes variation in hydrostatic pressure and buoyancy on tubular members caused by changes in wave and tide levels. These effects may be from any direction. Tides play a vital role in design elevations of structural elements, for example boat landings, fenders, decks and corrosion protection, splash zone treatment of steel members and upper limits of marine growth; they also play part in calculation of design forces on platform. Orientation of platform chosen depends on prevailing seas, winds, and currents and operational requirements. Wind force is also one of the criteria that influence the orientation of the platform. It acts upon the portion of the structure which is above water level like deck houses, derricks and equipment located on top side, but it is not dealt with as data with regard to directions are not sufficiently available.

5.4.1 South China Sea

Steel Jacket platform provides support (by piles driven into the seabed), and deck is placed on its top, which contains staff quarters, a drilling rig and production facilities. Wind is the most important parameter as it is not only primary and direct source of loading but also plays a big role in producing the waves as well as for some extent the currents also. Wind induces drag forces which are proportional to square of its velocity. Currents are formed by winds and ocean tides and induce drag forces on underwater tubular members of Jacket platforms. Waves are the major source of loading on offshore platform as it produces inertia, drag, lift, diffraction and buoyancy forces on the tubular members. This section focuses on determining the dominating directions of waves and currents in three regions of Malaysia. The data consist of twenty data sets at different locations from PMO, eleven at SBO and at SKO provided by local industry.

The environmental conditions change with geographical locations. In each region of the world, geography, foundation conditions, design wave heights, periods and tides may change, which has an impact on the design of offshore Jacket platform. ISO 19902 recommends each region to calibrate environmental load factors which are region specific. API RP2A-WSD and LRFD are available when an international code was developed with contributions from API (USA), Health and safety executive (HSE, UK), Norwegian Petroleum Directorate (NPD, Norway) and other countries [9]. In Malaysia, API RP2A WSD is still used for design of offshore Jacket platforms. For adopting LRFD design method, environmental load factors for this region need to be calculated by calibration process. In this book, environmental load factor and resistance factors are to be found by reliability-based calibration. ISO 19902 requires each offshore region to adopt region-specific environmental load factors.

The tropical cyclones which are called hurricane in Atlantic and typhoon in Pacific are to be looked into as these are responsible for extreme conditions which govern the design [10]. The region is not much affected by typhoons, but they do occur rarely. PMO has already seen one typhoon Vamei in 2001. This is the only typhoon reported in metocean (meteorological and oceanographic) reports available. SBO is located near Philippines which is subjected to many typhoons. Typhoon Greg passed this region in 1996. Metocean reports mention the direction towards W-SW of SBO. For SKO, there are two storms mentioned in metocean data. The closest typhoon came to this region was typhoon Percy in 1983 and the typhoon Greg which made fall in SBO in 1996.

Most often, the design practice for the design wave in GOM for fixed offshore platforms is to use a wave height (vertical distance between a crest and the preceding trough, where both are defined by zero-crossing periods, [11] with a 1 % annual probability of exceedance, i.e. 100-year return period [12]. It is the average period of time between successive occurrences of events at the site. Hundred-year event is taken for offshore structures, which means it has an exceedance probability (being equalled or exceeded) of 1 % (0.01) in any one year, i.e. probability = 1/100. The 100-year wind, 100-year wave and 100-year current are conservatively assumed to occur simultaneously and act in the same direction. This design load for a Jacket is much more severe than the true 100-year load as it is very much possible that wind, wave and current may not act simultaneously in the same direction [13]. From Hurricanes, the effect on platforms in GOM has been reported in the literature where it can be seen that wave direction plays a major part for the stability of the platform. Thus, directional wave and wind should be considered before design of platform.

Wind-driven waves produce environmental forces on Jacket platforms. These waves have no regular shape, varying height and length and reach structure from many directions at the same time; this makes their intensity and distribution of forces a very complex phenomenon. This requires determination of wave criteria for extreme and normal conditions. Design parameters for offshore structures depend largely on knowledge about water depths and tides. Tides and currents influence the determination of forces acting on platform. The wave data collected at site consist of many years of data. These data are mainly collected during approximately the past 10 years. The data are normalised with respect to the maximum at the said site. For example, at one site, wave height is 7.3, 5.8, 5.1 and 4.4 in NE, NW, SE and SW. Then, NE direction has 7.7/7.3 = 1, NW 5.8/7.3 = 0.79.

5.4.2 Wave

The environmental load on offshore platforms is a combination of waves, currents and wind though waves are the dominant factor [13]. Jacket platforms are naturally more sensitive to waves than wind and currents; that is, the peak response is expected to occur at the time of maximum wave height, whereas in compliant platform the peak response may happen at other time as it depends on magnitudes

and directions of three environmental parameters at each instant in time [12]. Table 5.1 shows the significant wave height values at three regions of Malaysia, which shows there are a lot of variations in these values.

Table 5.2 shows the normalised values of significant wave height with respect to maximum value in the governing direction.

These normalised values at region 1 at various locations ranging from a to t are shown in Table 5.3. From the table, it is clear that the direction of NE is governing wave direction for maximum sites except three sites. Then comes the NW, which though governing one site has also secondary effects. SE and SW are almost equal as they govern only some time and most of the time less than the NE and NW. Table 5.3 shows the normalised values of significant wave height at SBO at various locations a–g. Here, NW direction is governing most of the time; NE direction is governing two sites only. Then comes the SW, which though governs only one site has also some influence on platform. The wave effect from SE direction is very minimal.

Table 5.1 Maximum and critical values (in maximum direction) of significant wave height

Location	Significant wave height (Hs) varies between (m)	
	Maximum	Minimum (critical direction)
PMO	7.3	4.6
SBO	6.5	3.8
SKO	6.4	2.7

Table 5.2 100-year significant wave height (PMO)

Locations	NW	NE	SE	SW
a	1	0.79	0.6	0.51
b	0.87	1	0.62	0.64
c	0.74	1	0.51	0.43
d	0.75	1	0.52	0.44
e	0.71	1	0.57	0.45
f	0.75	1	0.55	0.45
g	0.78	1	0.48	0.63
h	0.73	1	0.5	0.42
i	0.57	0.46	0.75	1
j	0.75	1	0.49	0.42
k	0.71	1	0.79	0.71
l	0.8	1	0.51	0.67
m	0.66	1	0.51	0.51
n	0.71	1	0.57	0.45
o	0.8	1	0.51	0.67
p	0.79	1	0.49	0.68
q	0.7	1	0.54	0.42
r	0.79	1	0.48	0.54
s	0.54	0.46	0.77	1
t	0.6	0.8	0.96	1

Table 5.3 100-year significant wave height (SBO)

Locations	NW	NE	SE	SW
a	1	0.85	0.45	0.85
b	1	1	0.3	0.7
c	1	1	0.29	0.71
d	1	0.51	0.3	1
e	1	0.76	0.29	0.84
f	1	0.84	0.4	0.84
g	1	0.84	0.56	0.84

Table 5.4 100-year significant wave height (SKO)

Locations	NW	NE	SE	SW
a	1	1	0.31	0.6
b	1	0.9	0.51	0.69
c	1	0.32	0.32	0.74
d	1	0.87	0.32	0.87
e	1	0.9	0.51	0.69
f	1	0.59	0.41	1
g	1	0.3	0.3	0.8
h	1	0.91	0.3	0.7
i	1	0.9	0.51	0.69
j	1	1	0.61	0.8
k	1	1	0.45	0.77
l	1	1	0.45	0.77
m	1	1	0.51	0.8
n	1	0.9	0.51	0.71
o	1	0.89	1	1
p	1	1	0.38	0.67
q	1	1	0.52	0.78
r	1	1	0.54	0.75
s	1	1	0.52	0.7

Table 5.4 shows the normalised values of significant wave height at SKO at various locations ranging from a to s. From the table, it is clear that NW and NE directions are most of the time equally governing. Then comes the SW, which though governs only two places has also influence on platform. The wave flow in SE direction is again very minimal.

5.4.3 Current

Current influences the design, construction and operation of Jacket platforms. They are important with regard to (i) location and orientation of boat landings and barge bumpers/fenders, (ii) forces on the platform and (iii) sea floor scouring.

Boat landings and barge bumpers are located so as to allow the boat to engage the platform as it moves against the current. The speed and direction of current at specified elevation are indicated in the current profile. The current velocity varies through water column [14]. Total current profile related to sea state causing extreme waves is specified for platform design.

Table 5.5 shows the surface current speed at different locations of Jacket platform in the three regions of Malaysia. Table 5.6 shows the normalised values for current at PMO at various locations a–q. It is clear that NE is governing maximum currents flowing in this direction and then comes SW direction followed by SE, which governs two places, but in NW direction current seems to flow very occasionally and not governing any site.

Table 5.7 shows the normalised values for surface current at SKO1 at various locations of platforms a–g. Here, NE is governing maximum number of currents flowing in this direction and then comes SW direction which only governs one site followed by SE and NW direction with very few occurrences in this direction.

Table 5.5 Surface current at different regions for 100 years

Location	Platform	Surface current (m) for 100 years
PMO	a	1.47
	b	1.30
SBO	c	0.94
	d	0.87
SKO	e	1.05

Table 5.6 100-year surface current (PMO)

Locations	NW	NE	SE	SW
a	0.56	0.88	0.59	1
b	0.54	1	1	0.73
c	0.64	1	0.76	0.84
d	0.56	0.89	0.56	1
e	0.67	1	0.83	0.88
f	0.7	0.98	0.65	1
g	0.66	1	0.81	0.88
h	0.65	1	0.72	0.91
i	0.46	1	0.57	0.77
j	0.63	0.89	0.67	1
k	0.79	1	0.79	1
l	0.63	0.89	0.67	1
m	0.82	0.83	0.69	1
n	0.68	1	0.87	0.91
o	0.57	1	0.6	0.83
p	0.65	1	0.68	0.86
q	1	0.76	0.96	0.64

Table 5.7 100-year surface current (SKO1)

Locations	NW	NE	SE	SW
a	0.31	1	0.31	0.5
b	0.47	1	0.29	0.44
c	0.31	1	0.31	0.5
d	0.6	1	0.4	0.4
e	0.4	1	0.7	1
f	0.31	1	0.31	0.5
g	0.5	1	0.8	1

For SBO, only one data of current is available in which governing direction is NE, followed by SW.

The wave results show they have a clear bias towards NE in PMO, and for SBO, it is the NW, but at SKO it is balanced between NE and NW. Here, it can be considered that Jacket platforms are influenced from NE and NW directions. The data collection for waves as per international practice is 20 min in 3-h period.

5.5 Wave Load Models

The oceanographic data available for wave height have usually been of short period. From this small amount of data, we have to estimate extreme value of tail end of distribution and associated wave uncertainties for the large storm conditions which have extremely small probability of occurrence. Load uncertainty of significant wave height is of prime importance when evaluating the structural reliability. Coefficient of variation (COV) for annual extreme wave loading is more than 50 % in North Sea [3]. Heidman and Weaver report COV of 25 % for wave loads [3]. In this text, due to low mean values predicted by Weibull two parameter distributions, it is selected for structural reliability besides that it fitted well with existing available data.

5.5.1 PMO Region

Significant wave height defines the characteristic wave height of a random wave. It is the most important parameter of environmental data for offshore Jacket design. Tables 5.8 and 5.9 show significant wave heights distributed as per Weibull and Gumbel distributions in PMO for 12 platforms. Figures 5.1 and 5.2 show the extrapolated wave heights using CDF of respective distributions for PMO.

Table 5.8 Return period and significant wave (m), Weibull distribution PMO

PM	Return period in years				Weibull distribution parameters				
	10	10^2	10^3	10^4	Scale	Shape	Mean	SD	COV
A	4.9	5.3	5.53	5.70	4.46	8.83	4.22	0.57	0.14
B	4.8	5.2	5.43	5.60	4.36	8.66	4.12	0.57	0.14
C	5.2	5.6	5.83	6.00	4.76	9.35	4.51	0.58	0.13
D	5.5	6.5	7.08	7.50	4.50	4.15	4.09	1.11	0.27
E	5.1	5.5	5.69	5.90	4.66	9.18	4.41	0.58	0.13
F	4.9	5.4	5.69	5.90	4.36	7.13	4.08	0.67	0.17
G	4.3	4.6	4.77	4.90	3.96	10.28	3.78	0.44	0.12
H	5.7	6.8	7.44	7.90	4.61	3.93	4.17	1.19	0.29
I	4.5	4.9	5.13	5.30	4.06	8.14	3.83	0.56	0.15
J	4.4	4.7	4.87	5.00	4.06	10.51	3.87	0.44	0.11
K	4.6	5	5.23	5.40	4.16	8.31	3.93	0.56	0.14
L	4.5	4.8	4.97	5.10	4.16	10.74	3.97	0.45	0.11

Table 5.9 Return period and significant wave (m), Gumbel distribution PMO

PM	Return period in years				Gumbel distribution parameters				
	10	10^2	10^3	10^4	Scale	Location	Mean	SD	COV
A	4.9	5.3	5.69	6.08	5.87	4.52	4.62	0.22	0.05
B	4.8	5.2	5.59	5.98	5.87	4.42	4.52	0.22	0.05
C	5.2	5.6	5.99	6.38	5.87	4.82	4.92	0.22	0.04
D	5.5	6.5	7.48	8.46	2.35	4.54	4.79	0.55	0.11
E	5.1	5.5	5.89	6.28	5.87	4.72	4.82	0.22	0.05
F	4.9	5.4	5.89	6.37	4.70	4.42	4.54	0.27	0.06
G	4.3	4.6	4.89	5.18	7.83	4.01	4.09	0.16	0.04
H	5.7	6.8	7.87	8.96	2.14	4.65	4.92	0.60	0.12
I	4.5	4.9	5.29	5.68	5.87	4.12	4.22	0.22	0.05
J	4.4	4.7	4.99	5.28	7.83	4.11	4.19	0.16	0.04
K	4.6	5	5.39	5.78	5.87	4.22	4.32	0.22	0.05
L	4.5	4.8	5.09	5.38	7.83	4.21	4.29	0.16	0.04

The COV for wave, distributed as Weibull, gave variation between 12 and 29 %, whereas Gumbel gave COV between 4 and 12 %. Gumbel gave low COV values for corresponding wave height. The Weibull distribution mean values are lower than those estimated by Gumbel distribution. The Gumbel model overestimated the chance of large wave heights [15]. Due to this reason, Weibull distribution has been adopted for the reliability analysis of Jacket platforms as it proved to be a better fit. The same findings are reported by Monahan [16].

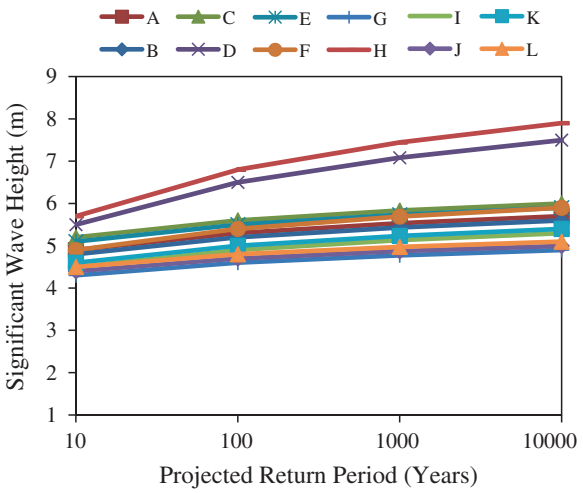

Fig. 5.1 Extrapolation of significant wave height (Weibull at PMO)

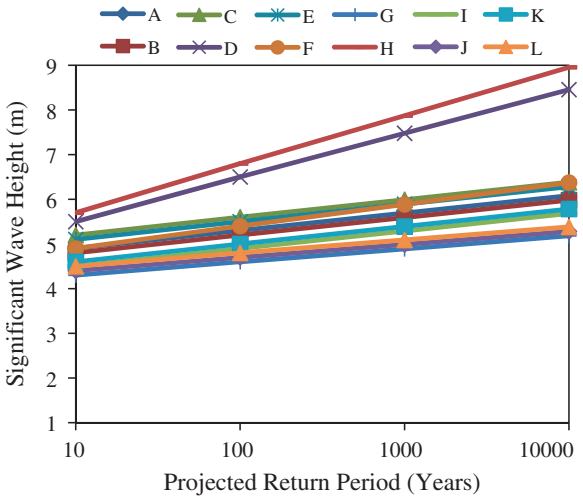

Fig. 5.2 Extrapolation of significant wave height (Gumbel at PMO)

5.5.2 SBO Region

Table 5.10 shows eight platforms' specific data from SBO using Weibull distribution, and Table 5.11 shows same platforms using Gumbel distribution. The range of 100-year wave height is 4.4–6.5 m, and for 10,000 years, it is 4.8–8.20 m as per the Weibull distribution shown in Fig. 5.3. Gumbel for same 10-year and 100-year wave height gave 10,000 return period of 5.27–9.83 m as shown in Fig. 5.4.

Table 5.10 Return period and significant wave (m), Weibull distribution SBO

SBO	Return period in years				Weibull distribution parameters				
	10	10^2	10^3	10^4	Scale	Shape	Mean	SD	COV
A	4.8	6.5	7.49	8.20	3.33	2.29	2.95	1.37	0.46
B	4.5	5.1	5.45	5.70	3.87	5.54	3.57	0.75	0.21
C	3.5	4.7	5.40	5.90	2.45	2.35	2.18	0.98	0.45
D	3.8	4.3	4.59	4.80	3.27	5.61	3.03	0.62	0.21
E	4.1	5.7	6.63	7.30	2.76	2.10	2.44	1.22	0.50
F	4.5	5.6	6.24	6.70	3.46	3.17	3.10	1.07	0.35
G	3.1	4.4	5.16	5.70	2.03	1.98	1.80	0.95	0.53
H	3.7	4.5	4.97	5.30	2.92	3.54	2.63	0.82	0.31

Table 5.11 Return period and significant wave (m), Gumbel distribution SBO

SBO	Return period in years				Gumbel distribution parameters				
	10	10^2	10^3	10^4	Scale	Location	Mean	SD	COV
A	4.8	6.5	8.16	9.83	1.38	3.17	3.59	0.93	0.26
B	4.5	5.1	5.69	6.27	3.92	3.93	4.07	0.33	0.08
C	3.5	4.7	5.87	7.05	1.96	2.35	2.65	0.65	0.25
D	3.8	4.3	4.79	5.27	4.70	3.32	3.44	0.27	0.08
E	4.1	5.7	7.26	8.83	1.47	2.57	2.96	0.87	0.29
F	4.5	5.6	6.68	7.76	2.14	3.45	3.72	0.60	0.16
G	3.1	4.4	5.67	6.95	1.81	1.86	2.17	0.71	0.33
H	3.7	4.5	5.28	6.06	2.94	2.93	3.13	0.44	0.14

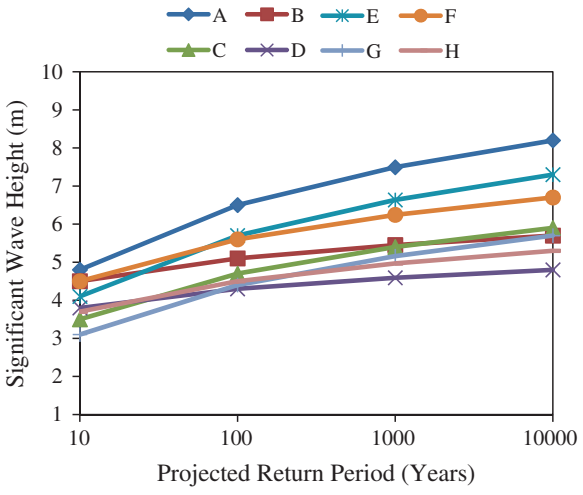

Fig. 5.3 Extrapolation of significant wave height (Weibull at SBO)

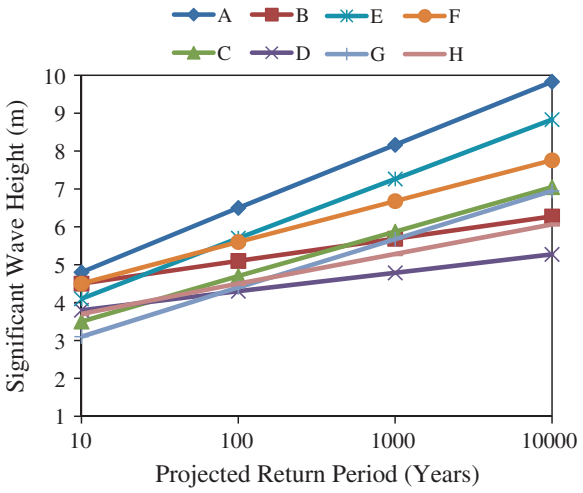

Fig. 5.4 Extrapolation of significant wave height (Gumbel at SBO)

5.5.3 SKO Region

Table 5.12 shows 13 platforms' specific data from SKO using Weibull distribution, and Table 5.13 shows same platforms using Gumbel distribution. The range of 100-year wave height is 4.4–6.4 m, and for 10,000 years, it is 5.0–8.10 m as per the Weibull distribution as shown in Fig. 5.5. The Gumbel for same 10-year and 100-year wave height gave 10,000-year return period wave heights of 5.57–9.73 m as shown in Fig. 5.6.

Table 5.12 Return period and significant wave (m) Weibull distribution SKO

SKO	Return period in years				Weibull distribution parameters				
	10	10^2	10^3	10^4	Scale	Shape	Mean	SD	COV
A	4	5.2	5.90	6.40	2.92	2.64	2.59	1.06	0.41
B	4	4.9	5.43	5.80	3.13	3.42	2.82	0.91	0.32
C	4.7	6.4	7.39	8.10	3.24	2.25	2.87	1.35	0.47
D	3.8	4.4	4.75	5.00	3.19	4.73	2.92	0.70	0.24
E	4.2	5.1	6.00	5.63	3.32	3.57	2.99	0.93	0.31
F	4.4	5.1	5.51	5.80	3.68	4.69	3.37	0.82	0.24
G	4.3	4.9	5.65	5.90	3.67	5.31	3.39	0.73	0.22
H	3.8	5.1	5.86	6.40	2.67	2.36	2.36	1.07	0.45
I	4.2	5.1	5.63	6.00	3.32	3.57	2.99	0.93	0.31
J	4.5	5.2	5.61	5.90	3.78	4.79	3.46	0.82	0.24
K	5	5.8	6.27	6.60	4.18	4.67	3.82	0.93	0.24
L	5.6	6.3	6.71	7.00	4.86	5.88	4.50	0.89	0.20
M	4.5	5.3	5.77	6.10	3.70	4.24	3.36	0.90	0.27

Table 5.13 Return period and significant wave (m), Gumbel distribution at SKO

SKO	Return period in years				Gumbel distribution parameters				
	10	10^2	10^3	10^4	Scale	Location	Mean	SD	COV
A	4	5.2	6.37	7.55	1.96	2.85	3.15	0.65	0.21
B	4	4.9	5.78	6.67	2.61	3.14	3.36	0.49	0.15
C	4.7	6.4	8.06	9.73	1.38	3.07	3.49	0.93	0.27
D	3.8	4.4	4.99	5.57	3.92	3.23	3.37	0.33	0.10
E	4.2	5.1	5.98	6.87	2.61	3.34	3.56	0.49	0.14
F	4.4	5.1	5.78	6.46	3.36	3.73	3.90	0.38	0.10
G	4.3	4.9	5.49	6.07	3.92	3.73	3.87	0.33	0.08
H	3.8	5.1	6.37	7.65	1.81	2.56	2.87	0.71	0.25
I	4.2	5.1	5.98	6.87	2.61	3.34	3.56	0.49	0.14
J	4.5	5.2	5.88	6.56	3.36	3.83	4.00	0.38	0.10
K	5	5.8	6.58	7.36	2.94	4.23	4.43	0.44	0.10
L	5.6	6.3	6.98	7.66	3.36	4.93	5.10	0.38	0.07
M	4.5	5.3	6.08	6.86	2.94	3.73	3.93	0.44	0.11

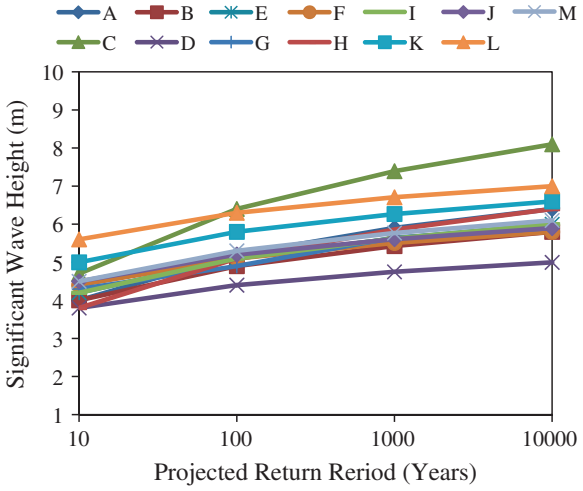

Fig. 5.5 Extrapolation of significant wave height (Weibull at SKO)

5.5.4 Gulf of Mexico (GOM) and North Sea (NS)

The data for GOM and North Sea are acquired from ISO code [14]. Table 5.14 and Fig. 5.7 show the Weibull distribution parameters for international waters. The waves are as high as 14.6 and 16.4 m for 100 years, and they are 20.70 and 18.50 m for 10,000 years. The COV is high for GOM with 79 % as compared to 29 % in North Sea. Table 5.15 and Fig. 5.8 show the Gumbel distribution parameters for international waters. For Gumbel, the GOM and North-North Sea 10,000-year return period wave gave 26.57 and 20.50 m. Gumbel gave 9–80 % of COV. The distributions depend on data acquired from ISO 19900-1.

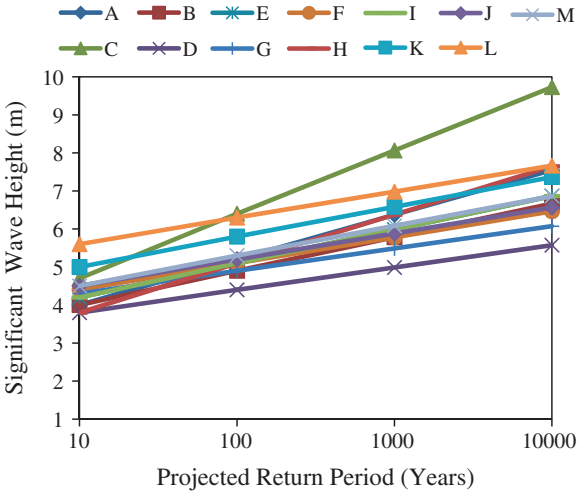

Fig. 5.6 Extrapolation of significant wave height (Gumbel at SKO)

Table 5.14 Return period and significant wave (m), Weibull at GOM and NS

	Return period in years				Weibull distribution parameters				
	10	10^2	10^3	10^4	Scale	Shape	Mean	SD	COV
GOM	8.5	14.6	18.17	20.70	4.43	1.28	4.11	3.23	0.79
SNS	7.5	9	9.88	10.50	6.02	3.80	5.44	1.60	0.29
CNS	11.8	13.6	14.65	15.40	9.95	4.88	9.12	2.13	0.23
NNS	14.3	16.4	17.62	18.50	12.13	5.06	11.14	2.52	0.23

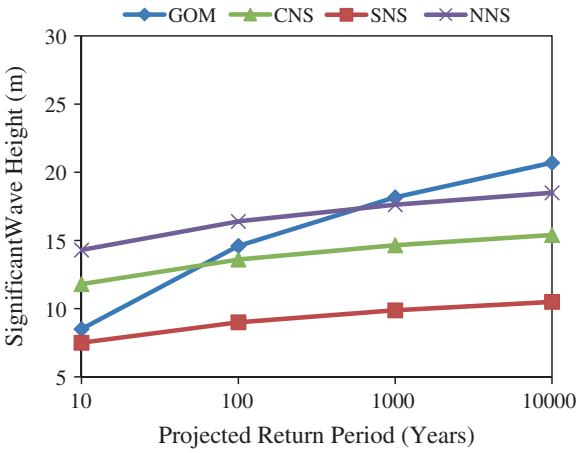

Fig. 5.7 Extrapolation of significant wave height, Weibull at GOM and NS

Table 5.15 Return period and significant wave (m), Gumbel at GOM and NS

	Return period in years				Gumbel distribution parameters				
	10	10^2	10^3	10^4	Scale	Location	Mean	SD	COV
GOM	8.5	14.6	20.59	26.57	0.39	2.66	4.16	3.33	0.80
SNS	7.5	9	10.47	11.94	1.57	6.06	6.43	0.82	0.13
CNS	11.8	13.6	15.36	17.13	1.31	10.08	10.52	0.98	0.09
NNS	14.3	16.4	18.45	20.50	1.12	12.29	12.80	1.15	0.09

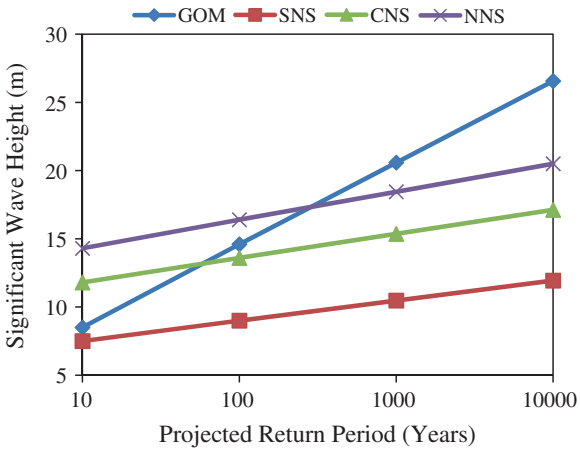

Fig. 5.8 Extrapolation of significant wave height, Gumbel at GOM and NS

5.6 Wind Load Model

Wind contributes less than 10 % of total base shear under extreme environmental loading. Wind loads contribute comparatively little to the total base shear [3]. Weibull and Gumbel distributions are fitted to the wind load model. Due to low mean values and data fitting well with existing values, 2-parameter Weibull distribution is selected.

5.6.1 PMO Region

From many previous studies, it has been shown that two-parameter Weibull distributions can fit well for surface wind speed on land and sea [16]. In this text, hourly mean wind speed is used which is measured at 10 m height. The COV is from Weibull distribution for wind speed in the range of 21–93 % and for Gumbel distribution between 8 and 137 %. The general tendency is low values of COV for Gumbel. This is shown in Tables 5.16 and 5.17 and Figs. 5.9 and 5.10. Data for ten platforms are analysed from PMO region.

Table 5.16 Return period and wind speed (m/s), Weibull distributions at PMO

PM	Return period in years				Weibull distribution parameters				
	10	10^2	10^3	10^4	Scale	Shape	Mean	SD	COV
A	20	33	40.60	45.99	10.95	1.38	10.00	7.31	0.73
B	20	23	24.75	26.00	16.90	4.96	15.51	3.58	0.23
C	22	26	28.33	29.99	17.99	4.15	16.34	4.44	0.27
D	22	34	41.01	45.99	13.03	1.59	11.69	7.51	0.64
E	20	38	51.83	59.30	9.24	1.08	8.97	8.31	0.93
F	22	25	26.75	28.00	18.86	5.42	17.40	3.70	0.21
G	20	34	42.17	47.98	10.56	1.31	9.75	7.53	0.77
H	22	25	26.75	28.00	18.86	5.42	17.40	3.70	0.21
I	21	40	54.83	62.72	9.67	1.08	9.40	8.75	0.93
J	20	28	32.67	35.99	13.34	2.06	11.82	6.02	0.51

Table 5.17 Return period and wind speed (m/s), Gumbel distribution at PMO

PM	Return period in years				Gumbel distribution parameters				
	10	10^2	10^3	10^4	Scale	Location	Mean	SD	COV
A	20	33	45.76	58.50	0.18	7.55	10.74	7.10	0.66
B	20	23	25.93	28.87	0.78	17.13	17.86	1.64	0.09
C	22	26	29.92	33.84	0.59	18.17	19.15	2.18	0.11
D	22	34	45.77	57.53	0.20	10.51	13.46	6.55	0.49
E	20	38	55.67	73.31	0.13	2.76	7.18	9.82	1.37
F	22	25	27.93	30.87	0.78	19.13	19.86	1.64	0.08
G	20	34	47.75	61.47	0.17	6.59	10.03	7.64	0.76
H	22	25	27.93	30.87	0.78	19.13	19.86	1.64	0.08
I	21	40	58.65	77.27	0.12	2.80	7.47	10.37	1.39
J	20	28	35.84	43.68	0.29	12.34	14.30	4.37	0.31

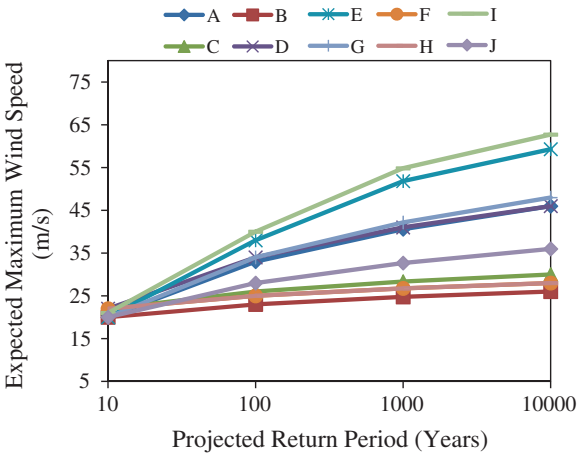

Fig. 5.9 Extrapolation of wind speed (Weibull at PMO)

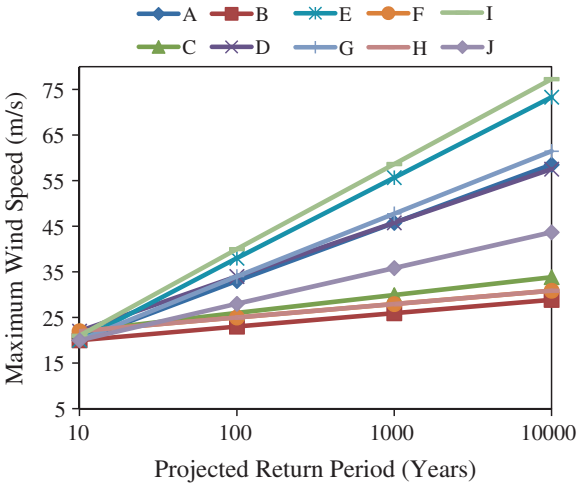

Fig. 5.10 Extrapolation of wind speed (Gumbel at PMO)

The Gumbel distribution gives higher mean wind values during extrapolation as compared to Weibull distribution. This means that extrapolation from Gumbel distribution overestimated the wind speed besides that Weibull also gives a better fit. Therefore, Weibull model is recommended for the reliability of Jacket platforms in offshore Malaysia.

5.6.2 SBO Region

Data for five Jacket platforms from SBO are analysed. Table 5.18 and Fig. 5.11 show the result for wind as per the Weibull distribution. The range for 100 years is 29–32 m/s. The corresponding 10,000-year values are in the range of 33–47 m/s. The Gumbel distribution is shown in Table 5.19 and Fig. 5.12. The 10,000-year value is shown as 36.84–61.42 m/s.

Table 5.18 Return period and wind speed (m/s), Weibull distribution at SBO

SBO	Return period in years				Weibull distribution parameters				
	10	10^2	10^3	10^4	Scale	Shape	Mean	SD	COV
A	18	31	38.60	43.99	9.36	1.28	8.68	6.86	0.79
B	19	32	39.59	44.99	10.15	1.33	9.33	7.09	0.76
C	25	29	31.33	33.00	20.91	4.67	19.12	4.66	0.24
D	17	32	40.77	47.00	7.94	1.10	7.67	7.01	0.91
E	24	31	35.07	37.97	17.64	2.71	15.69	6.25	0.40

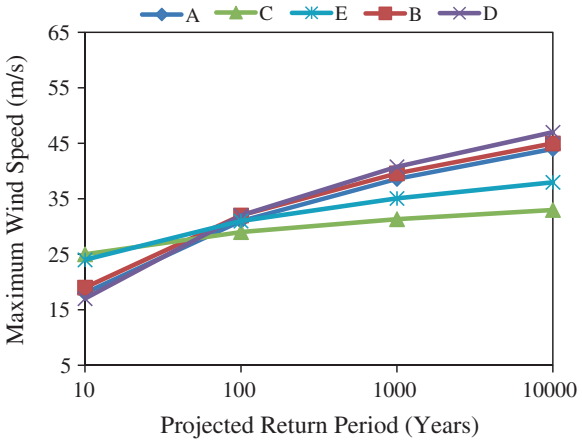

Fig. 5.11 Extrapolation of wind speed (Weibull at SBO)

Table 5.19 Return period and wind speed (m/s), Gumbel distribution at SBO

SBO	Return period in years				Gumbel distribution parameters				
	10	10^2	10^3	10^4	Scale	Location	Mean	SD	COV
A	18	31	43.76	56.50	0.18	5.55	8.74	7.10	0.81
B	19	32	44.76	57.50	0.18	6.55	9.74	7.10	0.73
C	25	29	32.92	36.84	0.59	21.17	22.15	2.18	0.10
D	17	32	46.72	61.42	0.16	2.63	6.32	8.19	1.30
E	24	31	37.87	44.73	0.34	17.30	19.02	3.82	0.20

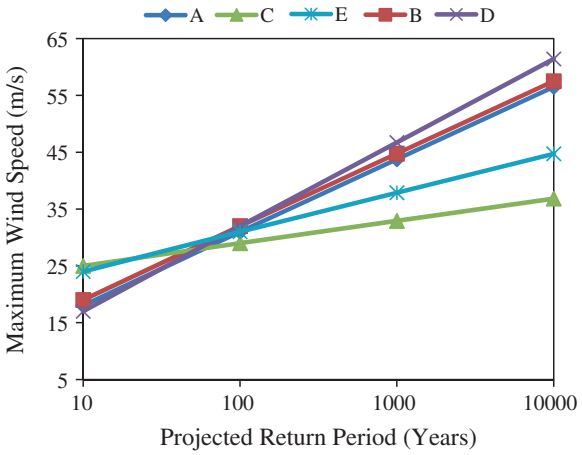

Fig. 5.12 Extrapolation of wind speed (Gumbel at SBO)

5.6.3 SKO Region

Data for eight Jacket platforms from this region are analysed. Table 5.20 and Fig. 5.13 show the result for wind as per the Weibull distribution. The range for 100 years is 20–36 m/s. The corresponding 10,000-year values are in the range of 22–52 m/s. The Gumbel distribution is shown in Table 5.21 and Fig. 5.14. The Gumbel 10,000-year values are in the range of 24–67 m/s.

5.6.4 Gulf of Mexico (GOM) and North Sea (NS)

The data from international waters are taken from ISO code [14]. Table 5.22 and Fig. 5.15 show the result for wind as per the Weibull distribution. The GOM for

Table 5.20 Return period and wind speed (m/s), Weibull distribution at SKO

SKO	Return period in years				Weibull distribution parameters				
	10	10^2	10^3	10^4	Scale	Shape	Mean	SD	COV
A	19	29	34.84	38.98	11.42	1.64	10.22	6.40	0.63
B	28	33	35.92	38.00	22.98	4.22	20.89	5.58	0.27
C	20	36	45.35	52.00	9.86	1.18	9.32	7.93	0.85
D	19	24	26.92	29.00	14.34	2.97	12.80	4.70	0.37
F	20	32	39.01	43.99	11.36	1.47	10.28	7.09	0.69
G	20	24	26.33	27.99	16.06	3.80	14.52	4.26	0.29
H	18	22	24.33	25.99	14.14	3.45	12.71	4.07	0.32
I	18	20	21.17	22.00	15.86	6.58	14.78	2.63	0.18

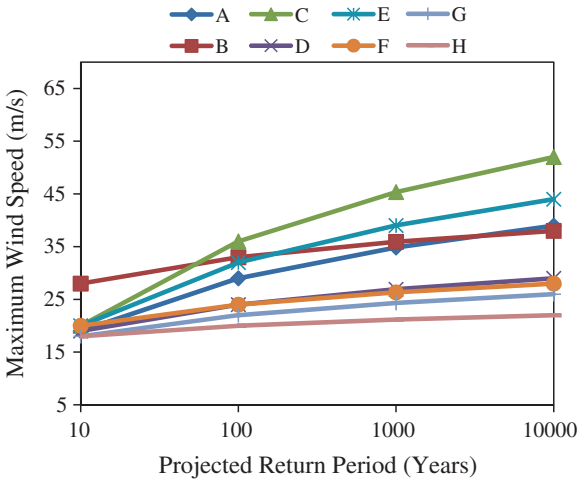

Fig. 5.13 Extrapolation of wind speed (Weibull at SKO)

Table 5.21 Return period and wind speed (m/s), Gumbel distribution at SKO

SKO	Return period in years				Gumbel distribution parameters				
	10	10^2	10^3	10^4	Scale	Location	Mean	SD	COV
A	19	29	38.81	48.61	0.23	9.42	11.88	5.46	0.46
B	28	33	37.90	42.80	0.47	23.21	24.44	2.73	0.11
C	20	36	51.71	67.00	0.15	4.68	8.61	8.73	1.01
D	19	24	28.90	33.80	0.47	14.21	15.44	2.73	0.18
F	20	32	43.78	55.53	0.20	8.51	11.46	6.55	0.57
G	20	24	27.92	31.84	0.59	16.17	17.15	2.18	0.13
H	18	22	25.92	29.84	0.59	14.17	15.15	2.18	0.14
I	18	20	21.96	24.00	1.17	16.08	16.58	1.09	0.07

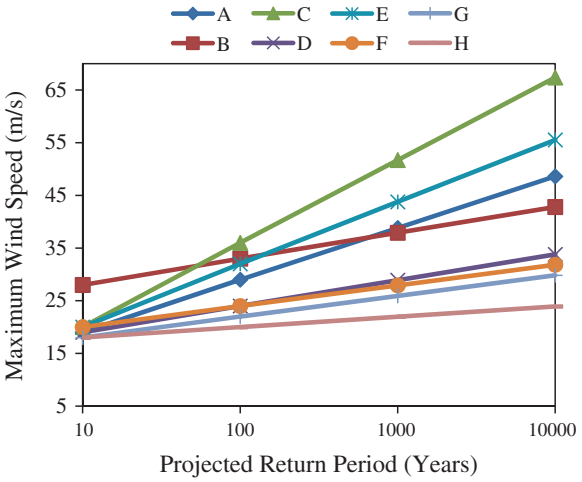

Fig. 5.14 Extrapolation of wind speed (Gumbel at SKO)

Table 5.22 Return period and wind speed (m/s), Weibull at GOM and NS

	Return period in years				Weibull distribution parameters				
	10	10^2	10^3	10^4	Scale	Shape	Mean	SD	COV
GOM	28.4	46.1	56.44	63.79	15.86	1.43	14.40	10.22	0.71
SNS	32	36	38.33	40.00	27.77	5.88	25.74	5.08	0.20
CNS	34	39	41.92	44.00	28.83	5.05	26.48	6.01	0.23
NNS	40	45	47.92	50.00	34.71	5.88	32.17	6.35	0.20

100 years is 46.1 m/s. The corresponding 10,000-year value is 63.79 m/s. For North Sea, 100-year wind is in the range of 36–45 m/s and 10,000 was 40–50 m/s. The Gumbel distribution is shown in Table 5.23 and Fig. 5.16. The 10,000-year GOM is 81 m/s, and for North Sea, it is 44–55 m/s.

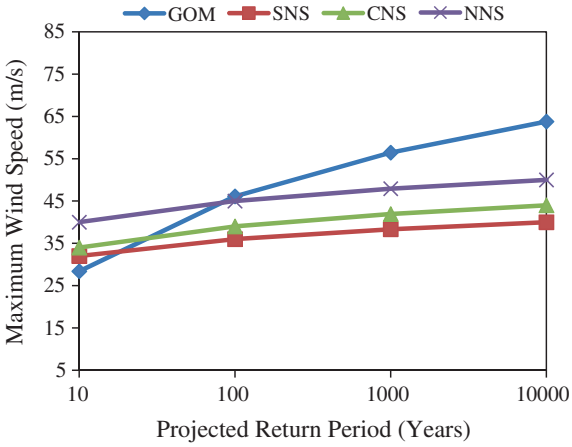

Fig. 5.15 Extrapolation of wind speed (Weibull at GOM and NS)

Table 5.23 Return period and wind speed (m/s), Gumbel at GOM and NS

	Return period in years				Gumbel distribution parameters				
	10	10^2	10^3	10^4	Scale	Location	Mean	SD	COV
GOM	28.4	46.1	63.47	81.00	0.13	11.45	15.80	9.66	0.61
SNS	32	36	39.92	44.00	0.59	28.17	29.15	2.18	0.07
CNS	34	39	43.90	49.00	0.47	29.21	30.44	2.73	0.09
NNS	40	45	49.90	55.00	0.47	35.21	36.44	2.73	0.07

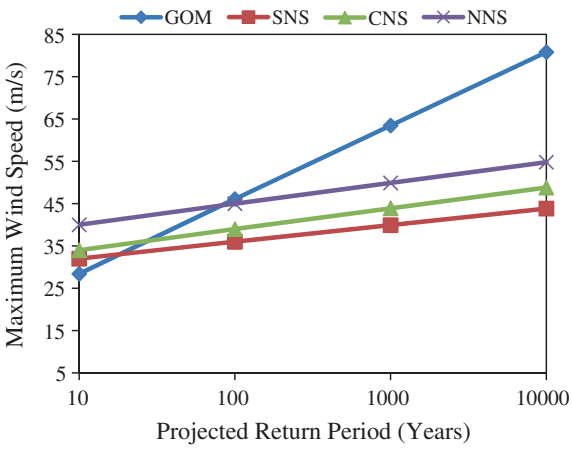

Fig. 5.16 Extrapolation of wind speed (Gumbel at GOM and NS)

5.7 Current Load Model

Due to low mean value of current and data fitting well with existing Weibull two parameter distribution, it is selected in this text.

5.7.1 PMO Region

Current data from fifteen platform surroundings are analysed for PMO region. Current distributed as per Weibull distribution gave COV in the range of 15–33 %, and Gumbel distribution gave 6–15 %. Thus, Gumbel distribution has low COV, but it gives higher extrapolated mean values. Tables 5.24 and 5.25 give basic current parameter for Weibull and Gumbel. The corresponding extrapolated values are shown in Figs. 5.17 and 5.18. The 100-year value lies in the range of 1.1–1.5, and 10,000-year Weibull is in the range of 1.22–1.63. The Gumbel 10,000-year value is in the range of 1.33–1.84.

5.7.2 SBO Region

Current data for six Jacket platforms from SBO are analysed. Table 5.26 and Fig. 5.19 show the result for current as per the Weibull distribution. The range for 100 years is 0.87–2.23 m/s. The corresponding 10,000-year values are in the range of 0.93–2.56 m/s. The Gumbel distribution is shown in Table 5.27 and Fig. 5.20. The 10,000-year value achieved is 0.98–2.87 m/s.

Table 5.24 Return period and current speed (m/s), Weibull distribution at PMO

PM	Return period in years				Weibull distribution parameters				
	10	10^2	10^3	10^4	Scale	Shape	Mean	SD	COV
A	0.98	1.1	1.17	1.22	0.85	6.00	0.79	0.15	0.19
B	1.14	1.25	1.31	1.36	1.02	7.52	0.96	0.15	0.16
C	1.15	1.3	1.39	1.45	0.99	5.65	0.92	0.19	0.20
D	1.15	1.35	1.47	1.55	0.95	4.32	0.86	0.23	0.26
E	1.05	1.2	1.29	1.35	0.89	5.19	0.82	0.18	0.22
F	1.06	1.2	1.28	1.34	0.91	5.59	0.84	0.17	0.21
G	1.05	1.21	1.30	1.37	0.89	4.89	0.81	0.19	0.23
H	1.07	1.2	1.27	1.33	0.93	6.05	0.87	0.17	0.19
I	1.37	1.5	1.57	1.63	1.23	7.65	1.15	0.18	0.15
J	1.1	1.35	1.49	1.60	0.86	3.38	0.77	0.25	0.33
K	1.16	1.37	1.49	1.58	0.95	4.17	0.86	0.23	0.27
L	1.05	1.26	1.38	1.47	0.84	3.80	0.76	0.22	0.29
M	1.12	1.26	1.34	1.40	0.97	5.88	0.90	0.18	0.20
N	1.19	1.34	1.43	1.49	1.03	5.84	0.96	0.19	0.20
O	1.05	1.19	1.27	1.33	0.90	5.54	0.83	0.17	0.21

Table 5.25 Return period and current speed (m/s), Gumbel distribution at PMO

PM	Return period in years				Gumbel distribution parameters				
	10	10^2	10^3	10^4	Scale	Location	Mean	SD	COV
A	0.98	1.1	1.22	1.33	19.58	0.87	0.89	0.07	0.07
B	1.14	1.25	1.35	1.46	21.36	1.03	1.06	0.06	0.06
C	1.15	1.3	1.44	1.59	15.67	1.01	1.04	0.08	0.08
D	1.15	1.35	1.55	1.74	11.75	0.96	1.01	0.11	0.11
E	1.05	1.2	1.34	1.49	15.67	0.91	0.94	0.08	0.09
F	1.06	1.2	1.33	1.47	16.78	0.93	0.96	0.08	0.08
G	1.05	1.21	1.37	1.52	14.69	0.90	0.94	0.09	0.09
H	1.07	1.2	1.32	1.45	18.08	0.95	0.98	0.07	0.07
I	1.37	1.5	1.62	1.75	18.08	1.25	1.28	0.07	0.06
J	1.1	1.35	1.59	1.84	9.40	0.86	0.92	0.14	0.15
K	1.16	1.37	1.57	1.78	11.19	0.96	1.01	0.11	0.11
L	1.05	1.26	1.46	1.67	11.19	0.85	0.90	0.11	0.13
M	1.12	1.26	1.39	1.53	16.78	0.99	1.02	0.08	0.07
N	1.19	1.34	1.48	1.63	15.67	1.05	1.08	0.08	0.08
O	1.05	1.19	1.32	1.46	16.78	0.92	0.95	0.08	0.08

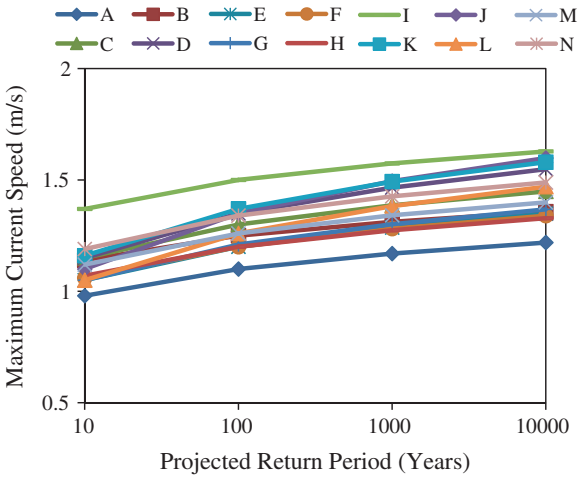

Fig. 5.17 Extrapolation of current speed (Weibull at PMO)

5.7.3 SKO Region

Current data for nine Jacket platforms from SKO are analysed. Table 5.28 and Fig. 5.21 show the result for wind as per the Weibull distribution. The range for 100 years is 1.0–1.8 m/s. The corresponding 10,000-year values are in the range of 1.14–2.10 m/s. The Gumbel distribution is shown in Table 5.29 and Fig. 5.22. The 10,000-year value is shown as 1.22–2.38 m/s.

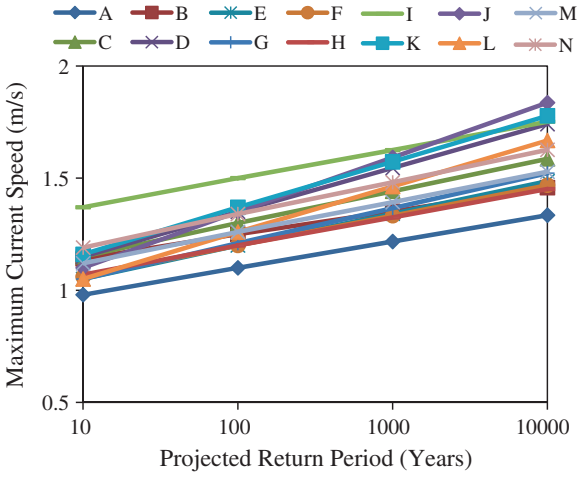

Fig. 5.18 Extrapolation of current speed (Gumbel at PMO)

Table 5.26 Return period and current speed (m/s), Weibull distribution at SBO

SBO	Return period in years				Weibull distribution parameters				
	10	10^2	10^3	10^4	Scale	Shape	Mean	SD	COV
A	1.9	2.23	2.42	2.56	1.57	4.33	1.43	0.37	0.26
B	0.81	0.87	0.90	0.93	0.74	9.70	0.71	0.09	0.12
C	1.13	1.26	1.33	1.39	0.99	6.37	0.92	0.17	0.18
D	0.78	0.94	1.03	1.10	3.71	0.62	0.56	0.17	0.30
E	1.11	1.26	1.35	1.41	0.95	5.47	0.88	0.19	0.21
F	1.2	1.35	1.44	1.50	1.04	5.88	0.97	0.19	0.20

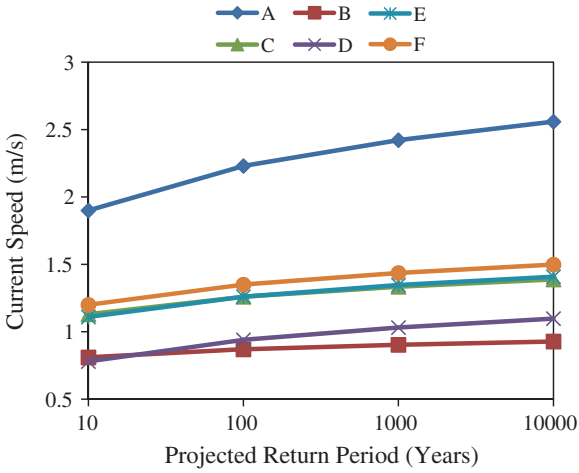

Fig. 5.19 Extrapolation of current speed (Weibull at SBO)

Table 5.27 Return period and current speed (m/s), Gumbel distribution at SBO

SBO	Return period in years				Gumbel distribution parameters				
	10	10^2	10^3	10^4	Scale	Location	Mean	SD	COV
A	1.9	2.23	2.55	2.87	7.12	1.58	1.67	0.18	0.11
B	0.81	0.87	0.92	0.98	39.16	0.75	0.77	0.03	0.04
C	1.13	1.26	1.38	1.51	18.08	1.01	1.04	0.07	0.07
D	0.78	0.94	1.10	1.25	14.69	0.63	0.67	0.09	0.13
E	1.11	1.26	1.40	1.55	15.67	0.97	1.00	0.08	0.08
F	1.2	1.35	1.49	1.64	15.67	1.06	1.09	0.08	0.07

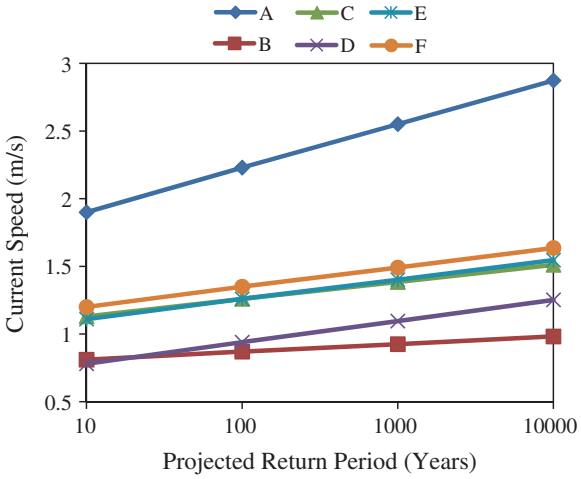

Fig. 5.20 Extrapolation of current speed (Gumbel at SBO)

Table 5.28 Return period and current speed (m/s), Weibull distribution at SKO

SKO	Return period in years				Weibull distribution parameters				
	10	10^2	10^3	10^4	Scale	Shape	Mean	SD	COV
A	0.96	1.05	1.10	1.14	0.86	7.73	0.81	0.12	0.15
B	1.5	1.8	1.97	2.10	1.20	3.80	1.09	0.32	0.29
C	1.53	1.74	1.86	1.95	1.31	5.39	1.21	0.26	0.21
D	1.55	1.75	1.87	1.95	1.34	5.71	1.24	0.25	0.20
E	0.87	1	1.07	1.13	0.74	4.98	0.68	0.16	0.23
F	1.1	1.25	1.34	1.40	0.94	5.42	0.87	0.19	0.21
G	0.83	1.21	1.43	1.59	0.53	1.84	0.47	0.26	0.56
H	1.05	1.2	1.29	1.35	0.89	5.19	0.82	0.18	0.22
I	1.3	1.5	1.62	1.70	1.09	4.84	1.00	0.24	0.24

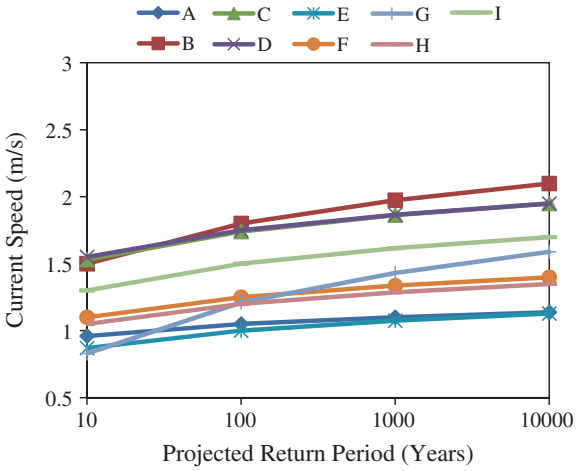

Fig. 5.21 Extrapolation of current speed (Weibull at SKO)

Table 5.29 Return period and current speed (m/s), Gumbel distribution at SKO

SKO	Return period in years				Gumbel distribution parameters				
	10	10^2	10^3	10^4	Scale	Location	Mean	SD	COV
A	0.96	1.05	1.14	1.22	26.11	0.87	0.90	0.05	0.05
B	1.5	1.8	2.09	2.38	7.83	1.21	1.29	0.16	0.13
C	1.53	1.74	1.94	2.15	11.19	1.33	1.38	0.11	0.08
D	1.55	1.75	1.95	2.14	11.75	1.36	1.41	0.11	0.08
E	0.87	1	1.12	1.25	18.08	0.75	0.78	0.07	0.09
F	1.1	1.25	1.39	1.54	15.67	0.96	0.99	0.08	0.08
G	0.83	1.21	1.58	1.95	6.18	0.47	0.56	0.21	0.37
H	1.05	1.2	1.34	1.49	15.67	0.91	0.94	0.08	0.09
I	1.3	1.5	1.70	1.89	11.75	1.11	1.16	0.11	0.09

5.7.4 Gulf of Mexico (GOM) and North Sea (NS)

The data from international waters are taken from ISO code [14]. Table 5.30 and Fig. 5.23 show the result for current as per the Weibull distribution. The GOM for 100 years is 2.3 m/s. The corresponding 10,000 year value is 3.30 m/s. For North Sea, 100-year value is in the range of 0.9–1.3 3 m/s and 10,000 was 1.1–1.41 m/s. The Gumbel distribution is shown in Table 5.31 and Fig. 5.24. The 10,000-year GOM is 4.26 m/s, and for North Sea, it is 1.29–1.49 m/s.

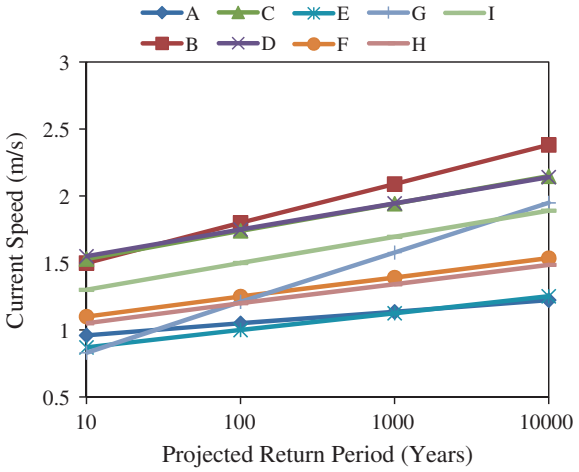

Fig. 5.22 Extrapolation of current speed (Gumbel at SKO)

Table 5.30 Return period and current speed (m/s), Weibull at GOM and NS

	Return period in years				Weibull distribution parameters				
	10	10^2	10^3	10^4	Scale	Shape	Mean	SD	COV
GOM	1.3	2.3	2.88	3.30	0.65	1.21	0.61	0.51	0.83
SNS	1.25	1.33	1.38	1.41	1.16	11.17	1.11	0.12	0.11
NNS	0.7	0.9	1.02	1.10	0.52	2.76	0.46	0.18	0.39

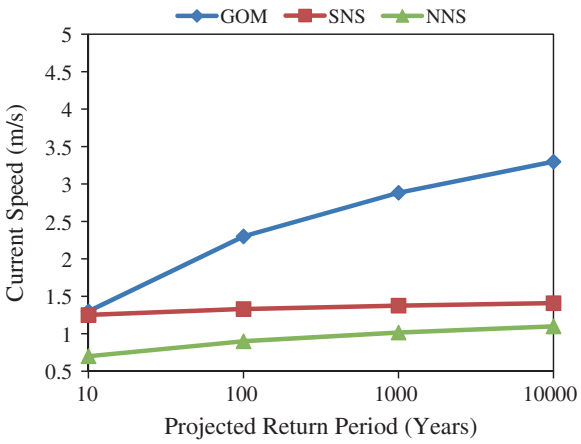

Fig. 5.23 Extrapolation of current speed (Weibull at GOM and NS)

Table 5.31 Return period and current speed (m/s), Gumbel at GOM and NS

	Return period in years				Gumbel distribution parameters				
	10	10^2	10^3	10^4	Scale	Location	Mean	SD	COV
GOM	1.3	2.3	3.28	4.26	2.35	0.34	0.59	0.55	0.93
SNS	1.25	1.33	1.41	1.49	29.37	1.17	1.19	0.04	0.04
NNS	0.7	0.9	1.10	1.29	11.75	0.51	0.56	0.11	0.20

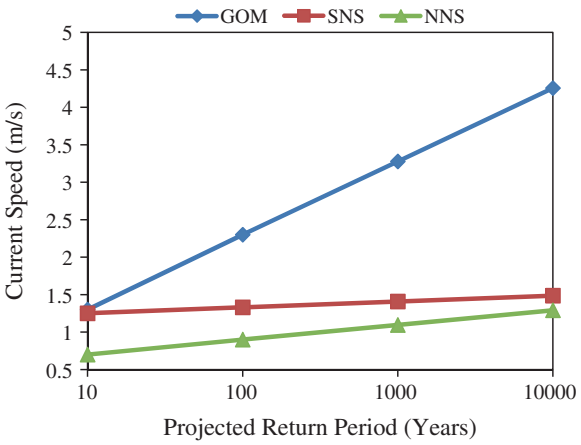

Fig. 5.24 Extrapolation of current speed (Gumbel at GOM and NS)

5.8 Summary

Environmental load uncertainty parameters are discussed in this chapter. This uncertainty is related to an estimation of parameters for extreme environmental load. This variable load is expected to occur near Jacket platform at any time during its design life time or beyond. The major findings are as follows:

1. The reliability determination requires that distribution parameters should be used for uncertain random variables. There are three parameters of uncertainty for Jacket platforms, i.e. wave, wind and current. In this text, Weibull and Gumbel distribution parameters are determined using 10-year and 100-year values.
2. Gumbel distribution overestimated the parameters of environmental load. Therefore, Weibull two-parameter distribution is recommended for the reliability of Jacket platforms in Malaysia.
3. The ISO 19902 requires that reassessment of Jacket platforms should be from 10,000-year return period. Weibull and Gumbel distributions are used to find significant wave height, current and wind speed extrapolations.

References

1. Tromans, P.: Extreme environmental load statistics in UK waters (2001)
2. Ochi, M.K.: Probabilistic extreme values and their implication for offshore structure design. In: Offshore Technology Conference, OTC 3161, Houston (1978)
3. Marley, M., Etterdal, B., Grigorian, H.: Structural Reliability Assessment of Ekofisk Jacket Under Extreme Loadin. Presented at the offshore technology conference, OTC 13190, Houston (2001)
4. DNV: Classification note 30.6 Structural reliability analysis of marine structures (1992)
5. Yiquan, Q., Zhizu, Z., Ping, S.: Extreme wind, wave and current in deep water of South China sea. Int. J. Offshore Polar Eng. **20**(1), 18–23 (2010)
6. Neelamani, S., Salem, K., Rakha, K.: Extreme waves in the Arabian Gulf. Presented at the proceedings of the 9th international coastal symposium, Australia (2007)
7. Prior-Jones, R.L., Beiboer, F.L.: Use of joint probability in deriving environmental design criteria. Presented at the environmental forces on offshore structures and their prediction, Netherlands (1990)
8. Soares, G.C., Scotto, M.: Modelling uncertainty in long-term predictions of significant wave height. Ocean Eng. **28**(3), 329–342 (2001)
9. Gudmestad, O.T., Daniell, K.: Wave current-interaction. Environmental forces on offshore structures and their prediction: society for underwater technology, pp. 81–110 (1990)
10. Driver, D.B., Borgman, L.E., Bole, J.B.: Typhoon Wind, Wave and Current Directionality in the South China Sea. OTC 7416. Houston, Texas (1994)
11. Jahns, H.O., Wheeler, J.D.: Long-term wave probabilities based on hindcasting of severe storms. Soc. Petrol. Eng. **3934**, 473–486 (1973)
12. Wen, Y.K., Banaon, H.: Development of environmental combination design criteria for fixed platforms in the Gulf of Mexico. Offshore Techonology Conference 6540 (1991)
13. Tromans, P., Vanderschuren, L.: Response based design conditions in the North Sea: application of a new method. Offshore Technology Conference 7683, pp. 387–397. Houston (1995)
14. ISO19901-1: Metocean design and operating considerations (2005)
15. Panchang, V.G., Li, D.C.: Large waves in the Gulf of Mexico caused by Hurricane Ivan. Am. Meteorol. Soc. **87**(4), 481–489 (2006)
16. Monahan, A.H.: The probability distribution of sea surface wind speeds. part I: theory and seawinds observations. J. Clim. **19**(4), 497–520 (2006)

Chapter 6
Tubular Strength Comparison of Offshore Jacket Structures Under API RP 2A and ISO 19902

Abstract Offshore platforms are only 67 years old and are fairly new compared to other types of civil engineering structures. Offshore Jacket platforms in Malaysia are designed using API RP2A Working Stress Design (WSD) code. API WSD code has proved its effectiveness and has been in use for long time, but it needs to be changed into load and resistance factor design (LRFD)-based code which is being followed by all building code agencies. In place of WSD, limit state design or LRFD has proved to be more rational as it considers probabilistic models. The reliability of Jacket platforms is maintained in API RP 2A-LRFD by setting target safety factor the same as that provided in WSD, which means structures designed as per LRFD code will have the same reliability as API RP 2A-WSD (which has already provided safe structures and the best available practice for design). When adopting LRFD methodology, the appropriate load and resistance factors can be optimised through the process of calibration. Knowledge of the strength equations in the different codes and the similarities and differences between them is useful for the calibration. The first step in the calibration process is the determination of reliability of structural tubular members of the Jacket designed as per existing practice of WSD and LRFD code. In this text, API RP 2A-WSD code and International Standard Organization (ISO 19902) (LRFD-based code) are taken into consideration for the reliability analysis. The relevant strength equations of three codes are identified and compared, and the similarities and differences are determined for tubular members which are the main part of Jacket structures.

6.1 Introduction

Offshore Jacket platforms are normally designed using one of the following offshore design codes: API RP2A Working Stress Design (WSD) [1], API RP2A load and resistance factor design (LRFD) [2] or ISO 19902 [3]. Locally,

Note This chapter is based on one of author's paper published Proceedings of the Ninth ISOPE Pacific/Asia Offshore Mechanics Symposium, Busan, Korea, November 14–17, 2010.

Z. Nizamani, *Environmental Load Factors and System Strength Evaluation of Offshore Jacket Platforms*, Ocean Engineering & Oceanography 4,
DOI 10.1007/978-3-319-15051-2_6

Malaysia has its version of the code, i.e. PETRONAS Technical Standards (PTS) [4], which is actually depend on the API RP 2A-WSD. The aim here is to determine the similarities and differences in resistance formulations provided in codes of API RP 2A-WSD, LRFD and ISO. Nine types of stresses are chosen for comparing the design resistance formulae, i.e. axial tension, axial compression, bending, shear, hydrostatic pressure, tension and bending, compression and bending, tension, bending and hydrostatic pressure and compression, bending and hydrostatic pressure. API RP 2A-LRFD and ISO 19902 codes are limit state design-based approaches for design of steel Jacket platforms. API WSD uses a common factor of safety for material where as in API LRFD and ISO factors are constant in value for the type of resistance under consideration. The growth of design codes is an indicator of development of structural design since the codes reflect engineering practice [5]. The tubular member design equations in three codes are considered, and main similarities and differences among them are identified. The equations for tubular members in all the above codes come from theory of shell buckling. Important dissimilarities are there in the equation for axial compression especially with regard to local buckling and some load interaction equations. The overall column buckling equation used in API WSD is same as the equation in API RP 2A-LRFD and ISO-19902 but has different coefficients; here, ISO gives lower capacity compared to LRFD. The interaction equation for tension/compression along with bending in ISO follows the API WSD and is linear, but the LRFD equation has a cosine form. For the numerical comparisons, tubular members of different diameters, thickness and lengths are chosen from an earlier analysis, and axial, bending and hoop strengths evaluated and compared. This chapter reviews and summarises the comparison of the three basic codes for offshore Jacket platforms and provides in detail the tubular member resistance. The load factors used in API RP 2A-LRFD and ISO are discussed along with inherent safety factor present in API RP 2A-WSD. Resistance formulae for the nine main stress conditions are chosen for evaluation, and their strengths and weaknesses are compared. In this text, the steel tubular member structural components are chosen which sustain the dead, live and environment load acting on the main structure. LRFD and ISO standards are basically limit state approaches which uses the partial safety factors (for loads) multiplied with characteristic loads to give design action effects and partial safety factors multiplied with characteristic resistances to give design resistances. The WSD is allowable strength design approach, whereas ISO and LRFD use factors which are constant in value for the type of resistance under consideration.

6.2 Design Codes for Jackets

The first design standard for offshore structures, the API WSD, was published in October 1969. The 21st edition of API RP 2A-WSD was published in 2000. After judging the advantages of LRFD in AISC [6], it was considered that the

time was ripe to have an API RP 2A-LRFD code which was ultimately published in 1993. The industry initially applied the WSD codes in international locations. The expansion of national standards and globalisation of major projects resulted in a desire for an international standard. The oil and gas industry, the Exploration and Production Forum and the API identified the International Organisation for Standardisation (ISO) as the entity to do this [7]. The ISO Technical Committee 67 was set up with 7 sub-committees. SC 7 addressed offshore structures [8]. This was followed by an international code/standard in 1998 with ISO 13819 [9] which has now been modified in ISO 19902 in 2007. In the development of the ISO, the base document is the API RP 2A-LRFD [10].

The member resistance formulae in WSD have undergone major changes three times [5]. The member resistance formulae were introduced in the 6th edition in 1975. Prior to this, WSD recommended the use of AISC provisions. The 1975 edition provided guidance on local buckling, hydrostatic pressure, interaction formulae for axial compression, bending stress, axial tension and hoop stress. In the 11th edition (1980), equations were introduced for allowable hoop stress, a formula for combined effects of axial compression, bending and hydrostatic pressure. In the 17th edition (1987), the allowable bending stress was increased from $0.66f_y$ to $0.75f_y$ for members not susceptible to local buckling. In 1993, when the LRFD version was introduced, some formulae were modified. This was incorporated in the 21st edition of WSD.

All the three codes that are compared provide equations for single load case as well as for combination of loads. Chord and bracing members of Jacket platforms suffer from combined stresses due to wave and current forces. Gravity loads dominate the leg member design, but environmental loads dominate the design of brace members [7]. In API WSD method, the allowable stresses are either expressed implicitly as a fraction of yield stress or buckling stress, or by applying a safety factor on the critical buckling stress [8]. In-place extreme environmental design conditions for the ultimate limit state or buckling failure modes are considered. For buckling, this is often the governing design condition for majority of structural components in offshore platforms. [8]. Utilisation ratio is equal to modelling uncertainty (experimental strength to predicted strength) [8]. The expressions for utilisation ratio are explicitly provided in the ISO but not in WSD and LRFD. Local buckling checks are required to be made for members with $D/t > 60$ in all codes [8]. Bracing members act as ties or struts depending on whether they carry tensile or compressive loading [8]. Chord and brace members have to withstand hydrostatic pressure and bending moment which arise due to wave and current forces and from load redistribution at the nodal points [8].

For thick-walled tubular members, ($d/T < 60$) the strength of very stocky columns reaches full yield even at the characteristic level due to strain hardening. At large slenderness (λ), API curve is similar to Euler buckling curve, but ISO curve lies 10 % below it. Greater differences are observed for thin-walled tubulars ($D/t = 120$). The difference between API LRFD and ISO is maximum, when thin-walled column is short (low λ) [9]. API LRFD and WSD load capacities have been

compared to ISO with all resistance, and load factors included with environmental to gravity load ratio are 2–4 [9]. The LRFD curve for smaller D/t ratio starts at unity and moves upward to 1.11 (1/0.9), and this shows LRFD has more capacity than ISO [9]. At greater D/t ratio, LRFD crosses the unity line, and short columns of ISO show more capacity than LRFD but less at higher slenderness, while API WSD curves lie constantly above ISO and LRFD specially for greater live to dead load ratios [9].

There is great difference between API and ISO for local buckling. In ISO formula, the material properties as well as the geometric properties influence the local buckling [9]. ISO and API LRFD provisions for hydrostatic pressure are identical but different for WSD. The pressure that can be sustained is directly proportional to tubular member which are nominally stronger according to ISO or API LRFD over the range where elastic buckling stress lies between 0.55 and 6.2 times yield stress [9]. LRFD and ISO remain near WSD when partial load and resistance factors are considered. However, WSD safety factor is 1.5, and ISO/LRFD load and resistance factors are 1.3 and 1.25, respectively. Thus, the overall factors are $1.5/(1.3 \times 1.25) = 0.92$ on the ISO/LRFD capacity relative to WSD [9]. Comparing the equations for combined loads, the ISO has utilised the simpler interaction equations of WSD which are linear, whereas the API LRFD uses a cosine interaction equation [9]. The D/t ratio of a pile shall be small so that local buckling is avoided at stresses up to yield strength. API WSD/LRFD gives minimum pile wall thickness, where continued hard driving of 820 blows per meter with biggest size hammer is used which is $t = 6.35 + D/100$. The API values for pile diameter and thickness vary between (610–3,048 mm) and (13–37), respectively. The minimum annulus (gap between pile and the sleeve) recommended by API RP 2A-WSD and API RP 2A-LRFD is 38 mm, while the ISO recommends an annulus of 40 mm. In ISO, wind actions on downstream components can be reduced due to shielding by upstream components. For perpendicular wind approach angles with respect to projected area, API provides common shape factor coefficient for cylindrical members, whereas ISO divides cylindrical members into four classes as shown in Table 6.1.

In ISO, the minimum capacity for joint requirement is only for primary or significant joints which influence reserve system strength (critical load paths) or secondary joints whose failure has important safety or environmental effects.

Table 6.1 Shape coefficients

Component		Shape coefficients (C_s)	
		WSD/LRFD	ISO
Cylinders	Smooth, $R_e > 5 \times 10^5$	0.5	0.65
	Smooth, $R_e \leq 5 \times 10^5$	0.5	1.20
	Rough, all R_e	0.5	1.05
	Covered with ice, all R_e	0.5	1.20

6.3 Numerical Analysis Background

This chapter compares the resistance formulae for different stress conditions in API RP 2A-WSD, API RP 2A-LRFD and ISO 19902 and the corresponding safety factors. The equations play a very vital role in finding the resistance factors for Jacket platforms in Malaysia as randomness and uncertainties are accurately accounted. The similarities between the codes are identified. Where there are differences, the source of the formula is identified. The limiting conditions for the use of the formulae provided by the different codes are also discussed. The structure contains uncertainty and randomness in itself, i.e. material resistance, geometric parameters, initial defects, etc. There is uncertainty in the physical models used to asses load effects and response of structure [11]. The characteristic loads are multiplied with safety factors to give design load effects, and divisors are applied to characteristic resistances to give design resistance [12]. There are differences in ISO and LRFD equations for the different types of resistance. The objective here is to review the differences in stress equations provided in the three major codes for the design of offshore Jacket platforms. These stresses are evaluated numerically by putting values in the given equation and then comparing them. After comparison, the differences are highlighted.

6.4 Comparison of Tubular Strength Equations in Different Codes

Jacket platform component failures include brace buckling, plastification of the section and punching of a chord by a brace [11]. Geometric slenderness D/t is limited in ISO up to 120, and material yield strength is limited to 500 MPa (taking lead from NORSOK code) as shown in Table 6.2. Failure criteria may be expressed as an interaction equation among member internal action and resistance variable. The parameters for tubular members are yield stress, strain hardening, Young's modulus, residual stresses, section parameters (diameter and

Table 6.2 Limit values for the variables in the three codes

Item	API WSD	API LRFD	ISO 19902
Wall thickness of member (mm)	≥6	≥6	≥6
D/t	<120[a]	<120[a]	<120
Yield strength (MPa)	<414	<414	<500
Yield strength to ultimate strength	–	–	0.85
Yield strength to ultimate tensile strength ratio	–	–	<0.9

[a]In the local buckling equations used for axial compression, bending and hydrostatic pressure, $D/t < 300$ is acceptable

thickness), out of roundness of the section and out of straightness of the member [11]. Comparing API LRFD and ISO, the average reduction in combined axial tension and bending capacity of ISO is observed to be 9 %; for axial compression, bending and pressure, the average reduction in ISO is found to be 7 %, while for combined tension, bending and pressure, the ISO formulation showed increase of capacities of 10 % [7].

6.4.1 Axial Tension

The allowable axial tension is taken as $0.6F_y$. This is from AISC and has remained unchanged from 1969 [5]. The LRFD and ISO expressions are identical. Due to low consequences of tension yielding, safety indices in ISO and LRFD for extreme loading are taken larger than used in WSD. The equations in LRFD and ISO are used for yielding of gross section of cylindrical members which covers vast majority of structures related to offshore engineering, whereas for non-tubular members, the analyses are made through AISC LRFD/WSD equations, respectively. In comparing design resistance with respect to partial safety factor, the ISO design resistance is 0.95/0.952 = 99.75 % of API LRFD resistance. Thus, the expressions are the same. This kind of stress, acting independently as a governing stress, occurs very rarely for offshore structures as shown in Table 6.3.

For comparison of equations, the safety factors have to be removed from above equations so that they will be at par with each other. Thus, they can be written as in Table 6.4.

Table 6.3 Comparison of axial tension equation

API RP 2A-WSD	API RP 2A-LRFD	ISO 19902
$F_t = 0.6 * F_y$	$f_t = \phi_t * F_y$	$\sigma_t = \frac{f_t}{\gamma_t}$
F_t = tensile stress	f_t = tensile stress	σ_t = tensile stress
Safety factor = 0.6	$\phi_t = 0.95$	f_t = tensile strength = f_y
F_y = yield strength	Safety factor = 0.95	$\gamma_t = 1.05$
		Safety factor = 0.9524

Table 6.4 Comparison of axial tension equation without factors

API RP 2A-WSD	API RP 2A-LRFD	ISO 19902
$F_t = F_y$	$f_t = F_y$	$\sigma_t = f_y$

6.4.2 Axial Compression

LRFD takes 0.85 as safety factor, whereas ISO takes 1.18 as a factor but both become equal when put in respective equations. Low D/t ratio members are not subject to local buckling under axial compression, and API recommends that unstiffened tubular members should be investigated for local buckling, when D/t ratio is greater than the limiting value. Unstiffened tubular members under axial compression have following failure modes [5]: (i) material yield, (ii) Euler column (overall) buckling, (iii) local buckling and (iv) combination of all.

6.4.2.1 Overall Column Buckling

Characteristic column strength is normalised with respect to the tubular yield stress, when partial safety factor is unity, for API RP 2A-LRFD and ISO 19902. The overall column buckling equation used in API WSD is adopted from AISC and is not similar to API LRFD or ISO. Equations provided in LRFD and ISO are similar in form, but different coefficients are used. Here, the capacity of ISO equation is lower than LRFD equation [9]. API WSD column strengths cannot be compared at a characteristic level because of WSD system. But total unfactored load capacities can be compared.

MSL has compared LRFD, and WSD loads are compared to ISO loads, with all resistance and load partial factors included in the computation [13]. The load capacities are dependent on assumed environmental to gravity load ratio with a range of 2–4 [9]. As partial load factors for API LRFD and ISO are same, LRFD curves remained same [9]. The LRFD curve started at unity and climbed to 1.11 (=1/0.9), and this shows that LRFD will give more capacity than ISO [9]. The LRFD thin curve crosses the unity line, and the short columns of ISO give greater capacity than LRFD but less at higher slenderness. The API WSD curves consistently lie above both ISO and LRFD and far higher.

For overall column buckling, the WSD formula is from the AISC [5]. The expressions in LRFD and ISO are similar, there being a difference in the constant in the expressions (0.25 in LRFD and 0.278 in ISO). Also, the limiting value for λ is $\sqrt{2}$ in LRFD and 1.34 in ISO. There is also a small variation in the expressions for $\lambda > \sqrt{2}$ or 1.34 where the ISO expressions are factored using 0.9.

Cylindrical shells with low D/t ratio are not prone to local buckling under axial compression and are designed on the basis of material failure, i.e. local buckling stress is taken same as yield stress, but as compared to this, high D/t cylindrical shell must be checked for local shell buckling. In its commentary clause 13.2.3.2, ISO gives separate equation for a member composed of two or more separate cross section along member length; however, there is no provision mentioned in API codes. The axial compressive strength is determined as follows:

(i) Find elastic buckling strength P_e for whole member taking into consideration end restraints and variable cross-sectional properties.
(ii) Find effective length factor of member.
(iii) The axial compressive strength $P_{c,r}$ is determined by Eqs. 6.1 and 6.2:

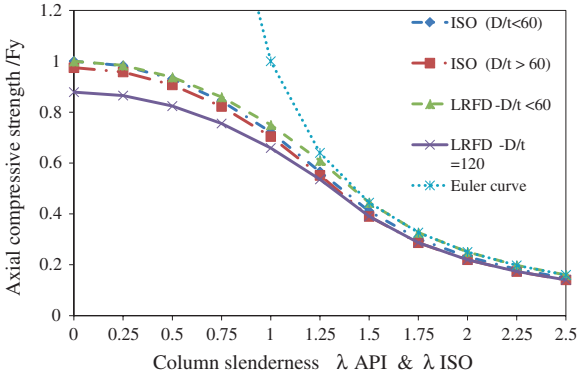

Fig. 6.1 Comparison of characteristic column curve strength of ISO 19902 and API LRFD

$$P_{c,r} = \left[1 - 0.278\frac{P_{yc,r}}{P_e}\right]P_{yc,r} \quad \text{for} \quad \left(\frac{P_{yc,r}}{P_e}\right)^{0.5} \leq 1.34 \tag{6.1}$$

$$P_{c,r} = 0.9P_e \quad \text{for} \quad \left(\frac{P_{yc,r}}{P_e}\right)^{0.5} > 1.34 \tag{6.2}$$

The axial compressive stress of each section is acquired by dividing $P_{c,r}$ by the respective cross-sectional area A_i.

In Fig. 6.1, characteristic column strength is normalised with the yield stress of cylindrical member (without partial safety factor). This normalised strength is plotted against the column slenderness (λ). From this, it is clear that LRFD equation matches with Euler buckling curve for $\lambda \geq \sqrt{2}$, when $D/t > 60$. Few strength equations ever match with their elastic critical buckling curves, for values of non-dimensional slenderness quite near to unity [7]. Slenderness is related to critical stress where cylindrical member can withstand local buckling failure. For thick cross-sectional columns, this critical stress is the yield stress and, thus, λ for ISO and LRFD is equal, which makes LRFD and ISO strength points fall on same vertical line [9].Thin-walled cylindrical member subject to local buckling will have displaced points because of different equations used in different codes.

6.4.2.2 Local Buckling

Circular members with low D/t ratio are not subject to local buckling under axial compression and are designed with respect to material failure (local buckling stress is taken equal to yield stress). But as D/t ratio increases, elastic buckling strength decreases, and now member should be checked for local buckling.

6.4.2.3 Elastic Buckling

Unstiffened thin-walled cylinders under axial compression and bending can fail at loads below buckling loads as predicted by small deflection shell theory, and there is sudden drop in load carrying capacity upon buckling. This buckling load is also affected along with geometric imperfections by boundary conditions and residual stresses, which cause inelastic action to commence before nominal stresses due to applied loads reach yield strength. Local buckling should be checked whenever $d/t > 60$, and $d/t = 60$ is suitable for commonly used offshore platform steel, i.e. $F_y = 242$ to 414 MPa (35–60 Ksi). The expressions for local buckling in WSD and LRFD are identical for $D/t \leq 60$ and also $D/t > 60$. Note that the limits given are geometrical limits. The expression in ISO is similar to the NORSOK [12] and dependent on material factor limits.

6.4.2.4 Inelastic Buckling

Offshore cylindrical members as per LRFD fall into the inelastic range normally [3]. Inelastic local buckling as compared to elastic buckling can be taken as less sensitive to geometric imperfections and residual stresses.

6.4.2.5 Effective Length Factor (*K*)

Effective length factor of bracing member is reduced in ISO code. Clause 3.3.1.d of API RP 2A-WSD, clause D3.2.3 of LRFD and clause 13.5 of ISO provide the effective length factor and moment reduction factors for different members, which is reproduced in Tables 6.5 and 6.6, respectively. The former two are the same. The effective length is found by a rational analysis considering joint restraints, joint flexibility and joint movement. Studies indicate that buckling lengths determined from refined analysis improved design predictions. Studies on X-frame have been done by Knapp and Dixon [14] and Livesley [15]. API follows the AISC effective length alignment charts, whereas ISO has its values presented through its commentary clause A.13.5. The length to which the effective length factor is applied is normally measured from centreline to centreline of the end joints. For members framing into legs, two cases are follows: (a) face of leg to face of leg for main diagonal braces and (b) face of leg to centreline of end joint for *K*-braces. C_m is used to obtain an equivalent moment for the moment pattern to which a beam–column is subjected to.

Figure 6.2 compares local buckling strengths, normalised with respect to yield stress, as a function of cylindrical slenderness (D/t). API equation provides single curve, which is independent of yield stress, whereas ISO equation provides different curves related to yield stress. Aside from relatively small region near $D/t = 60$ and for higher strength steels, lower buckling strengths are shown by API.

Table 6.5 Effective length factor (K)

Structural component	API RP 2A-WSD	API RP 2A-LRFD	ISO 19902
Topside legs			
Braced	1	1	1
Portal (unbraced)	See note	See note	See note
Structure legs and piling			
Grouted composite section	1	1	1
Ungrouted legs	1	1	1
Ungrouted piling between shim points	1	1	1
Structure brace members			
Primary diagonals and horizontals	0.8	0.8	0.7
K-braces	0.8	0.8	0.7
X-braces	0.9	0.9	0.8
Longer segment length (full length)	–	–	0.7
Secondary horizontals	0.7	0.7	0.7

Note The effective length alignment chart provided in all three codes is to be used. The alignment charts are provided in AISC and section A 13.5 of the ISO

Table 6.6 Moment reduction factors

Structural component	API RP 2A-WSD	API RP 2A-LRFD	ISO 19902
Topside legs			
Braced	0.85	1	0.85
Portal (unbraced)	0.85	0.85	0.85
Structure legs and piling			
Grouted composite section	*C*	1	*C*
Ungrouted legs	*C*	1	*C*
Ungrouted piling between shim points	*B*	1	*B*
Structure brace members			
Primary diagonals and horizontals	*B* or *C*	0.8	*B* or *C*
K-braces	*C*	0.8	*B* or *C*
X-braces	–		
Longer segment length	*C*	0.9	*B* or *C*
Full length	–	–	*B* or *C*
Secondary horizontals		0.7	*B* or *C*

Where $B = 0.6 - 0.4\ (M_1/M_2)$, but not less than 0.4, not more than 0.85
$C = 1 - 0.4(f_a/F_{e'})$, or 0.85, whichever is less

Figure 6.3 shows the ratio of API local buckling strength to that of ISO. This ratio applies to very stocky but short columns, and for long columns, overall buckling starts first, and thus, local buckling effects are not significant.

Figure 6.4 shows that for $D/t = 60$ and yield stresses in excess of 350 N/mm^2, the ISO provision is more burdensome than LRFD, whereas in yield buckling interaction region ($D/t \geq 60$), the ISO equation is more optimistic than LRFD.

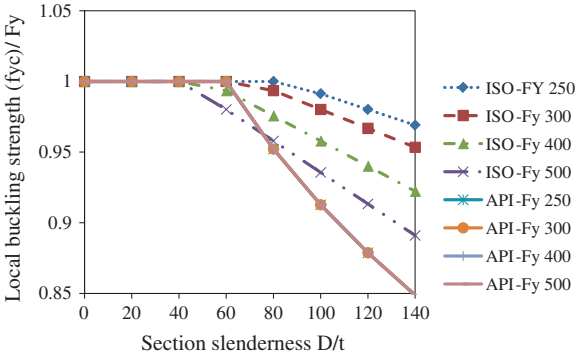

Fig. 6.2 Comparison of API and ISO local buckling strength

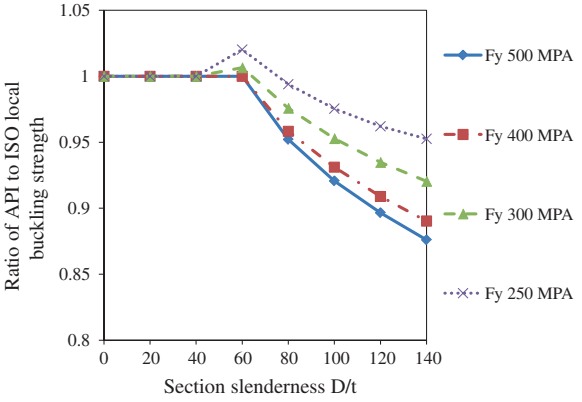

Fig. 6.3 Comparison of ISO and API (LRFD or WSD) local buckling strengths

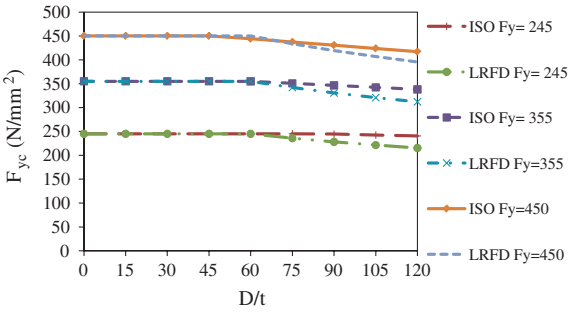

Fig. 6.4 Comparison of API and ISO local buckling strength

Figure 6.5 shows that (i) ISO is independent of yield stress, but LRFD provides different requirements for different values of yield stress. This should not occur in non-dimensional structural strength frame. (ii) ISO gives more structural efficiency in comparison with LRFD.

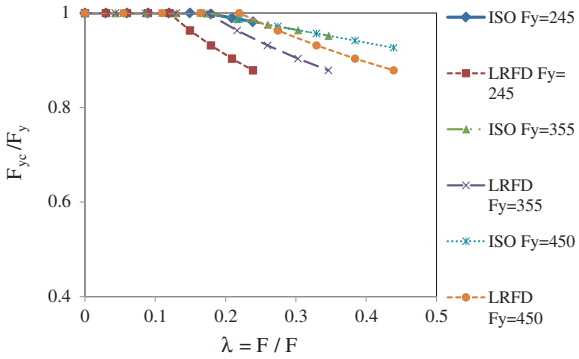

Fig. 6.5 Comparison of API and ISO local buckling strength

6.4.3 Bending

For $D/t \leq 10{,}340/f_y$, the bending strength formula for WSD is $0.75f_y$. In comparing design resistance formulae with respect to partial safety factor, the ISO design resistance is $0.95/(1/1.05) = 100$ % of API LRFD resistance. The expressions are the same. The limits given in WSD and LRFD are geometric (D/t), whereas the limits used in ISO are having material strength and Young's modulus. The upper limit for D/t given in WSD and LRFD is 300. Failure of cylindrical members in pure bending is precipitated by localised axis symmetric bulges on the compression side of the cylinders [5]. Like local buckling (in axial compression), buckling behaviour depends on D/t ratio, and at larger D/t ratios, both moment and rational capacities of tube decrease. Tubular members of Jacket may have bending stresses due to any of the following three material regions:

(a) Inelastic,
(b) elastic to plastic,
(c) elastic.

As per API LRFD, simply supported beam tests have smaller moment capacities than fixed end beam tests. Reduction in moment capacity is considered with the reduction in support rigidity. On the other hand, end conditions have little influence on rotational capacity of cylinder. At low F_y d/t, plastic hinge mechanism forms over short length of tubular. Now when end support rigidity is reduced, hinge is formed over a longer segment of cylinder. F_y d/t for tubular shell increases, whereas moment as well as rotational capacities decreases. Behaviour of cylindrical shell is defined, when behaviour of cylinder subjected to bending is separated into three regions:

(a) High rotational capacity: Ductile failure mode, i.e. load decay is gradual
(b) Intermediate rotational capacity: Semi-ductile failure mode, i.e. load decay is even more gradual
(c) Low rotational capacity: Little post-yield ductility, i.e. load decay is rapid and is susceptible to local buckling.

From above region (a), extending up to F_y D/t = 10,340 allows to develop full plastic moment capacity. This is reduced to 10 % in excess of yield moment capacity (M_u/M_y = 1.10) at F_y D/t = 20,680 MPa in region (b). LRFD nominal bending stress defines full plastic capacity of tubular section in region (a), while WSD formulation for allowable bending stress increased by (1.67—safety factor) yields less full plastic capacity [3]. In WSD, allowable stresses for cylinders under bending have been derived by using a safety factor of 1.67 against ultimate bending capacities at lower bound. WSD and LRFD depend on same relationship with ultimate moment capacity normalised with respect to yield moment capacity (M_u/M_y). In ISO, bending strength of fabricated tubular members is achieved by dividing the ultimate plastic moment strength by elastic yield moment. Here, ultimate bending moment strength is called full plastic moment of member. Members with f_y = 345 MPa and E = 205,000 MPa full plastic moment can be developed if $D/t \leq 30$, when $D/t \approx 60$, the strength is linearly reduced to about 10 % in excess of yield strength.

6.4.4 Shear

Two types of shear are identified, namely the beam shear and torsional shear. For beam shear, the expressions in all the three codes are similar when the factors are removed. In the WSD, the allowable beam shear stress is taken as 0.4 times the yield strength. The representative shear strength is taken as $f_y/\sqrt{3} = 0.58f_y$ in ISO, the partial resistance factor being 1.05. In LRFD, the resistance factor is 0.95 which is same as in ISO (i.e. 1/1.05 ≈ 0.95). For torsional shear, the expressions in all the three codes are similar when the factors are removed. In the WSD, the allowable torsional shear stress is taken as 0.4 times the yield strength. The partial resistance factor is 1.05 in the ISO. In LRFD, the resistance factor is 0.95 which is same as in ISO.

6.4.5 Hydrostatic Pressure (Hoop Buckling)

Equations of API LRFD and ISO are same, whereas WSD differs. Here, elastic hoop buckling stress Fhe is same in LRFD and ISO codes, but critical hoop buckling stress Fhc is different in WSD, which is shown in Fig. 6.6. External pressure acts radially on submerged tubular members either with or without axial component [12]. In former case, pressure load effect is termed as “hydrostatic”, while the radial pressure with no axial component is usually called as “lateral” and gives rise only to hoop stresses [13].

In WSD, the design formula is given as $f_h \leq F_{hc}/SF$, and for the F_{hc}, expressions are given for four elastic stress ranges. In comparing design resistance formulae of ISO and LRFD with respect to partial safety factor, the ISO design

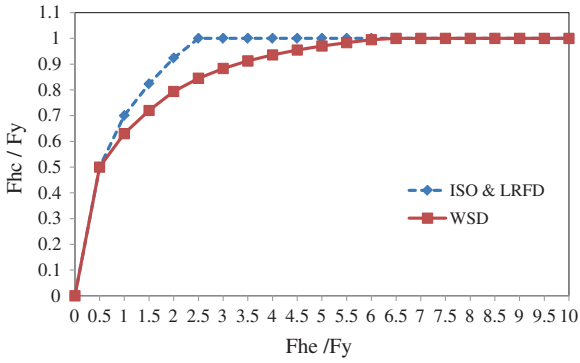

Fig. 6.6 Hoop buckling strength as a function of elastic buckling stress

resistance is 0.80/(1/1.25) = 100 % of API LRFD resistance. The equations in LRFD and ISO are identical. However, LRFD provides only a single expression for critical hoop buckling, whereas ISO provides formula for three ranges of elastic hoop buckling strength. The expression for design hydrostatic head provided in WSD and LRFD is identical. Same expressions are provided for circumferential stiffening ring design in WSD and LRFD. However, the ISO gives additional guidance on (a) external and internal rings, (b) guidance for avoidance of local buckling of ring stiffeners with and without flanges. Hoop buckling occurs when tubular members subjected to external pressure. Hoop buckling stress is determined through following: (i) material yield strength with respect to elastic hoop buckling stress and (ii) design equations are valid in the range of $F_y < 60$ Ksi and $D/t < 120$.

Along with hoop stresses external hydrostatic pressure imposes a capped-end axial compression force in the member if ends are capped; on the other hand external radial pressure only imposes hoop compression in tubular member and no capped-end compression. As hoop and capped-end axial stresses from external pressure are always in compression, they are assumed to have positive sign [5]. Unstiffened circular members under external hydrostatic pressure go through local buckling of shell wall anywhere between restraints. Effect of external pressure on circular member is magnified by an original geometric imperfection/out of roundness. For closed-end circulars such as braces, hydrostatic pressure also imposes an axial compressive stress of $0.5f_h$, some of which is taken by the structure and some of which passes into the member [16]. Hoop stress is shown in Eq. 6.3.

$$\text{Hoop stress} \leq \frac{\text{Critical hoop buckling capacity}}{\text{Hoop buckling safety factor}} \tag{6.3}$$

Critical hoop buckling capacity F_{hc} in API WSD is same as used in API LRFD (without resistance factor) [5]. Elastic hoop buckling stress F_{he} is same in LRFD and ISO codes, but critical hoop buckling stress F_{hc} is different in WSD, which is shown in Fig. 6.6.

6.4.6 Combined Stresses Without Hydrostatic Pressure

Here, circular members acted upon by combined axial as well as bending stresses are considered. The secondary moments from factored global stresses and bending stresses (P − Δ) effects are not considered except in cases of large axial force or flexible component is under consideration. P − Δ effects are found to be important in the design of unbraced deck legs, piles and laterally flexible structures [4]. For combined equations of tension and bending or compression and bending, ISO has taken a linear form as WSD, but LRFD has given a cosine form as indicated by Fig. 6.7. This cosine equation can be exploited with low D/t ratios like $D/t > 25$ [14]. Due to this nonlinear approach by LRFD, the given equations are not a good measure for component's usage in resistance equations especially for combined hydrostatic pressure [5]. PAFA reports that cosine equation for combined stresses in local buckling may be appropriate for stocky sections, i.e. low D/t, but the result is not corroborated due to insufficiency of test reports [7]. ISO has made two changes in the combined equations, i.e. when combined stresses act with hydrostatic pressure, hydrostatic pressure do affect local buckling strength, but there is no effect on overall buckling. Interaction equation between bending, tension and pressure becomes conservative with increasing cross-sectional slenderness. These results will affect the reduction in member size compared with existing practice. Here, two types of analysis are recognised one when capped-end forces are considered and other when they are not taken into consideration.

6.4.6.1 Tension and Bending

In WSD, the safety factor on axial component is 0.6. The expression given in WSD is shown in Eq. 6.4 and is a modification of the expression AISC, namely

$$\frac{f_a}{0.6F_y} + \frac{f_{bx}}{F_{bx}} + \frac{f_{by}}{F_{by}} \leq 1.0 \tag{6.4}$$

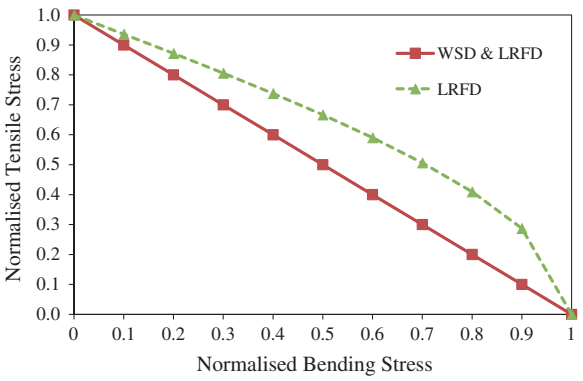

Fig. 6.7 Normalised interaction curve for combined axial tension and bending

Equation 6.4 was modified for LRFD version where resistance factor comes into effect. In comparing the design resistance formulae with respect to partial safety factor, the LRFD has partial safety factors of $\phi_\tau = 0.95$ and $\phi_b = 0.95$, whereas ISO has $\gamma_{R,\tau} = 1.05$ and $\gamma_{R,b} = 1.05$. Hence, the factors are identical. Here, the components experiencing combined axial tension and bending actions are checked at all cross sections along their length. If bending stress is greater than the axial tension, the local buckling effect (due to bending on compression side) is considered in bending strength (F_{bn}) [3]. The API LRFD interaction formula is in the cosine form. Neither API WSD nor ISO uses the cosine form.

6.4.6.2 Compression and Bending

API LRFD and ISO use AISC-ASD beam–column stability interaction equation (first), and this gives conservative results when used for large-scale offshore members where imperfections and residual stresses are comparatively more (LRFD code). From LRFD interaction equation governing overall buckling, the compression partial resistance factor applied to Euler stress in bending term, is deleted in ISO, which may lead to less conservative design as compared to LRFD. This change will tend to compensate for conservative outcome introduced by linear form of local buckling equation [7]. However, outcome may not be clear as it is not certain that local or overall requirement may govern the member design in the presence of compression and bending.

The WSD formula is from the AISC [5]. In WSD, two interaction equations have to be complied (i) for member stability and (ii) for plasticity. All three codes use two equations, i.e. (i) involving overall compressive strength and $P - \delta$ amplified bending stress and (ii) involving local buckling strength and unamplified bending stress. When axial component is small, i.e. $f_a/F_a \leq 0.15$, an alternate equation is provided. In comparing the design resistance with respect to partial safety factors, both use equal factors, and the LRFD has partial safety factors of $\phi_c = 0.85$ and $\phi_b = 0.95$, whereas ISO has $\gamma_{R,c} = 1.18$ and $\gamma_{R,b} = 1.05$. This type of stresses indicates beam–column nature of action of stress. Two equations are provided here: first is for beam–column stability check and the second is for strength check for components under combined axial compression and bending [4].

6.4.7 Combined Stresses with Hydrostatic Pressure

Tubular member under the water line is subjected to hydrostatic pressure if it has not been filled with water [4]. Fluid is allowed in hollow legs due to upending and placement and for pile installation [3]. Members filled with water under in-place conditions are subjected by hydrostatic pressure during launch and installation [4]. Hydrostatic pressure effects are taken into account when conducting member checks like axial compression of capped-end pressures [4]. When longitudinal

tensile stresses due to axial tension and bending and hoop compressive stresses (collapse) due to hydrostatic pressure occur simultaneously, then the interaction equations are used [1]. Cylindrical members subjected to hydrostatic pressure are checked against (1) hoop buckling under hydrostatic pressure, (2) tensile yielding under combination of action effects (capped-end forces result in tension in member), (3) compression yielding and local buckling when combined action effects like due to capped-end forces producing compression in member and (4) column buckling when force effects, excluding that coming from capped-end actions results in compression [4].

6.4.7.1 Tension, Bending and Hydrostatic Pressure

In comparing design resistance with respect to partial safety factor, the LRFD has partial safety factors of $\phi_\tau = 0.95$, $\phi_b = 0.95$ and $\phi_h = 0.80$, whereas ISO has $\gamma_{R,\tau} = 1.05$, $\gamma_{R,b} = 1.05$ and $\gamma_{R,h} = 1.25$. Outside hydrostatic pressure has three main effects in existence of tensile forces: (i) decrease of axial tension due to capped-end axial compression, (ii) decrease in axial tensile strength (f_t) caused by hoop compression, results in $f_{t,h}$ and (iii) decrease of bending strength (f_b) caused by hoop compression results in $f_{b,h}$. Axial tension hydrostatic pressure interaction is similar to bending–hydrostatic pressure interaction [4].

6.4.7.2 Compression, Bending and Hydrostatic Pressure

Capped-end axial compressive stress due to hydrostatic pressure does not produce column buckling of a tubular under combined external compressive stress as well as hydrostatic pressure. For stability check, calculated axial compression, i.e. external axial compressive stress is used only. In comparing design resistance with respect to partial safety factor, the LRFD has partial safety factors of $\phi_c = 0.85$, $\phi_b = 0.95$ and $\phi_h = 0.80$, whereas ISO has $\gamma_{R,c} = 1.18$, $\gamma_{R,b} = 1.05$ and $\gamma_{R,h} = 1.25$.

6.5 Summary

The code equations of cylindrical members are almost similar for stresses acting independently or in group, e.g. API RP 2A-WSD, LRFD and ISO have identical equations for axial tension, bending and hydrostatic pressure. The equations provided in the three codes for nine different stress conditions have been compared through descriptions and graphs. Some of the underlying factors for these differences were identified. These equations are valid for cylindrical members of offshore Jacket platforms at all depths [17–19]. The following conclusions are drawn after comparing the three codes:

ISO 19902 considers steel with yield stress up to 500 MPa, whereas in API codes, this limit is 414 MPa. Due to low consequences of tension yielding, safety indices in ISO and LRFD for extreme loading are taken larger than in WSD. Effective length factor (K) of bracing member is 0.8 in API, whereas it is 0.7 in ISO 19902 which shows the conservativeness of ISO. Local buckling check depends on only geometric parameter in API WSD and API LRFD, whereas in ISO, it depends on geometric and elastic modulus of members. Additional information is provided by ISO 19902 for (i) external and internal rings and (ii) guidance for avoidance of local buckling of ring stiffeners with and without flanges. In the local buckling equations used for axial compression, bending and hydrostatic pressure, the API allows the upper limit of D/t ratio up to 300, whereas ISO 19902 permits up to 120 only. ISO 19902 gives separate equations when two or more separate cross sections are combined in a member under compressive stress, unlike in the API codes. The bending stress equation in ISO contains modulus of elasticity and the yield strength, whereas the API equation has only yield strength. Shear stress factors in API LRFD and ISO 19902 remain same, whereas WSD has more reduced factors. Linear interaction equations are introduced in ISO following API RP 2A-WSD, whereas cosine interaction equations are given by API RP 2A-LRFD. The criteria, for slender beam–column strength, are made through reduction below elastic buckling. Capped-end forces from hydrostatic pressure could be included in or excluded from analysis of Jacket structures with subsequent strength formulations. In WSD, design formulae are provided for four elastic stress ranges. The equation in LRFD and ISO is identical. LRFD provides only a single equation for critical hoop buckling, while ISO provides equation for three ranges of elastic hoop buckling strength.

Members subjected to combined compression and flexure must be proportioned in such a way that they satisfy strength as well as stability criteria throughout their length. When design storm environmental conditions enforce stresses due to lateral and vertical forces, WSD (AISC) stresses are increased by 1/3.

References

1. API RP 2A-WSD: Planning, Designing and Constructing Fixed Offshore Platforms—Working Stress Design, 21st edn. American Petroleum Institute (2000)
2. API RP 2A-LRFD: Planning, Designing and Constructing Fixed Offshore Platforms—Load and Resistance Factor Design, 1st edn. Reaffirmed 16 May 2003 (1993)
3. ISO 19902: Petroleum and Natural Gas Industries—Fixed Steel Offshore Structures (2007)
4. PTS 34.19.10.30: Design of Fixed Offshore Structures, PETRONAS Technical Standards. PETRONAS Carigalli Sdn Bhd (2010)
5. Advanced Mechanics and Engineering Ltd.: Assessment of the historical development of fixed offshore structural design codes. Offshore Technology Report, OTO 1999-015. Prepared for HSE UK (1999)
6. American Institute of Steel Construction (AISC): Manual of Steel Construction—Load and Resistance Factor Design (1994)
7. PAFA Consulting Engineers: For HSE, Implications for the assessment of existing fixed steel structures of proposed ISO 13819-2 member strength formulations. Final Report (2000)

8. Advance Mechanics & Engineering Ltd. For HSE, Buckling of offshore structures: assessment of code limitations. Offshore Technology Report-OTO 97-049
9. MSL Engineering Ltd.: For HSE, Load factor calibration for ISO 13819 regional annex: component resistance. Offshore Technology Report 2000/072
10. Wisch, D.J.: Fixed Steel Standard: ISO and API Developments—ISO TC 67/SC 7/WG3. OTC 8423, Houston, Texas (1997)
11. Guenard, Y., Goyet, J., Labeyrie, J.: Structural safety evaluation of steel jacket platforms. The Society of Naval Architects and Marine Engineers, Virginia, 5–6 Oct 1987
12. Bomel Ltd.: For HSE, Comparison of tubular member strength provisions in codes and standards. Offshore Technology Report 2001/084
13. Advance mechanics & Engineering Ltd.: For HSE, Buckling of offshore structures: assessment of code limitations. Offshore Technology Report-OTO 97 049
14. Knapp, A.E., Dixon, D.A.: The use of x-bracing in fixed offshore platform. In: Proceedings of the 5th Offshore Technology Conference. OTC 1663, Houston (1972)
15. Livesley, R.K.: The application of an electronic digital computer to some problems of structural analysis. Struct Eng 34, 1 (1956)
16. ISO 13819-2.: Offshore Structures—Part 2: Fixed Steel Structures. ISO 19902 cancels and replaces ISO 13819 (1995)
17. Mangiavacchi, A.: API Offshore Structures Standards: 2006 and Beyond. OTC 17698, Houston (2005)
18. Snell, R.: ISO Offshore Structures Standard. OTC 8421, Houston, Texas, 5–8 May 1997
19. Hellan, O., Moan, T., Drange, S.O.: Use of non-linear pushover analysis in ultimate limit state design and integrity assessment of jacket structures. In: Proceedings of 7th International Conference on the Behaviour of Offshore Structures BOSS (1994)

Chapter 7
Component Reliability and Environmental Load Factor

Abstract Behaviour of structure can be measured by probability of failure or reliability index. Target reliability of components is found as per API RP2A WSD. Load factors are developed in such a way that the reliability index of Jacket is at predefined target level. The reliability indices of ISO LRFD design for a range of load factors are determined. When ISO load factors are plotted against the corresponding API target reliabilities, the intersection point gave the proposed load factor. Not only the Jacket reliability designed as per new load factors will be higher than the target, but also it will ensure safer Jacket.

7.1 Introduction

Reliability is defined as an ability to fulfil the particular requirements including the design working life of Jacket [1]. This chapter presents the structural reliability analysis of tubular components of four Jacket platforms in Malaysia. After reliability is determined, the corresponding environmental load factors are developed. They are compared with load factors used in other regions, and finally, load factors for offshore Malaysia region are recommended. Figures 7.1 and 7.2 are taken by the author during the site visit for determination of variability of resistance uncertainty.

7.2 Selection of Members

The method followed here depends on ISO LRFD 19902, which is explained by BOMEL [2]. Primary members are selected from Jacket for reliability analysis. These members include leg, vertical diagonal, horizontal at periphery and horizontal diagonals of Jacket. Table 7.1 shows some typical members selected for finding the reliability index. They are selected from the slenderness $\frac{k \times l}{r}$ and diameter-to-thickness ratio. This table is based on one of the four selected platforms.

Z. Nizamani, *Environmental Load Factors and System Strength Evaluation of Offshore Jacket Platforms*, Ocean Engineering & Oceanography 4,
DOI 10.1007/978-3-319-15051-2_7

Fig. 7.1 Tubular component of a brace member assembly

Fig. 7.2 Tubular brace member under construction

Table 7.1 Member selection for calibration–slenderness ratio and *d*/*t* ratio

Diameter (*D*) mm	Wall thickness (*T*) mm	Length (*L*) mm	*K* factor	Slenderness (%)	*D*/*T*
1,650	25.0	9,344	1.0	0.23	66.00
1,630	15.0	17,500	1.0	0.43	108.7
660	12.7	15,370	0.7	0.65	51.97
711	15.0	11,000	0.7	0.43	47.40
610	12.7	11,800	0.7	0.54	48.03
660	19.0	11,940	0.7	0.51	34.74
406	12.7	12,000	0.7	0.83	31.97
508	12.7	12,400	0.7	0.68	40.00

7.3 Component Target Reliability

Reliability index for offshore Jacket platforms can be taken as minimum lower bounds of safety levels acceptable to the public. Load and resistance factor design requires the development of target reliability levels. Theophanatos et al. 1992 [3] suggested the selection of target reliability using (API WSD/API LRFD/ISO 19902) for the selection of target safety index and separate partial factors for individual component and load effect types to be determined. The best possible safety required for the structure depends on the cost of failure of structure [4]. Optimum safety can be determined by minimum expected cost or with maximum utility [4, 5]. The target reliability indices are chosen so that it can give consistent and uniform safety margin for all components.

Primary members are the main element of the Jacket, whose failure may cause serious damage to the structure. Target reliability of secondary components can be fixed at a lower value than the primary members. Serviceability limit state (SLS) has a lower level of consequences of failure than ultimate limit states (ULS). For ultimate limit states, calculated reliability indices represent component reliability [4, 5]. Therefore, in this book, only ultimate limit state has been considered for finding the reliability index. Tables 7.2 and 7.3 show the values used for the calibration of ISO code, taking into effect of North Sea platforms. Reliability indices are for different Jacket components and load factors [2].

Table 7.2 ISO target reliability [6]

Load effect	API RP2A WSD	ISO ($\gamma = 1.35$)
	β	β
Compression and bending	3.49	3.84
Tension and bending (brace)	3.64	3.85
All	3.50	3.85

Table 7.3 Reliability index against different environmental load factors [2]

Code		Brace	Brace compression and bending	Leg
API (WSD)		3.70	3.70	3.49
ISO	$\gamma_w = 1.20$	3.66	3.69	3.57
	$\gamma_w = 1.25$	3.75	3.79	3.66
	$\gamma_w = 1.30$	3.84	3.88	3.76
	$\gamma_w = 1.35$	3.93	3.97	3.84
	$\gamma_w = 1.40$	4.02	4.05	3.94
	$\gamma_w = 1.45$	4.11	4.14	4.02

7.4 Component Reliability Analysis

API and ISO are component-based design codes. The element is designed, and then the system is checked using overall system analysis. In this book, it is divided into different bays and subdivided into types of members. SACS software is used for the analysis of Jackets. However, W_e/G ratios above 10 may not actually occur in this region, but still they are included in this book to check the effects of higher load. The most pertinent W_e/G ratio lies in between 0.5 and 2.0. Design code equations for components are shown in Appendix A and relevant MATLAB codes are shown in Appendix C.

7.4.1 Code Stresses

API and ISO codes specify seven types of stresses a component undergoes during its design life. These can be single or two or three combined stresses. Here, limit state equation for seven types is used to find the reliability.

7.4.1.1 Single Stresses

Jacket members under pure axial tension are not found during the analysis. For finding reliability against tensile stresses, only those members that are predominantly influenced by axial tensile stresses and with minimum bending stresses are selected. The reliability is determined for the member, to find the effect of API and ISO codes using different environmental-to-gravity load ratios. The basic equations for API and ISO are found to be similar, i.e. depending on the yield strength (F_y) except safety factors. Figure 7.3 shows component reliability of member under axial tension. The ISO LRFD with a load factor of 1.35 gave higher values of reliability as compared to API WSD. ISO LRFD (MS) proposes a load factor of 1.25 as shown in Fig. 7.41. Here, ISO LRFD is plotted with an environmental load

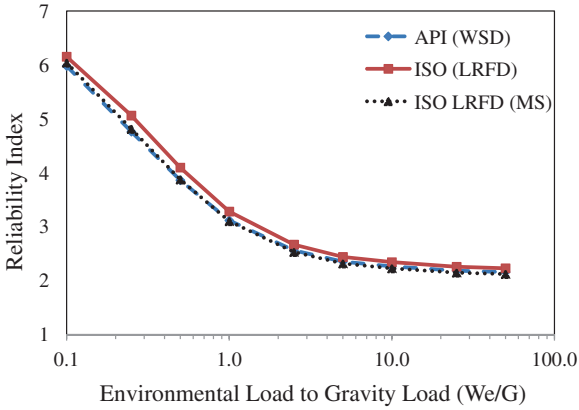

Fig. 7.3 Variation of W_e/G ratio versus reliability index for components in axial tension for API WSD, ISO (MS), and ISO LRFD codes at SKO1

factor of 1.35 as given by ISO code. ISO LRFD (MS) stands for this region with a load factor of 1.25. When the ratio of W_e/G increases, the reliability decreases. It can be seen that with the increase of W_e/G ratio, reliability decreases for all cases. The ISO (LRFD) code gave higher values as compared to API (WSD), which shows the consistency of the ISO code.

The same trend is observed in the case of axial compression as shown in Fig. 7.4. Here also, the ISO code gave higher reliability index at different W_e/G ratios. It is found that metocean parameters are more influencing as compared to other variables for this type of stresses.

Figure 7.5 shows reliability for members under isolated bending stress which are not encountered during the Jacket analysis. Here, selected members are those which showed high ratio of bending stresses as compared to axial stress. The results showed the same trend, and ISO is again higher as compared to API. ISO LRFD (MS) comes in between both codes for compression and bending cases as shown in Figs. 7.4 and 7.5. During Jacket analysis, compression stress is the only isolated stress present in components out of the above three isolated stresses.

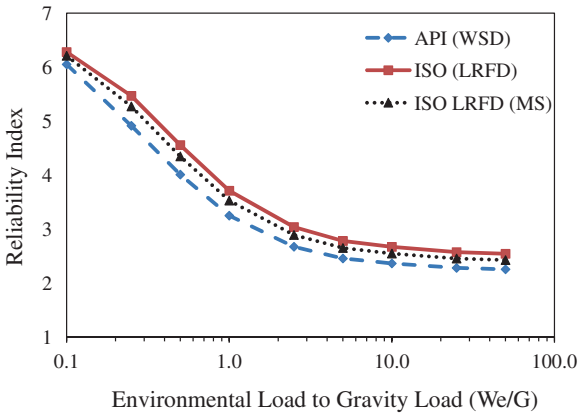

Fig. 7.4 Variation of W_e/G ratio versus reliability index for components in compression for API WSD, ISO (MS), and ISO LRFD codes at SKO1

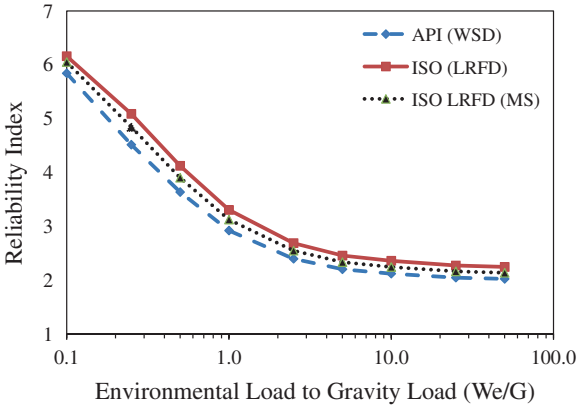

Fig. 7.5 Variation of W_e/G ratio versus reliability index for components in bending for API WSD, ISO (MS), and ISO LRFD codes at SKO1

7.4.1.2 Combined Two Stresses

Figures 7.6 and 7.7 depend on the reliability of combined two stresses which are found in the actual member analysis. The code equations are similar in API WSD and ISO LRFD, but the only difference is in safety factors. The ratio of axial to bending stress used here is 0.5, which is from actual stresses as explained in Chap. 3. The result shows that the ISO reliability is again higher, but in the case of compression and bending, not only both curves are close together but also at higher gravity load, API gave higher values. This book proposes values that are in between the curves with a load factor of 1.25. Combined stress ratio used for reliability analysis is based on 50 % for axial tension/compression and 50 % for bending. This is the ratio available from the Jacket and also used for ISO code development [2].

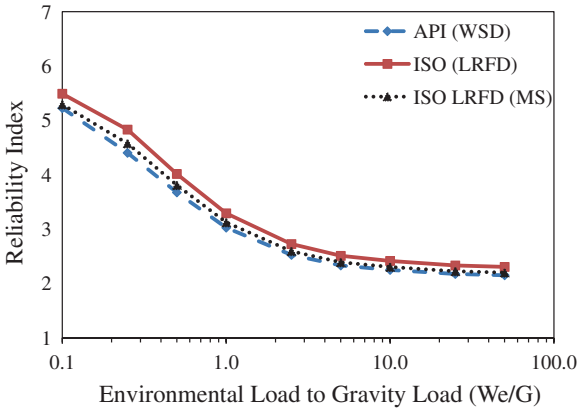

Fig. 7.6 Variation of W_e/G ratio versus reliability index for components in tension and bending for API WSD, ISO (MS), and ISO LRFD codes at SKO1

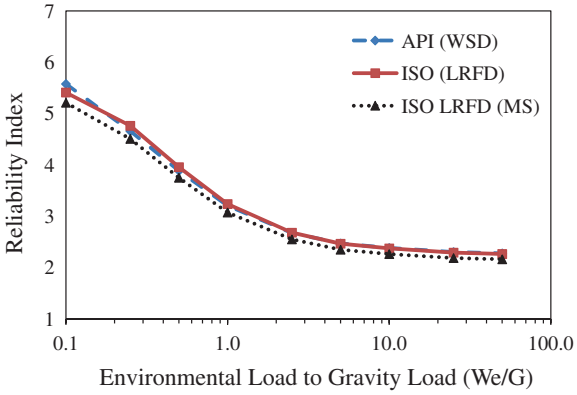

Fig. 7.7 Variation of W_e/G ratio versus reliability index for components in compression and bending for API WSD, ISO (MS), and ISO LRFD codes at SKO1

7.4.1.3 Combined Three Stresses

The ratio for combined three stresses used in this book for axial to bending stress is 0.4–0.6. The result in Figs. 7.8 and 7.9 shows the same trend as is found for ISO. Steepness reduced at higher values of W_e/G as compared to low values. The ISO LRFD value gave higher reliability as compared to API WSD, and this book proposes load factor of 1.25. Figure 7.9 shows reliability values proposed in this book which are less than the target reliability index, but on average, the results showed that 1.25 is agreed upon. Combined stress ratio used for reliability analysis is based on 40–60 % for axial tension/compression and bending. This is the ratio available from the Jacket and also used for ISO code development [2].

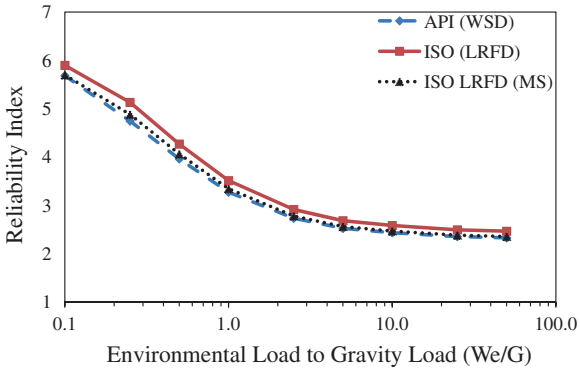

Fig. 7.8 Variation of W_e/G ratio versus reliability index for components in tension, bending, and hydrostatic pressure for API WSD, ISO (MS), and ISO LRFD codes at SKO1

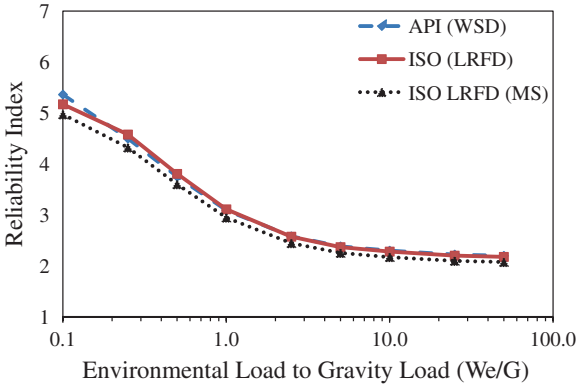

Fig. 7.9 Variation of W_e/G ratio versus reliability index for components in compression, bending, and hydrostatic pressure for API WSD, ISO (MS), and ISO LRFD codes at SKO1

7.4.2 Sensitivity Analysis

All variables of random input do not have equal influence on reliability index output. Sensitivity analysis can be used to quantify the influence of each basic random variable [7]. Table 7.4 shows the sensitivity index for the variables used in this research. The most important influence is made by significant wave height, current, environmental load model uncertainty, stress model uncertainty, and yield strength. This means that these parameters have high weightage for reliability index and geometrical parameters are less sensitive. The same is achieved for study conducted in Mediterranean Sea [8] and for ISO [2]. ISO recommends that most sensitive α values for resistance should have value of 0.8 and for load −0.7 [9]. The significant wave height of Malaysian regions is lower as compared to GOM and NS, which plays important role in reliability analysis as shown in Table 7.4. Thus, comparative target reliability is achieved using a reduced load factor of 1.25. Sensitivity analysis indicated that environmental load parameters strongly influenced the reliability of Jacket [10].

Table 7.4 Sensitivity analysis of random variables' axial tension

Basic variable	Reliability index is achieved at these values of random variables	Sensitivity factor (α)
Yield strength	414.42	−0.1028
Diameter	1855	−0.0036
Thickness	52.15	−0.0378
Significant wave height	4.7	0.8783
Current	0.85	0.1160
Environmental load uncertainty model	0.86	−0.4325
Dead load	1.0	0.000787
Live load	1.0	0.0013
Stress model uncertainty	1.24	−0.127

7.4.3 Effect of Variation of Environmental Load Factor

The effect of environmental load to gravity load variations for ISO code equations is shown in Figs. 7.10, 7.11, 7.12, 7.13, 7.14, 7.15, 7.16 and 7.17. This shows variation in reliability index with respect to change in environmental load factors. With high W_e/G ratios, the steepness reduced, and thus, reliability decreased with the increase in W_e/G ratios. These figures show clearly that the reliability index follows the same trend in the case of single, two, or three stresses. Higher reliability is achieved with increases in load factor.

7.4.4 Effect of Column Slenderness Ratio

The effect of slenderness on component reliability is not much varying. The variation of reliability index is small with wide range of columns having slenderness ratio in the range of 0.2–1.15. Column buckling ISO code equation that is used for

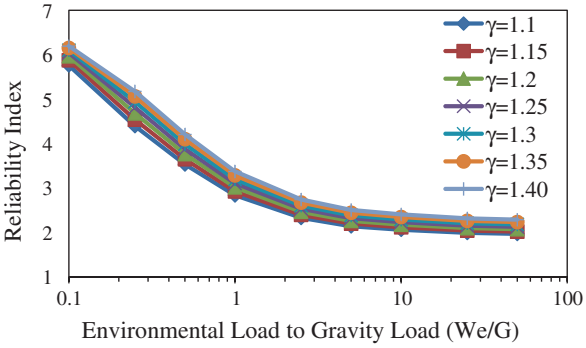

Fig. 7.10 Variation of reliability index versus W_e/G for axial tension (leg) using ISO code for different values of environmental load factor (γ)

Fig. 7.11 Variation of reliability index versus W_e/G for compression (leg) using ISO code for different values of environmental load factor (γ)

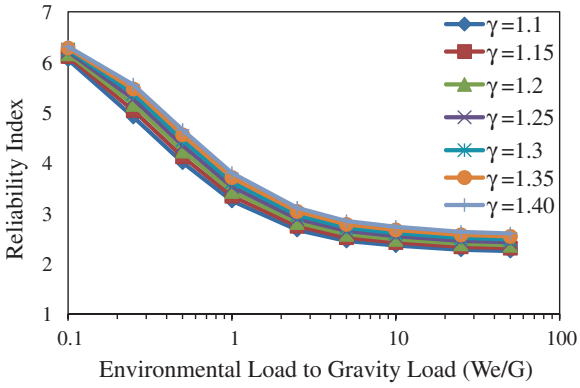

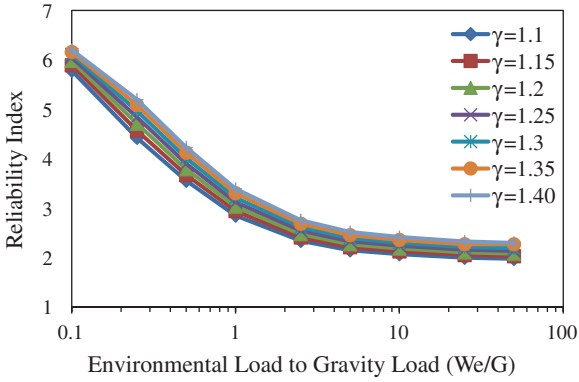

Fig. 7.12 Variation of reliability index versus W_e/G for bending (leg) using ISO code for different values of environmental load factor (γ)

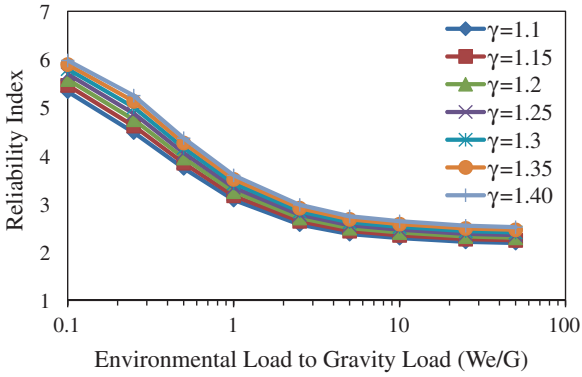

Fig. 7.13 Variation of reliability index versus W_e/G for tension and bending (leg) using ISO code for different values of environmental load factor (γ)

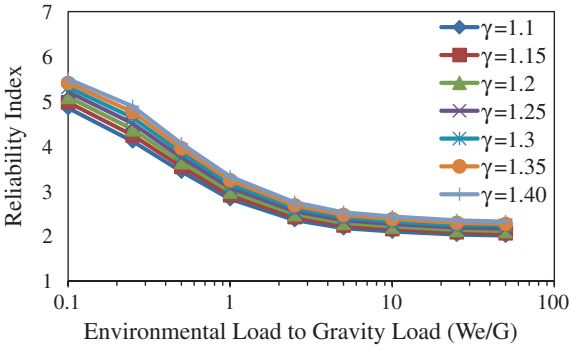

Fig. 7.14 Variation of reliability index versus W_e/G for compression and bending (leg) using ISO code for different values of environmental load factor (γ)

the reliability is evaluated with range of W_e/G ratio. Therefore, it can be concluded that reliability index is not sensitive to slenderness ratio as shown in Fig. 7.18.

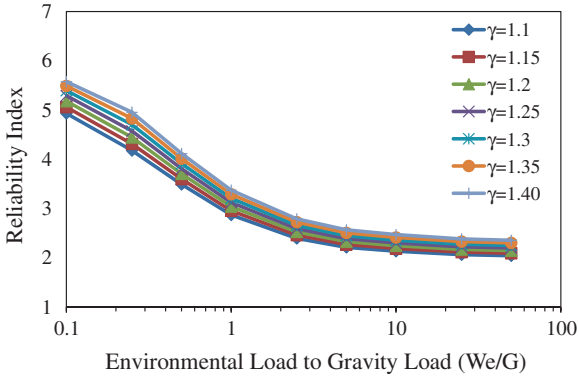

Fig. 7.15 Variation of reliability index versus W_e/G for tension, bending, and hydrostatic pressure (leg) using ISO code for different values of environmental load factor (γ)

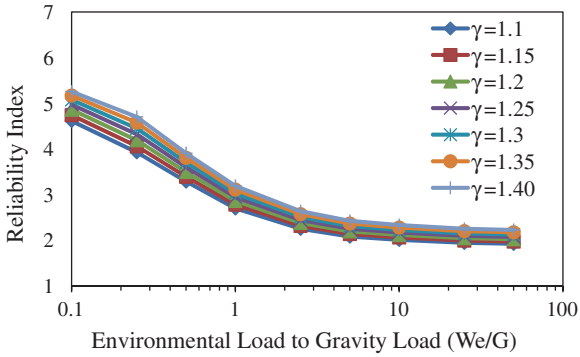

Fig. 7.16 Variation of reliability index versus W_e/G for compression, bending, and hydrostatic pressure (leg) using ISO code for different values of environmental load factor (γ)

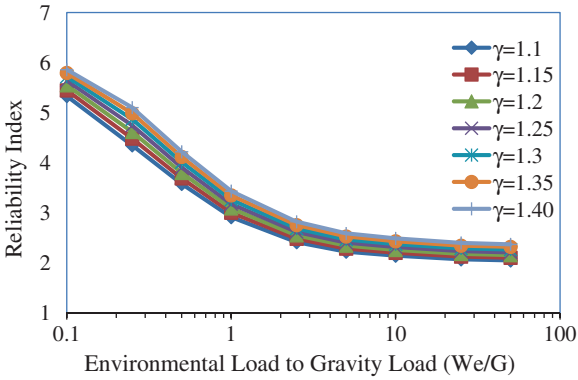

Fig. 7.17 Variation of reliability index versus W_e/G for combined stresses (leg) using ISO code for different values of environmental load factor (γ)

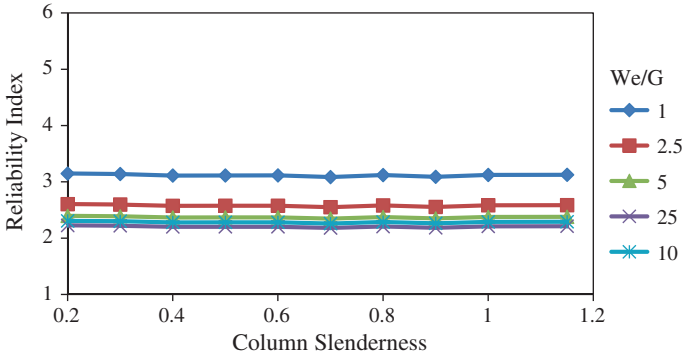

Fig. 7.18 Column slenderness versus reliability index for various W_e/G ratios

7.4.5 Calibration Points for Jackets

Calibration points are used to evaluate the effects of component reliability on both codes. It is seen that both codes gave results which are consistent and not much varied. Table 7.5 shows reliability index for this book compared with ISO study. Figures 7.19 and 7.20 show the calibration points for Jacket members for all types of model stresses. API WSD showed more consistency for all stresses. The calibration points of API are much close together as compared to ISO. The reliability index obtained in this book is comparable with ISO.

7.4.6 Selection of Environmental Load Factor

Load factors are multiplied with design/characteristic load with an intention so that this new factored load will be higher than the actual load. The criterion for selection of load and resistance factors is the closeness to the target reliability level [4, 5]. The factors must be based on the target reliability which should be equal to

Table 7.5 Reliability index for jacket members

Load type	MS		BOMEL [11]	
	ISO (LRFD)	API (WSD)	ISO (LRFD)	API (WSD)
Compression and bending	3.65	3.82	3.97	3.70
Tension and bending	4.53	4.09	3.85	3.64
Compression, bending, and hydrostatic	4.25	3.93	4.09	3.80
Tension, bending, and hydrostatic	4.37	3.74	3.72	3.85
Average	4.20	3.90	3.91	3.75

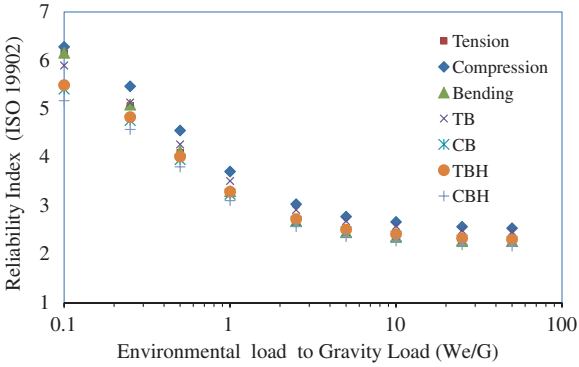

Fig. 7.19 Calibration of jacket members under ISO for all types of model stresses with W_e/G ratios versus ISO reliability indices

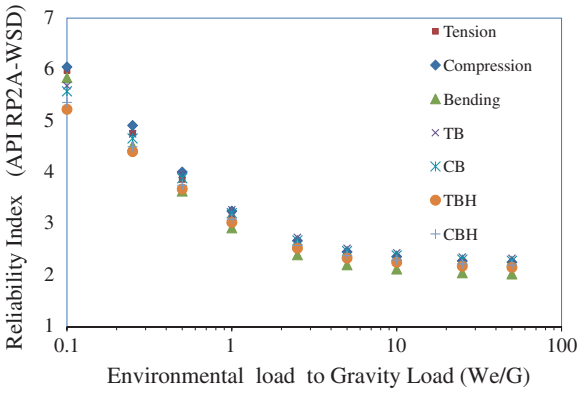

Fig. 7.20 Calibration of jacket members under API WSD for all types of model stresses with W_e/G ratios versus API WSD reliability indices

or greater than the preselected target reliability, and in this case, it is API WSD. Here, environmental load and resistance factors are calibrated so that the one close to target reliability can be selected. The point where ISO code overtakes the target reliability can be taken as the load factor. API (WSD) and ISO (LRFD) load factors are evaluated at W_e/G ratio of 1.0 as was determined by BOMEL [2]. The variation of load factors is influenced by the sensitivity of random variables as shown in Table 7.4. This method is used to find load factors based on target reliability from API WSD code which has proved its robustness and notional level of probability of failure is considered. This is done for AISC and ACI 318 codes. Target reliability is based on API WSD which has already proved it to be a reliable code.

7.4.7 PMO Platform

Figures 7.21, 7.22, 7.23, 7.24, and 7.25 show the environmental load factor for the PMO region for all the four components of Jacket. Figure 7.21 shows the

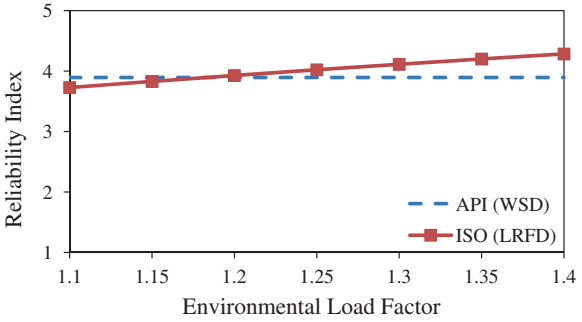

Fig. 7.21 Reliability index versus environmental load factor for HP at PMO using ISO 19902 and API WSD

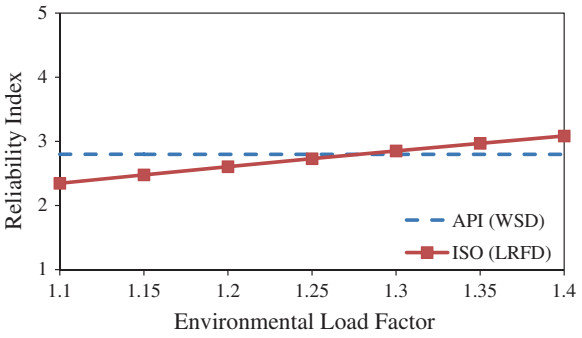

Fig. 7.22 Reliability index versus environmental load factor for HD at PMO using ISO 19902 and API WSD

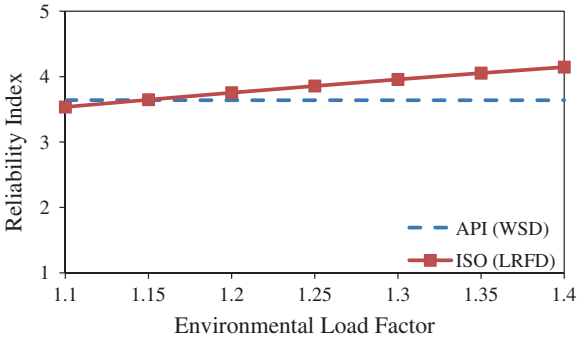

Fig. 7.23 Reliability index versus environmental load factor for VD at PMO using ISO 19902 and API WSD

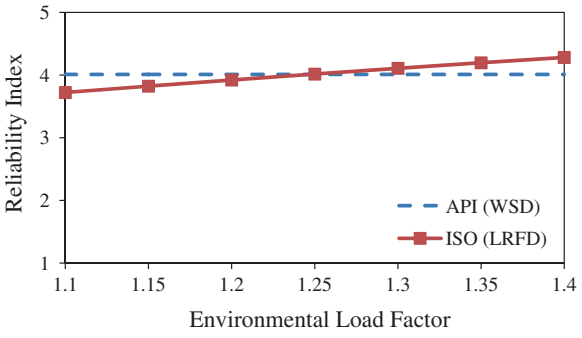

Fig. 7.24 Reliability index versus environmental load factor for leg at PMO using ISO 19902 and API WSD

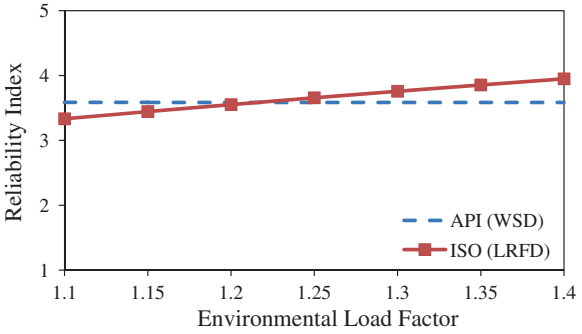

Fig. 7.25 Reliability index versus environmental load factor for component at PMO using ISO 19902 and API WSD

load factor for horizontal periphery brace member with a load factor of 1.20. Horizontal diagonal load factor of 1.27 is shown in Fig. 7.22. Figure 7.23 shows vertical diagonal load factor of 1.15, and finally, leg members shown in Fig. 7.24 have a load factor of 1.25. The averaged load factor for this region is evaluated to be 1.25 as shown in Fig. 7.25 with a API WSD target reliability index of 3.59. For the platform at PMO, the horizontal diagonal members are highly stressed. The least stressed members are vertical diagonals. The highest target reliability used is 4.0 for leg members.

7.4.8 SBO Platform

Figures 7.26, 7.27, 7.28, 7.29, and 7.30 show the environmental load factor for the SBO region for all the four types of components of Jacket. Figure 7.26 shows horizontal periphery brace member with a load factor of 1.25. Horizontal diagonal load factor of 1.25 is shown in Fig. 7.27. Figure 7.28 shows vertical diagonal load factor of 1.25, and finally, leg member is shown in Fig. 7.29 with a load factor of 1.25. The averaged load factor for this region is evaluated to be 1.27 as shown in Fig. 7.30, with average target reliability index of 4.30. The results from this

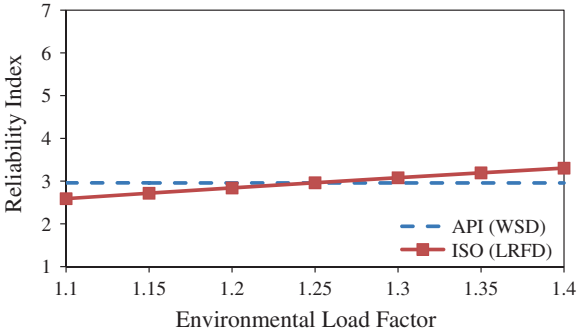

Fig. 7.26 Reliability index versus environmental load factor for HP at SBO using ISO 19902 and API WSD

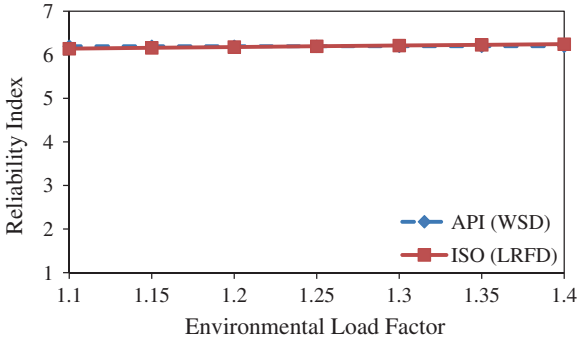

Fig. 7.27 Reliability index versus environmental load factor for HD at SBO using ISO 19902 and API WSD

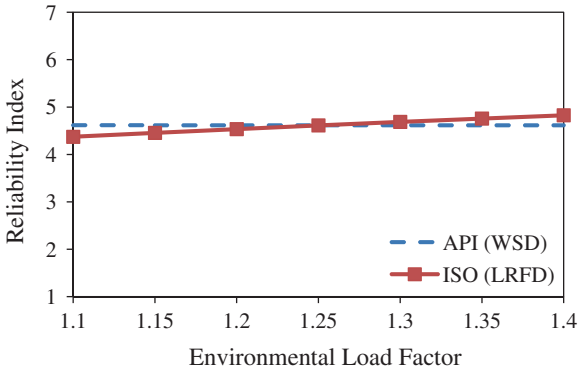

Fig. 7.28 Reliability index versus environmental load factor for VD at SBO using ISO 19902 and API WSD

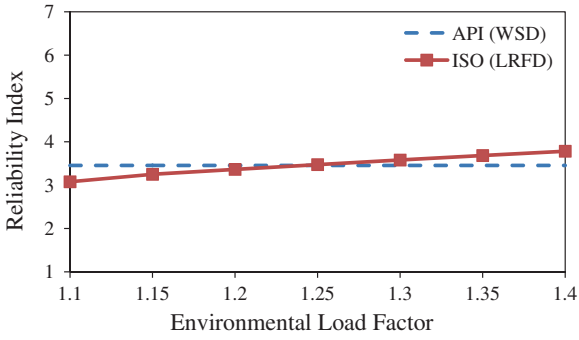

Fig. 7.29 Reliability index versus environmental load factor for leg at SBO using ISO 19902 and API WSD

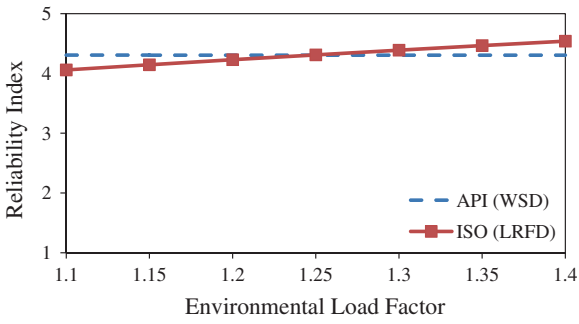

Fig. 7.30 Reliability index versus environmental load factor for component at SBO using ISO 19902 and API WSD

platform are the most consistent among all the platforms. This shows that members are equally stressed, though the target reliability is different for all the members. The highest reliability is found for horizontal diagonal member with target reliability of 6.1, and the lowest is for horizontal brace at periphery. The API WSD target reliability of 4.3 is evaluated for this platform.

7.4.9 SKO Region

From SKO region, two Jackets are selected for analysis, and results are presented here.

7.4.9.1 SKO1 Platform

Figures 7.31, 7.32, 7.33, 7.34, and 7.35 show the environmental load factor for the SKO1 Jacket, for all the four types of components of Jacket. Figure 7.31 shows the horizontal periphery brace member with a load factor of 1.15. Horizontal diagonal load factor of 1.25 is shown in Fig. 7.32. Figure 7.33 shows vertical diagonal load factor of 1.25, and finally, leg members in Fig. 7.34 show a load factor of

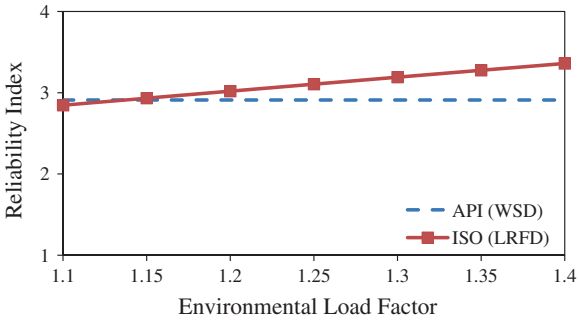

Fig. 7.31 Reliability index versus environmental load factor for HP at SKO1 using ISO 19902 and API WSD

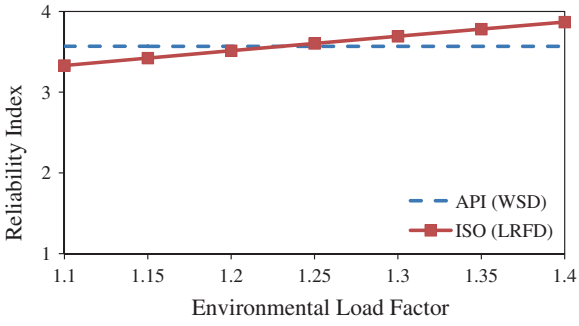

Fig. 7.32 Reliability index versus environmental load factor for HD at SKO1 using ISO 19902 and API WSD

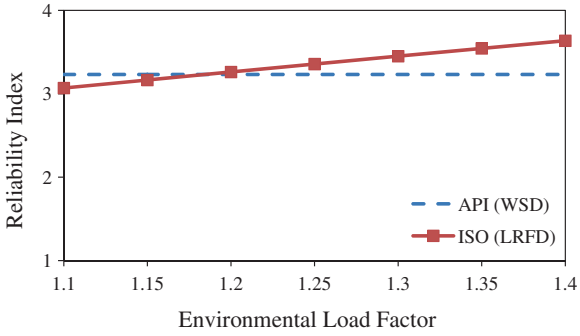

Fig. 7.33 Reliability index versus environmental load factor for VD at SKO1 using ISO 19902 and API WSD

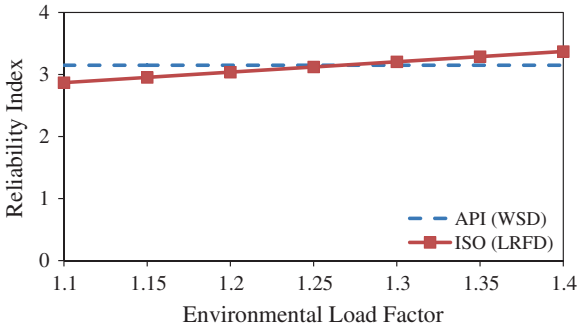

Fig. 7.34 Reliability index versus environmental load factor for leg at SKO1 using ISO 19902 and API WSD

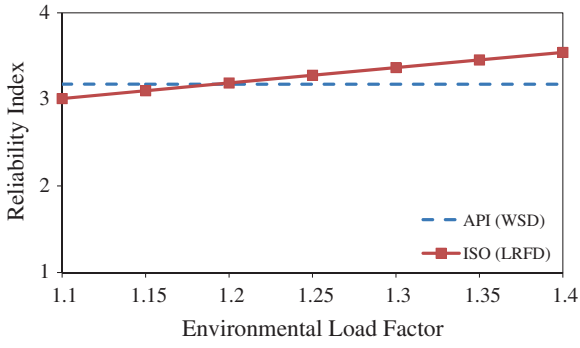

Fig. 7.35 Reliability index versus environmental load factor for component at SKO1 using ISO 19902 and API WSD

1.25. The averaged load factor for this region is 1.20 as shown in Fig. 7.35. The average target reliability index is 3.17 for this platform in SKO region.

For the platform at SKO1, the leg members are highly stressed. The least stressed members are braces at horizontal periphery and vertical diagonals. The target reliability of 3.6 is the highest for horizontal diagonal members.

7.4.9.2 SKO2 Platform

Figures 7.36, 7.37, 7.38, 7.39 and 7.40 show the environmental load factor for SKO2 Jacket, for all the four types of components of Jacket that are analysed. Figure 7.36 show horizontal periphery brace member with environmental load factor of 1.25. Horizontal diagonal load factor of 1.20 is shown in Fig. 7.37. Figure 7.38 shows vertical diagonal member with environmental load factor of

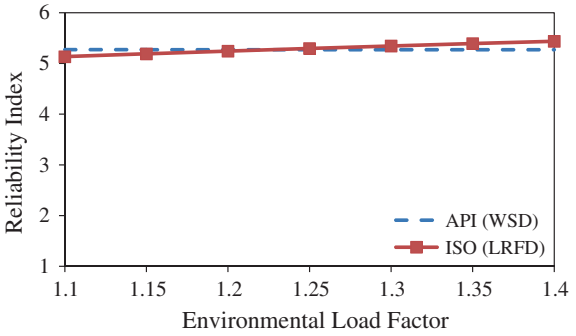

Fig. 7.36 Reliability index versus environmental load factor for HP at SKO2 using ISO 19902 and API WSD

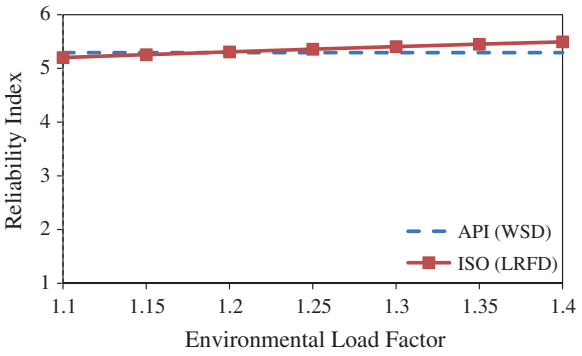

Fig. 7.37 Reliability index versus environmental load factor for HD at SKO2 using ISO 19902 and API WSD

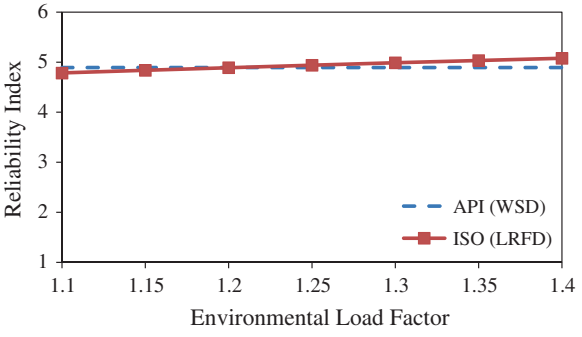

Fig. 7.38 Reliability index versus environmental load factor for VD at SKO2 using ISO 19902 and API WSD

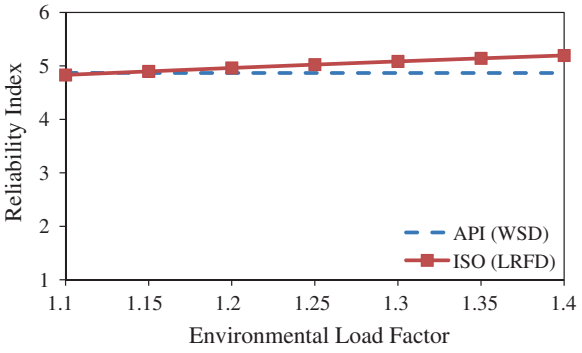

Fig. 7.39 Reliability index versus environmental load factor for leg at SKO2 using ISO 19902 and API WSD

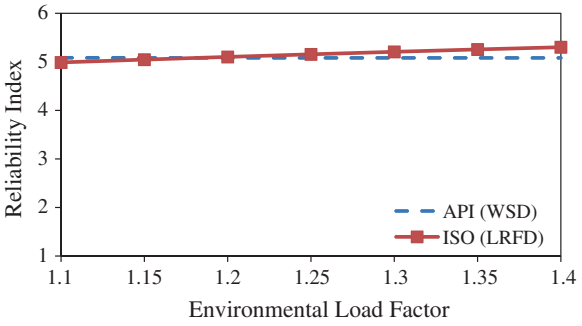

Fig. 7.40 Reliability index versus environmental load factor for component at SKO2 using ISO 19902 and API WSD

1.20, and finally, leg members in Fig. 7.39 show a load factor of 1.15. The averaged load factor shown in Fig. 7.40 for this Jacket came out to be 1.25. The average target reliability index is 5.08 for this platform. For the platform at SKO2, the horizontal members at periphery and vertical diagonals are highly stressed. The least stressed members are leg members. All members have high target reliability, and the maximum is found for horizontal members with target reliability of 5.2.

7.5 All Regions and All Components Combined Result

When all stress conditions and regions are added and averaged together, the environmental load factor for Jacket platform components in Malaysia is 1.25 as shown in Fig. 7.41. This work establishes that the common load factor of 1.35 used by ISO code is on the higher side. Even with reduced load, factor reliability of Jacket will be higher as compared to API RP2A WSD code. It is reported that the higher the reliability index is, the larger the structural safety margin will be and the more the corresponding cost will be and vice versa [12]. Target reliability index used in one study in China was 4.2 [13] and 2.8 in other study which is also conducted in China [14], but the later uses the Gumbel distribution for environmental load.

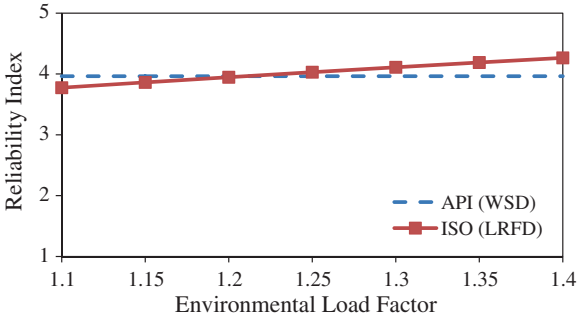

Fig. 7.41 Reliability index versus environmental load factor for Jacket platforms in Malaysia at SKO2 using ISO 19902 and API WSD

Table 7.6 API (WSD) target reliability and ISO (LRFD) reliability

Code		Reliability index (Malaysia)	Reliability index (North Sea/GOM) [2]
API (WSD)		3.96	3.70
ISO (LRFD)	$\gamma_w = 1.10$	3.78	–
	$\gamma_w = 1.15$	3.86	–
	$\gamma_w = 1.20$	3.95	3.70
	$\gamma_w = 1.25$	4.03	3.80
	$\gamma_w = 1.30$	4.11	3.88
	$\gamma_w = 1.35$	4.19	3.97
	$\gamma_w = 1.40$	4.27	4.10

Table 7.6 shows the target reliability index for Malaysia and reliability index against increasing load factors. These are compared with ISO LRFD code.

7.6 Resistance Factor

The characteristic resistance of tubular members is reduced by the resistance factors. Safety is ensured through common understanding that factored resistance is less than or equal to factored environmental load. Here, environmental load factor of 1.25 is used to find the resistance factor of component. Two types of stress conditions are considered here, i.e. axial tension and axial compression. The ISO 19902 resistance factors for axial tension and compression are 1.05 and 1.18, which are equal to API RP2A LRFD with a environmental load factor of 1.35 [15].

7.6.1 Axial Tension

The resistance factor for axial tension in ISO code is 1.05. In this book, load factor of 1.25 gave equivalent resistance factor of 1.05. Therefore, for axial tension, same resistance factor is suggested to be used for offshore Malaysia as shown in Fig. 7.42.

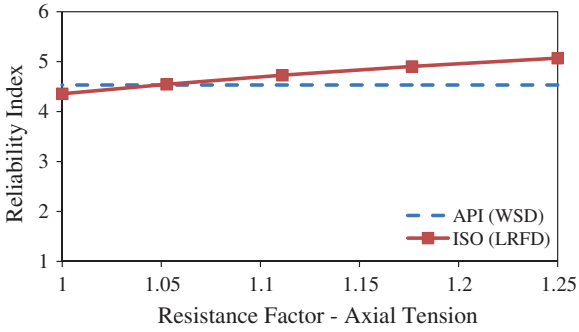

Fig. 7.42 Reliability index versus environmental load factor for jacket platforms in Malaysia using ISO 19902 and API WSD axial tension resistance factor for components

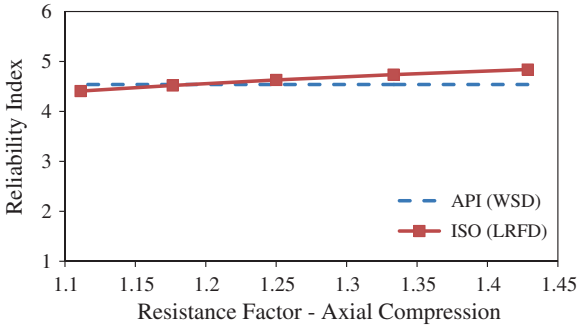

Fig. 7.43 Reliability index versus environmental load factor for jacket platforms in Malaysia at SKO2 using ISO 19902 and API WSD axial compression resistance factor for components

7.6.2 Axial Compression

The resistance factor for axial compression in ISO code is 1.18. In this book, load factor of 1.25 gave equivalent resistance factor of 1.18. Therefore, for axial compression, same resistance factor is suggested to be used for offshore Malaysia as shown in Fig. 7.43.

7.7 Summary

Structural reliability analysis of Jacket platforms provides a rational basis for finding the load and resistance factors for Jacket platforms. The load factor is taken as the value which gives at least similar or higher reliability level as compared to API WSD code. From calibration of both code results, it is clear that reliability-based ISO LRFD factors can provide uniform safety levels for Jackets in Malaysia. The environmental load factor results obtained are as follows:

(1) For the platform in PMO region, environmental load factor is in the range of 1.15–1.27. The range of target reliability as per API WSD here is 2.80–4.01.
(2) For the platform in SBO region, environmental load factor is in the range of 1.23–1.27. The range of target reliability as per API WSD here is 2.96–6.20.
(3) For the platform SKO1 in SKO region, environmental load factor is in the range of 1.15–1.26. The range of target reliability as per API WSD here is 2.90–3.57.
(4) For the platform SKO2 in SKO region, environmental load factor is in the range of 1.14–1.24. The range of target reliability as per API WSD here is 4.27–5.29.

When the above load factors are averaged, the outcome is the common environmental load factor for offshore Malaysia that is determined to be 1.25. With this modified load factor, the resistance factors are checked for the Jacket component. Two cases are considered, i.e. axial tension and axial compression. It is found that the resistance factors for axial tension and compression are the same as per ISO 19902 code, i.e. 1.05 and 1.18 with new load factor. Thus, it can be recommended that with the load factor of 1.25, the same resistance factor can be used.

References

1. Gulvanessian, H., Calgaro, J.A., Holicky, M.: Designer's Guide to EN 1990 Eurocode: Basis of Structural Design. Thomas Telford, London (2002)
2. BOMEL: Component based calibration of North western European annex environmental load factors for the ISO fixed steel offshore structures code 19902 (2003)
3. Theophanatos, A., Cazzulo, R., Berranger, I., Ornaghi, L., Wittengerg, L.: Adaptation of API RP2A-LRFD to the mediterranean sea. In: Presented at the Offshore Technology Conference, OTC 6932, Houston (1992)
4. Nowak, A.S., Maria, M.S.: Structural reliability as applied to highway bridges. Structural Engineering Material vol. 2(2), pp. 218-224, Wiley (2000)
5. Nowak, A.S., Raymond, J.T.: Reliability-based design criteria for timber bridges in Ontario. Canadian J Civil Eng **13**(1), 1–7 (1986)
6. Moses F.: Application of reliability to formulation of fixed offshore design codes. In: Presented at the Marine Structural Reliability Symposium (1995)
7. Chakrabarty, B., Bhar, A.: Sensitivity analysis in structural reliability of Marine structures. In: Presented at the 3rd International ASRANet Colloquium, Glasgow (2006)
8. Theophanatos, A., Wickham, A.H.S.: Modelling of environmental loading for adaptation of API RP 2A-Load and resistance factor design in UK offshore structural design practice. In: Proceedings of Institution of Civil Engineers, pp. 195–204, (1993)
9. ISO-2394 General principles on reliability for structures, ISO-2394, in ISO (1998)
10. Gierlinski, J.T., Yarmier, E.: Integrity of fixed offshore structures: a case study using RASOS software. In: 12th International Conference on Offshore Mechanics and Arctic Engineering (OMAE), Glasgow (1993)
11. BOMEL Comparison of tubular member strength provisions in codes and standards (2001)
12. Lind, N.C.: Target reliability levels from social indicators. In: Proceedings of the Sixth International Conference of Structural Safety and Reliability, ICOSSAR-93, Rotterdam (1994)

13. Zhou, D.C., Duan, Z.D., Ou, J.P.: Calibration of LRFD for steel jacket offshore platform in China offshore area (2); load, resistance and load combination factors. China Ocean Eng **20**(2), 199–212 (2006)
14. Jin, W., Hu, Q., Shen, Z., Shi, Z.: Reliability-based load and resistance factors design for offshore jacket platforms in the Bohai bay: calibration on target reliability index. China Ocean Eng **23**(1), 15–26 (2009)
15. API. American Petroleum Institute RP2A LRFD (2003)

Chapter 8
Joint Reliability Analysis and Environmental Load Factor

Abstract Due to critical nature of joints, API and ISO code recommend them to be stronger than components. The joint types are K-, T/Y- or X-joint, and they are classified as based on the geometry and loads acting on the member. The joints are analysed for four types of stresses. Their respective environmental load factors have been determined and reported.

8.1 Introduction

To safeguard the structure against uncertainties, safety margins are introduced in design by means of various load and resistance factors. This is due to imprecise knowledge and inherent randomness in the design parameters. Joint design is an important part for the Jacket platforms. Design code equations for joints are shown in Appendix B and relevant MATLAB codes are shown in Appendix C. Figures 8.1 and 8.2 show Jacket joints under fabrication.

8.2 Selection of Joints

Joints for this book are arranged in groups chosen from the four platforms. They are based on chord diameter and brace diameter ratio, joint types and angle. These different joints are grouped, and the representative joints are analysed. Table 8.1 shows selection of joints from one platform.

8.2.1 K-Joints

For axial stresses and in-plane bending, ISO LRFD gave higher reliability index values as compared to API WSD. For OPB case, it is API WSD which gave higher values. With increase of environmental load, the reliability decreased significantly.

Z. Nizamani, *Environmental Load Factors and System Strength Evaluation of Offshore Jacket Platforms*, Ocean Engineering & Oceanography 4,
DOI 10.1007/978-3-319-15051-2_8

Fig. 8.1 Tubular joint view at the fabrication yard

Fig. 8.2 Tubular joint view for a brace at the fabrication yard

Table 8.1 Joint selected for calibration

Joint type	Chord diameter (D), mm	Chord wall thickness (T), mm	Brace diameter (d), mm	Brace wall thickness (t), mm	Angle (°)
K	1,854	51	660	19	60
	908	41	604	29	50
T/Y	1,880	64	908	41	87
	610	16	610	13	90
X	660	25	660	13	72
	502	22	502	16	83

Figures 8.3, 8.4 and 8.5 show the reliability index with respect to increasing W_e/G ratios. The ISO LRFD with a load factor of 1.35 gave higher values of reliability as compared to API WSD. In this book, ISO LRFD (MS) environmental load factor of 1.25 is proposed as will be shown later. ISO LRFD is plotted with an environmental load factor of 1.35 as recommended by ISO code. ISO LRFD (MS) stands for this region with a load factor of 1.25. Figure 8.3 shows the reliability values for tension/compression condition of the K-joint. Figures 8.3, 8.4 and 8.5

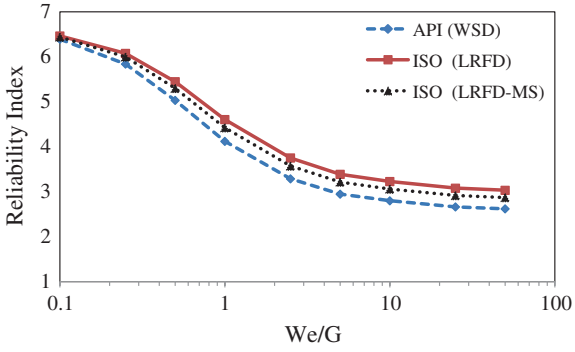

Fig. 8.3 Variation of W_e/G ratio versus reliability index for K-joint tension/compression for API WSD, ISO-MS and ISO LRFD codes at SKO1

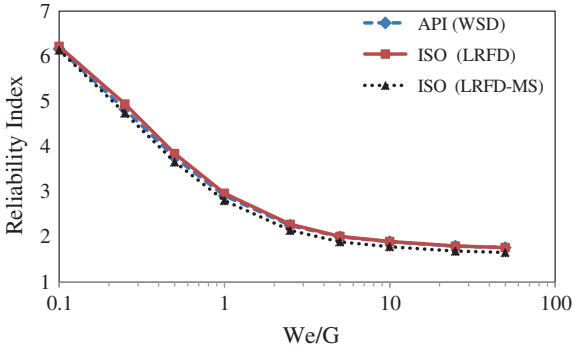

Fig. 8.4 Variation of W_e/G ratio versus reliability index for K-joint IPB for API WSD, ISO-MS and ISO LRFD codes at SKO1

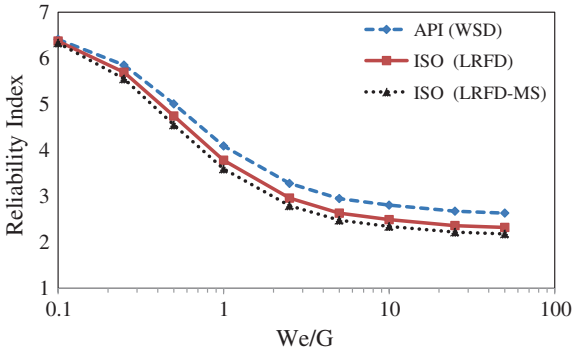

Fig. 8.5 Variation of W_e/G ratio versus reliability index for K-joint OPB for API WSD, ISO-MS and ISO LRFD codes at SKO1

Table 8.2 ISO reliability index for K-joints

Stress type	Reliability index MS, $\gamma_w = 1.25$	Reliability index MS, $\gamma_w = 1.35$	Reliability index ISO $\gamma_w = 1.35$ [1]
Axial tension	3.98	4.16	3.90
Axial compression	3.98	4.16	3.90
IPB	2.79	3.01	4.10
OPB	3.03	3.25	3.79
Average	3.45	3.66	3.90

show the proposed reliability values for in-plane and out-plane bending. Table 8.2 shows the reliability index for K-joint for one platform. In this book, reliability index is found out at environmental load factor of 1.25 and 1.35. Offshore Malaysia values are compared with ISO code values. The environmental load factor of 1.25 gave good results as compared to ISO code values with given target reliability.

8.2.2 T/Y-Joints

For axial stresses and in-plane bending, ISO LRFD gave higher reliability index values as compared to API WSD. For OPB case, it is API WSD which gave higher values. With increase of environmental load, the reliability decreased significantly as shown in Figs. 8.6, 8.7, 8.8 and 8.9. The ISO LRFD value gave higher values of reliability as compared to API WSD values. This book proposes a load factor of 1.25. Table 8.3 shows the reliability index for T/Y-joint for one platform. In this book, reliability index is found out at environmental load factor of 1.25 and 1.35. Offshore Malaysia values are compared with ISO LRFD code values. The load factor of 1.25 gave good results as compared to ISO code values.

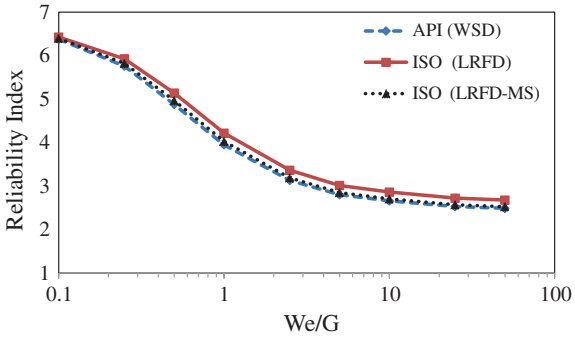

Fig. 8.6 Variation of W_e/G ratio versus reliability index for T/Y-joint in tension for API WSD, ISO-MS and ISO LRFD codes at SKO1

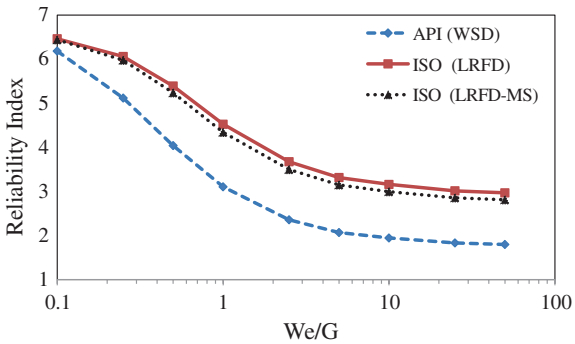

Fig. 8.7 Variation of W_e/G ratio versus reliability index for T/Y-joint in C for API WSD, ISO-MS and ISO LRFD codes at SKO1

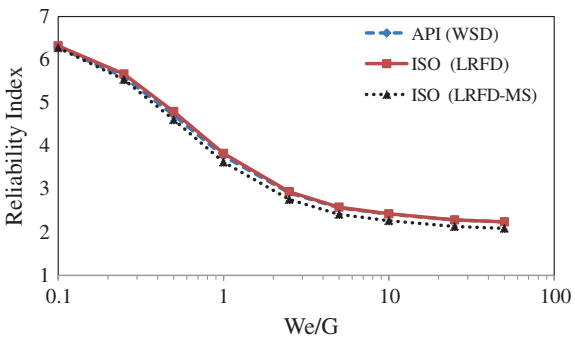

Fig. 8.8 Variation of W_e/G ratio versus reliability index for T/Y-joint in IPB for API WSD, ISO-MS and ISO LRFD codes at SKO1

8.2.3 X-Joints

For axial stresses and IPB, ISO LRFD gave higher reliability index as compared to API WSD. For OPB case, it is API which gave higher values. With increase of environmental load, the reliability decreased significantly as shown in Figs. 8.10, 8.11, 8.12 and 8.13. The ISO LRFD gave higher values of reliability as compared to API WSD. This text proposes 1.25 as environmental load factor. Table 8.4

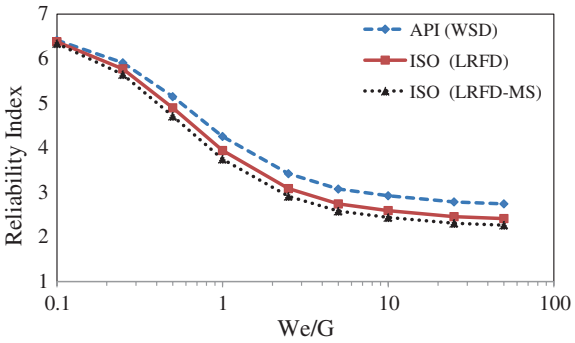

Fig. 8.9 Variation of W_e/G ratio versus reliability index for T/Y-joint in OPB for API WSD, ISO-MS and ISO LRFD codes at SKO1

Table 8.3 ISO reliability index for T/Y-joints

Stress type	Reliability index MS, $\gamma_w = 1.25$	Reliability index MS, $\gamma_w = 1.35$	Reliability index North Sea $\gamma_w = 1.35$ [1]
Axial tension	3.81	4.02	4.13
Axial compression	3.58	3.78	4.04
IPB	3.37	3.58	4.04
OPB	3.94	4.12	4.11
Average	3.68	3.88	4.06

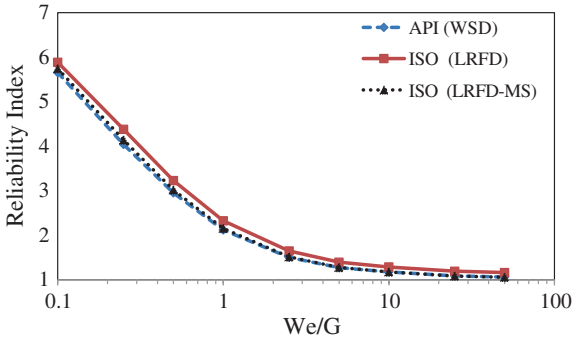

Fig. 8.10 Variation of W_e/G ratio versus reliability index for X-joint in tension for API WSD, ISO-MS and ISO LRFD codes at SKO1

shows the reliability index for X-joint for one platform. In this text, reliability index is found at environmental load factor of 1.25 and 1.35. Offshore Malaysia values are compared with ISO code values. The environmental load factor of 1.25 gave good results as compared to ISO code values.

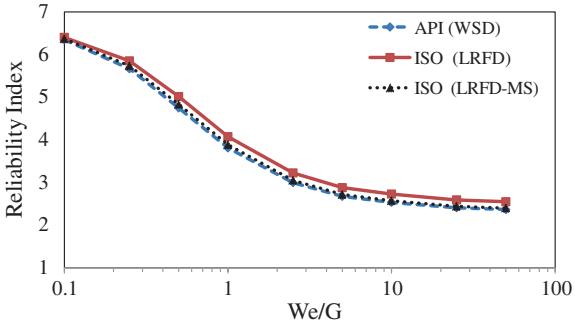

Fig. 8.11 Variation of W_e/G ratio versus reliability index for X-joint in compression for API WSD, ISO-MS and ISO LRFD codes at SKO1

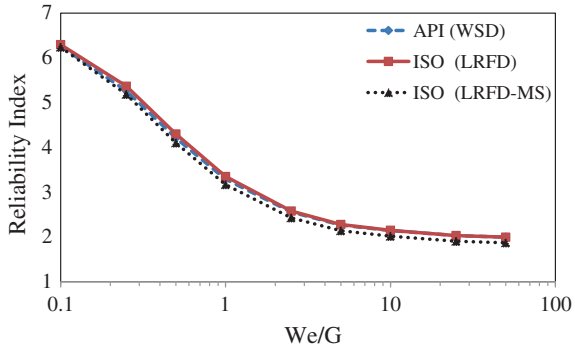

Fig. 8.12 W_e Variation of W_e/G ratio versus reliability index for X-joint in IPB for API WSD, ISO-MS and ISO LRFD codes at SKO1

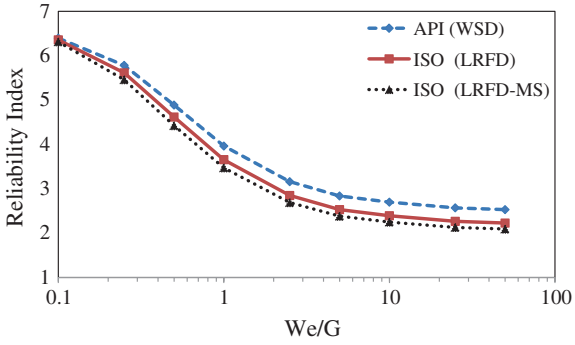

Fig. 8.13 Variation of W_e/G ratio versus reliability index for X-joint in OPB for API WSD, ISO-MS and ISO LRFD codes at SKO1

Table 8.4 ISO reliability index for X-joints

Stress type	Reliability index MS, $\gamma_w = 1.25$	Reliability index MS, $\gamma_w = 1.35$	Reliability index North Sea $\gamma_w = 1.35$ [1]
Axial tension	4.28	4.45	4.07
Axial compression	4.38	4.52	3.98
IPB	4.61	4.75	4.20
OPB	4.29	4.45	4.00
Average	4.39	4.54	4.03

8.3 Beta Factor (β) Effects (d/D) on Reliability Index

Here, brace diameter (d) to chord diameter (D) are varied and all other parameters are made constant, to evaluate the effect of beta factor. The results are shown below:

8.3.1 K-Joints

ISO LRFD code except OPB stresses gave same reliability index, thus the variation has significant effect on OPB equation only as shown in Figs. 8.14, 8.15 and 8.16. The API WSD code is very sensitive to the beta ratio as the reliability varied much with respect to this ratio. Except in the case of axial stresses (up to β ratio = 0.4), the reliability of ISO is higher compared to API WSD code.

8.3.2 T/Y-Joints

Except OPB, ISO LRFD code is not sensitive to beta ratios and maintained constant reliability as shown in Figs. 8.17, 8.18, 8.19 and 8.20. For axial stresses

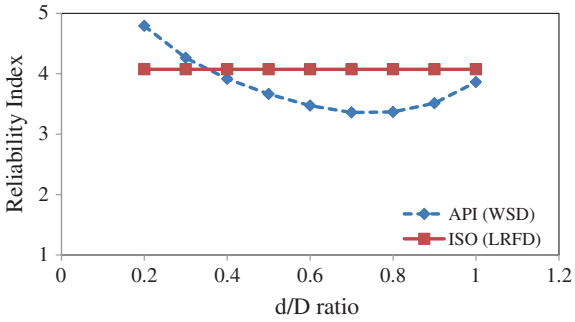

Fig. 8.14 Effect of β ratio on reliability index, K-joint in tension/compression at SKO1

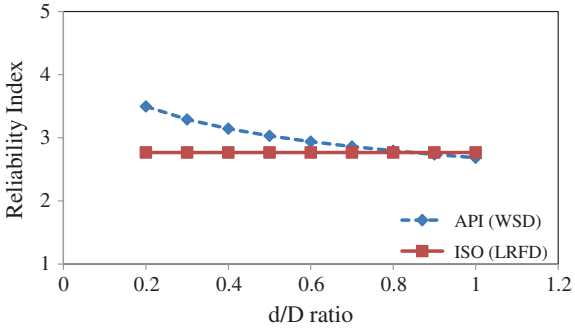

Fig. 8.15 Effect of β on reliability index of K-joint in IPB at SKO1

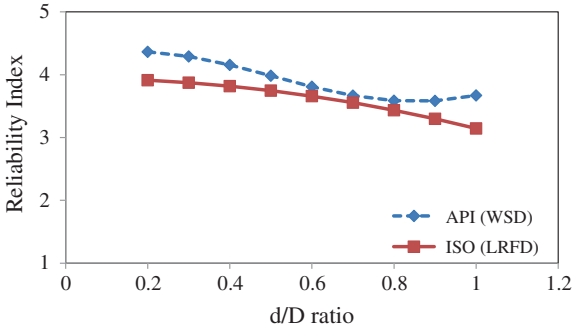

Fig. 8.16 Effect of β on reliability index of K-joint in OPB at SKO1

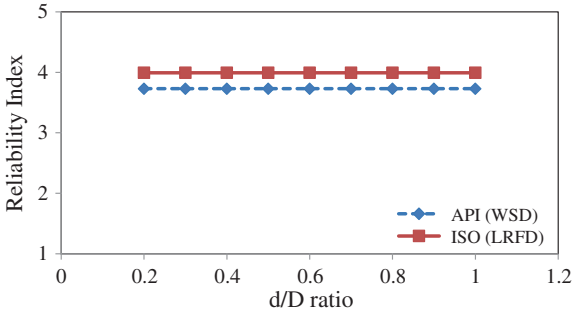

Fig. 8.17 Effect of β on reliability index of T/Y-joint in tension at SKO1

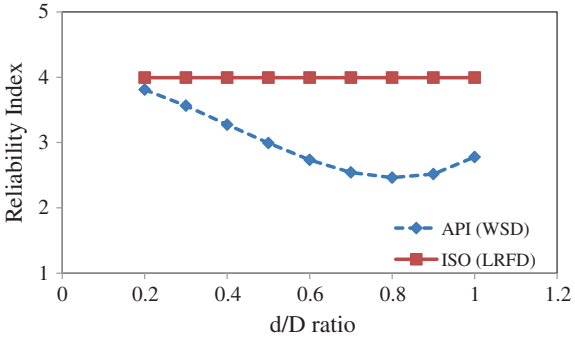

Fig. 8.18 Effect of β on reliability index of T/Y-joint in compression at SKO1

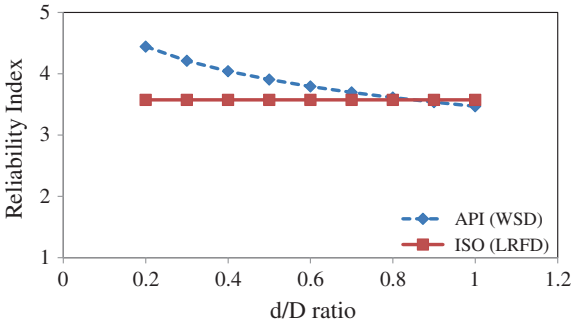

Fig. 8.19 Effect of β on reliability index of T/Y-joint in IPB at SKO1

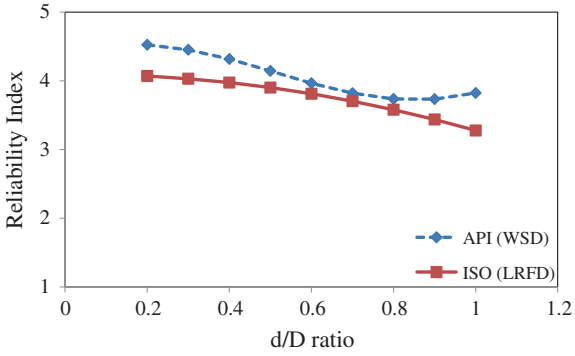

Fig. 8.20 Effect of β on reliability index of T/Y-joint in OPB at SKO1

alone, ISO LRFD gave higher reliability index always, but when combined with bending, it gave lower values. API WSD is always sensitive to beta ratios except for axial tension case.

8.3.3 X-Joints

Except OPB, ISO LRFD code is not sensitive to beta ratios and maintained constant reliability as shown in Figs. 8.21, 8.22, 8.23 and 8.24. For axial stresses, ISO gave always higher reliability index but low when bending is involved. API WSD is always sensitive to beta ratios except axial stresses case.

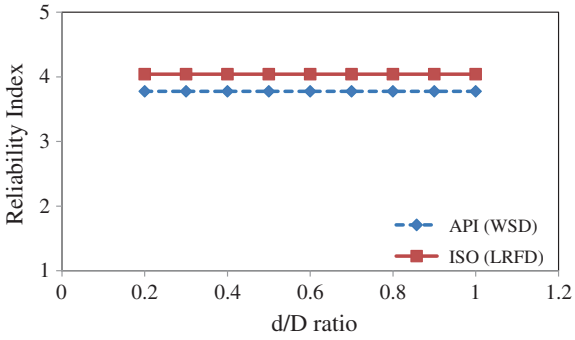

Fig. 8.21 Effect of β on reliability index of X-joint tension at SKO1

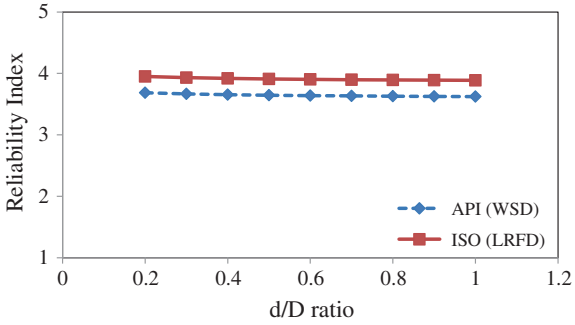

Fig. 8.22 Effect of β on reliability index of X-joint in compression at SKO1

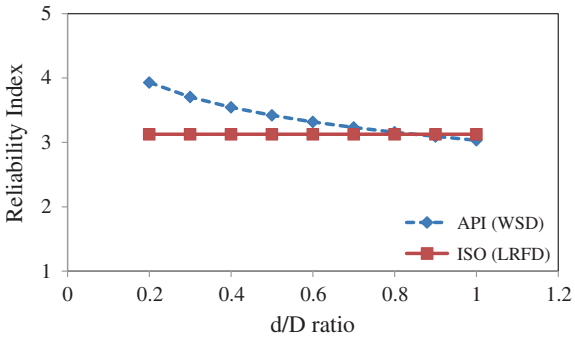

Fig. 8.23 Effect of β on reliability index of X-joint in IPB at SKO1

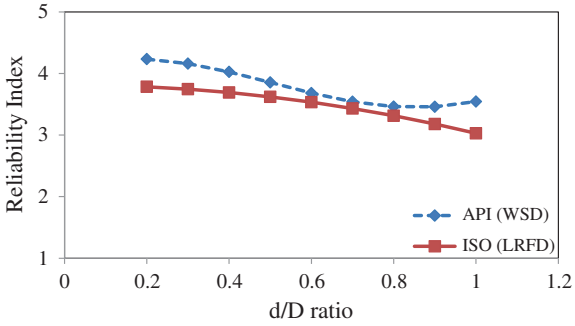

Fig. 8.24 Effect of β on reliability index of X-joint in OPB at SKO1

8.4 Gamma Factor (γ) Effects ($D/2T$)

The variation of Gamma factor ($D/2T$) is checked to find its effect on reliability analysis.

8.4.1 K-Joints: Tension/Compression

Figures 8.25, 8.26 and 8.27 show the variability of gamma effect on reliability. It can be seen that ISO LRFD code maintains almost constant reliability except in the case of OPB where it gave minor variability. Thus, ISO LRFD is not sensitive to gamma ratios. The API WSD code shows large variability for all three stresses, and thus, it can be concluded that it has sensitiveness to the gamma ratio. ISO LRFD code shows higher reliability except for OPB stresses.

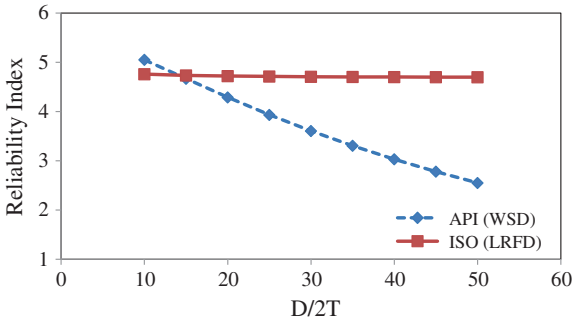

Fig. 8.25 Effect of γ on reliability index, K-joint tension and compression at SKO1

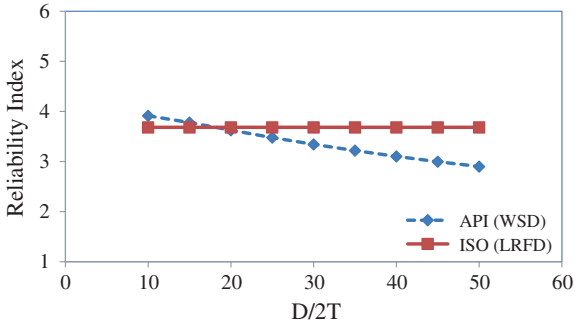

Fig. 8.26 Effect of γ on reliability index of K-joint in IPB at SKO1

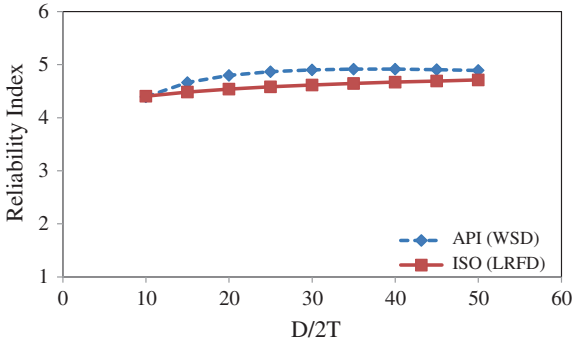

Fig. 8.27 Effect of γ on reliability index of K-joint in OPB at SKO1

8.4.2 T/Y-Joints

The gamma effect on ISO LRFD code is again not susceptible to changes in gamma ratio except the case of OPB as shown in Figs. 8.28, 8.29, 8.30 and 8.31. The API WSD code shows its sensitiveness to the gamma factor except for axial tension. ISO LRFD code shows higher reliability except for OPB stresses.

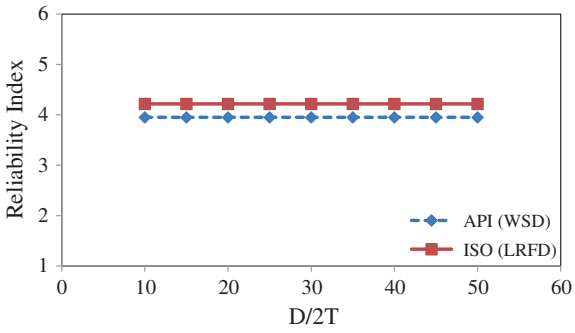

Fig. 8.28 Effect of γ on reliability index of T/Y-joint in tension at SKO1

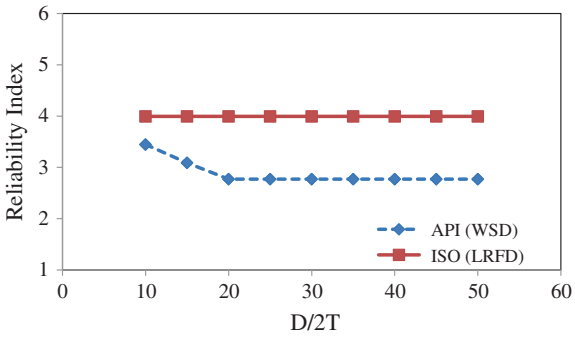

Fig. 8.29 Effect of γ on reliability index of T/Y-joint in compression at SKO1

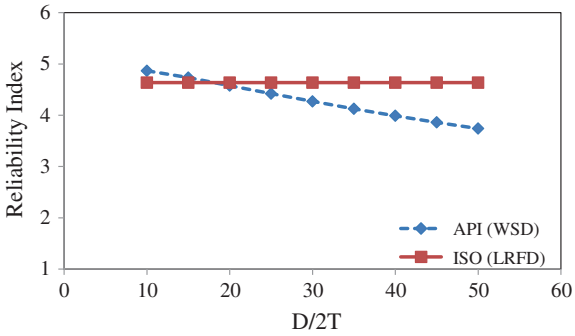

Fig. 8.30 Effect of γ on reliability index of T/Y-joint in IPB at SKO1

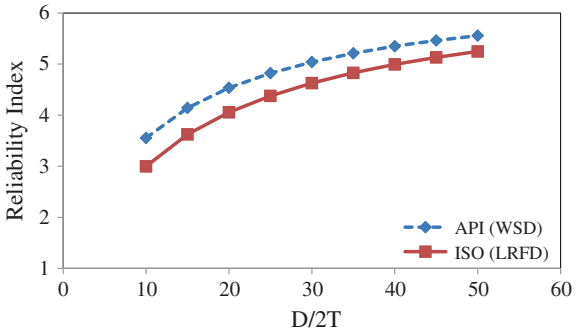

Fig. 8.31 Effect of γ on reliability index of T/Y-joint in OPB at SKO1

8.4.3 X-Joints

Here, both codes show sensitiveness in case of IPB and OPB, otherwise they maintained constant reliability as shown in Figs. 8.32, 8.33, 8.34 and 8.35. In all cases, ISO shows higher reliability except in the case of OPB stresses.

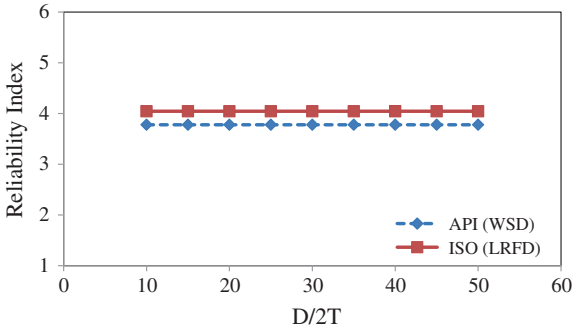

Fig. 8.32 Effect of γ on reliability index of X-joint in tension at SKO1

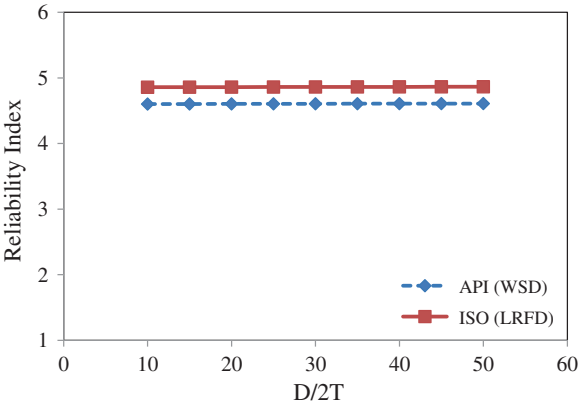

Fig. 8.33 Effect of γ on reliability index of X-joint in compression at SKO1

Fig. 8.34 Effect of γ on reliability index of X-joint in IPB at SKO1

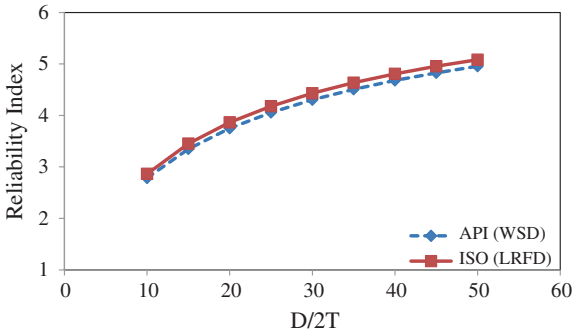

Fig. 8.35 Effect of γ on reliability index of X-joint in OPB at SKO1

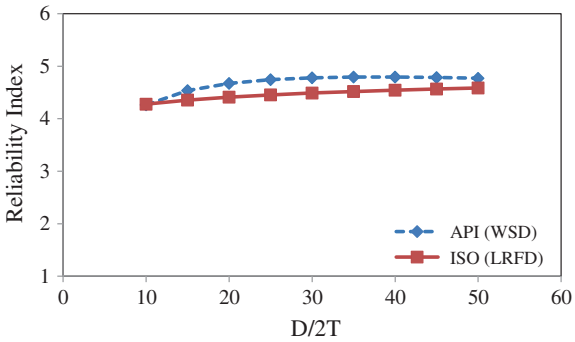

8.5 Variation of Environmental Load Factor

Figures 8.36, 8.37 and 8.38 show environmental load variation for K-, T/Y- and X-joints. There is large variation with respect to W_e/G ratios. When dead load ratio governs, it gives higher reliability index as compared to the case when environmental load ratio is governing. The reliability continued to decrease with increase of environmental load factors as was observed by [1]. The same effects are observed during the component reliability analysis.

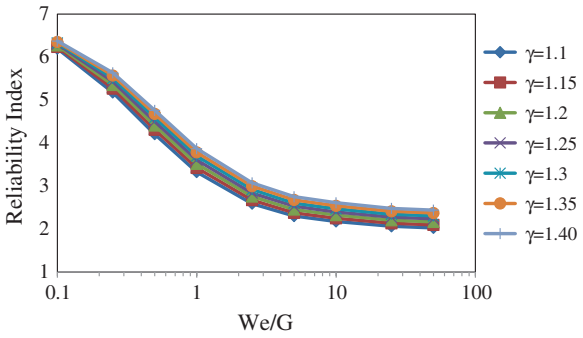

Fig. 8.36 Variation of reliability index versus W_e/G for K-joint using ISO code for different values of environmental load factor (γ)

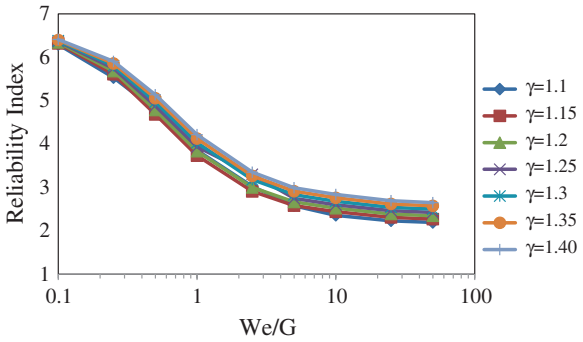

Fig. 8.37 Variation of reliability index versus W_e/G for T/Y-joint using ISO code for different values of environmental load factor (γ)

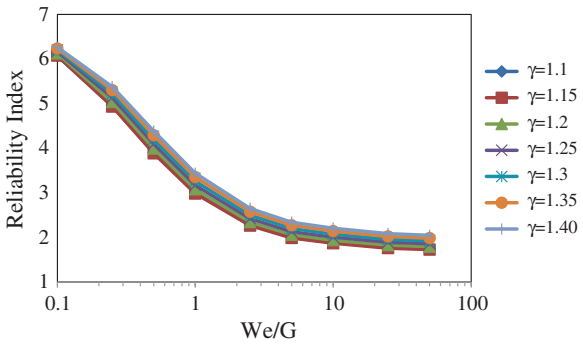

Fig. 8.38 Variation of reliability index versus W_e/G for X-joint using ISO code for different values of environmental load factor (γ)

8.6 Calibration of API (WSD) and ISO (LRFD) Reliability Index

To evaluate the effects of both codes on reliability analysis of joints, the calibration points in ISO LRFD and API WSD codes are evaluated, as shown in Tables 8.5 and 8.6. It is seen that both codes give results which are consistent and not much dispersion is observed. The calibration of reliability index for IPB and OPB in Figs. 8.39 and 8.40 showed that the ISO (LRFD) has less variance as compared to API (WSD).

Table 8.5 Joints reliability index under stresses—ISO 19902 code [1]

ISO				
Stress type	K-joints	T-joints	X-joints	Average
Compression	4.60	4.52	4.08	4.40
Tension	4.60	4.22	2.32	3.71
IPB	2.97	3.83	3.35	3.38
OPB	3.78	3.94	3.66	3.79
Average	3.99	4.13	3.35	3.82

Table 8.6 Joints reliability index under stresses—API RP2A WSD code [1]

API WSD				
Stress type	K-joints	T-joints	X-joints	Average
Compression	4.12	3.10	3.81	3.68
Tension	4.12	3.95	2.12	3.40
IPB	2.92	3.76	3.29	3.32
OPB	4.09	4.25	3.96	4.10
Average	3.81	3.77	3.30	3.63

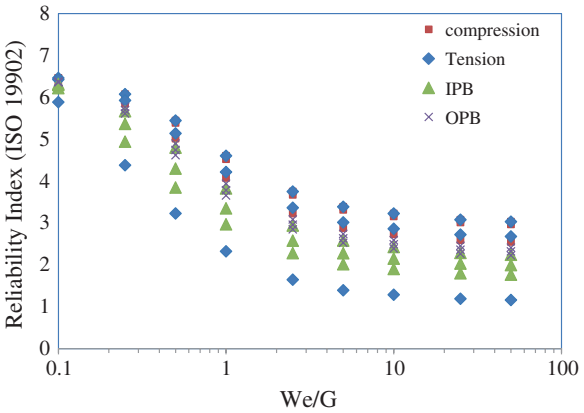

Fig. 8.39 Calibration of Jacket joint under ISO for all types of model stresses with W_e/G ratios versus ISO reliability indices

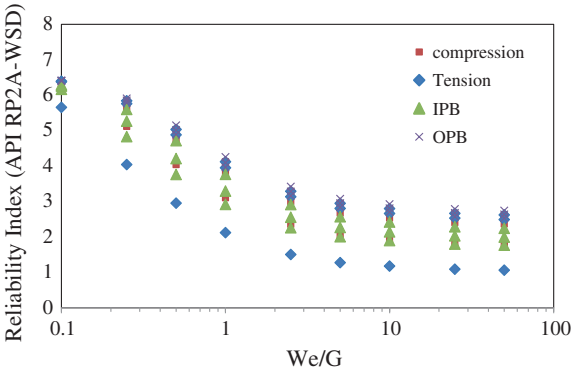

Fig. 8.40 Calibration of Jacket joint under API WSD for all types of model stresses with W_e/G ratios versus API WSD reliability indices

8.7 Environmental Load Factor

The target reliabilities for Jacket platforms in Malaysia are based on calibration of API (WSD). Environmental load is calibrated, so that the one near to target reliability is recommended for future platforms in Malaysia. The environmental load factor for joint of three regions is derived and presented in following sections.

8.7.1 PMO Region Platform

Figures 8.41, 8.42, 8.43 and 8.44 show the environmental load factors for the PMO region Jacket, for all three types of joints of Jacket. Figure 8.41 shows the load factor for K-joint as 1.30. T/Y-joints load factor of 1.20 is shown in Fig. 8.42. Figure 8.43 shows X-joint load factor of 1.30. The averaged load factor for this region, shown in Fig. 8.44, is 1.25. The target reliability is 3.92 for PMO region.

In PMO region, it can be seen that X- and K-joint are most stressed. The target reliability of for X-joint is 4.95, the highest among other types. Nowadays, the codes prefer X-joints for Jackets due to ductility. This shows that the platform designed is using maximum capacity of this joint.

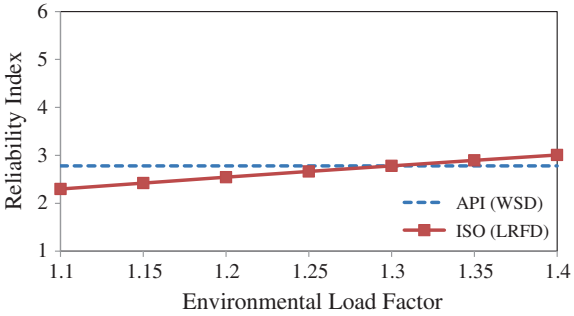

Fig. 8.41 Reliability index versus environmental load factor for K-joint at PMO using ISO 19902 and API WSD

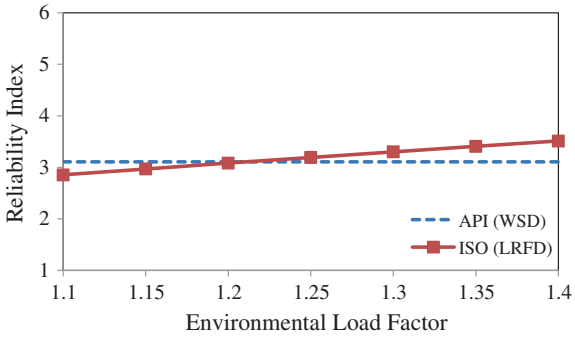

Fig. 8.42 Reliability index versus environmental load factor for T/Y-joint at PMO using ISO 19902 and API WSD

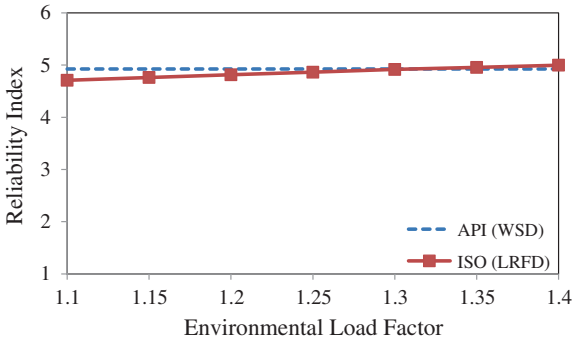

Fig. 8.43 Reliability index versus environmental load factor for X-joint at PMO using ISO 19902 and API WSD

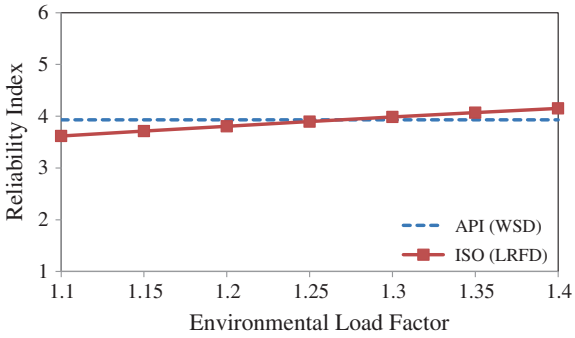

Fig. 8.44 Reliability index versus environmental load factor for all joints at PMO using ISO 19902 and API WSD

8.7.2 SBO Region Platform

Figures 8.45, 8.46, 8.47 and 8.48 show the environmental load factor for the SBO region Jacket, for all three types of joints of Jacket. Figure 8.45 shows the load factor for K-joint as 1.25. T/Y-joints load factor of 1.25 is shown in Fig. 8.46.

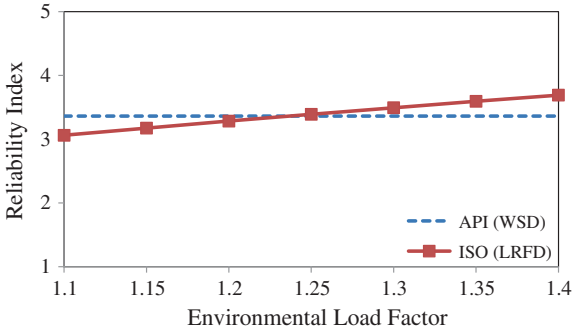

Fig. 8.45 Reliability index versus environmental load factor for K-joint at SBO using ISO 19902 and API WSD

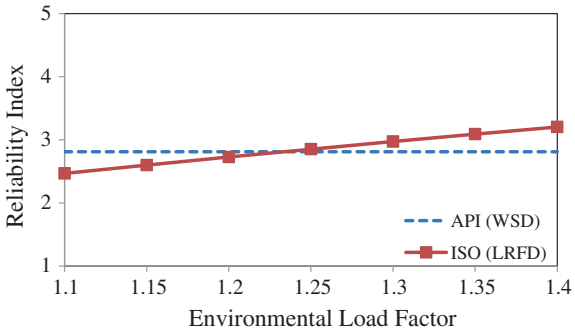

Fig. 8.46 Reliability index versus environmental load factor for T/Y-joint at SBO using ISO 19902 and API WSD

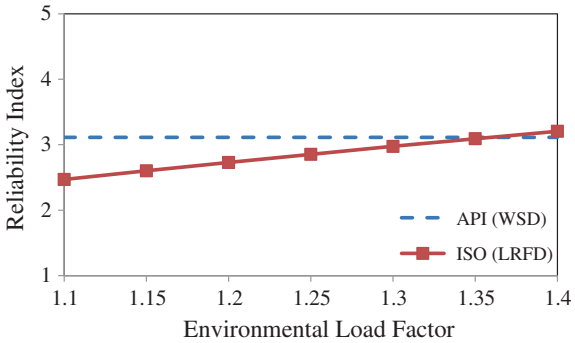

Fig. 8.47 Reliability index versus environmental load factor for X-joint at SBO using ISO 19902 and API WSD

Figure 8.47 shows X-joint load factor of 1.35. The averaged load factor for this region shown in Fig. 8.48 is 1.25. The target reliability index is 3.11 for SBO region. In SBO region, it can be seen that X-joints are the most stressed. The target reliability for X-joint is 3.05, and for K-joint, it was 3.4. It is highest target reliability among other types of joints at this platform.

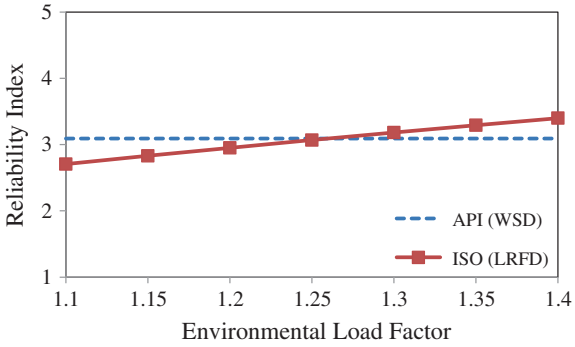

Fig. 8.48 Reliability index versus environmental load factor for all joints at SBO using ISO 19902 and API WSD

8.7.3 SKO Region

From SKO region, two Jackets are selected for analysis and results are produced below:

8.7.3.1 SKO1 Platform

Figures 8.49, 8.50, 8.51 and 8.52 show the environmental load factor for the SKO region with SKO1 Jacket, for all three types of joints of Jacket. Figure 8.49 shows the load factor for K-joint as 1.25. T/Y-joints load factor of 1.20 is shown in Fig. 8.50. Figure 8.51 shows X-joint load factor of 1.30. Averaged load factor for this region shown in Fig. 8.52 is 1.25. The target reliability index is 3.64 for this platform in SKO region. In SKO1 region, it can be seen that again, X-joints are the most stressed and its target reliability is 3.40. For K-joint, target reliability is 3.95, the highest among other types at this platform.

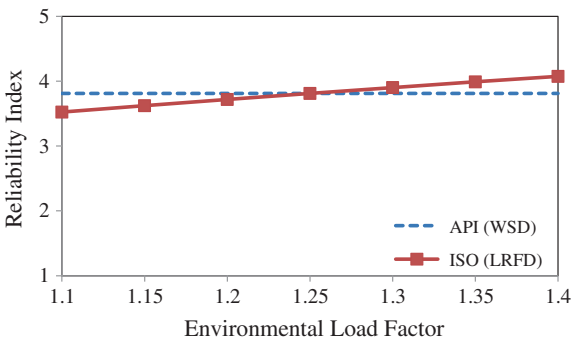

Fig. 8.49 Reliability index versus environmental load factor for K-joint at SKO1 using ISO 19902 and API WSD

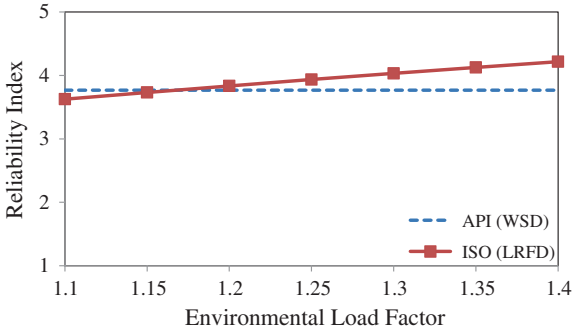

Fig. 8.50 Reliability index versus environmental load factor for T/Y-joint at SKO1 using ISO 19902 and API WSD

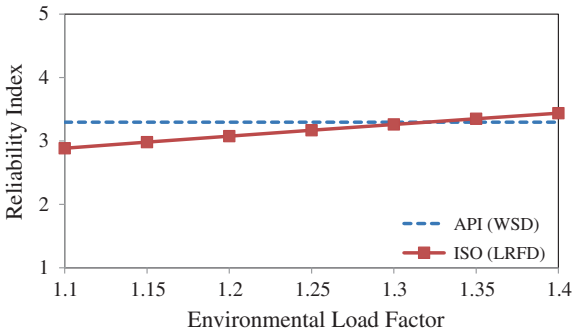

Fig. 8.51 Reliability index versus environmental load factor for X-joint at SKO1 using ISO 19902 and API WSD

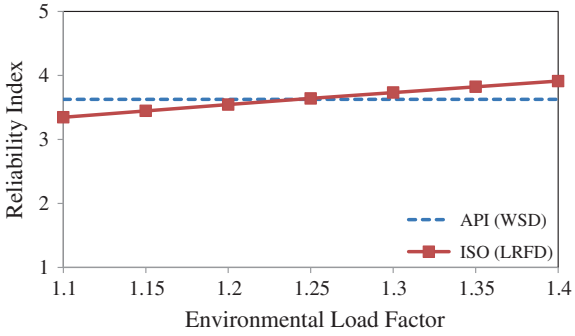

Fig. 8.52 Reliability index versus environmental load factor for all joints at SKO1 using ISO 19902 and API WSD

8.7.3.2 SKO2 Platform

Figures 8.53, 8.54, 8.55 and 8.56 show the environmental load factor for the SKO region at SKO2 Jacket, for all three joints of Jacket. Figure 8.53 shows the load factor for K-joint 1.30. T/Y-joints load factor of 1.25 is shown in Fig. 8.54. Figure 8.55 shows X-joint load factor of 1.25. Averaged load factor for this region shown in 8.56 is 1.30. The target reliability index is 4.73 for this platform in SKO region. In SKO2 region, it can be seen that again K- and X-joint are the most stressed and their target reliability is almost equal to 5.0.

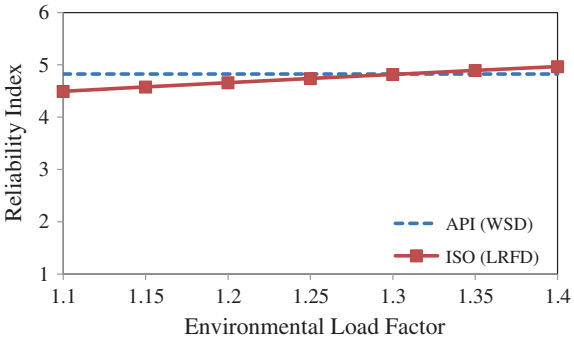

Fig. 8.53 Reliability index versus environmental load factor for K-joint at SKO2 using ISO 19902 and API WSD

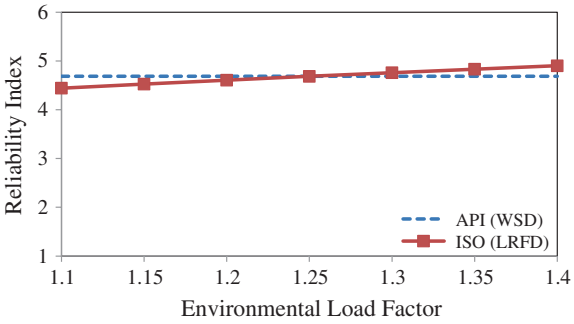

Fig. 8.54 Reliability index versus environmental load factor for T/Y-joint at SKO2 using ISO 19902 and API WSD

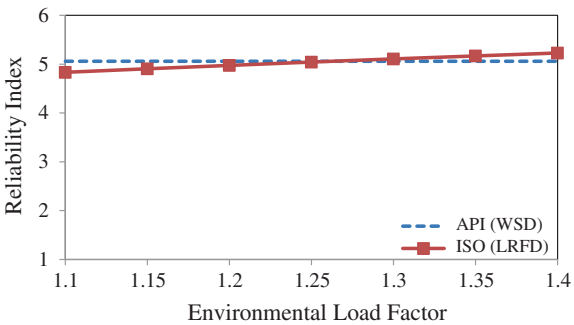

Fig. 8.55 Reliability index versus environmental load factor for X-joint at SKO2 using ISO 19902 and API WSD

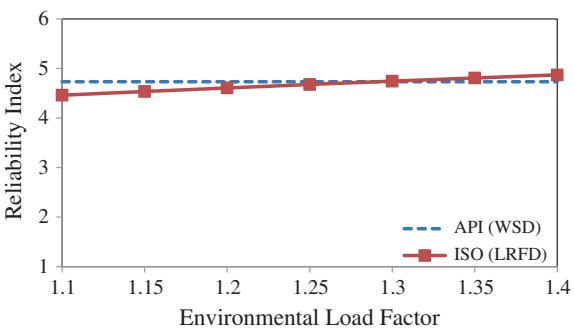

Fig. 8.56 Reliability index versus environmental load factor for all joint at SKO2 using ISO 19902 and API WSD

8.8 All Regions and All Joints Combined Result

The reliability index for API WSD came out to be 3.96, and it is 3.94 when load factor is 1.25 as shown in Table 8.7 and Fig. 8.57. When all conditions and regions are added and averaged together, the environmental load factor for Jacket platform joints in Malaysia is proposed to be 1.25. The values have been compared with ISO LRFD values are also shown in the Table 8.7. The high values of reliability indices show that members are oversized. This may be due to provisions to withstand transportation and installation of Jacket [2].

Table 8.7 (WSD) Target reliability and ISO (LRFD) reliability for joints

Code		Reliability index (Malaysia)	Reliability index (North Sea/GOM) [1]
API (WSD)		3.96	3.42
ISO(LRFD)	$\gamma_w = 1.10$	3.66	–
	$\gamma_w = 1.15$	3.75	–
	$\gamma_w = 1.20$	3.85	3.74
	$\gamma_w = 1.25$	3.94	3.83
	$\gamma_w = 1.30$	4.0	3.92
	$\gamma_w = 1.35$	4.12	4.0
	$\gamma_w = 1.40$	4.20	4.1

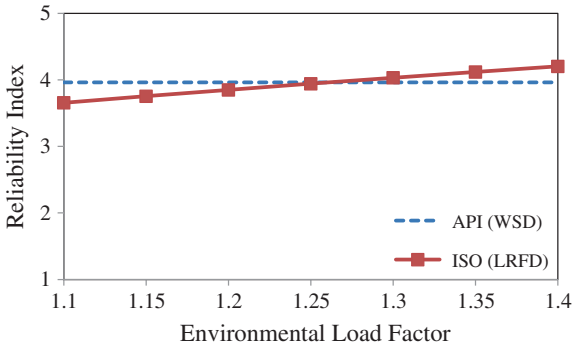

Fig. 8.57 Reliability index versus environmental load factor for all joint for all platforms using ISO 19902 and API WSD

8.9 Summary

Environmental load factor for joints used by API RP2A LRFD and ISO is same, i.e., 1.35. The wave conditions for 100-year design vary too much for many regions. Therefore, applied load is not similar to the conditions in offshore Malaysia. The ISO code reports that joints should be made stronger than the components, and this makes them safe as compared to component [3–5]. In this book, four platforms are used to find the effect of load factor representing each region of offshore Malaysia. All three types of joints are analysed with four different types of stresses. The environmental load factor results obtained are as follows:

1. The platform in PMO region is in range of 1.2–1.29. The range of target reliability as per API WSD is 2.78–4.93.
2. The platform in SBO region is in range of 1.23–1.33. The range of target reliability as per API WSD is 2.81–3.36.
3. The platform in SKO1 region is in range of 1.17–1.31. The range of target reliability as per API WSD is 3.30–3.81.
4. The platform in SKO2 region is in range of 1.24–1.29. The range of target reliability as per API WSD is 4.69–5.06.

The averaged load factor proposed in this research is 1.27.

References

1. BOMEL: Component based calibration of North western European annex environmental load factors for the ISO fixed steel offshore structures code 19902 (2003)
2. Birades, M., Cornell, C.A., Ledoigt, B.: Load factor calibration for the gulf of guinea adaptation of APIRP2A-LRFD, in behaviour of offshore structures. London (2003)
3. Karsan, D.I., Marshall, P.W., Pecknold, D.A., Mohr, W.C., Bucknell, J.: The new API RP2A, Tubular joint design practice, 22nd edn. In Offshore Technology Conference, OTC 17236, Houston, USA (2005)
4. Pecknold, D., Marshall, P.W., Bucknell, J.: New API RP2A Tubular Joint Strength Design Provisions. In Offshore Technology Conference, OTC 17310. Houston, USA (2005)
5. Thandavamoorthy, T.S.: Finite element modelling of the behaviour of internally ring stiffened T-joints of offshore platforms. J. Offshore Mech. Arctic Eng. OMAE **131**(4) (2002)

Chapter 9
System Reliability-Based Environmental Loading

Abstract Codes applicable to Jacket platforms, such as API WSD, API LRFD and ISO 19902, are based on component and joint design. If Design codes are followed properly, the strength of member will always exceed the load effect as utility ratio is always maintained less than one while designing the Jacket. Codes consider overall structural integrity, redundancy and multiple failure paths only indirectly by using structural integrity assessment methods. Before going for reassessment in this chapter environmental load factor has been evaluated using system reliability.

9.1 Introduction

When analysing overall system, the first or initial failure cannot represent the strength of platform. Thus, failure of a single component does not mean that the capacity of platform has reached the strength limit. In earlier chapters environmental load factor is determined for component and joint reliability, this chapter deals with environmental load factor using system reliability. Figure 9.1 shows Jacket assembly in progress.

9.2 System Strength Reliability

System reliability is defined as probability that when using given environmental conditions, the system will perform its intended function satisfactorily for a given period of time [1]. It has been proved that without incurring weight penalty, Jacket can be designed not only to achieve governing elastic design criteria but also to provide reserve strength beyond the design requirements. This reserve strength will act as insurance against extreme events or unforeseen operational changes which arise during its life [2]. System strength of Jacket is evaluated using collapse analysis module of SACS. Wave loads are the major loads faced

Z. Nizamani, *Environmental Load Factors and System Strength Evaluation of Offshore Jacket Platforms*, Ocean Engineering & Oceanography 4,
DOI 10.1007/978-3-319-15051-2_9

Fig. 9.1 Jacket structure assembly in progress

by the Jacket platform during its life, and here, wave height is increased to find the RSR. Probability of exceedance is ascertained for the design/assessment of Jacket. Existing Jacket platform after surviving severe loading environment for some years/storm events are considered safe for such type of storms if ever they recur. This theory has already been applied on land-based structures, such as proof loading used against existing structures to gauge the strength of structure through measurement of deflection. This method has been recommended by ISO for the reassessment of structure [3].

9.2.1 Wave and Current

Here in this book, four platforms are analysed for collapse analysis, one from PMO, one from SBO and two from SKO. In SKO itself, the platform SKO2 is analysed for two conditions, i.e. one with legs fixed at mud line and other with pile soil interaction. For a given sea-state, wave height and current profile are kept fixed [4]. Topside deck comes under wave attack as wave height increases. The results of four platforms are shown in Figs. 9.2, 9.3, 9.4, 9.5 and 9.6 using the API WSD code. This shows that there is significant increase of load at higher wave heights. This is achieved for platform at PMO with 16 m, at SBO with 11.6 m, with SKO1 with 17.5 m and SKO2 with 17.6 m. Same wave height is taken for SKO2a. This is due to waves hitting the deck, which produced higher base shear.

9.2.2 Curve Fitting

Stoke's fifth-order wave theory is used by SACS for producing wave loading on the Jacket. During collapse analysis, environmental load increases in steps. To establish the relationship between wave and current load and response of Jacket, curve fitting is done to find the coefficients of response surface equation. This

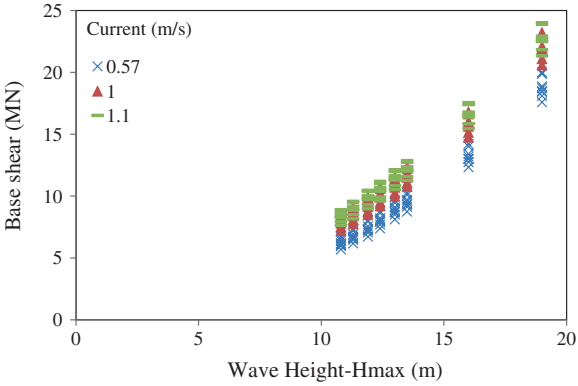

Fig. 9.2 Base shear against wave heights and current speed at PMO

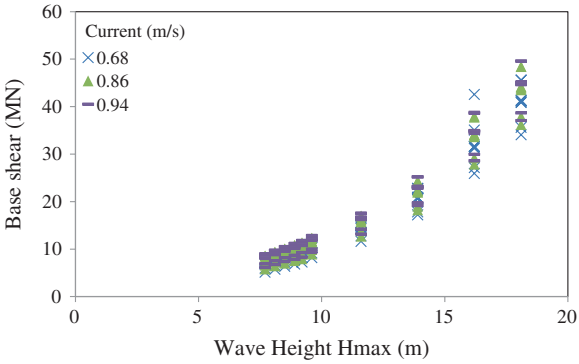

Fig. 9.3 Base shear against wave heights and current speed at SBO

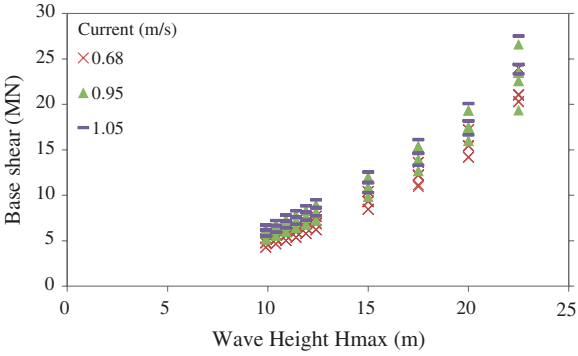

Fig. 9.4 Base shear against wave heights and current speed at SKO1

relationship was established by Heideman's Equation (2.15) and which has been used for curve fitting as shown in [5]. Figures 9.7, 9.8, 9.9, 9.10 and 9.11 represent the curve fitting of Jackets. Figure 9.7 shows clearly that the current also plays important part in reliability analysis as the difference in values of base shear is quite high, as compared to 0.57 and 1.0.

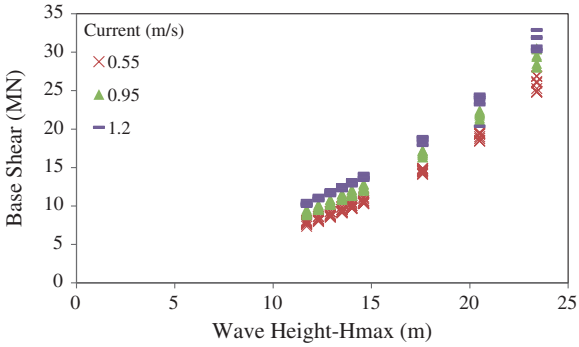

Fig. 9.5 Base shear against wave heights and current speed at SKO2

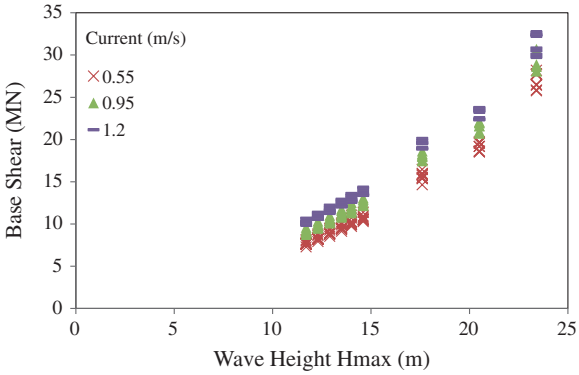

Fig. 9.6 Base shear against wave heights and current speed at SKO2a

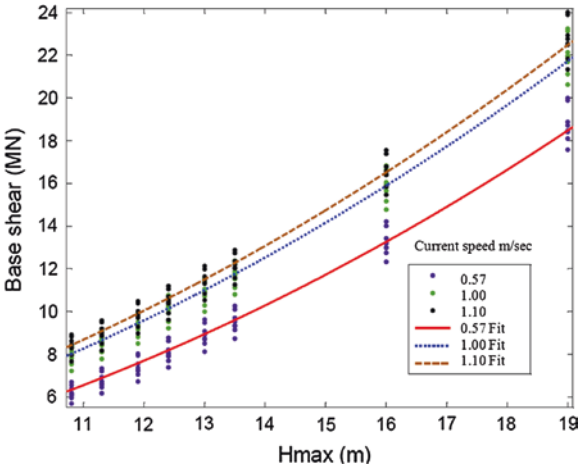

Fig. 9.7 Curve fitting model for platform "PMO"

Table 9.1 provides the parameters for wave and current for the platforms obtained from curve fitting. Separate parameters are obtained for each current speed. Here, the design current speed used is based on 100 years as required by ISO/API codes. These values are used to find the probability of failure and reliability index.

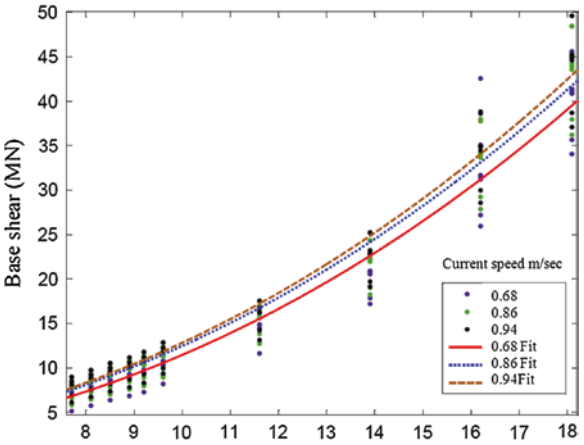

Fig. 9.8 Curve fitting model for platform "SBO"

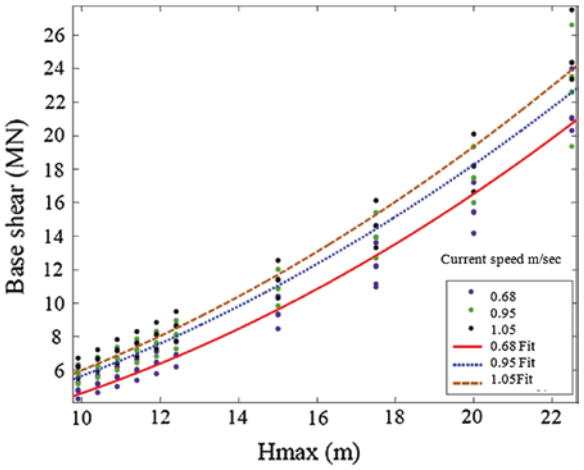

Fig. 9.9 Curve fitting model for platform "SKO1"

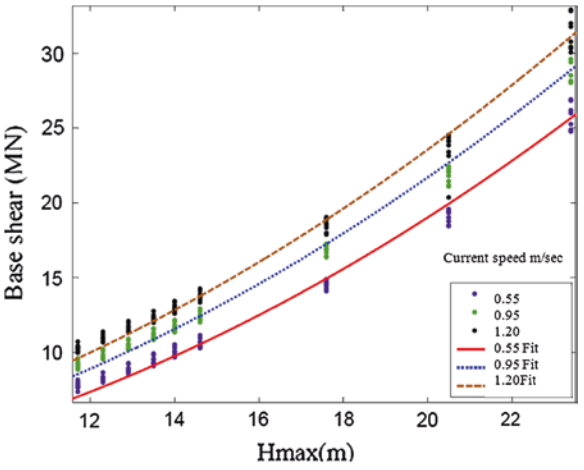

Fig. 9.10 Curve fitting model for platform "SKO2"

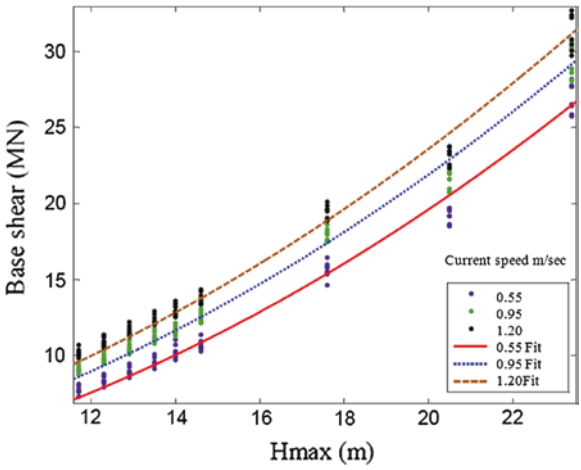

Fig. 9.11 Curve fitting model for platform "SKO2a"

Table 9.1 Parameters of wave and current for system reliability

Platform	Current	a_1	a_2	a_3	R^2
PMO	0.57	0.03237	2.7	2.1	0.9831
	1	0.0339	2.7	2.1	0.984
	1.1	0.03419	2.7	2.1	0.9841
SBO	0.68	0.0428	2	2.3	0.956
	0.86	0.04335	2	2.3	0.964
	0.94	0.04459	2	2.3	0.9649
SKO1	0.68	0.026	2.8	2.091	0.9719
	0.95	0.03053	2.8	2.05	0.9703
	1.05	0.03144	2.8	2.05	0.9712
SKO2	0.55	0.03513	2.8	2.05	0.9877
	0.95	0.03614	2.8	2.05	0.9899
	1.2	0.03687	2.8	2.05	0.9856
SKO2a	0.55	0.03624	2.8	2.05	0.9856
	0.95	0.03649	2.8	2.05	0.9864
	1.2	0.03693	2.8	2.05	0.9856

9.2.3 Selection of RSR for Jackets in Malaysia

The collapse analysis is done for the given platforms, and results achieved are shown in Tables 9.2, 9.3, 9.4, 9.5 and 9.6. The members which failed initially are diagonal braces, horizontal braces and legs. The base shear varied in each direction. The RSR achieved is on higher sides and minimum RSR achieved is 2.0 at platform in PMO. API WSD and ISO LRFD give minimum RSR of 1.58 and 1.86, respectively, for the manned platforms. The range fixed for RSR to find environmental load and probability of failure is 1.5–2.25. The probability of failure of 10^{-7} with reliability index of 5.0 is considered practical enough for this book.

Table 9.2 RSR and system redundancy at platform PMO

Direction	Member group	Base shear (KN)		RSR	Peak load	100-Year/ Peak load	System redundancy
		First member failure	100-Year load		Base shear (KN)		
0	VD6	19,027	9,062	2.10	23,564	0.385	1.38
45	HD4	26,042	10,020	2.60	26,042	0.385	1.38
90	VF1	30,346	10,467	2.90	31,395	0.333	1.33
135	VB5	33,944	10,461	3.24	33,944	0.308	1.31
180	VD6	29,030	9,674	3.00	31,053	0.312	1.31
225	HD3	30,934	10,664	2.90	30,934	0.345	1.34
270	VE5	25,374	10,570	2.40	26,431	0.400	1.40
315	VB5	20,592	10,296	2.00	20,592	0.500	1.50

Table 9.3 RSR and system redundancy at platform SBO

Direction	Member group	Base shear		RSR	Peak load	100-year/ peak load	System redundancy
		First member failure	100-Year load		Base shear (KN)		
0	L13	35,162	3,702	4.90	46,633.97	0.079	1.079
45	L13	42,296.38	12,818.31	3.30	76,867.37	0.167	1.167
90	LG6	39,767.77	12,428.01	3.20	49,707.7	0.250	1.250
135	LG6	39,176.36	12,243.33	3.20	92,806.79	0.132	1.132
180	L19	42,919.1	8,941.835	4.80	75,007.79	0.119	1.119
225	L19	34,896.13	12,463.53	2.80	84,723.34	0.147	1.147
270	XF1	34,798.45	12,428.34	2.80	84,492.46	0.147	1.147
315	L13	35,380.36	12,636.78	2.80	75,810.72	0.167	1.167

Table 9.4 RSR and system redundancy at platform SKO1

Direction	Member group	Base Shear		RSR	Peak load	100-Year/ peak load	System redundancy
		First member failure	100-Year load		Base shear (KN)		
0	LGC	22,022	4,782	4.61	23,937	0.20	1.20
45	LGC	17,346	3,527	4.92	17,718	0.20	1.20
90	V2A	22,626	7,768	2.91	36,448	0.21	1.21
135	LGC	21,670	6,757	3.21	33,882	0.20	1.20
180	LG2	24,342	7,494	3.25	37,472	0.20	1.20
225	LG2	18,022	8,000	2.25	22,054	0.36	1.36
270	LG2	25,291	9,188	2.75	41,652	0.22	1.22
315	LG2	18,405	4,905	3.75	24,573	0.20	1.20

Table 9.5 RSR and system redundancy at platform SKO2

Direction	Member group	Base shear		RSR	Peak load	100-Year/ peak load	System redundancy
		First member failure	100-Year load		Base shear (KN)		
0	VB9	21,215	9,752.54	2.18	42,222	0.23	1.23
45	VB19	35,240	9,487	3.71	45,500	0.21	1.21
90	VBF	36,252	8,982	4.04	42,012	0.21	1.21
135	VB9	31,086	9,349	3.33	45,050	0.21	1.21
180	VB9	25,348	9,413	2.69	46,903	0.20	1.20
225	VBJ	29,666	9,191	3.23	42,000	0.22	1.22
270	VBJ	22,751	9,237	2.46	40,860	0.23	1.23
315	VB9	22,327	9,104	2.45	39,300	0.23	1.23

Table 9.6 RSR and system redundancy at platform SKO2a

Direction	Member group	Base Shear		RSR	Peak load	100-Year/ peak load	System redundancy
		First member failure	100-year load		Base shear (KN)		
0	VB9	20,857	8,141	2.56	39,791	0.20	1.20
45	L32	32,056	13,017	2.46	36,665	0.36	1.36
90	102	29,980	8,877	3.38	42,488	0.21	1.21
135	VAA	30,907	9,195	3.36	34,472	0.27	1.27
180	VB9	26,138	9,317	2.81	39,133	0.24	1.24
225	VBJ	23,266	9,102	2.56	25,768	0.35	1.35
270	VBJ	23,544	9,190	2.56	32,483	0.28	1.28
315	VB9	23,141	9,096	2.54	31,663	0.29	1.29

9.3 System Environmental Load Factor

RSR values are evaluated from existing platforms based on design of API WSD. Here, the environmental load factor proposed for all three regions of Malaysia is using minimum RSR of 2. This is done to build maximum optimised structures which are not only safe as per API but also will economise the cost. It has been suggested that minimum target probability of failure for system reliability should be taken as 3×10^{-5} [6, 7] with a reliability index of 4.0. This reliability index is related to ductile failure of system with reserve capacity and dangerous failure implications for Jacket platforms. Melchers reports that minimum system reliability index should be 3.58 RSR. For Figs. 9.12, 9.13, 9.14, 9.15 and 9.16, reliability index has been determined with respect to different We/G ratios and range of environmental loads. For platforms from three regions, reliability index is high when

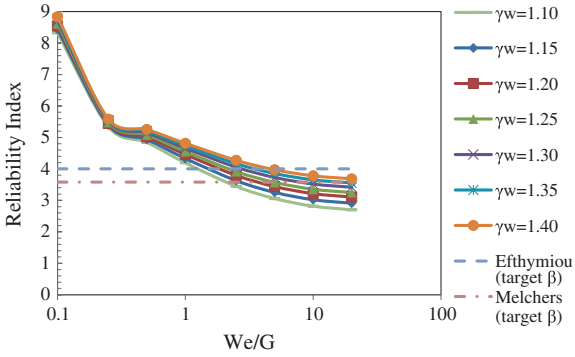

Fig. 9.12 Variation of reliability index versus We/G ratio using ISO 19902 code for different environmental load factors (γ_w) at PMO

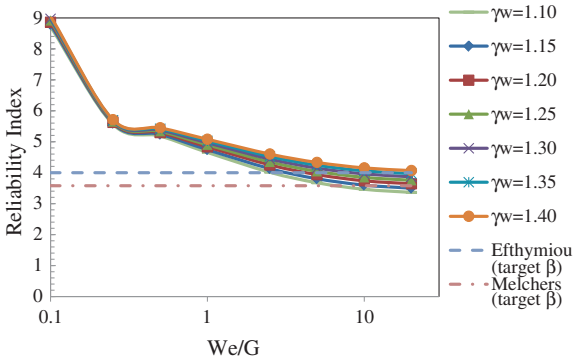

Fig. 9.13 Variation of reliability index versus We/G ratio using ISO 19902 code for different environmental load factors (γ_w) at SBO

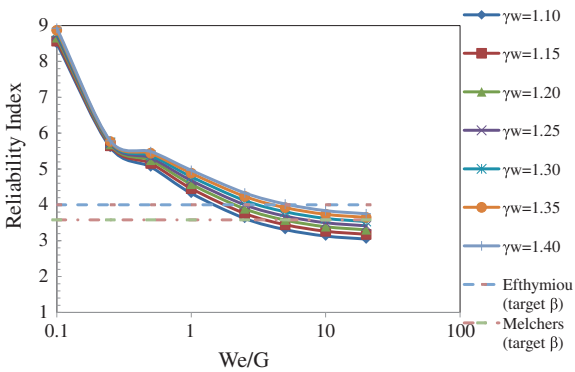

Fig. 9.14 Variation of reliability index versus We/G ratio using ISO 19902 code for different environmental load factors (γ_w) at SKO1

gravity load is more, but as environmental load increased, the reliability index became stable and curve straightened up. The other influence of higher gravity load is that from 0.1 to 0.5, the spread of difference between load factors is not large, but as environmental load increased, spread became more visible. This trend is representative for all regions. The same is also present for ISO code [8]. The curves are steeper between 0.2 and 0.3 but became flatter after 1.0.

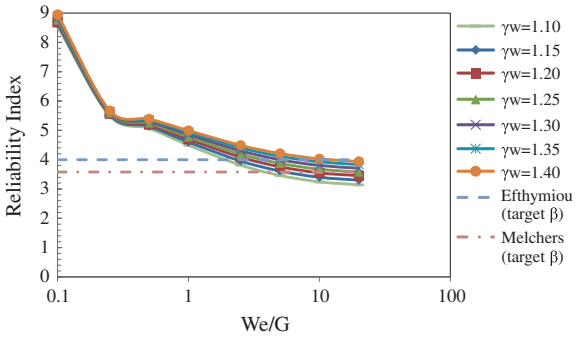

Fig. 9.15 Variation of reliability index versus We/G ratio using ISO 19902 code for different environmental load factors (γ_w) at SKO2

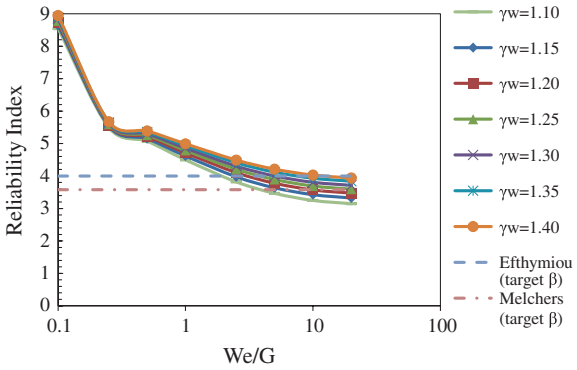

Fig. 9.16 Variation of reliability index versus We/G ratio using ISO 19902 code for different environmental load factors (γ_w) at SKO2a

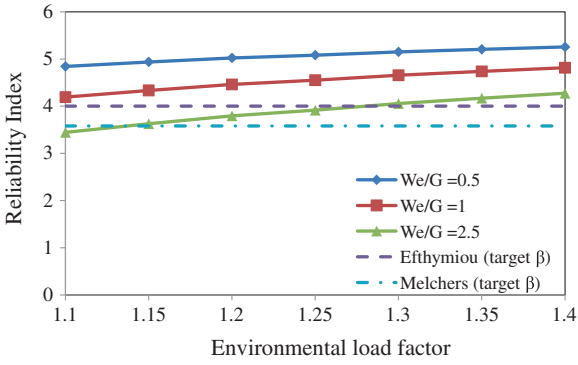

Fig. 9.17 Effect of γ_w on reliability index against W_e/G ratio of 0.5, 1 and 2.5 at PMO

Figures 9.17, 9.18, 9.19, 9.20 and 9.21 show reliability index with respect to different load factors and We/G ratios of 0.5, 1 and 2.5. These figures show that except with We/G ratio of 2.5, other ratios are well above the target reliability. When wave load impact increased, the reliability index became lower and vice versa. The reliability index increased with increasing percentage contribution of dead load which is more predictable with less variability [7].

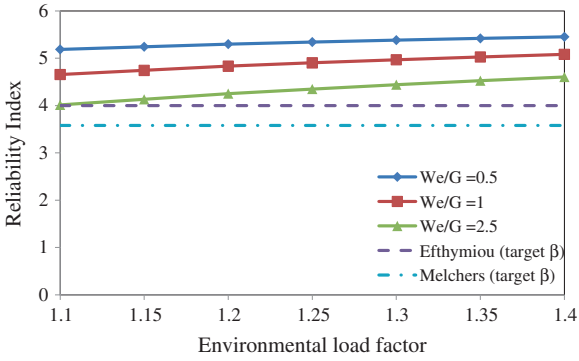

Fig. 9.18 Effect of γ_w on reliability index against W_e/G ratio of 0.5, 1 and 2.5 at SBO

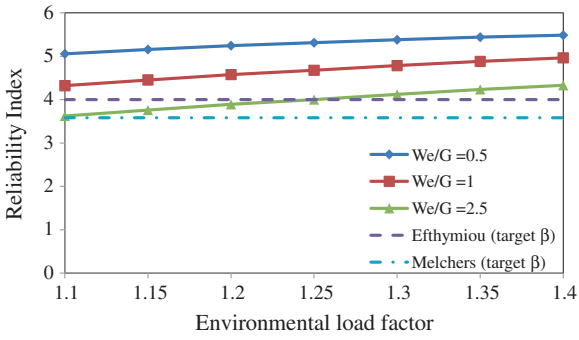

Fig. 9.19 Effect of γ_w on reliability index against W_e/G ratio of 0.5, 1 and 2.5 at SKO1

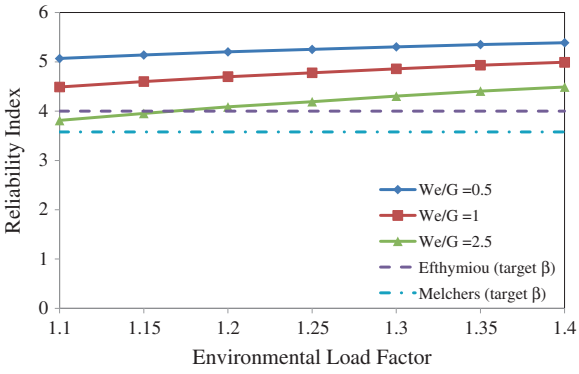

Fig. 9.20 Effect of γ_w on reliability index against W_e/G ratio of 0.5, 1 and 2.5 at SKO2

Figures 9.22, 9.23, 9.24, 9.25 and 9.26 show reliability index with respect to varying We/G ratios for the environmental load factor of 1.1. From these figures, it is clear that load factor of 1.1 is higher than the notional target reliabilities. Thus, any reliability above the accepted reliable Jacket will be safe for the Jacket assessed for ductility.

Figures 9.27, 9.28, 9.29, 9.30 and 9.31 show that the proposed load factor for Malaysia of 1.1 is well above the target reliabilities.

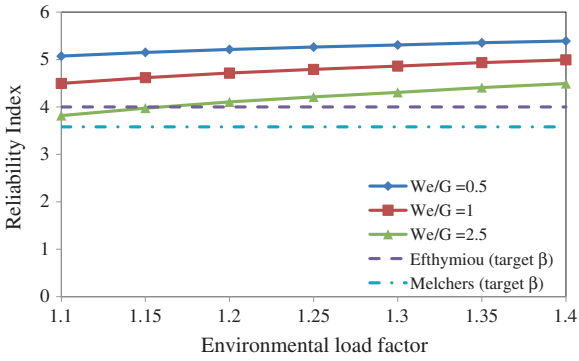

Fig. 9.21 Effect of γ_w on reliability index against W_e/G ratio of 0.5, 1 and 2.5 at SKO2a

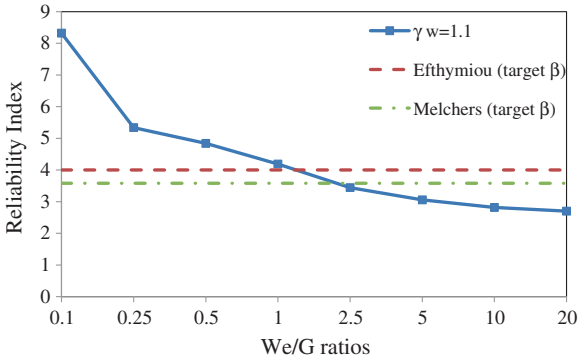

Fig. 9.22 Reliability index versus We/G ratios with $\gamma_w = 1.10$ and target reliability at PMO

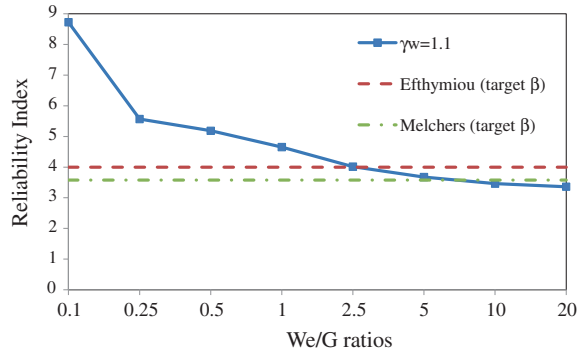

Fig. 9.23 Reliability index versus We/G ratios with $\gamma_w = 1.10$ and target reliability at SBO

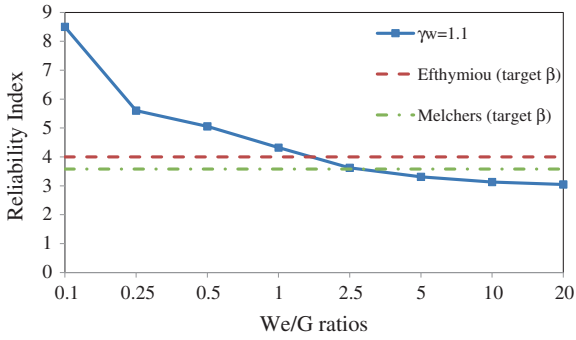

Fig. 9.24 Reliability index versus We/G ratios with $\gamma_w = 1.10$ and target reliability at SKO1

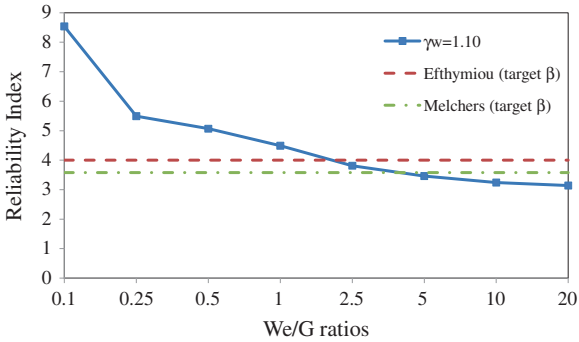

Fig. 9.25 Reliability index versus We/G ratios with $\gamma_w = 1.10$ and target reliability at SKO2

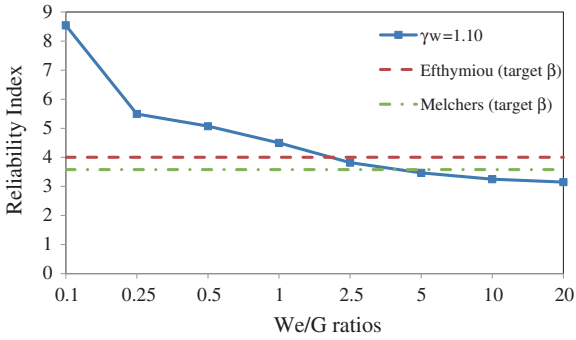

Fig. 9.26 Reliability index versus We/G ratios with $\gamma_w = 1.10$ and target reliability at SKO2a

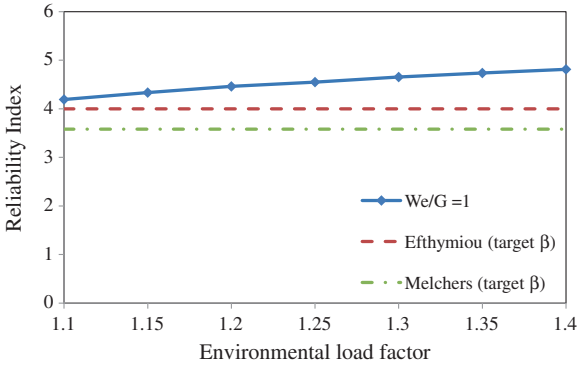

Fig. 9.27 Reliability index versus environmental load factor, We/G = 1 at PMO

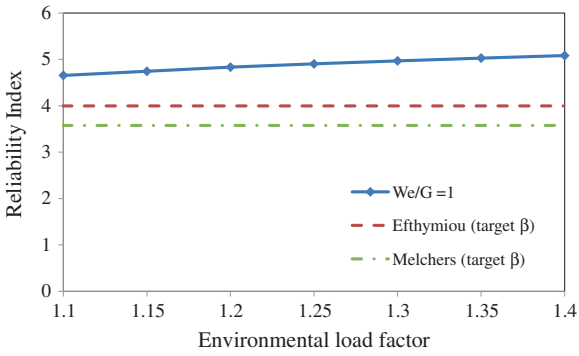

Fig. 9.28 Reliability index versus environmental load factor, We/G = 1 at SBO

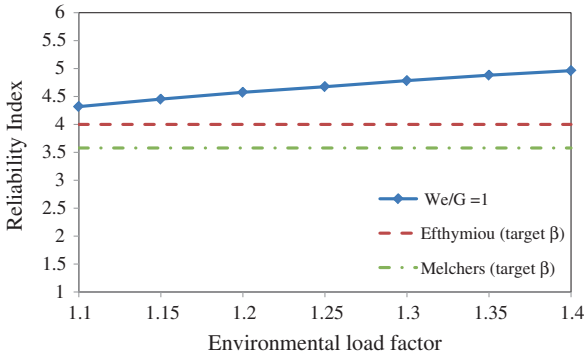

Fig. 9.29 Reliability index versus environmental load factor, We/G = 1 at SKO1

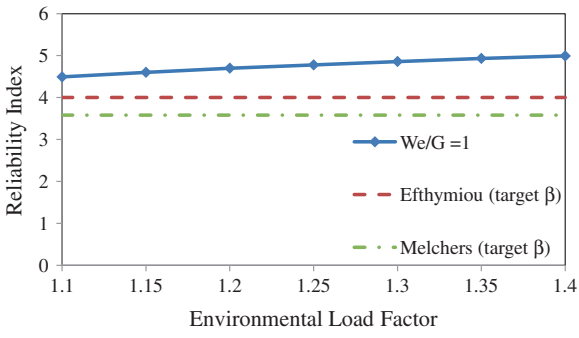

Fig. 9.30 Reliability index versus environmental load factor, We/G = 1 at SKO2

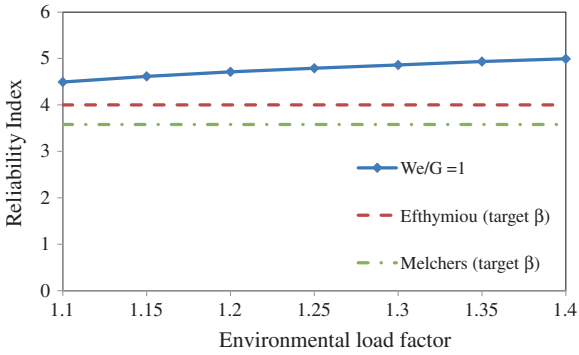

Fig. 9.31 Reliability index versus environmental load factor, We/G = 1 at SKO2a

9.4 Summary

The load factor is determined for all three regions and four Jacket platforms. Due to system ductility with given RSR, the environmental load factor is much lower as compared to component and joint. For system, the target reliability index is 4.0 and 3.8 based on notional system reliability index proposed by Efthymiou and Melchers, respectively. The load factor evaluated for all regions is found to be 1.1, with W_e/G ratio of 1.0. The same trend of component and joint is present for reliability index of system with regard to W_e/G ratios. The reliability index decreased with increase of environmental load. The load factor of 1.1 can be proposed for offshore Malaysia using the referred target reliability.

References

1. Furnes, O., Sele, A.: Offshore structures-implementation of reliability. In: Extreme Loads Response Symposium, Integrity of offshore structures, Society of Naval Architects and Marine Engineers (1982)
2. Titus, P.G., Banon, H.: Reserve strength analysis of offshore platforms. Paper 88179 presented at the 7th Offshore Southeast Asia Conference, Singapore (1988)
3. ISO-2394: General principles on reliability for structures, ISO-2394. In: ISO (1998)
4. Sigurdsson, G., Skallerud, B., Skjong, R., Amdahl, J.: Probabilistic collapse analysis of Jackets. In: Presented at the OMAE, Houston (1994)
5. Heideman, J.: Parametric response model for wave/current joint probability. Report Submitted to API TAC 88-20 for API LRFD1980
6. Efthymiou, M., Graaf, G.W., Tromans, P.S., Hines, I.M.: Reliability based criteria for fixed steel offshore platforms. J. Offshore Mech. Arct. Eng. OMAE **119**(2), 120–124 (1997)
7. Ingebrigtsen, T., Loset, O., Nielsen, S.G.: Fatigue design and overall safety of grouted pile sleeve connections. In: Offshore technology conference, OTC 6344, Houston (1990)
8. BOMEL: System-based calibration of North West European annex environmental load factors for the ISO fixed steel offshore structures code 19902 (2003)

Chapter 10
Extension of Life of Jacket Platforms

Abstract Jacket platforms are frequently checked when loading and resistance parameters are changed or at the end of design life and if hydrocarbon reserves are still there to be extracted, it must be checked for extension of life. Therefore, the probability of failure is used to check its strength at all the stages. Bayesian updating is a technique to be used for updating probability of failure taking into consideration probability of failure.

10.1 Introduction

Reassessment of old platforms using component-based approach becomes unviable as now, the whole system is now working under the given conditions. So instead of component reliability, system strength analysis method is used to check the reserve strength of the platform and find its redundancy. The next step is to find wave properties through base shear. Wave height is increased so that a wave height which gives RSR of 1.0 could be evaluated. This wave height is used for Bayesian updating of Jacket platform.

10.2 Collapse Analysis of Jacket

Failure can be defined as global collapse, i.e. loads exceeding the ultimate capacity of Jacket [1]. Appendix F shows the RSR values with respect to applied H_{max} in different ranges starting from design wave. This analysis is done to overload the Jacket and find its response near failure condition [2, 3]. The minimum acceptable safe condition for Jacket is set at RSR of 1.0. The corresponding wave height is further used to find the probability of failure. It can be seen that at low wave height, RSR is high, but as wave heights increased, the RSR reduced. The same trend is observed at all three regions. The RSR of 1.0 corresponding to the given wave load made us confident about the Jacket strength and ductility.

Z. Nizamani, *Environmental Load Factors and System Strength Evaluation of Offshore Jacket Platforms*, Ocean Engineering & Oceanography 4,
DOI 10.1007/978-3-319-15051-2_10

10.2.1 Wave Effect on Collapse Load

Figures 10.1, 10.2, 10.3, 10.4 and 10.5 show the base shear against wave height effects of Jacket response. The variation in base shear is due to difference of top-side weight, Jacket height, water depth and wave heights. Here, each wave height is analysed in eight directions along with three current speeds. Thus, there are

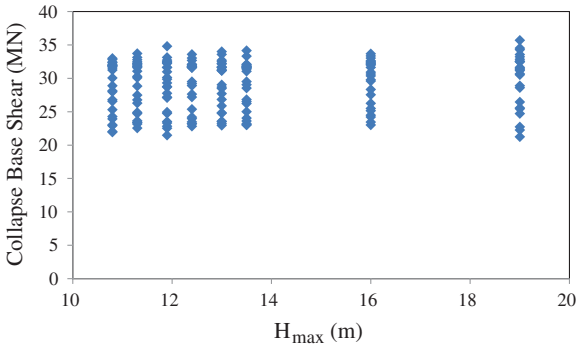

Fig. 10.1 Collapse base shear against H_{max} for PMO

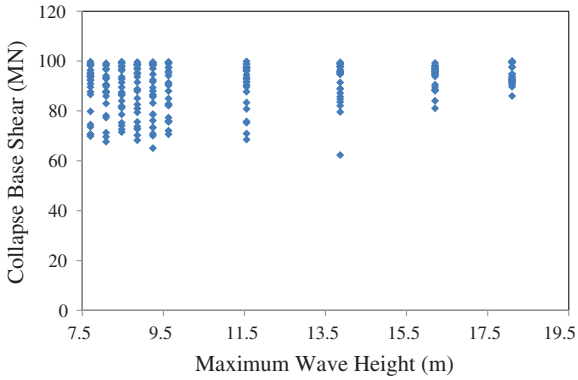

Fig. 10.2 Collapse base shear against H_{max} for SBO

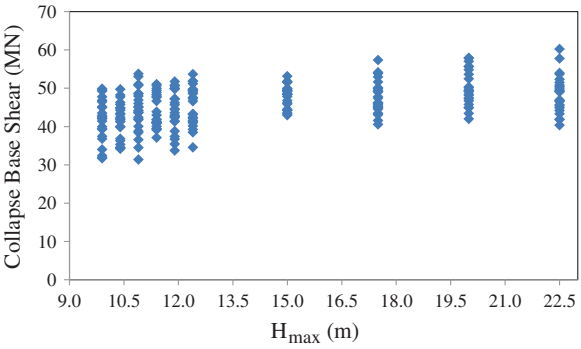

Fig. 10.3 Collapse base shear against H_{max} for SKO1

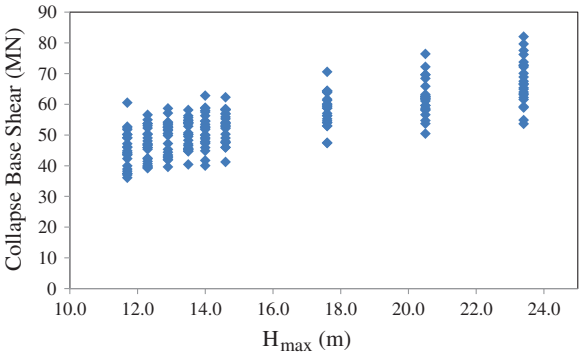

Fig. 10.4 Collapse base shear against H_{max} for SKO2

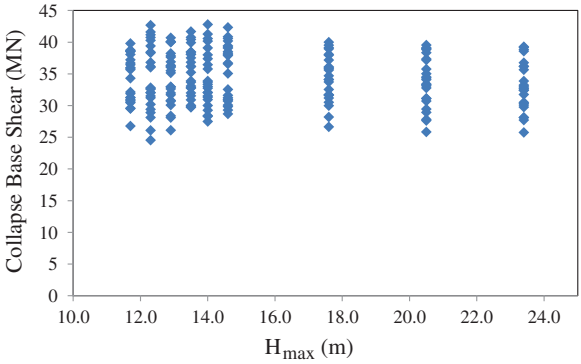

Fig. 10.5 Collapse base shear against H_{max} for SKO2a

24 analyses for each wave. The high variation in base shear is due to increase in wave height. The scatter at different wave heights is due to system redundancy in Jackets for different directions.

10.2.2 Directional Base Shear

Figures 10.6, 10.7, 10.8, 10.9 and 10.10 show collapse base shear with eight wave directions. Here, Jackets vary in their strength when loads act in different directions. The scatter at PMO is less as compared to other regions.

10.2.3 Wave Directional Effects on Collapse Base Shear

Figures 10.11, 10.12, 10.13, 10.14, 10.15, 10.16, 10.17 and 10.18 show the effect of collapse base shear against H_{max} with varying current speed in eight directions for PMO region. Here, effect of each wave height is placed separately. Collapse

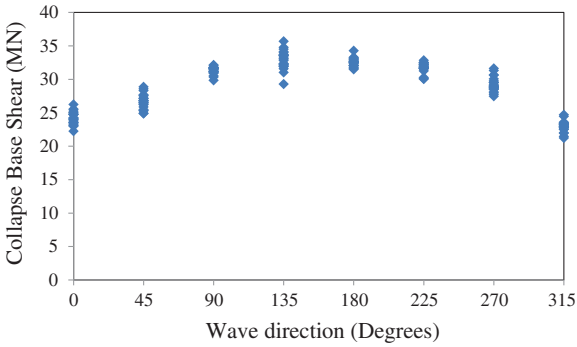

Fig. 10.6 Collapse base shear against wave direction at PMO

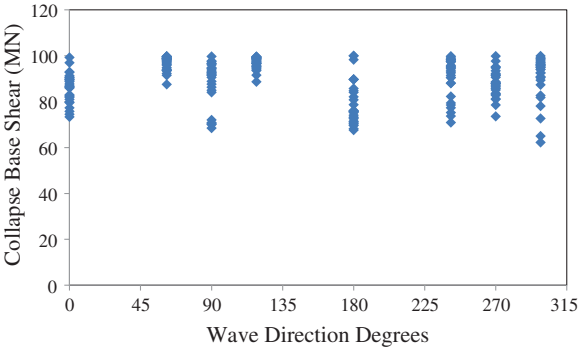

Fig. 10.7 Collapse base shear against wave direction at SBO

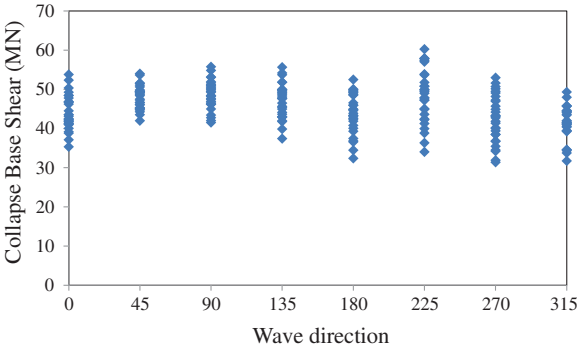

Fig. 10.8 Collapse base shear against wave direction at SKO1

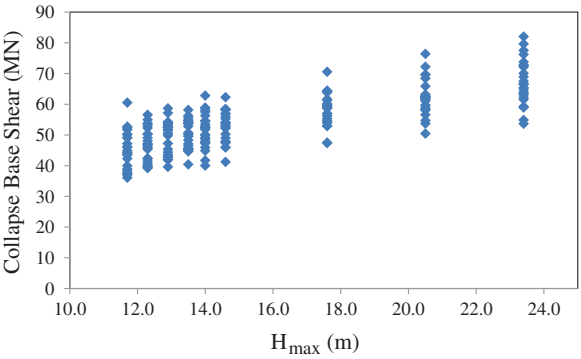

Fig. 10.9 Collapse base shear against wave direction at SKO2

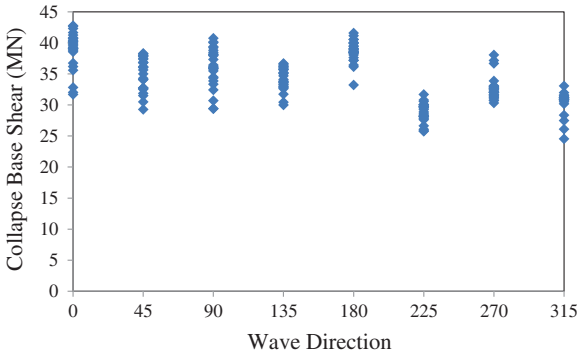

Fig. 10.10 Collapse base shear against wave direction at SKO2a

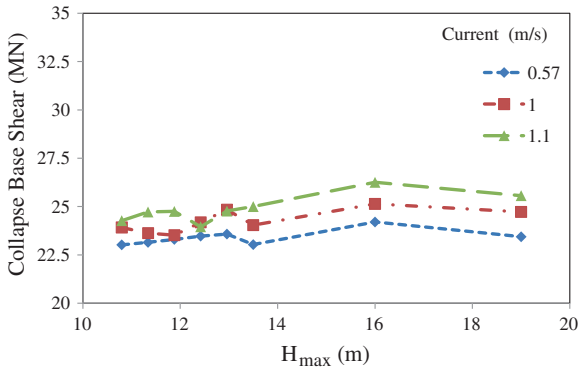

Fig. 10.11 Collapse base shear against H_{max} wave with varying currents for PMO for 0°

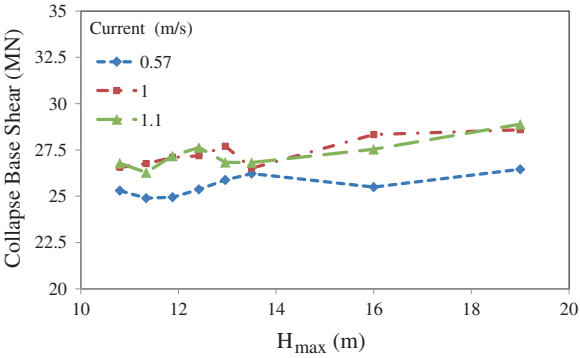

Fig. 10.12 Collapse base shear against H_{max} wave with varying currents for PMO for 45°

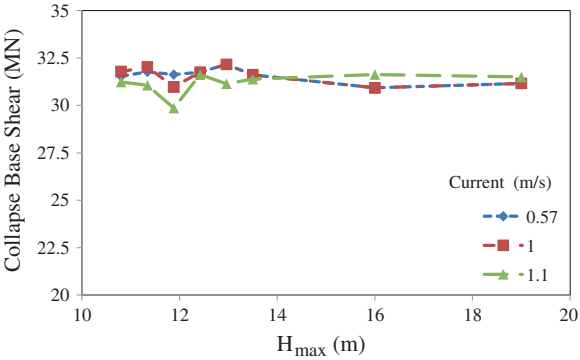

Fig. 10.13 Collapse base shear against H_{max} wave with varying currents for PMO for 90°

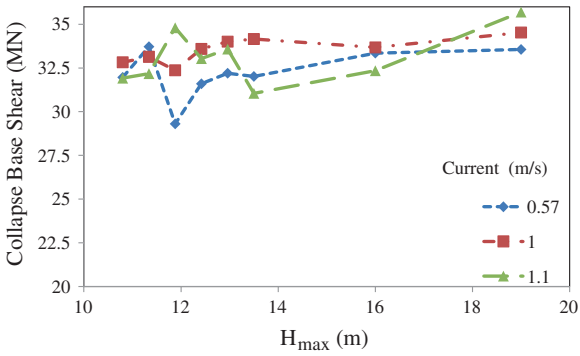

Fig. 10.14 Collapse base shear against H_{max} wave with varying currents for PMO for 135°

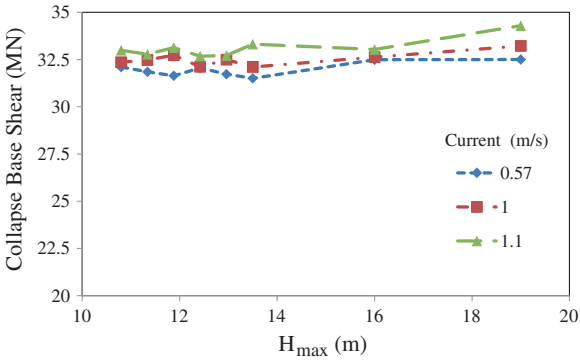

Fig. 10.15 Collapse base shear against H_{max} wave with varying currents for PMO for 180°

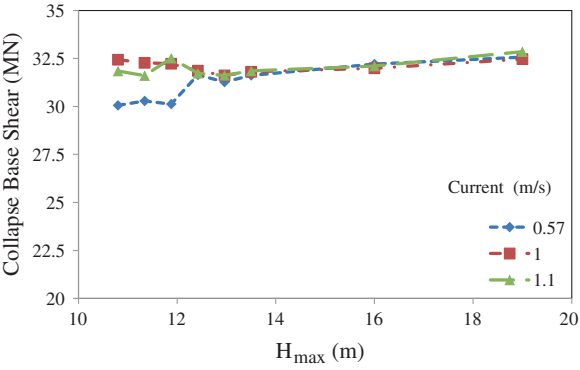

Fig. 10.16 Collapse base shear against H_{max} wave with varying currents for PMO for 225°

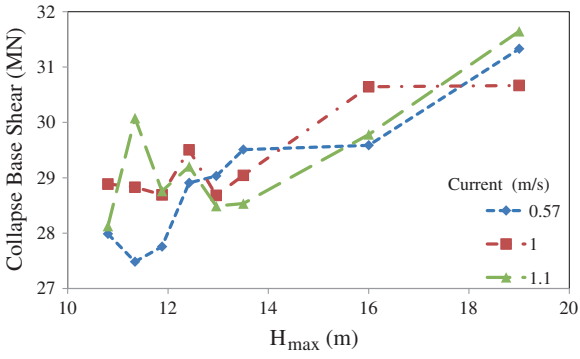

Fig. 10.17 Collapse base shear against H_{max} wave with varying currents for PMO for 270°

base shear varied as wave heights increase, due to system strength of Jacket. The effect of directions is predominant in all cases. Results from SBO, SKO1 and SKO2, SKO2a regions are shown in Appendix E.

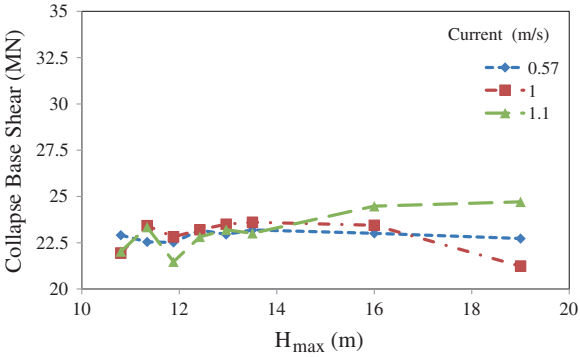

Fig. 10.18 Collapse base shear against H_{max} wave with varying currents for PMO for 315°

10.2.4 System Redundancy

Appendix F shows the system redundancy against the wave loads. It shows that system redundancy did not depend on increased wave heights. It is the direction of wave which played important role in this regard.

10.3 Updating the Probability of Failure

Evaluating probability of failure becomes extremely important in case of any damage to the Jacket, change of loading pattern, application of new loads, routine check-up after some years or when extension of life is required. Most of the existing Jacket platforms in offshore Malaysia have already completed their life, and they are constantly being evaluated for extension of life. Here, first probability of failure is checked for design and 10,000-year load. The Bayesian updating technique is applied for evaluating the probability of failure at design load and extremely high load when RSR of Jacket equals to 1.0.

10.3.1 Sensitivity Analysis

The effect of uncertainty has already been seen in earlier chapter for load and resistance. Here, effects of load and resistance model uncertainty on overall system probability of failure are evaluated.

10.3.1.1 Effect of Load Uncertainty Model

Figures 10.19, 10.20, 10.21, 10.22 and 10.23 show the effect on uncertainty model due to load with resistance model uncertainty of 5 and 10 % and RSR of 1.5 and 2.0. When RSR is 2, probability of failure is decreasing as compared to RSR of

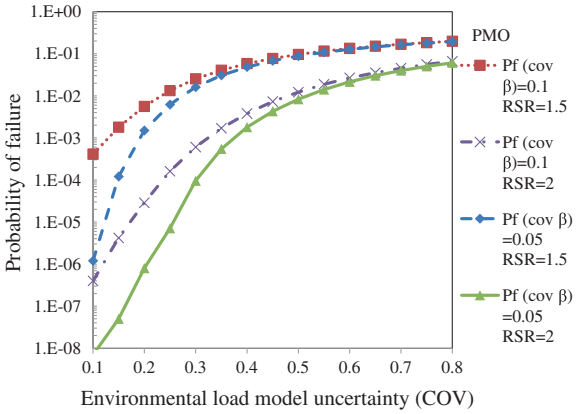

Fig. 10.19 Variation of load model uncertainty on resistance model uncertainty at PMO

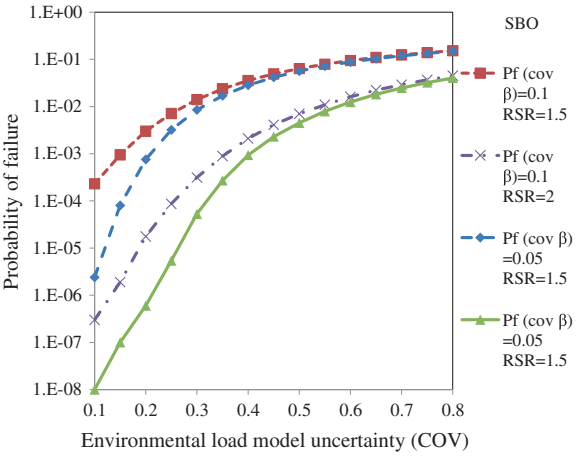

Fig. 10.20 Variation of load model uncertainty on resistance model uncertainty at SBO

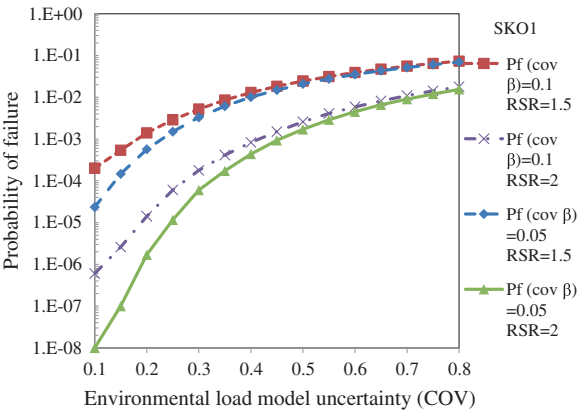

Fig. 10.21 Variation of load model uncertainty on resistance model uncertainty at SKO1

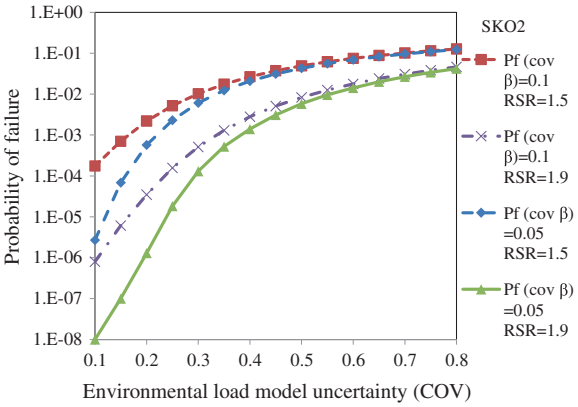

Fig. 10.22 Variation of load model uncertainty on resistance model uncertainty at SKO2

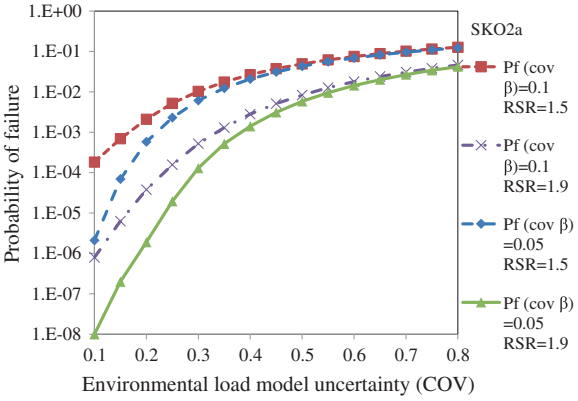

Fig. 10.23 Variation of load model uncertainty on resistance model uncertainty at SKO2a

1.5. The variability in load model uncertainty lies between 10 and 40 %. The variability of probability of failure with RSR of 1.5 is 1×10^{-2} to 1×10^{-6}. With RSR of 2.0, this varied from 1×10^{-3} to 1×10^{-8}. Even with resistance model, when variability is kept constant at 10 %, the variability at RSR of 1.5 is between 1×10^{-2} and 1×10^{-4} , and with RSR of 2.0, this variability reaches to 1×10^{-3} to 1×10^{-7}. This shows that the effects of the parameters of reliability are high, and thus, fixed-target reliability is difficult to achieve for Jacket platforms. Thus, it can be said that reliability is always based on personal judgment.

10.3.1.2 Probability of Failure and RSR Sensitivity

Figures 10.24, 10.25, 10.26, 10.27 and 10.28 show the effect of RSR on probability of failure with load model uncertainty in range of 0.15–0.45. These figures show that the risk increases with reduction in RSR value, i.e. probability of failure decreased sharply with increase of RSR. It shows that with RSR value of 2.5, the risk became extremely rare with probability of failure reaching up to 1×10^{-8} for

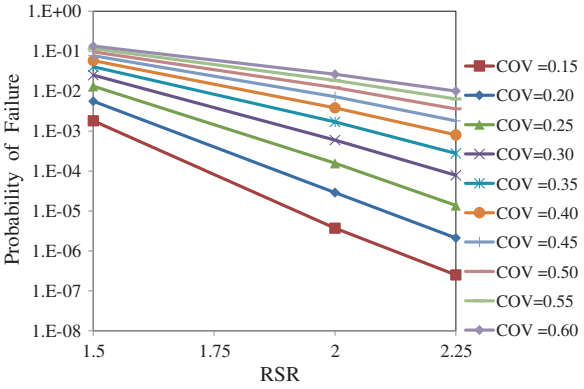

Fig. 10.24 Variation of load model uncertainty and RSR on probability of failure, with $\beta = 0.10$ at PMO

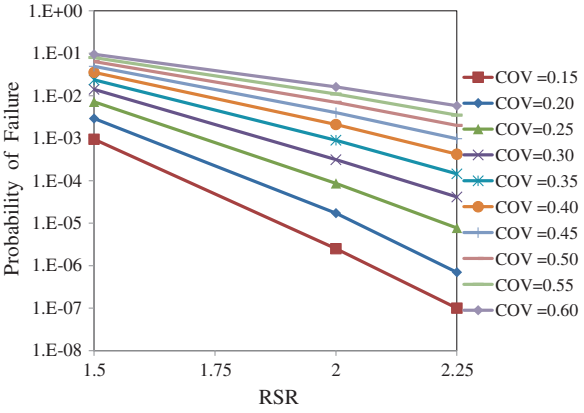

Fig. 10.25 Variation of load model uncertainty and RSR on probability of failure, with $\beta = 0.10$ at SBO

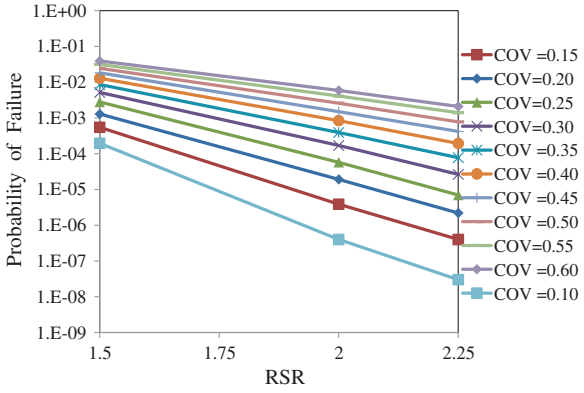

Fig. 10.26 Variation of load model uncertainty and RSR on probability of failure, with $\beta = 0.10$ at SKO1

COV of load of 0.15. In case of COV of 0.45, the probability of failure reached up to 1×10^{-4} with RSR of 2.5. Here, in this text, COV of 0.15 on load is used, and that is the reason why RSR value of 1.5–2.5 is considered safe for analysis. This results in minimum RSR in range of 2.0–2.5 and depends on COV of load model uncertainty.

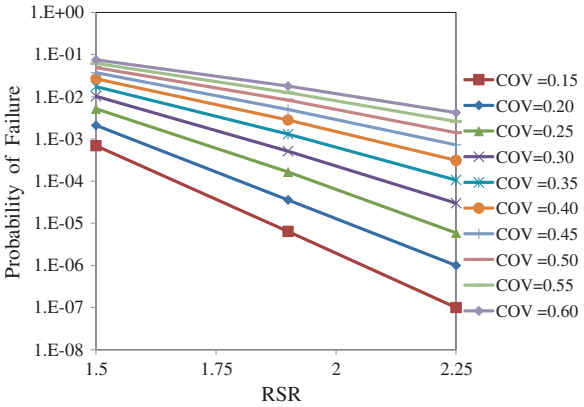

Fig. 10.27 Variation of load model uncertainty and RSR on probability of failure, with $\beta = 0.10$ at SKO2

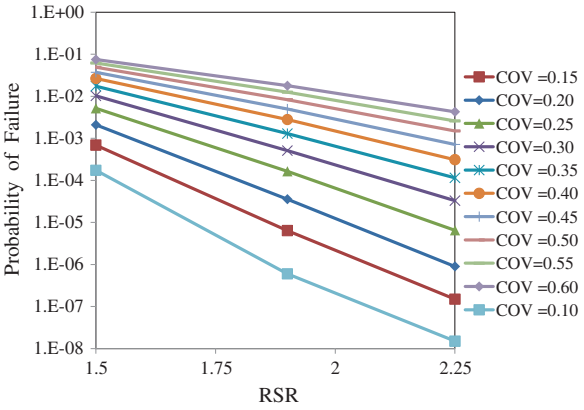

Fig. 10.28 Variation of load model uncertainty and RSR on probability of failure, with $\beta = 0.10$ at SKO2a

10.3.1.3 Effect of Model Uncertainty of Environmental Load on Probability of Failure

Figures 10.29, 10.30, 10.31, 10.32 and 10.33 show the effects of experienced waves on probability of failure. The effect of variation of wave height on probability of failure is significant with variation of COV of load model uncertainty. Failure probability increased with increase in wave height.

10.3.2 Bayesian Updating the Probability of Failure

The probability of failure is evaluated using an RSR value of 1.5 and 2.0. Table 10.1 and Figs. 10.34, 10.35, 10.36, 10.37 and 10.38 show the probability of failure with design load and updated probability of failure with increased load. It can be seen that with Bayesian updating, probability of failure decreases.

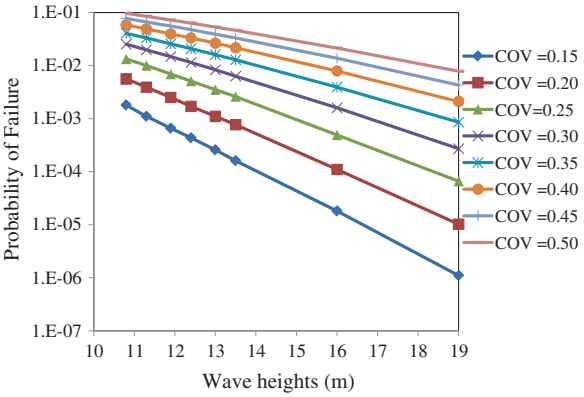

Fig. 10.29 Effect of wave heights and load model uncertainty on probability of failure at PMO

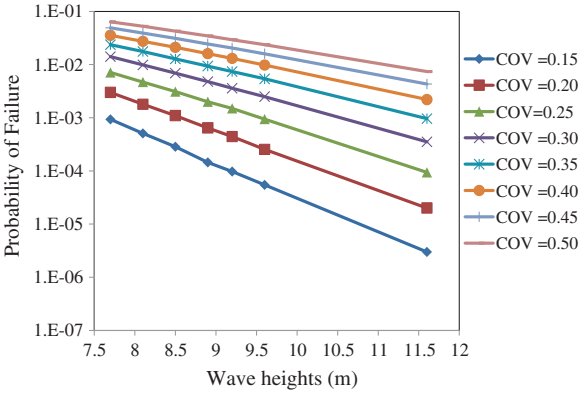

Fig. 10.30 Effect of wave heights and load model uncertainty on probability of failure at SBO

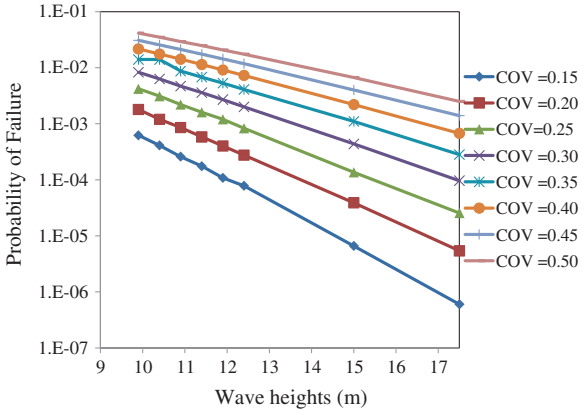

Fig. 10.31 Effect of wave heights and load model uncertainty on probability of failure at SKO1

With experienced resistance and load, it could be predicted how much load can be resisted by the Jacket. Thus, extension of life as well as assessment of Jacket can be predicted. The main advantage here is that the platform is considered safe

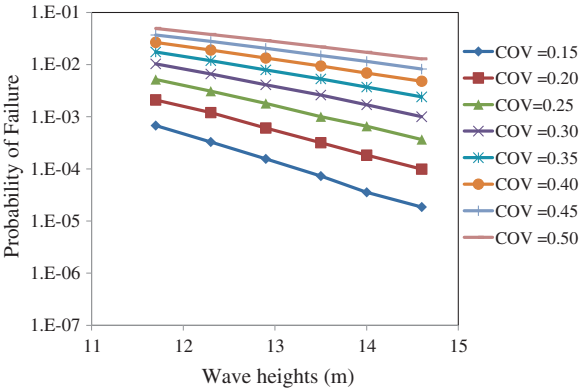

Fig. 10.32 Effect of wave heights and load model uncertainty on probability of failure at SKO2

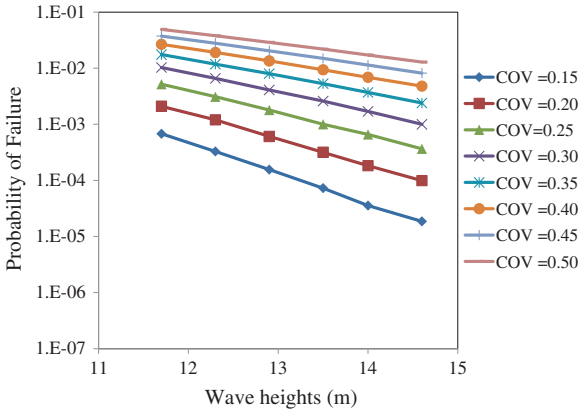

Fig. 10.33 Effect of wave heights and load model uncertainty on probability of failure at SKO2a

Table 10.1 Design and updated probability of failure

	Design Pf (RSR) = 1.5	Updated Pf (RSR) = 1.5	Design Pf (RSR = 2.0)	Updated Pf (RSR) = 2.0
PMO	9.20E−03	1.26E−03	3.01E−05	2.04E−05
SBO	9.23E−04	1.14E−04	3.00E−06	1.95E−06
SKO1	6.24E−04	1.80E−04	2.90E−06	2.48E−06
SKO2	6.78E−04	9.94E−05	5.90E−06	3.45E−06
SKO2a	6.78E−04	9.96E−05	6.70E−06	3.92E−06

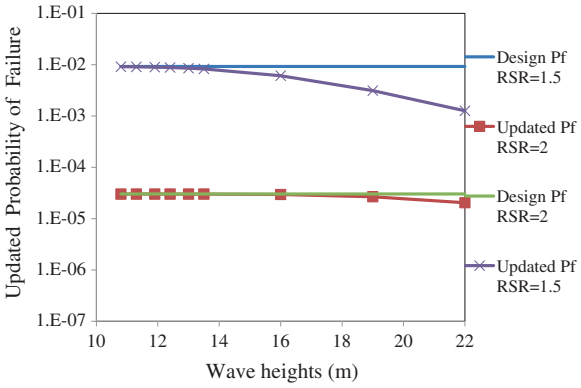

Fig. 10.34 Effect of wave heights and RSR on updated probability of failure at PMO

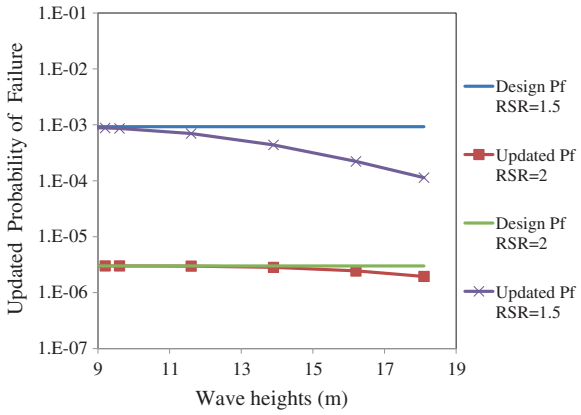

Fig. 10.35 Effect of wave heights and RSR on updated probability of failure at SBO

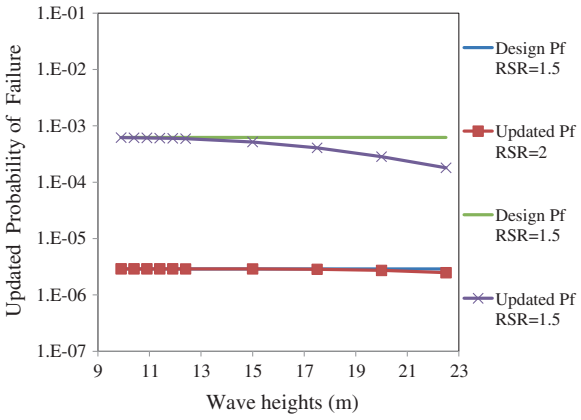

Fig. 10.36 Effect of wave heights and RSR on updated probability of failure at SKO1

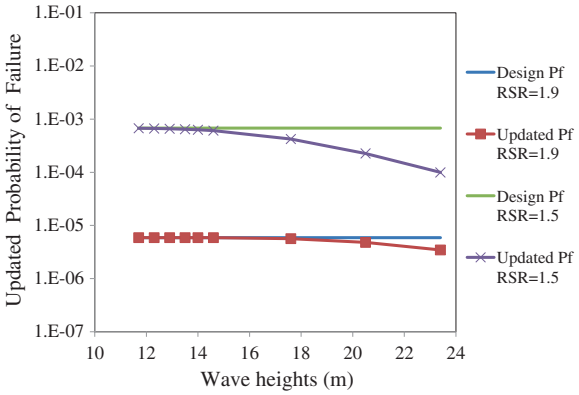

Fig. 10.37 Effect of wave heights and RSR on updated probability of failure at SKO2

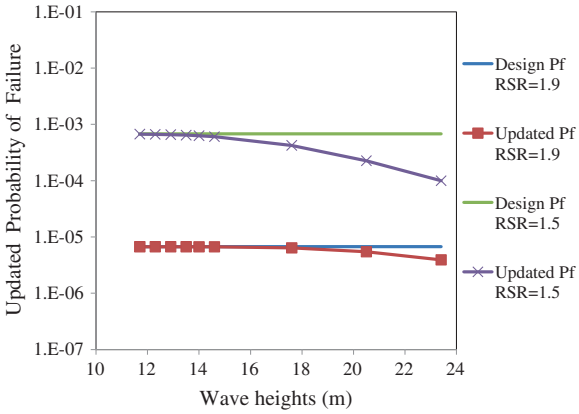

Fig. 10.38 Effect of wave heights and RSR on updated probability of failure at SKO2a

against a wave of 10,000-year return period as recommended by ISO, when updating is made. With design probability of failure, an existing Jacket at PMO cannot be recommended for extension of life if it has an RSR of 1.5, but we have seen in Table 10.2 that as it has minimum RSR of 2.0, it can be given extension of life.

Table 10.2 Reduced capacity for PMO Jacket with damaged members

X-brace	Base shear at 100-year load (KN)	Collapse base shear (KN)	Damaged strength ratio	Reduced capacity factor	Capacity reduction
Intact	9,060.0	20,380.0	2.25	1.00	1.00
One member removed	9,043.0	15,822.0	1.75	0.78	0.78
Two members removed	9,030.0	13,548.0	1.50	0.86	0.67

10.3.3 Bayesian Updating Probability of Failure with Damaged Members

When Jacket members fail, the overall capacity of Jacket reduces as shown in Table 10.2, 10.3, 10.4, 10.5 and 10.6. Damaged strength factor is found using Eq. 3.68. This reduced capacity is used to find updated probability of failure (UPF) as shown in Figs. 10.39, 10.40, 10.41, 10.42, 10.43, 10.44, 10.45, 10.46, 10.47 and 10.48. The capacity is reduced about 50 % in case of three member failures, and therefore, probability of failure is determined up to two member failures. Table 10.7 shows that with experienced waves, the probability of failure decreases. Though in all cases probability of failure is very high, with experienced waves, it decreased and reached a level where it can sustain 10,000 years load.

Table 10.3 Reduced capacity for SBO Jacket with damaged members

X-brace	Base shear at 100-year load (KN)	Collapse base shear (KN)	Damaged strength ratio	Reduced capacity factor	Capacity reduction
Intact	12,636.8	35,380.4	2.80	1.00	1
One member removed	12,555.0	31,387.0	2.50	0.89	0.893
Two members removed	12,494.0	24,987.0	2.00	0.80	0.714

Table 10.4 Reduced capacity for SKO1 Jacket with damaged members

X-brace	Base shear at 100-year load (KN)	Collapse base shear (KN)	Damaged strength ratio	Reduced capacity factor	Capacity reduction
Intact	8,000	18,022	2.25	1.00	1
One member removed	7,932.0	15,904.0	2.01	0.89	0.89
Two members removed	7,833.0	13,714.0	1.75	0.87	0.78

Table 10.5 Reduced capacity for SKO2 Jacket with damaged members

X-brace	Base shear at 100-year load (KN)	Collapse base shear (KN)	Damaged strength ratio	Reduced capacity factor	Capacity reduction
Intact	9,752.54	21,215	2.18	1.00	1
One member removed	9,739.0	21,660.0	2.22	1.02	1.02
Two members removed	9,738.0	19,253.0	1.98	0.89	0.91

Table 10.6 Reduced capacity for SKO2a with damaged members

X-brace	Base shear at 100-year load (KN)	Collapse base shear (KN)	Damaged strength ratio	Reduced capacity factor	Capacity reduction
Intact	8,141	20,857	2.56	1.00	1
One member removed	9,758.0	21,650.0	2.22	0.87	0.87
Two members removed	9,756.0	19,271.0	1.98	0.89	0.77

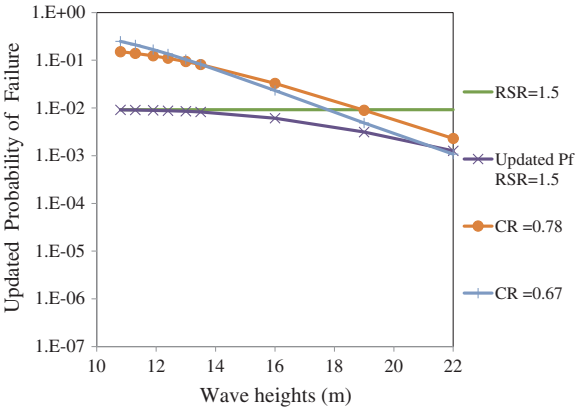

Fig. 10.39 Effect of wave heights and collapse ratio on updated probability of failure with damaged members and RSR of 1.5 at PMO

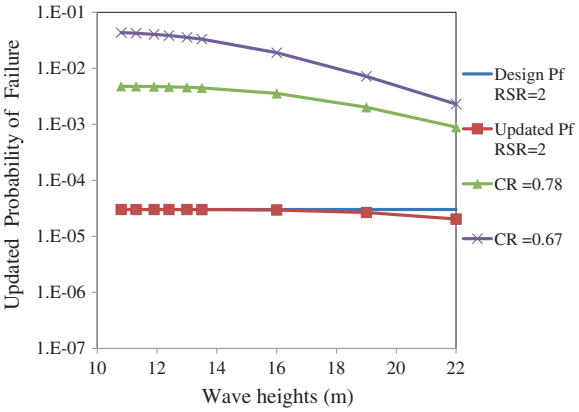

Fig. 10.40 Effect of wave heights and collapse ratio on updated probability of failure with damaged members and RSR of 2.0 at PMO

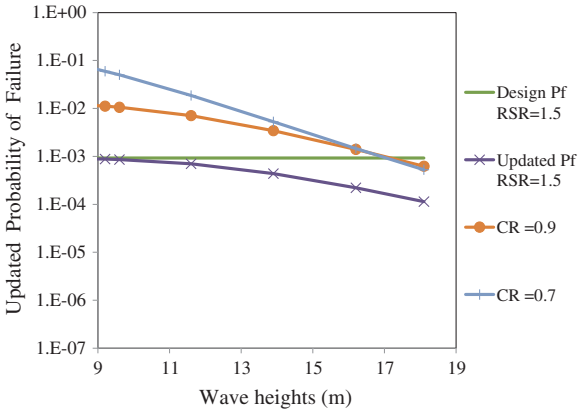

Fig. 10.41 Effect of wave heights and collapse ratio on updated probability of failure with damaged members and RSR of 1.5 at SBO

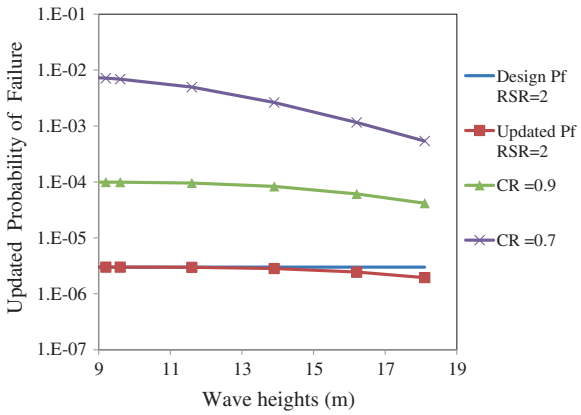

Fig. 10.42 Effect of wave heights and collapse ratio on updated probability of failure with damaged members and RSR of 2.0 at SBO

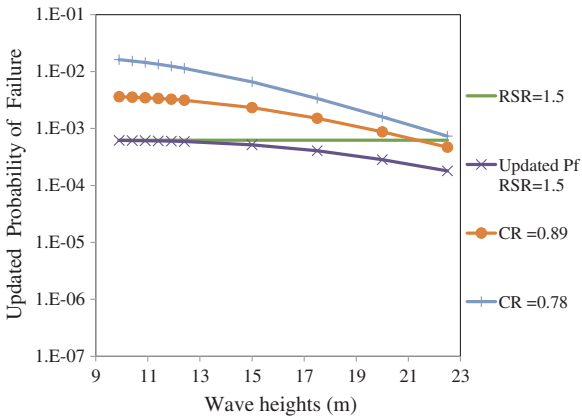

Fig. 10.43 Effect of wave heights and collapse ratio on updated probability of failure with damaged members and RSR of 1.5 at SKO1

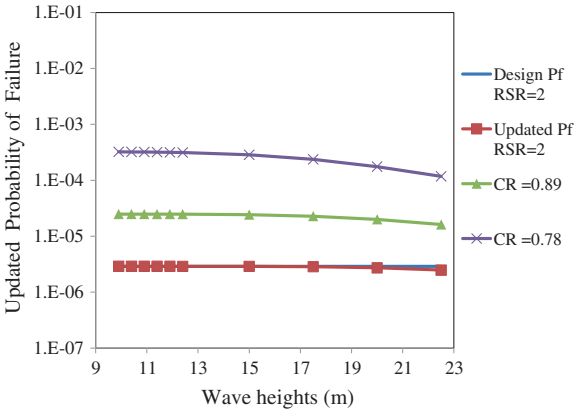

Fig. 10.44 Effect of wave heights and collapse ratio on updated probability of failure with damaged members and RSR of 2.0 at SKO1

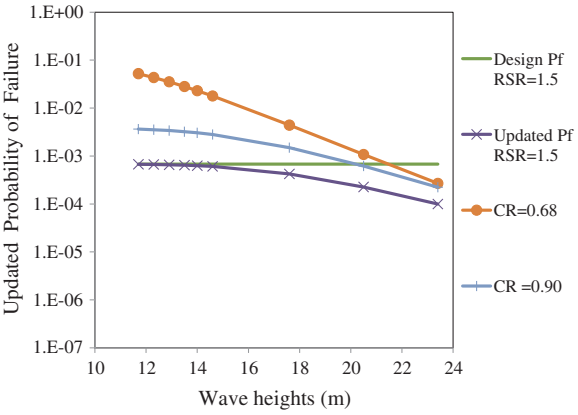

Fig. 10.45 Effect of wave heights and collapse ratio on updated probability of failure with damaged members and RSR of 1.5 at SKO2

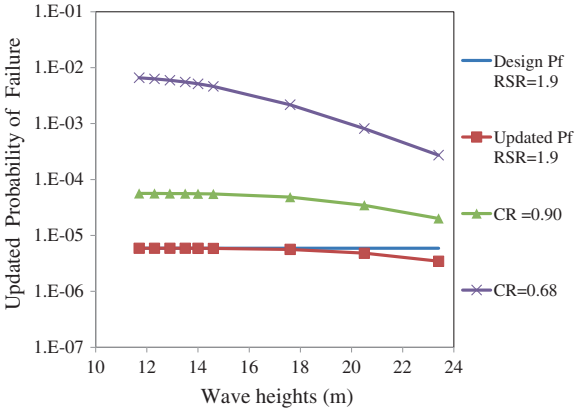

Fig. 10.46 Effect of wave heights and collapse ratio on updated probability of failure with damaged members and RSR of 2.0 at SKO2

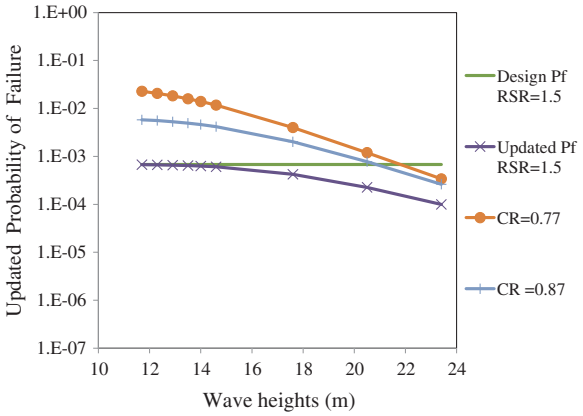

Fig. 10.47 Effect of wave heights and collapse ratio on updated probability of failure with damaged members and RSR of 1.5 at SKO2a

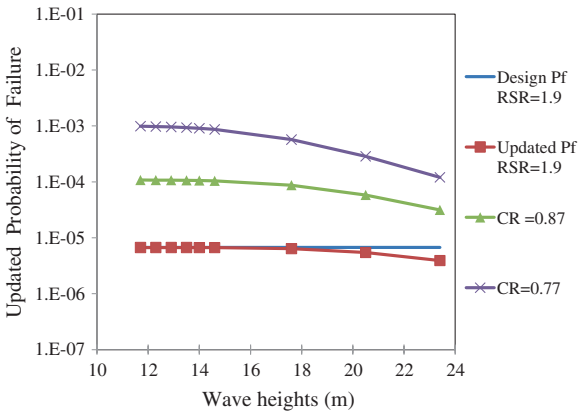

Fig. 10.48 Effect of wave heights and collapse ratio on updated probability of failure with damaged members and RSR of 2.0 at SKO2a

Table 10.7 Probability of failure of Jacket with damaged members

Regions	Collapse ratio	RSR	
		1.5	2.0
PMO	0.78	2.30E−03	8.91E−04
	0.67	1.08E−03	2.30E−03
SBO	0.9	6.25E−04	4.17E−05
	0.7	5.26E−04	5.38E−04
SKO1	0.89	4.70E−04	1.62E−05
	0.78	7.36E−04	1.18E−04
SKO2	0.9	5.90E−06	2.01E−05
	0.68	3.45E−06	2.73E−04
SKO2a	0.87	6.70E−06	3.15E−05
	0.77	3.92E−06	1.20E−04

10.4 Summary

Once component and joint environmental load has been evaluated, it becomes mandatory to assess the load factor for Jacket using system strength and RSR. Here, we are interested for minimum RSR as this would give us the most economical Jacket. The minimum RSR specified by API WSD and ISO 19902 is 1.58 and 1.85, respectively. The minimum RSR is compared with return period of load. PMO region has minimum RSR of 2.0, SBO has 2.8, SKO1 has 2.25, SKO2 2.18 and SKO2a 2.54. In this text, RSR of 1.5, 2.0 and 2.5 are considered, as higher values will give costly and non-economical Jackets.

Furthermore, collapse analysis is made to evaluate the effect of waves against collapse base shear. When Jacket platforms reaches their design age of 30 years, and hydro carbon resources are still there to be extracted, then it becomes mandatory to evaluate the strength of Jacket based on system reliability. The ISO and API have set criteria for checking the system strength integrity assessment of Jacket. Failure of Jacket platforms due to overloading from wave and current action is considered here.

Existing platforms after surviving severe environmental load for some years are found to be very safe against such loads. The increase of load becomes significant after higher wave heights due to wave forces striking the deck of topside. High RSR values show how strong these platforms are designed. The updating of probability of failure showed its advantages over non-updated probability of failure.

References

1. Marley, M., Etterdal, B., Grigorian, H.: Structural reliability assessment of ekofisk jacket under extreme loading. Presented at the Offshore Technology Conference, OTC 13190, Houston (2001)
2. Gerhard, E.: Assessment of existing offshore structures for life extension. Doctor of Philosophy, Department of Mechanical and Structural Engineering and Material Science, University of Stavanger, Stavanger, Norway (2005)
3. Gerhard, E., Sorensen, J.D., Langen, I.: Updating of structural failure probability based on experienced wave loading. Presented at the International Offshore and Polar Engineering Conference Honolulu, Hawaii, USA (2003)

Chapter 11
Conclusions and Recommendations

Abstract The codes of practice for API WSD and ISO LRFD are used in this book to find the reliability of Jacket platforms in Malaysia. ISO code uses LRFD methodology and its benefits are shown. Its advantages are highlighted for design of Jackets in offshore Malaysia. ISO code requires that environmental load factors should be location dependent. This code also requires that resistance and load uncertainty should be determined. Based on actual uncertainty, environmental load factors are ascertained using component, joint and system reliability. Reassessment of Jacket strength is performed using design load probability of failure with 10,000-year return period load. Probability of failure is updated using Bayesian updating technique with higher loads. The main conclusions, findings and achievements are listed in the following sections.

11.1 Uncertainty

11.1.1 (a) Resistance Uncertainty

Resistance variable played an important role for the reliability analyses specially yield strength which is shown through sensitivity analysis in Chap. 7. Although difference is very little between normal and lognormal distribution, using Anderson–Darling and Kolmogorov–Smirnov fitting tests, the best fit is taken for reliability analysis. Thus, the best fit is Gaussian distribution in all cases.

The other variables are thickness, diameter, tensile strength and elongation and their properties have been evaluated. Statistical models are developed using ISO code stress equations for component and joints resistance. The model equations are used to find the variability in types of stresses. As the basic distribution is Gaussian, the uncertainty models are also Gaussian.

Z. Nizamani, *Environmental Load Factors and System Strength Evaluation of Offshore Jacket Platforms*, Ocean Engineering & Oceanography 4,
DOI 10.1007/978-3-319-15051-2_11

11.1.2 (b) Environmental Load Uncertainty

The reliability determination requires that distribution parameters should be used for uncertain random load variables. The main focus of this research is based on extreme values, and therefore, extreme value distributions are used to fit the data. For this purpose, two types of extreme value distributions, i.e. Weibull and Gumbel are used to fit the statistical parameters for wave, wind and current. The data used here considers 10 and 100 years values. Gumbel distribution overestimated the mean value parameters of environmental load. Therefore, Weibull two parameter distribution is recommended for the reliability analysis of Jacket platforms in offshore Malaysia.

11.2 Load Factors

11.2.1 Component Reliability and Environmental Load Factor

Component reliability is found for Jacket platforms using API WSD and ISO LRFD codes. Environmental load factor for different regions are shown below:

- The platform in PMO region is in the range of 1.15–1.27.
- The platform in SBO region is in the range of 1.23–1.27.
- The platform SKO1 in SKO region is in the range of 1.15–1.26.
- The platform SKO2 in SKO region is in the range of 1.14–1.24.

The average load factor of 1.25 is recommended for Jacket platforms in offshore Malaysia based on the target reliability index of 3.96. The resistance factor is checked with proposed load factor of 1.25. It is found that there is no significant effect on resistance factor thus with new environmental load factor the current ISO 19902 resistance factors could be used.

11.2.2 Joint Reliability and Joint-based Environmental Load Factor

ISO LRFD and API LRFD recommend environmental load factors of 1.35, which is considered to be higher even by ISO itself for regions with mild climate is checked in this book for offshore Malaysia. This is due to difference in local ocean geography for each region. In most cases, this could save steel; thus, Jacket design would become economical. All three types of joints are analysed with four different types of stresses. Environmental load factor for different regions are shown below:

Environmental load factor for different regions are shown below:

- The platform in PMO region is in the range of 1.20–1.29.
- The platform in SBO region is in the range of 1.23–1.23.
- The platform SKO1 in SKO region is in the range of 1.17–1.31.
- The platform SKO2 in SKO region is in the range of 1.24–1.29.

The average load factor of 1.27 is recommended for Jacket platforms in offshore Malaysia based on the target reliability index of 3.96.

11.2.3 System-based Environmental Load Factor

System-based load factor for Jacket platform is determined using system global strength. Here, minimum RSR is used as it would give economical and safe Jacket and the Jacket will be highly utilised. Minimum RSR specified by API WSD and ISO 19902 are 1.58 and 1.85. In this book, RSR of 1.5, 2.0 and 2.5 are considered. The load factor is determined for all three regions and four Jacket platforms. For system, the target reliability index is 4.0 and 3.8 based on notional system reliability index proposed by Efthymiou as reported by BOMEL [1] and Melchers [2], respectively. The reliability index decreased with increase of W_e/G ratio. The load factors are determined for W_e/G ratio of 1.0. The load factor of 1.1 is achieved with a target reliability of 4.0. Thus, it can be set as load factor for offshore Malaysia using system reliability.

11.3 Bayesian Updating of Probability of Failure for Reassessment

The same methodology is followed here for four platforms by overloading them with wave and current loads. The load increase became significant after higher wave heights due to wave forces striking the deck of topside. With experienced resistance and load, it can be predicted how much load can be resisted by the Jacket with a minimum RSR of 1.0. It can be seen that without Bayesian updating, some Jackets would never have succeeded in getting a probability of failure below 1×10^{-4}, a major requirement for life extension and assessment qualification. Bayesian updating method made SBO and SKO1 platform probability of failure less than 1×10^{-4} which would not have been possible otherwise.

11.4 Future Work

Following are the studies which are suggested for future-related work:

11.5 Time Variant Reliability

Fatigue and corrosion are the time variant random variables. The fatigue-based limit state is not evaluated in this book and should be looked into in future works. This can be based on simulation or with available data. Fatigue crack in joint can cause local member or system failure. Fatigue becomes critical for operating conditions of environmental load. Similarly corrosion variable should also be looked into for reliability analysis of Jacket, TLP, SPAR or any other offshore structure.

11.6 Accidental Limit State

Some codes define accidental limit state. The reliability should also be evaluated for this condition. In case of accident, this limit state could play a major role in the stability of Jacket.

11.7 Operational Condition Reliability

Due to mild climate, Jacket platforms in Malaysia may be governed by operating conditions. The operating loading conditions have not been dealt with in this text, and they should be looked into in future works. This will still reduce the environmental load factor for Jacket design in offshore Malaysia for operating load conditions.

11.8 Structural Reliability of Floaters

Deep-sea platforms have now become necessity due to scarcity of hydrocarbon near continental shelf. Structural reliability analysis for floaters should be conducted for offshore Malaysia. The data from Kikeh Spar in Malaysia, with water depth of 1,300 m, can be obtained, and its reliability analysis evaluated.

11.9 Environmental Load Parameter Modelling

With more data collected on environmental load parameters and more realistic modelling of wave, wind, current and time period could be used to find accurate reliability for offshore structures in Malaysia.

11.10 Reassessment of Jacket

Vortex-induced vibrations have not been considered for loading in this text; it is an important aspect and should be checked for assessment of Jacket. Degradation of platform should also be considered in future work for reassessment of strength.

11.11 Bayesian Updating Due to Change of Conditions

Corrosion, earthquake, marine growth, boat impact and evaluation of pile strength need to be incorporated in the Bayesian updating of probability of failure.

11.12 Reliability of Offshore Mooring Foundations

Reliability analysis of offshore mooring foundations under operational and extreme environment can be determined. The local geographic environment may have significant effect on foundations.

References

1. BOMEL: System-based calibration of North West European annex environmental load factors for the ISO fixed steel offshore structures code 19902, 2003
2. Melchers, R.E.: Structural Reliability Analysis and Prediction, 2nd edn. Wiley, New York (2002)

Appendix A
Tubular Member API WSD and ISO 19902 Code Provisions

(a) Single stresses

API RP2A-WSD	ISO 19902
Axial tension $F_t = 0.6F_y$	Axial tension $\sigma_t \leq \frac{f_t}{\gamma_{R,t}},\ \gamma_{R,t} = 1.05$
Axial compression	Axial compression $\sigma_c \leq \frac{f_c}{\gamma_{R,c}},\ \gamma_{R,c} = 1.18$
Column buckling $F_a = \frac{\left[1-\frac{(Kl/r)^2}{2C_c^2}\right]F_y}{\frac{5}{3}+\frac{3\left(\frac{Kl}{r}\right)}{8C_c}-\frac{(Kl/r)^3}{8C_c^3}}$ for $\frac{Kl}{r} < C_c$ $F_a = \frac{12\pi^2 E}{23(Kl/r)^2}$ for $\frac{Kl}{r} \geq C_c$ $C_c = \left[\frac{2\pi^2 E}{F_y}\right]^{1/2}$	Column buckling $f_c = \left(1 - 0.278\lambda^2\right)f_{yc}$ for $\lambda \leq 1.34$ $f_c = \frac{0.9}{\lambda^2}f_{yc}$ for $\lambda > 1.34$ $\lambda = \sqrt{\frac{f_{yc}}{f_e}} = \frac{KL}{\pi r}\sqrt{\frac{f_{yc}}{E}}$
Local buckling $F_{xe} = 2CE\ t/D,\ C = 0.3$ $F_{xc} = F_y\left[1.64 - 0.23\left(\frac{D}{t}\right)^{\frac{1}{4}}\right] \leq F_{xe}, {}_{D}/_{t} > 60$ $F_{xe} = F_y$, for $(D/t) \leq 60$	Local buckling $F_{yc} = F_y$ for $\frac{f_y}{f_{xe}} \leq 0.170$ $f_{yc} = \left[1.047 - 0.274\frac{f_y}{f_{xe}}\right]f_y,\quad$ for $0.170 < \frac{f_y}{f_{xe}}$ $F_{xe} = 2C_x Et/D$ $C_x = 0.3$
Bending $F_b = 0.75F_y\ {}^{D}/_{t} \leq \frac{10340}{F_y}$ $F_b = \left[0.84 - 1.74\frac{F_y D}{Et}\right]F_y,\ \frac{10340}{F_y} < \frac{D}{t} \leq {}^{20680}/_{F_y}$ $F_b = \left[0.72 - 0.58\frac{F_y D}{Et}\right]F_y,\ \text{for } {}^{3000}/_{F_y} < {}^{D}/_{t} \leq 300$	Bending $\sigma_b = \frac{M}{Z_e} \leq \frac{f_b}{\gamma_{R,b}},\ \gamma_{R,b} = 1.05$ $f_b = \left(\frac{Z_P}{Z_e}\right)f_y\quad$ for $\frac{f_y D}{Et} \leq 0.0517$ $f_b = \left[1.13 - 2.58\left(\frac{f_y D}{Et}\right)\right]\left(\frac{Z_p}{Z_e}\right)f_y,\quad$ for $0.0517 < \frac{f_y D}{Et} \leq 0.1034$ $f_b = \left[0.94 - 0.76\left(\frac{f_y D}{Et}\right)\right]\left(\frac{Z_p}{Z_e}\right)f_y,\quad$ for $0.1034 < \frac{f_y D}{Et} \leq 120\frac{f_y}{E}$

Z. Nizamani, *Environmental Load Factors and System Strength Evaluation of Offshore Jacket Platforms*, Ocean Engineering & Oceanography 4,
DOI 10.1007/978-3-319-15051-2

(b) Combined stresses

API RP2A-WSD	ISO 19902
Tension and bending $\frac{f_a}{0.6F_{xc}} + \frac{\sqrt{f_{bx}^2+f_{by}^2}}{F_b} \le 1.0$	Tension and bending $\frac{\gamma_{R,t}\sigma_t}{f_t} + \frac{\gamma_{R,b}\sqrt{\sigma_{b,y}^2+\sigma_{b,Z}^2}}{f_b} \le 1.0$
Compression and bending $\frac{f_a}{F_b} + \frac{C_m\sqrt{f_{bx}^2+f_{by}^2}}{\left(1-\frac{f_a}{F_e'}\right)F_b} \le 1.0$ $\frac{f_a}{F_a} + \frac{\sqrt{\left[\frac{C_{mx}f_{bx}}{1-\frac{f_a}{F_{ex}'}}\right] + \left[\frac{C_{my}f_{by}}{1-\frac{f_a}{F_{ey}'}}\right]}}{F_b} \le 1.0$ $\frac{f_a}{0.6F_a} + \frac{\sqrt{f_{bx}^2+f_{by}^2}}{F_b} \le 1.0$	Compression and bending $\frac{\gamma_{R,c}\sigma_c}{f_c} + \frac{\gamma_{R,b}}{f_b}\left[\left(\frac{C_{m,y}\sigma_{b,y}}{1-\sigma_c/f_{e,y}}\right)^2 + \left(\frac{C_{m,z}\sigma_{b,z}}{1-\sigma_c/f_{e,z}}\right)^2\right]^{0.5} \le 1.0$ $\frac{\gamma_{R,c}\sigma_c}{f_{yc}} + \frac{\gamma_{R,b}\sqrt{\sigma_{b,y}^2+\sigma_{b,z}^2}}{f_b} \le 1.0$ $f_{e,y} = \frac{\pi^2 E}{(K_y L_y/r)^2}$ $f_{e,z} = \frac{\pi^2 E}{(K_z L_z/r)^2}$
Hydrostatic pressure (hoop buckling) $f_h \le F_{hc}/SF_{hc}$	Hydrostatic pressure (hoop buckling) $\sigma_h = \frac{pD}{2t} \le \frac{f_h}{\gamma_{R,h}},\ \sigma_h = 1.25$
Critical hoop buckling stress $F_{hc} = F_{he},\ F_{he} \le 0.55F_y$ $F_{hc} = 0.45F_y + 0.18F_{he}, 0.55 < F_{he} \le 1.6F_y$ $F_{hc} = \frac{1.31F_y}{1.15 + (F_y/F_{hc})} 1.6F_y < F_{he} < 6.2F_y$ $F_{hc} = F_y, F_{he} > 6.2F_y$	$f_h = f_y$ for $f_{he} > 2.44f_y$ $f_h = 0.7\left(f_{he}/f_y\right)^{0.4} f_y \le f_y$ for $0.55f_y < f_{he} \le 2.44f_y$ $f_h = f_{he}$ for $f_{he} \le 0.55f_y$
Elastic hoop buckling stress $F_{he} = 2C_hEt/D$ $C_h = 0.44t/D$ $C_h = 0.44(t/D) + \frac{0.21\left(\frac{D}{t}\right)^3}{M^4}, 0.825\frac{D}{t} \le M < \frac{1.6D}{t}$ $C_h = 0.736/(M-0.636), 3.5 \le M < 0.825D/t$ $C_h = 0.755(M-0.559), 1.5 \le M < 3.5$ $C_h = 0.8 \quad M < 1.5$ $M = \frac{L}{D}(2D/t)^{1/2}$	$f_{he} = 2C_hEt/D, C_h = \frac{0.44t}{D}$ for $\mu \ge 1.6D/t$ $C_h = 0.44t/D + 0.21\left(D/t\right)^3 \mu^4$ for $0.825D/t \le \mu < 1.6D/t$ $C_h = 0.737/(\mu - 0.579)$ for $1.5 \le \mu < 0.825D/t$ $C_h = 0.80$ for $\mu < 1.5$ $\mu = \frac{L_r}{D}\sqrt{\frac{2D}{t}}$

Appendix B
Tubular Joints API WSD and ISO 19902 Code Provisions

(a) ISO 19902 Code Provisions

Axial tension	Axial compression	In-plane bending	Out-plane bending
K-joint			
$(1.9+19\beta)Q_\beta^{0.5}Q_g$	$(1.9+19\beta)Q_\beta^{0.5}Q_g$	$4.5\beta\gamma^{0.5}$	$3.2\gamma^{(0.5\beta^2)}$
T/Y joint			
30β	$(1.9+19\beta)Q_\beta^{0.5}$	$4.5\beta\gamma^{0.5}$	$3.2\gamma^{(0.5\beta^2)}$
X-joint			
23β for $\beta \le 0.9$ $20.7+(\beta-0.9)(17\gamma-220)$ for $\beta > 0.9$	$\left[2.8+(12+0.1\gamma)\beta\right]Q_\beta$	$4.5\beta\gamma^{0.5}$	$3.2\gamma^{(0.5\beta^2)}$

Q_β = Geometrical factor	Q_g = Gap factor
$Q_\beta = \frac{0.3}{\beta(1-0.833\beta)}$ for $\beta > 0.6$ $Q_\beta = 1.0$ for $\beta \le 0.6$	$Q_g = 1.9-0.7\gamma^{-0.5}\left(g/T\right)^{0.5}$ for $\left(g/T\right) \ge 2.0$ but $Q_g \ge 1.0$ $Q_g = 0.13+0.65\emptyset\gamma^{0.5}\left(g/T\right)^{0.5}$ for $\left(g/T\right) \le -2.0$ $\emptyset = \frac{t*f_{yb}}{(T*f_y)}$

$$Q_f = 1-\lambda q_A^2$$

where $\lambda = 0.03$ (brace axial force), 0.045 (brace IPB), 0.021 (brace OPB)

$$q_A = \left[C_1\left(\frac{P_c}{P_y}\right)^2 + C_2\left(\frac{M_c}{M_p}\right)^2_{ipb} + C_2\left(\frac{M_c}{M_p}\right)^2_{opb}\right]^{0.5}\gamma_{Rq}$$

Z. Nizamani, *Environmental Load Factors and System Strength Evaluation of Offshore Jacket Platforms*, Ocean Engineering & Oceanography 4,
DOI 10.1007/978-3-319-15051-2

Table: coefficients C_1 and C_2

Joint type	C_1	C_2
Y-joint	25	11
X-joint	20	22
K-joint	14	43

(b) API WSD Code Provisions

Axial tension	Axial compression	In-plane bending	Out-plane bending
K-joint			
$(16+1.2\gamma)\beta^{1.2}Q_g$ but $\leq 40\,\beta^{1.2}Q_g$	$(16+1.2\gamma)\beta^{1.2}Q_g$ but $\leq 40\,\beta^{1.2}Q_g$	$(5+0.7\gamma)\beta^{1.2}$	$2.5+(4.5+0.2\gamma)\beta^{2.6}$
T/Y joint			
30β	$2.8+(20+0.8\gamma)\beta^{1.6}$ but $\leq 2.8+36\,\beta^{1.6}$	$(5+0.7\gamma)\beta^{1.2}$	$2.5+(4.5+0.2\gamma)\beta^{2.6}$
X-joint			
23β for $\beta \leq 0.9$ $20.7+(\beta-0.9)(17\gamma-220)$ for $\beta > 0.9$	$[2.8+(12+0.1\gamma)\beta]Q_\beta$	$(5+0.7\gamma)\beta^{1.2}$	$2.5+(4.5+0.2\gamma)\beta^{2.6}$

Q_β = Geometrical factor	Q_g = Gap factor
$Q_\beta = 1.0$ for $\beta \leq 0.6$ $Q_\beta = \frac{0.3}{\beta(1-0.833\beta)}$ for $\beta > 0.6$	$Q_g = 1+0.2\left[1-2.8g/D\right]^3$ for $g/D \geq 0.05$ but ≥ 1.0 $Q_g = 0.13+0.65\emptyset\gamma^{0.5}\left(g/T\right)^{0.5}$ for $\left(g/T\right) \leq -2.0$ $\emptyset = \frac{t*f_{yb}}{(T*f_y)}$

$$Q_f = \left[1 + C_1\left(\frac{FSP_c}{P_y}\right) - C_2\left(\frac{FSM_{ipb}}{M_p}\right) - C_3A^2\right]$$

$$A = \left[\left(\frac{FSP_c}{P_y}\right)^2 + \left(\frac{FSM_c}{M_p}\right)^2\right]^{0.5},\ \text{FS} = 1.2$$

Table: coefficients C_1, C_2 and C_3

Joint type	C_1	C_2	C_3
K-joint	0.2	0.2	0.3
T/Y-joint	0.3	0	0.8
X-joint			
$\beta \leq 0.9$	0.2	0	0.5
$\beta = 1.0$	–0.2	0	0.2

Appendix C
MATLAB Programing

This MATLAB code is based on FERUM an open source code developed by University of California, Berkeley.

Matlab Programme for Determining the Variability of Compression Resistance for Column Buckling Case

```
function ComRes2
disp('This program determines stastical parameters of the Compression Resistance for column Buckling')
disp('The assumptions are: Fy - Lognormal, D and T are both Normal Distributed')
Nsim = input('Number if Simulation = ');
Fyn = input('Nominal Fy = ');%Nominal Yield Strength
Tn = input('Nominal T = ');% Nominal Thickness of component
Dn = input('Nominal D = ');% Nominal Diameter of component
En = 210000;% Nominal Elastic Modulus
Kn = 1.0; % Nominal Effective Length Factor
Ln = input('Nominal L = ');
An = (pi()./4).*(Dn.^2 - (Dn-2.*Tn).^2); % Nominal Area
In = (pi()./64).*(Dn.^4 - (Dn-2.*Tn).^4); % Nominal Moment of Inertia
rn = sqrt(In./An);
Slrn = (Kn.*Ln./(pi.*rn)).*sqrt(Fyn./En);
if Slrn <= 1.34 %#ok<BDSCI>
   Fcn = (1-0.278.*Slrn.^2).*Fyn;
else % Slri >1.34 %#ok<BDSCI>
   Fcn = (0.9./Slrn.^2).*Fyn;
end
Rn = Fcn*An/1000; % Nominal Resistance
```


Z. Nizamani, *Environmental Load Factors and System Strength Evaluation of Offshore Jacket Platforms*, Ocean Engineering & Oceanography 4,
DOI 10.1007/978-3-319-15051-2

```
%3.3.1 Effective length factor Statistical Parameters (mu = Mean, std = Stand Devi.) : Normally Distributed
Kmu = 0.875;
Ksd = 0.097;
%3.3.2 Unbraced length Statistical Parameters (mu = Mean, std = Stand Devi.) : Normally Distributed
Lmu = 1;
Lsd = 0.0025;
%3.3.3 Young's Modulus Statistical Parameters (mu = Mean, std = Stand Devi.) : Normally Distributed
Emu = 1;
Esd = 0.05;
%3.1 Diameter Statistical Parameters (mu = Mean, std = Stand Devi.): Normally Distributed
Dmu = 0.99932;
Dsd = 0.00182;
%3.2 Thickness Statistical Parameters (mu = Mean, std = Stand Devi.): Normally Distributed
Tmu = 1.0242;
Tsd = 0.01616;
%3.3 Yield Strength Statistical Parameters (mu = Mean, std = Stand Devi.): Log Normally Distributed
Fymu = 1.2336;
Fysd = 0.04502;
Fyi = Fyn*normrnd(Fymu,Fysd,Nsim,1);% Random Yield Strength
Ti = Tn*normrnd(Tmu,Tsd,Nsim,1);% Random Thickness
Di = Dn*normrnd(Dmu,Dsd,Nsim,1);% Random Diameter
Li = Ln*normrnd(Lmu,Lsd,Nsim,1);% Random Length
Ki = Kn*normrnd(Kmu,Ksd,Nsim,1); % Random Effective Length Factor
Ei = En*normrnd(Emu,Esd,Nsim,1);% Random Elastic modulus
Ai = (pi()./4).*(Di.^2 - (Di-2.*Ti).^2); % Random Area
Ii = (pi()./64).*(Di.^4 - (Di-2.*Ti).^4); % Random Moment of Inertia
ri = sqrt(Ii./Ai);
Slri = (Ki.*Li./(pi.*ri)).*sqrt(Fyi./Ei);
if Slri <= 1.34 %#ok<BDSCI>
   Fcni = (1-0.278.*Slri.^2).*Fyi;
else % Slri >1.34 %#ok<BDSCI>
   Fcni = (0.9./Slri.^2).*Fyi;
end
Ri = Fcni.*Ai./1000;% Random Resistance
BiasRi = Ri/Rn;
%disp('Resistance Bias');
%disp([Ri BiasRi]);
ToExcel = [Ri BiasRi];
save ComRes.xls ToExcel -ascii
```

Matlab Programme for Determining the Variability of Compression Resistance for Local Buckling Case

```
function ComRes3
disp('This program determines stastical parameters of the Compression Resistance
Local Buckling')
disp('The assumptions are: Fy - Lognormal, D and T are both Normal Distributed')
Nsim = input('Number if Simulation = ');
Fyn = input('Nominal Fy = ');%Nominal Yield Strength
Tn = input('Nominal T = ');% Nominal Thickness of component
Dn = input('Nominal D = ');% Nominal Diameter of component
En = 210000;% Nominal Elastic Modulus
An = (pi()./4).*(Dn.^2 - (Dn-2.*Tn).^2);% Nominal Area
C = 0.3;% Nominal elastic critical buckling coefficient
Fxen = 2*C.*En.*Tn./Dn;
if Fyn./Fxen <= 0.170; %#ok<BDSCA>
   Fycn = Fyn;
Else
   Fycn = (1.047-0.274.*(Fyn./Fxen)).*Fyn;
end
Rn = Fycn.*An/1000;
%3.3.3 Young's Modulus Statistical Parameters (mu = Mean, std = Stand Devi.) :
Normally Distributed
Emu = 1;
Esd = 0.05;
%3.1 Diameter Statistical Parameters (mu = Mean, std = Stand Devi.): Normally
Distributed
Dmu = 0.99932;
Dsd = 0.00182;
%3.2 Thickness Statistical Parameters (mu = Mean, std = Stand Devi.): Normally
Distributed
Tmu = 1.0242;
Tsd = 0.01616;
%3.3 Yield Strength Statistical Parameters (mu = Mean, std = Stand Devi.): Log
Normally Distributed
Fymu = 1.2336;
Fysd = 0.04502;
Fyi = Fyn*normrnd(Fymu,Fysd,Nsim,1);% Random Yield Strength
Ti = Tn*normrnd(Tmu,Tsd,Nsim,1);% Random Thickness
Di = Dn*normrnd(Dmu,Dsd,Nsim,1);% Random Diameter
Ei = En*normrnd(Emu,Esd,Nsim,1);% Random Elastic modulus
Ai = (pi()./4).*(Di.^2 - (Di-2.*Ti).^2);% Random Area
C = 0.3;% Nominal elastic critical buckling coefficient
Fxei = 2*C.*Ei.*Ti./Di;
```

```
if Fyi./Fxei <= 0.170 %#ok<BDSCA>
   Fyci = Fyi;
else % Fyi./Fxei > 0.170 %#ok<BDSCA>
   Fyci = (1.047-0.274.*(Fyi./Fxei)).*Fyi;
end
Ri = Fyci.*Ai/1000;% Random Resistance
BiasRi = Ri/Rn;
%disp('Resistance Bias');
%disp([Ri BiasRi]);
ToExcel = [Ri BiasRi];
save ComRes.xls ToExcel -ascii
```

Matlab Program for Component Reliability for Tensiot Stress Limit State Function

```
function g = gfun_t(Fy,D,T,Hs,Vc,Xw,Dd,Lv,Xm)
%% This function defines the Limit State Function of Simple Tensile Strength
% as per ISO / API RP2A WSD (21st (2008) Ed
%DATA FIELDS IN 'ENVIRONMENTAL LOAD'
% Environmental Loads - Surface Response Method used to obtain the following
% Given as the Output load from SACS on a Particular member!
%DATA FIELDS IN 'REPRESENTATIVE TENSILE STRENGHT'
A = (pi()./4).*(D.^2 - (D-2.*T).^2);% Random area
Resistance = Fy.*A.*Xm;
%This functions is intented to evaluate the nominal resistance of typical
%joint using it's nominal geometrical and material properties
% No factor is included.
Fyn = 345; % Nominal Yield Strength
Dn = 508; % Nominal Diameter
Tn = 9.5;% Nominal Thickness
An = (pi()/4)*(Dn^2-(Dn-2*Tn)^2); % Nominal area
ResISO = Fyn.*An; %ISO Resistance Nominal
ResWSD = (0.6.*Fyn).*An; % API WSD Resistance Nominal
% Environmnetal Load Action Eveluation
Hmx = 2.00.*Hs;% Maximum height
Wn = 0.01515.*Hmx.^2-0.2782.*Hmx+0.7592.*Vc.^2-1.673.*Vc+3.741;% Envi-
ronmental Load Model
% Applied loads on the Joints[Through the BRACE]
% Lr = (0.45.*Dd+0.45.*Lv+0.09.*Wn./Xw);
% Lr = (0.40.*Dd+0.40.*Lv+0.20.*Wn./Xw);
% Lr = (0.33.*Dd+0.33.*Lv+0.33.*Wn./Xw);
Lr = (0.25.*Dd+0.25.*Lv+0.50.*Wn./Xw); % Load Ratios
% Lr = (0.14.*Dd+0.14.*Lv+0.72.*Wn./Xw);
```

```
% Lr = (0.08.*Dd+0.08.*Lv+0.84.*Wn./Xw);
% Lr = (0.05.*Dd+0.05.*Lv+0.90.*Wn./Xw);
% Lr = (0.02.*Dd+0.02.*Lv+0.96.*Wn./Xw);
% Lr = (0.01.*Dd+0.01.*Lv+0.98.*Wn./Xw);
% FS = 4/(3*1.67); % not used
FS = 1.333; %Used Factor of safety for API WSD
Load = Lr.*ResWSD.*FS; %Axial Load [API WSD]
% FS = (0.9524.*(Dd+Lv+Wn./Xw))./(1.1.*Dd+1.1.*Lv+1.40.*Wn./Xw); % Factor
% of safety for ISO 19902
% Load = Lr.*ResISO.*FS; %Axial Load [ISO 19902]
%Limit State Function
g = Resistance -Load;
```

Input File for Tension Reliability

```
%DATA FIELDS IN 'PROBDATA'
% Names of random variables. Default names are 'x1', 'x2', …, if not explicitely
defined.
% probdata.name = { 'name1' 'name2' … } or { 'name1' 'name2' … }'
%>>> Tubular Joint Input Variables <<<<
probdata.name = { 'Fy'
'D'
'T'
'Hs'
'Vc'
'Xw'
'Dd'
'Lv'
'Xm'};

% Marginal distributions for each random variable
% probdata.marg = [ (type) (mean) (stdv) (startpoint) (p1) (p2) (p3) (p4) (input_
type); … ];
probdata.marg = [ 1 424.350 17.250 345.000 nan nan nan nan 0 ;
1 508.000 0.914 508.000 nan nan nan nan 0 ;
1 9.728 0.152 9.500 nan nan nan nan 0 ;
16 4.220 0.570 4.220 nan nan nan nan 0 ;
16 0.790 0.150 0.790 nan nan nan nan 0 ;
1 1.000 0.150 1.000 nan nan nan nan 0 ;
1 1.000 0.060 1.000 nan nan nan nan 0 ;
1 1.000 0.100 1.000 nan nan nan nan 0 ;
1 1.260 0.050 1.260 nan nan nan nan 0 ;];
% Correlation matrix
```

```
probdata.correlation = eye(9); %Non-Correlated variables, function eye(n) displays the identitiy matrix
probdata.transf_type = 3;%Natal Joint Distribution - Transformation matrix
probdata.Ro_method = 1;%Method for computation of Nataf Corr Matrix - Solved numerically
probdata.flag_sens = 1;%Computation of sensitivities w.r.t - all sensitivities assessed
analysisopt.multi_proc = 1; % 1: block_size g-calls sent simultaneously
% - gfunbasic.m is used and a vectorized version of gfundata.expression is available.
% The number of g-calls sent simultaneously (block_size) depends on the memory
% available on the computer running FERUM.
% - gfunxxx.m user-specific g-function is used and able to handle block_size computations
% sent simultaneously, on a cluster of PCs or any other multiprocessor computer platform.
% 0: g-calls sent sequentially
analysisopt.block_size = 100; % Number of g-calls to be sent simultaneously
% FORM analysis options
analysisopt.i_max = 1000; % Maximum number of iterations allowed in the search algorithm
analysisopt.e1 = 1e-5; % Tolerance on how close design point is to limit-state surface
analysisopt.e2 = 1e-5; % Tolerance on how accurately the gradient points towards the origin
analysisopt.step_code = 0; % 0: step size by Armijo rule, otherwise: given value is the step size
analysisopt.Recorded_u = 1; % 0: u-vector not recorded at all iterations, 1: u-vector recorded at all iterations
analysisopt.Recorded_x = 1; % 0: x-vector not recorded at all iterations, 1: x-vector recorded at all iterations
% FORM, SORM analysis options
analysisopt.grad_flag = 'ffd'; % 'ddm': direct differentiation, 'ffd': forward finite difference
analysisopt.ffdpara = 1000; % Parameter for
1000 for basic limit-state functions, 50 for FE-based limit-state functions
analysisopt.ffdpara_thetag = 1000; % Parameter for
% Simulation analysis (MC,IS,DS,SS) and distribution analysis options
analysisopt.num_sim = 100000; % Number of samples (MC,IS), number of samples per subset step (SS) or number of directions (DS)
analysisopt.rand_generator = 1; % 0: default rand matlab function, 1: Mersenne Twister (to be preferred)
% Simulation analysis (MC, IS) and distribution analysis options
analysisopt.sim_point = 'origin'; % 'dspt': design point, 'origin': origin in standard normal space (simulation analysis)
```

```
analysisopt.stdv_sim = 1; % Standard deviation of sampling distribution in simulation analysis
% Simulation analysis (MC, IS)
analysisopt.target_cov = 0.05; % Target coefficient of variation for failure probability
analysisopt.lowRAM = 0; % 1: memory savings allowed, 0: no memory savings allowed
gfundata(1).evaluator = 'basic';
gfundata(1).type = 'expression'; % Do no change this field!
% Expression of the limit-state function:
gfundata(1).expression = 'gfun_t(Fy,D,T,Hs,Vc,Xw,Dd,Lv,Xm)';
gfundata(1).flag_sens = 0;
femodel = [];
randomfield = [];
```

Matlab Program for Joint Reliability for Tension Stress Limit State Function for T/Y Joint

```
function g = gfun_tt(Fy,Dcd,Tcd,Dbc,Tbc,Agl,Hs,Vc,Xw,Dd,Lv,Xm)
%% This function defines the Limit State Function of Simple Tubular Joint
% as per ISO
% DATA FIELDS IN 'ENVIRONMENTAL LOAD'
% Environmental Loads - Surface Response Method used to obtain the following
% Given as the Output load from SACS on a Particular Joints!
% DATA FIELDS IN 'GEOMETRIC PROPERTIES'
% Evaluation Geometric Propoerties of the Joint
% BRACE to CHORD Variation[0.2 to 1.0]
bta = Dbc./Dcd; %BRACE to CHORD Diameter Ratio

% Parametric Studies Considering "bta" as a Variable
% bta = 0.2;
% bta = 0.3;
% bta = 0.4;
% bta = 0.5;
% bta = 0.6;
% bta = 0.7;
% bta = 0.8;
% bta = 0.9;
% bta = 1.0;
% CHORD Gemometric ratio Variation[10 to 50]
%gma = Dcd./(2*Tcd);%CHORD Gemometric ratio
% Parametric Studies Considering "gma" as a Variable
% gma = 10;
% gma = 15;
```

```
% gma = 20;
% gma = 25;
% gma = 30;
% gma = 35;
% gma = 40;
%gma = 45;
% gma = 50;
% Evaluation of Stength Factor: Qu for K-Joint in In-Plane Bending Qu
%if bta>0.6 %#ok<BDSCI>
%Qbta = 0.3./(bta.*(1-0.833.*bta));
%else
%Qbta = 1.0;
%end
%GAP FACTOR
%ISO K-Joint Gap Factor and QuISO
%gap = 50; % Joint Gap - Gap between BRACEs connecting into the joint
%if gap./Tcd >= 2.0; %#ok<BDSCA>
%Qg = 1.9-0.7.*(gma.^-0.5).*(gap./Tcd).^0.5;
% if Qg <= 1.0;
% Qg = 1.0;
%end
%elseif gap./Tcd <= -2.0; %#ok<BDSCA>
% fyb = Fy;
% phi = (Tbc.*fyb)./(Tcd.*Fy);
% Qg = 0.13 + 0.65.*phi.*gma.^0.5;
%else %-2.0<Rat < 2.0; %Interpolation between the above values
%Qg1 = 1.9-0.7.*(gma.^(-0.5))*(2).^0.5;
%fyb = Fy;
% phi = (Tbc.*fyb)./(Tcd.*Fy);
% Qg2 = 0.13+0.65.*phi.*(gma.^0.5);
% Qg = Qg1+(Qg2-Qg1).*(gap./Tcd-2)./(-4);
%end
%Qu = (1.9+19.*bta).*Qg.*Qbta.^0.5;
Qu = 30.*bta;
% Qf Values
% Parametric Studies Considering "Qf" as a Variable
% Qf = 0.1;
% Qf = 0.2;
% Qf = 0.3;
% Qf = 0.4;
% Qf = 0.5;
% Qf = 0.6;
% Qf = 0.7;
% Qf = 0.8;
% Qf = 0.9;
% Qf = 1.0;
```

```
% DATA FIELDS IN 'REPRESENTATIVE STRENGHT FOR SIMPLE JOINT'
%Represenatative Strength of Simple Tubular Joint[Qf = 1.00, ISO factor = 1.00]
Resistance = Fy.*(Tcd.^2).*Qu./sind(Agl).*Xm; %Axial Resistance
%DATA FIELDS IN 'NOMINAL STRENGHT FOR SIMPLE JOINT for UC = 1'
%This functions is intented to evaluate the nominal resistance of typical
%joint using it's nominal geometrical and material properties
% No factor is included.
Fyn = 306;
Dcdn = 1200;
Tcdn = 40;
Dbcn = 711;
% Tbcn = 15;
Agln = 90.00;
beta = Dbcn./Dcdn; %BRACE to CHORD Diameter Ratio
% beta = bta; % BRACE to CHORD Variation[0.2 to 1.0]
gama = Dcdn./(2*Tcdn);%CHORD Gemometric ratio
%gama = gma; % CHORD Gemometric ratio Variation[10 to 50]
% Evaluation of Stength Factor: Qu for K-Joint in Axial Compression Qu
%if beta>0.6 %#ok<BDSCI>
% Qbeta = 0.3./(beta.*(1-0.833.*beta));
%else
%Qbeta = 1.0;
%end

%GAP FACTOR
%ISO K-Joint Gap Factor and QuISO
%gap = 50; % Joint Gap - Gap between BRACEs connecting into the joint
%if gap./Tcdn >= 2.0; %#ok<BDSCA>
% QgISO = 1.9-0.7.*(gama.^-0.5).*(gap./Tcdn).^0.5;
% if QgISO <= 1.0;
% QgISO = 1.0;
% end
%elseif gap./Tcd <= -2.0; %#ok<BDSCA>
%fyb = Fyn;
%phi = (Tbcn.*fyb)./(Tcdn.*Fyn);
% QgISO = 0.13 + 0.65.*phi.*gama.^0.5;
%else %-2.0<Rat< 2.0; %Interpolation between the above values
% QgISO1 = 1.9-0.7.*(gama.^(-0.5))*(2).^0.5;
% fyb = Fyn;
% phi = (Tbcn.*fyb)./(Tcdn.*Fyn);
% QgISO2 = 0.13+0.65.*phi.*(gama.^0.5);
% QgISO = QgISO1+(QgISO2-QgISO1).*(gap./Tcdn-2)./(-4);
%end
%QuISO = (1.9+19.*beta).*QgISO.*Qbeta.^0.5;
%ResISO = (Fyn*(Tcdn^2)*QuISO/sind(Agln));
QuISO = 30.*beta;
```

```
ResISO = Fyn.*(Tcdn.^2).*QuISO./sind(Agln);
%WSD K- Joint Gap Factor and QuWSD
%if gap./Dcdn >= 0.05; %#ok<BDSCA>
% QgWSD = 1+0.2.*(1-2.8.*gap./Dcdn).^3;
% if QgWSD <= 1.0;
% QgWSD = 1.0;
%end
%elseif gap./Dcdn <= -0.05; %#ok<BDSCA>
% fyb = Fyn;
% phi = (Tbcn.*fyb)/(Tcdn.*Fyn);
% QgWSD = 0.13 + 0.65.*phi.*gama.^0.5;
%else %-2.0<Rat< 2.0; %Interpolation between the above values
%QgWSD1 = 1+0.2.*(1-2.8.*gap./Dcdn).^3;
% fyb = Fyn;
% phi = (Tbcn.*fyb)./(Tcdn.*Fyn);
% QgWSD2 = 0.13+0.65.*phi.*(gama.^0.5);
% QgWSD = QgWSD1+(QgWSD2-QgWSD1).*(gap./Tcdn-2)./(-4);
%end
%QuWSD = (16+1.2.*gama).*QgWSD.*beta.^1.2;
%ResWSD = (Fyn*(Tcdn^2)*QuWSD/sind(Agln)); % WSD
QuWSD = 30.*beta;
ResWSD = Fyn.*(Tcdn.^2).*QuWSD./sind(Agln);
% DATA FIELDS IN 'LOAD ACTIONS'
% Environmnetal Load Action Eveluation
Hmx = 1.80.*Hs;
Wn = 0.006709.*Hmx.^2+0.03511.*Hmx-0.1821.*Vc.^2+0.5931.*Vc-0.1821;
% Applied loads on the Joints[Through the BRACE]
% Lr = (0.45.*Dd+0.45.*Lv+0.09.*Wn./Xw);
% Lr = (0.40.*Dd+0.40.*Lv+0.20.*Wn./Xw);
% Lr = (0.33.*Dd+0.33.*Lv+0.33.*Wn./Xw);
Lr = (0.25.*Dd+0.25.*Lv+0.50.*Wn./Xw);
% Lr = (0.14.*Dd+0.14.*Lv+0.72.*Wn./Xw);
% Lr = (0.08.*Dd+0.08.*Lv+0.84.*Wn./Xw);
% Lr = (0.05.*Dd+0.05.*Lv+0.90.*Wn./Xw);
% Lr = (0.02.*Dd+0.02.*Lv+0.96.*Wn./Xw);
% Lr = (0.01.*Dd+0.01.*Lv+0.98.*Wn./Xw);
% FS = 4/(3*1.67);
% Load = Lr.*ResWSD.*FS; %Axial Load [WSD]
FS = (0.95.*(Dd+Lv+Wn./Xw))./(1.1.*Dd+1.1.*Lv+1.40.*Wn./Xw);
Load = Lr.*ResISO.*FS; %Axial Load [ISO]

% DATA FIELDS IN 'lIMIT STATE FUCTION'(gfun)
%Limit State Function
g = Resistance -Load;
```

Input File for Tension Stress Joint Reliability for T/Y Joint

```
% DATA FIELDS IN 'PROBDATA'
% Names of random variables. Default names are 'x1', 'x2', , if not explicitely
  defined.
% probdata.name = { 'name1' 'name2' … } or { 'name1' 'name2' … }'
%>>> Tubular Joint Input Variables <<<<
probdata.name = { 'Fy'
'Dcd'
'Tcd'
'Dbc'
'Tbc'
'Agl'
'Hs'
'Vc'
'Xw'
'Dd'
'Lv'
'Xm'};
% Marginal distributions for each random variable
% probdata.marg = [ (type) (mean) (stdv) (startpoint) (p1) (p2) (p3) (p4) (input_
type); … ];
probdata.marg = [ 1 376.380 15.30 306.00 nan nan nan nan 0 ;
  1 1201.20 1.68 1200.0 nan nan nan nan 0 ;
1 40.960 0.640 40.0 nan nan nan nan 0 ;
1 711.0 1.280 711.0 nan nan nan nan 0 ;
1 15.36 0.240 15.00 nan nan nan nan 0 ;
1 90.0 0.253 90.0 nan nan nan nan 0 ;
16 3.030 0.620 3.030 nan nan nan nan 0 ;
16 0.56 0.170 0.560 nan nan nan nan 0 ;
1 1.000 0.150 1.000 nan nan nan nan 0 ;
1 1.000 0.060 1.000 nan nan nan nan 0 ;
1 1.000 0.100 1.000 nan nan nan nan 0 ;
1 1.300 0.100 1.300 nan nan nan nan 0 ;];
% Correlation matrix
probdata.correlation = eye(12); %Non-Correlated variables, function eye(n) dis-
  plays the identitiy matrix
probdata.transf_type = 3;%Natal Joint Distribution - Transformation matrix
probdata.Ro_method = 1;%Method for computation of Nataf Corr Matrix -
  Solved numerically
probdata.flag_sens = 1;%Computation of sensitivities w.r.t - all sensitivities
  assessed
% DATA FIELDS IN 'ANALYSISOPT' %
analysisopt.multi_proc = 1; % 1: block_size g-calls sent simultaneously
```

```
% - gfunbasic.m is used and a vectorized version of gfundata.expression is available.
% The number of g-calls sent simultaneously (block_size) depends on the memory
% available on the computer running FERUM.
% - gfunxxx.m user-specific g-function is used and able to handle block_size computations
% sent simultaneously, on a cluster of PCs or any other multiprocessor computer platform.
% 0: g-calls sent sequentially
analysisopt.block_size = 100; % Number of g-calls to be sent simultaneously
% FORM analysis options
analysisopt.i_max = 1000; % Maximum number of iterations allowed in the search algorithm
analysisopt.e1 = 1e-5; % Tolerance on how close design point is to limit-state surface
analysisopt.e2 = 1e-5; % Tolerance on how accurately the gradient points towards the origin
analysisopt.step_code = 0; % 0: step size by Armijo rule, otherwise: given value is the step size
analysisopt.Recorded_u = 1; % 0: u-vector not recorded at all iterations, 1: u-vector recorded at all iterations
analysisopt.Recorded_x = 1; % 0: x-vector not recorded at all iterations, 1: x-vector recorded at all iterations
% FORM, SORM analysis options
analysisopt.grad_flag = 'ffd'; % 'ddm': direct differentiation, 'ffd': forward finite difference
analysisopt.ffdpara = 1000; % Parameter for computation of FFD estimates of gradients - Perturbation = stdv/analysisopt.ffdpara;
% Recommended values: 1000 for basic limit-state functions, 50 for FE-based limit-state functions
analysisopt.ffdpara_thetag = 1000; % Parameter for computation of FFD estimates of dbeta_dthetag
% perturbation = thetag/analysisopt.ffdpara_thetag if thetag ~= 0 or 1/analysisopt
.ffdpara_thetag if thetag == 0;
% Recommended values: 1000 for basic limit-state functions, 100 for FE-based limit-state functions
% Simulation analysis (MC,IS,DS,SS) and distribution analysis options
analysisopt.num_sim = 100000; % Number of samples (MC,IS), number of samples per subset step (SS) or number of directions (DS)
analysisopt.rand_generator = 1; % 0: default rand matlab function, 1: Mersenne Twister (to be preferred)
% Simulation analysis (MC, IS) and distribution analysis options
analysisopt.sim_point = 'origin'; % 'dspt': design point, 'origin': origin in standard normal space (simulation analysis)
analysisopt.stdv_sim = 1; % Standard deviation of sampling distribution in simulation analysis
% Simulation analysis (MC, IS)
```

```
analysisopt.target_cov = 0.05; % Target coefficient of variation for failure probability
analysisopt.lowRAM = 0; % 1: memory savings allowed, 0: no memory savings allowed

%%data fields in 'gfundata' (one structure per gfun)
% Type of limit-state function evaluator:
% 'basic': the limit-state function is defined by means of an analytical expression or a Matlab m-function,
% using gfundata(lsf).expression. The function gfun.m calls gfunbasic.m, which evaluates gfundata(lsf).expression.
% 'xxx': the limit-state function evaluation requires a call to an external code. The function gfun.m calls gfunxxx.m,
% which evaluates gfundata(lsf).expression where gext variable is a result of the external code.
gfundata(1).evaluator = 'basic';
gfundata(1).type = 'expression'; % Do no change this field!
% Expression of the limit-state function:
gfundata(1).expression = 'gfun_tt(Fy,Dcd,Tcd,Dbc,Tbc,Agl,Hs,Vc,Xw,Dd,Lv,Xm)';
% Flag for computation of sensitivities w.r.t. thetag parameters of the limit-state function
% 1: all sensitivities assessed, 0: no sensitivities assessment
gfundata(1).flag_sens = 0;
%data fields in 'femodel' %
femodel = [];
% data fields in 'randomfield'
randomfield = [];
```

System Reliability

```
function g = gfun_SYSAbu(Xw,Hs,Dd,Lv,Xm)
%This function defines the Limit State Function of system reliability in
%E11R-C
% uncertain load
Hmx = 2.0.*Hs;
Wn = 0.03.*(Hmx+2.7*0.68).^2.1; % Load Model
Sn = 2.0.*(0.03.*Dd+0.02.*Lv+0.95.*(Wn./Xw)); % Load
%Uncertain Resistance of component evaluated using ISO, without partial factors
% Axial Compression
Rn = (0.03.*(10.8+2.7*0.68).^2.1).*1.65.*1.44.*1.52.*Xm; % Resistance
g = Rn - Sn;
end
```

Updating the Probability of Failure Using System Reliability

```
function Abu_3ua
clear all
clc
%disp('This program determines the probability of failure of system RSR');
disp('The input data comprises of, RSR,')
%1.0 Input of Nominal/Design basic Variables
%Nrun = input('Number of Runs = ');
Nsim = 1e7;
%Nsim = input('Number of Simulations = ');
%RSR = input('RSR values = ');
RSR = 1.5;
Hd = 10.80; % Design wave
c1 = 0.03237; % load coefficient
c2 = 2.7;
c3 = 2.1;
%Ho = 0.00;
% Hc = 4.46; % Scale parameter
% r = 8.83; % Shape parameter
% N = 5e6;
% F = rand(Nsim,1);
% D = (1-F.^(1/N));
% A = (-1.*(log(D))).^(1./r);
% Acmu = 1.96; % Convertion factor for Hmax given the Hs.[Hmax = A*Hs]
% Acsd = 0.05;
% Aci = normrnd(Acmu,Acsd,Nsim,1);% Convertion Factor Values
% H = 1.96.*(Ho+((Hc-Ho).*A))
% Hs_values = wblrnd(Hc,r,Nsim,1);
% Hmx = 2.0.*Hs_values;
% (mu = Mean, std = Stand Devi.): Normally Distributed
Bmu = 1.000;
Bsd = 0.1;
%2 Statistical Parameters (mu = Mean, std = Stand Devi.): Normally Distributed
amu = 1.000;
asd = 0.15;
% resistance uncertainty model
Bi = normrnd(Bmu,Bsd,Nsim,1);
% Load uncertainty model
Ai = normrnd(amu,asd,Nsim,1);
% Resistance
R = 0.67.*Bi.*RSR.*c1.*(Hd+(c2.*0.57).^c3);
% Load
```

```
%L = Ai.*c1.*H.^c3; % as per Erdsal Paper Model
L = Ai.*c1.*(Hd+(c2.*0.57).^c3); % As per Ersdal Thesis Model
%4.2 Evaluation of the Safety Margin
G = R-L;
pf = sum(G<0)/Nsim;
%Results = [Ri];
disp('The probability of failure is');
disp(pf);
Beta = -norminv(pf,0,1);
disp('The Beta is');
disp(Beta);
```

Updated Probability of Failure

```
unction Abu_3ub
clear all
clc
%disp('This program determines the Updated probability of failure of system RSR');
disp('The input data comprises of, RSR,')
%1.0 Input of Nominal/Design basic Variables
%Nrun = input('Number of Runs = ');
Nsim = 1e7;
%Nsim = input('Number of Simulations = ');
%RSR = input('RSR values = ');
RSR = 2.0;
Hdu = input('Hdu values = ');
Hd = 10.80; % Design wave
c1 = 0.03237; % load coefficient
c2 = 2.7;
c3 = 2.1;
% Ho = 0.00;
% Hc = 4.46; % Scale parameter
% r = 8.83; % Shape parameter
% N = 5e6;
% F = rand(Nsim,1);
% D = (1-F.^(1/N));
% A = (-1.*(log(D))).^(1./r);
% Acmu = 1.96; % Convertion factor for Hmax given the Hs.[Hmax = A*Hs]
% Acsd = 0.05;
% Aci = normrnd(Acmu,Acsd,Nsim,1);% Convertion Factor Values
% H = 1.96.*(Ho+((Hc-Ho).*A))
% Hs_values = wblrnd(Hc,r,Nsim,1);
```

```
% Hmx = 1.95.*Hs_values;
% (mu = Mean, std = Stand Devi.): Normally Distributed
Bmu = 1.000;
Bsd = 0.1;
%2 Statistical Parameters (mu = Mean, std = Stand Devi.): Normally Distributed
amu = 1.000;
asd = 0.15;
% resistance uncertainty model
Bi = normrnd(Bmu,Bsd,Nsim,1);
% Load uncertainty model
Ai = normrnd(amu,asd,Nsim,1);
% Resistance
R = 0.67.*Bi.*RSR.*c1.*(Hd+(c2.*0.57).^c3);
% Load
%L = Ai.*c1.*H.^c3; % as per Erdsal Paper Model
% L = Ai.*(Wi+c1.*Hmx.^c3); % As per Ersdal Thesis Model
L1 = Ai.*c1.*(Hdu+(c2.*0.57).^c3); % As per Ersdal Thesis Model
%4.2 Evaluation of the Safety Margin
% G = R-L;
F = R-L1;
pf = sum(F>0)/Nsim;
%Results = [Ri];
disp('The probability of failure is');
disp(pf);
Beta = -norminv(pf,0,1);
disp('The Beta is');
disp(Beta);
```

Appendix D
Load Ratios

Develop w, d, l ratios for given condition of $\frac{w_e}{G} = 0.1$

$$w + d + l = 1.0$$

Assuming dead and live ratio is same

$$w + 2d = 1.0 \tag{D.1}$$

Case study: given ratio of $\frac{w_e}{G} = 0.1$

It can be shown by,

$$\frac{w}{2d} = 0.1$$

$$w = 0.2d$$

Using Eq. (1) and putting value of w,

$$0.2d + 2d = 1.0$$

$$d = \frac{1}{2.2}$$

Now again putting value of d in Eq. (1),

$$w + 2 * \left(\frac{1}{2.2}\right) = 1.0$$

$$w = 0.0909$$

Now the given ratio is $\frac{w}{d+l} = 0.1$

$$\frac{0.0909}{d + l} = 0.1$$

$$0.1(d + l) = 0.0909$$

Z. Nizamani, *Environmental Load Factors and System Strength Evaluation of Offshore Jacket Platforms*, Ocean Engineering & Oceanography 4,
DOI 10.1007/978-3-319-15051-2

$$G = d + l = 0.909$$

$$70\,\% \text{ of } d = 0.7 * 0.909 = 0.64$$
$$30\,\% \text{ of } l = 0.3 * 0.909 = 0.27$$

Appendix E
Wave Load Against Corresponding Base Shear in 8 Directions at SBO, SKO1, SKO2 and SKO2a Jacket Platforms

See Figs. E.1, E.2, E.3, E.4, E.5, E.6, E.7, E.8, E.9, E.10, E.11, E.12, E.13, E.14, E.15, E.16, E.17, E.18, E.19, E.20, E.21, E.22, E.23, E.24, E.25, E.26, E.27, E.28, E.29, E.30, E.31 and E.32.

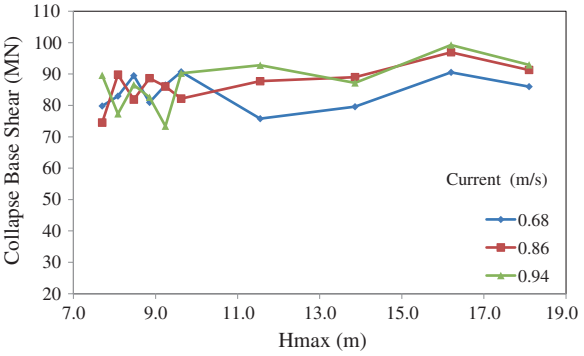

Fig. E.1 Collapse base shear against H_{max} wave with varying currents at SBO for 0°

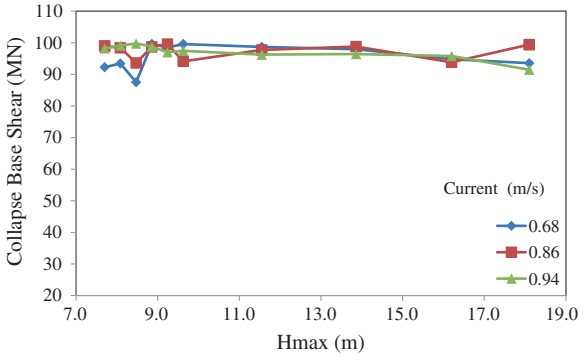

Fig. E.2 Collapse base shear against H_{max} wave with varying currents at SBO for 61.59°

Z. Nizamani, *Environmental Load Factors and System Strength Evaluation of Offshore Jacket Platforms*, Ocean Engineering & Oceanography 4,
DOI 10.1007/978-3-319-15051-2

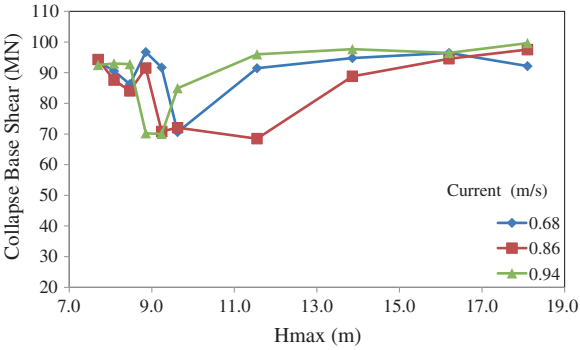

Fig. E.3 Collapse base shear against H_{max} wave with varying currents at SBO for 90°

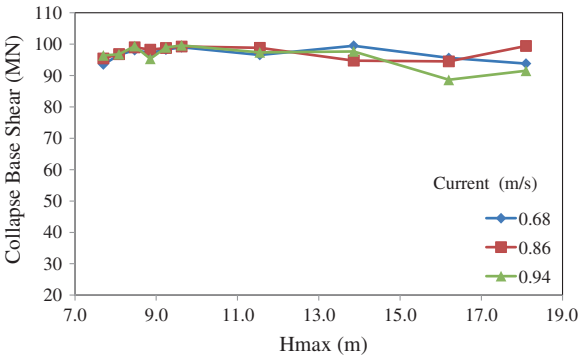

Fig. E.4 Collapse base shear against H_{max} wave with varying currents at SBO for 118.41°

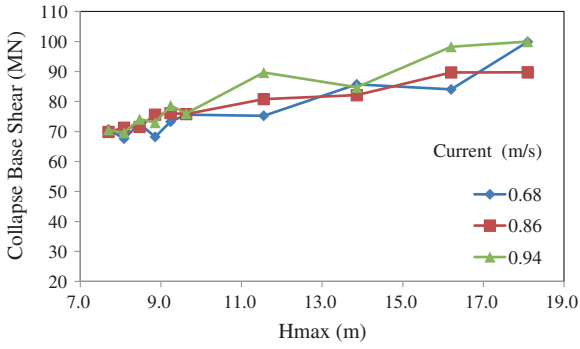

Fig. E.5 Collapse base shear against H_{max} wave with varying currents at SBO for 180°

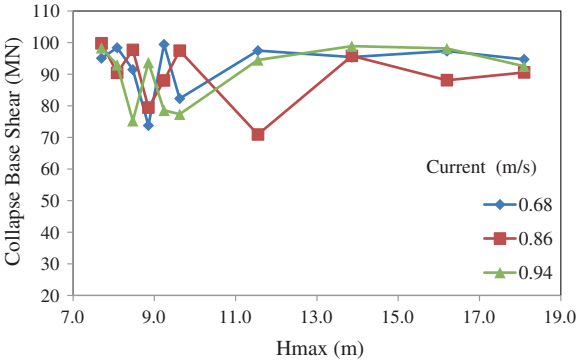

Fig. E.6 Collapse base shear against H_{max} wave with varying currents at SBO for 241.59°

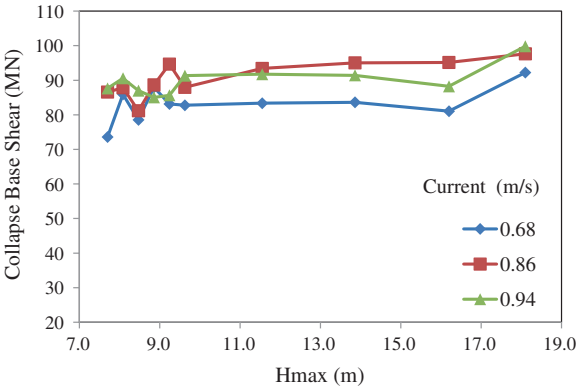

Fig. E.7 Collapse base shear against H_{max} wave with varying currents at SBO for 270°

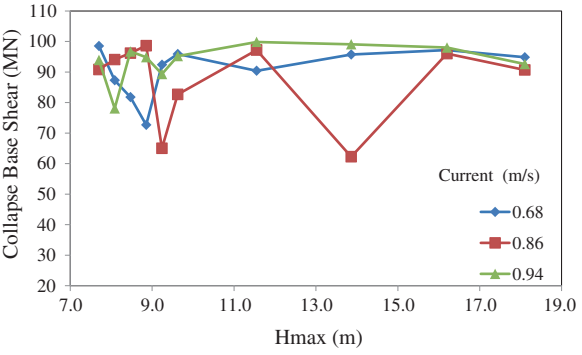

Fig. E.8 Collapse base shear against H_{max} wave with varying currents at SBO for 298.41°

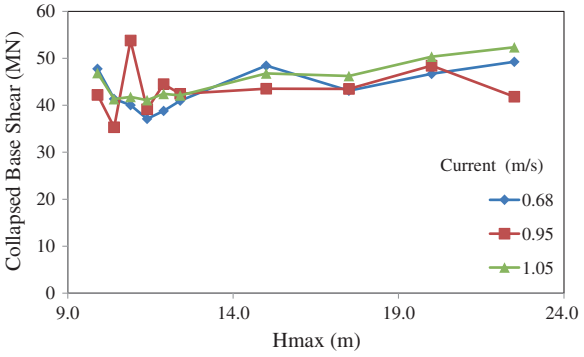

Fig. E.9 Collapse base shear against H_{max} wave with varying currents at SKO1 for 0°

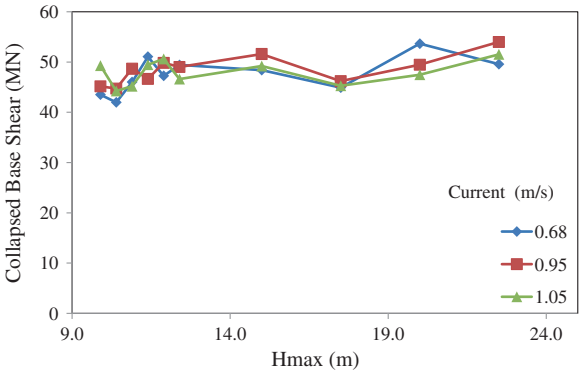

Fig. E.10 Collapse base shear against H_{max} wave with varying currents at SKO1 for 45°

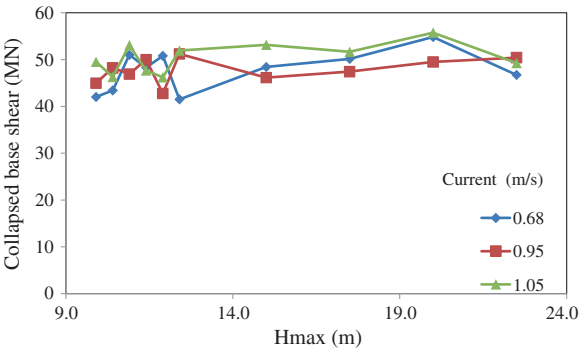

Fig. E.11 Collapse base shear against H_{max} wave with varying currents at SKO1 for 90°

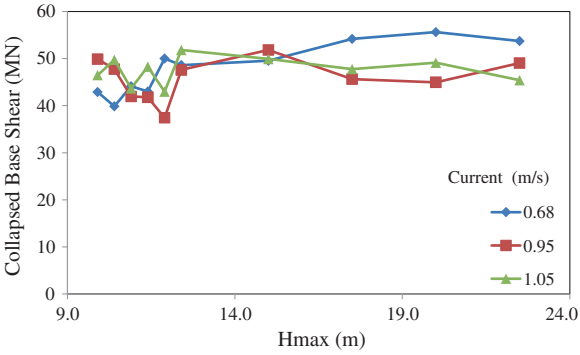

Fig. E.12 Collapse base shear against H_{max} wave with varying currents at SKO1 for 135°

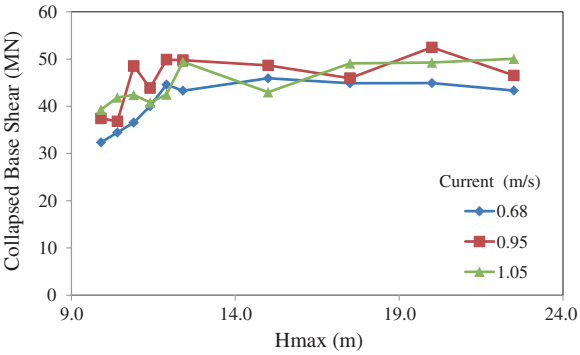

Fig. E.13 Collapse base shear against H_{max} wave with varying currents at SKO1 for 180°

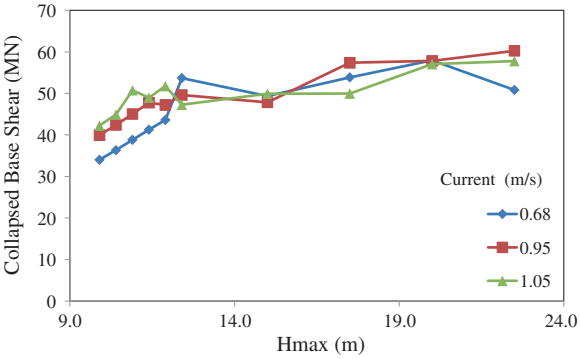

Fig. E.14 Collapse base shear against H_{max} wave with varying currents at SKO1 for 225°

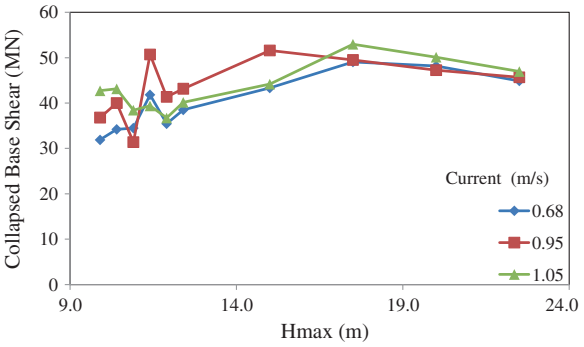

Fig. E.15 Collapse base shear against H_{max} wave with varying currents at SKO1 for 270°

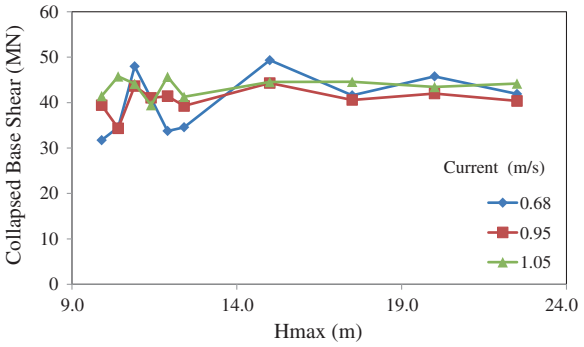

Fig. E.16 Collapse base shear against H_{max} wave with varying currents at SKO1 for 315°

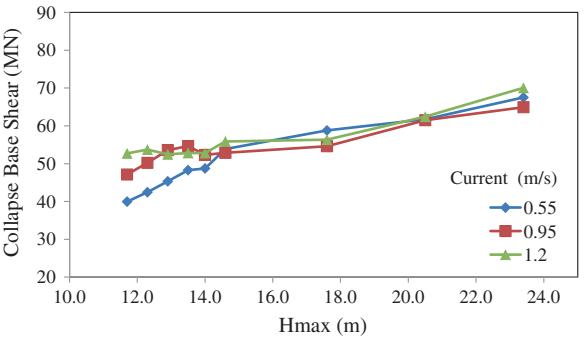

Fig. E.17 Collapse base shear against H_{max} wave with varying currents at SKO2 for 0°

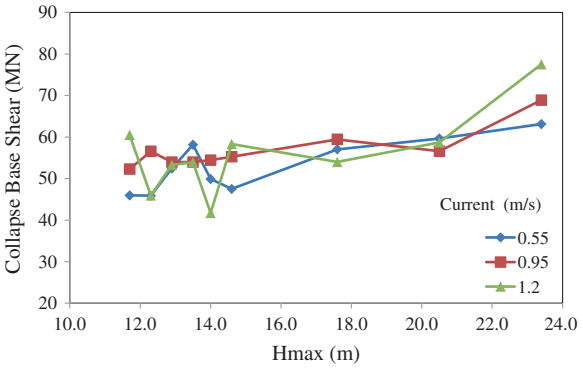

Fig. E.18 Collapse base shear against H_{max} wave with varying currents at SKO2 for 45°

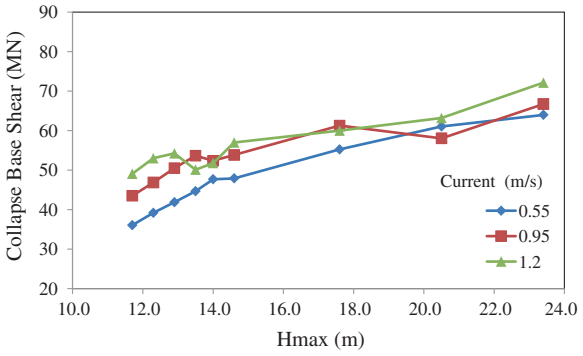

Fig. E.19 Collapse base shear against H_{max} wave with varying currents at SKO2 for 90°

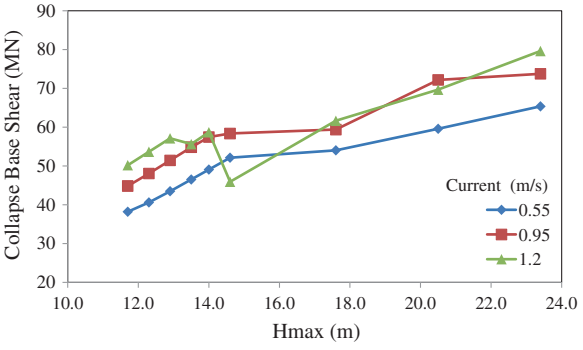

Fig. E.20 Collapse base shear against H_{max} wave with varying currents at SKO2 for 135°

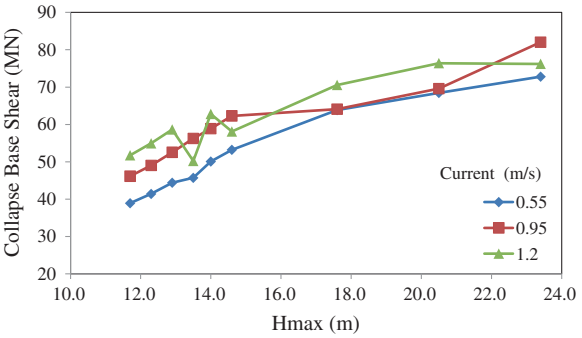

Fig. E.21 Collapse base shear against H_{max} wave with varying currents at SKO2 for 180°

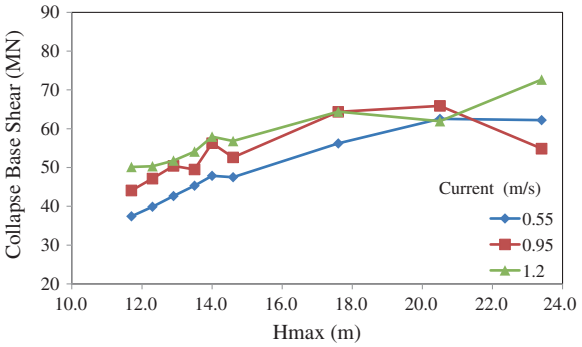

Fig. E.22 Collapse base shear against H_{max} wave with varying currents at SKO2 for 225°

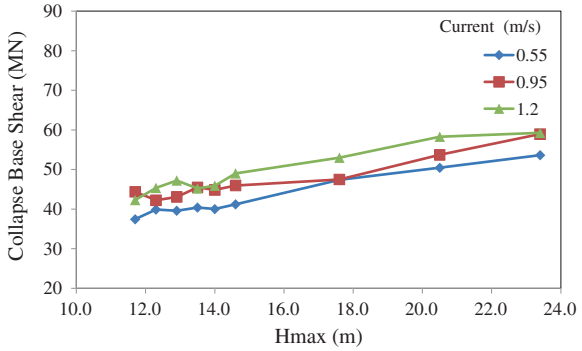

Fig. E.23 Collapse base shear against H_{max} wave with varying currents at SKO2 for 270°

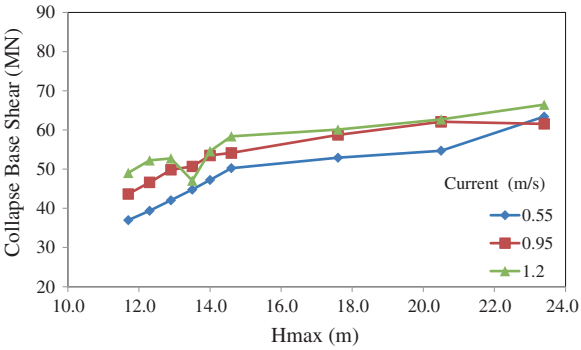

Fig. E.24 Collapse base shear against H_{max} wave with varying currents at SKO2 for 315°

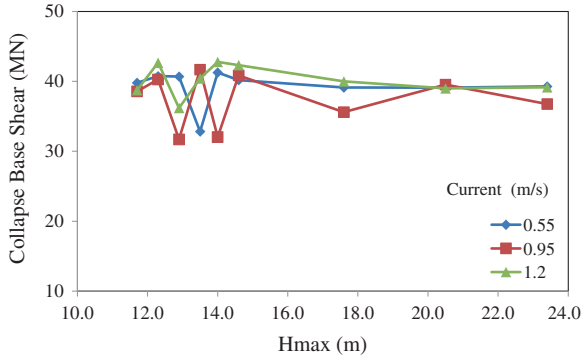

Fig. E.25 Collapse base shear against H_{max} wave with varying currents at SKO2a for 0°

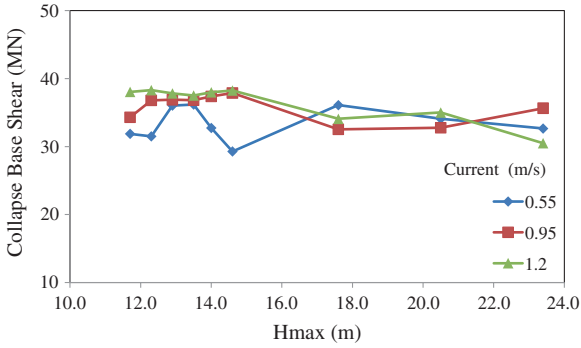

Fig. E.26 Collapse base shear against H_{max} wave with varying currents at SKO2a for 45°

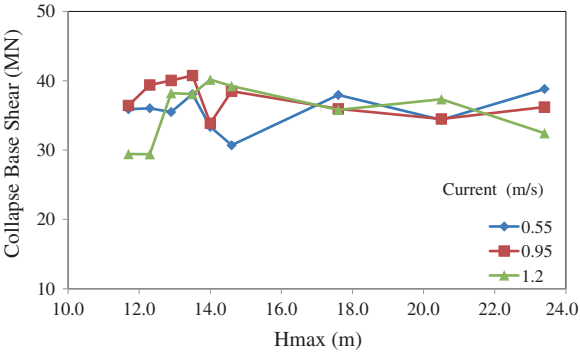

Fig. E.27 Collapse base shear against H_{max} wave with varying currents at SKO2a for 90°

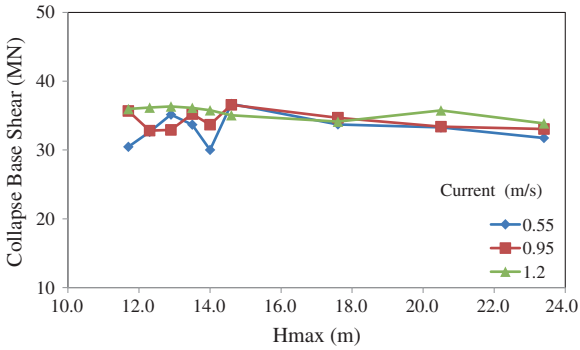

Fig. E.28 Collapse base shear against H_{max} wave with varying currents at SKO2a for 135°

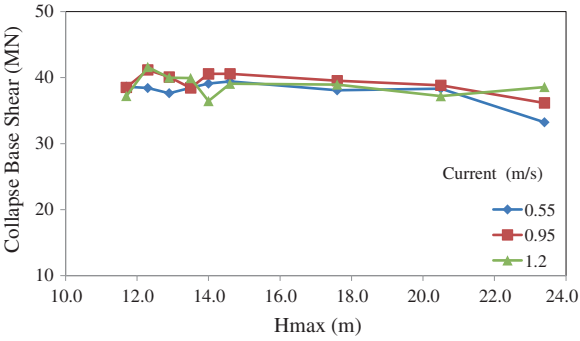

Fig. E.29 Collapse base shear against H_{max} wave with varying currents at SKO2a for 180°

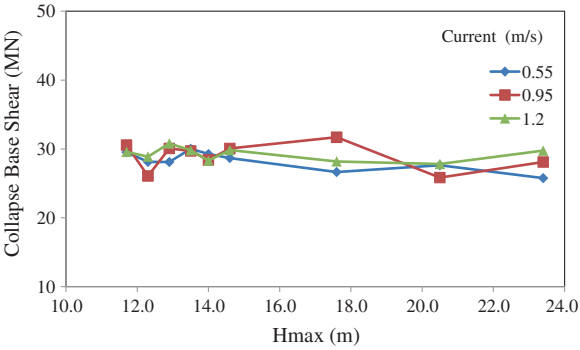

Fig. E.30 Collapse base shear against H_{max} wave with varying currents at SKO2a for 225°

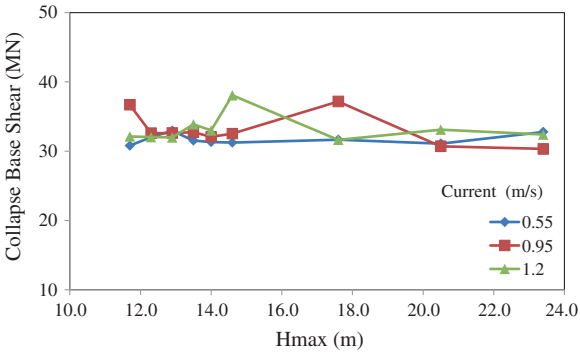

Fig. E.31 Collapse base shear against H_{max} wave with varying currents at SKO2a for 270°

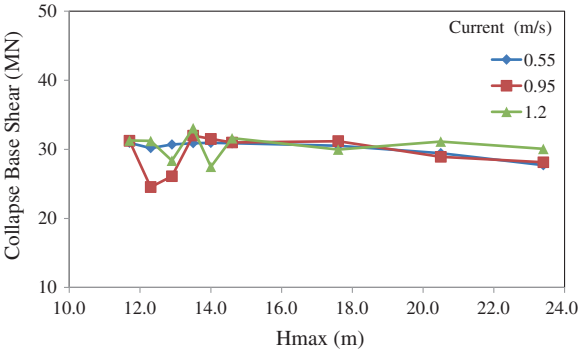

Fig. E.32 Collapse base shear against H_{max} wave with varying currents at SKO2a for 315°

Appendix F
Evaluation of RSR of 1.0 and System Redundancy

(a) PMO Jacket:

Direction	Wave period (Sec)	Wave height (m)	Current (cm/s)	Base shear (KN)		RSR	Peak load (KN)	100 year/ peak load	System redundancy
				Collapse load (KN)	100 year load (KN)				
0	10	10.8	0.57	19305	7427	2.60	23023	0.32	1.32
0	10	10.8	1	20233	9199	2.20	23919	0.38	1.38
0	10	10.8	1.1	20385	9709	2.10	24274	0.40	1.40
0	10.1	11.3	0.57	19153	7982	2.40	23149	0.34	1.34
0	10.1	11.3	1	20669	9844	2.10	23628	0.42	1.42
0	10.1	11.3	1.1	20596	10300	2.00	24722	0.42	1.42
0	10.3	11.9	0.57	19846	8630	2.30	23303	0.37	1.37
0	10.3	11.9	1	21375	10689	2.00	23519	0.45	1.45
0	10.3	11.9	1.1	21370	11249	1.90	24751	0.45	1.45
0	10.5	12.4	0.57	20650	9388	2.20	23472	0.40	1.40
0	10.5	12.4	1	21875	11515	1.90	24184	0.48	1.48
0	10.5	12.4	1.1	21556	11977	1.80	23958	0.50	1.50
0	10.7	13.0	0.57	21523	10250	2.10	23579	0.43	1.43
0	10.7	13.0	1	22346	12416	1.80	24836	0.50	1.50
0	10.7	13.0	1.1	22156	13034	1.70	24769	0.53	1.53
0	10.9	13.5	0.57	29834	10967	2.72	23035	0.48	1.48
0	10.9	13.5	1	22700	13354	1.70	24042	0.56	1.56
0	10.9	13.5	1.1	22221	13887	1.60	25001	0.56	1.56
0	11.8	16	0.57	22681	15122	1.50	24201	0.62	1.62
0	11.8	16	1	23340	17954	1.30	25141	0.71	1.71
0	11.8	16	1.1	24366	18744	1.30	26253	0.71	1.71
0	12.8	19	0.57	23439	21194	1.11	23439	0.90	1.90

(continued)

Z. Nizamani, *Environmental Load Factors and System Strength Evaluation of Offshore Jacket Platforms*, Ocean Engineering & Oceanography 4,
DOI 10.1007/978-3-319-15051-2

(continued)

Direction	Wave period (Sec)	Wave height (m)	Current (cm/s)	Base shear (KN)		RSR	Peak load (KN)	100 year/ peak load	System redundancy
				Collapse load (KN)	100 year load (KN)				
0	12.8	19	1	24728	24728	1.00	24728	1.00	2.00
0	12.8	19	1.1	25565	25565	1.00	25565	1.00	2.00
45	10	10.8	0.57	25301	8437	3.00	25301	0.33	1.33
45	10	10.8	1	26557	10418	2.55	26557	0.39	1.39
45	10	10.8	1.1	26784	10935	2.45	26784	0.41	1.41
45	10.1	11.3	0.57	23986	9055	2.65	24893	0.36	1.36
45	10.1	11.3	1	25648	11154	2.30	26765	0.42	1.42
45	10.1	11.3	1.1	26282	11684	2.25	26282	0.44	1.44
45	10.3	11.9	0.57	23964	9784	2.45	24943	0.39	1.39
45	10.3	11.9	1	25287	12045	2.10	27094	0.44	1.44
45	10.3	11.9	1.1	25913	12643	2.05	27179	0.47	1.47
45	10.5	12.4	0.57	23782	10573	2.25	25368	0.42	1.42
45	10.5	12.4	1	25890	12948	2.00	27187	0.48	1.48
45	10.5	12.4	1.1	26281	13480	1.95	27630	0.49	1.49
45	10.7	13	0.57	24727	11504	2.15	25877	0.44	1.44
45	10.7	13	1	26315	13853	1.90	27701	0.50	1.50
45	10.7	13	1.1	26831	14506	1.85	26831	0.54	1.54
45	10.9	13.5	0.57	25000	12198	2.05	26220	0.47	1.47
45	10.9	13.5	1	26517	14734	1.80	26517	0.56	1.56
45	10.9	13.5	1.1	26818	15327	1.75	26818	0.57	1.57
45	11.8	16	0.57	27959	16448	1.70	25490	0.65	1.65
45	11.8	16	1	26861	19537	1.37	28330	0.69	1.69
45	11.8	16	1.1	27537	20399	1.35	27537	0.74	1.74
45	12.8	19	0.57	26176	22762	1.15	26453	0.86	1.86
45	12.8	19	1	28591	26594	1.08	28591	0.93	1.93
45	12.8	19	1.1	27509	27509	1.00	28887	0.95	1.95
90	10	10.8	0.57	29607	8585	3.45	31542	0.27	1.27
90	10	10.8	1	31786	10597	3.00	31786	0.33	1.33
90	10	10.8	1.1	31237	11158	2.80	31237	0.36	1.36
90	10.1	11.3	0.57	29903	9348	3.20	31774	0.29	1.29
90	10.1	11.3	1	32030	11441	2.80	32030	0.36	1.36
90	10.1	11.3	1.1	31067	11951	2.60	31067	0.38	1.38
90	10.3	11.9	0.57	30605	10205	3.00	31628	0.32	1.32
90	10.3	11.9	1	30975	12392	2.50	30975	0.40	1.40
90	10.3	11.9	1.1	29862	12986	2.30	29862	0.43	1.43
90	10.5	12.4	0.57	29561	10951	2.70	31752	0.34	1.34
90	10.5	12.4	1	31809	13255	2.40	31809	0.42	1.42

(continued)

(continued)

Direction	Wave period (Sec)	Wave height (m)	Current (cm/s)	Base shear (KN)		RSR	Peak load (KN)	100 year/ peak load	System redundancy
				Collapse load (KN)	100 year load (KN)				
90	10.5	12.4	1.1	31625	13751	2.30	31625	0.43	1.43
90	10.7	13	0.57	30970	11914	2.60	32163	0.37	1.37
90	10.7	13	1	31182	14175	2.20	31182	0.45	1.45
90	10.7	13	1.1	31142	14831	2.10	31142	0.48	1.48
90	10.9	13.5	0.57	30347	12647	2.40	31613	0.40	1.40
90	10.9	13.5	1	31755	15123	2.10	31755	0.48	1.48
90	10.9	13.5	1.1	31388	15695	2.00	31388	0.50	1.50
90	11.8	16	0.57	30926	17182	1.80	30926	0.56	1.56
90	11.8	16	1	30357	20238	1.50	30357	0.67	1.67
90	11.8	16	1.1	31631	21087	1.50	31631	0.67	1.67
90	12.8	19	0.57	31163	23971	1.30	31163	0.77	1.77
90	12.8	19	1	30526	27750	1.10	30526	0.91	1.91
90	12.8	19	1.1	31501	28636	1.10	31501	0.91	1.91
135	10	10.8	0.57	31963	8606	3.71	31963	0.27	1.27
135	10	10.8	1	32826	10608	3.09	32826	0.32	1.32
135	10	10.8	1.1	31916	11170	2.86	31916	0.35	1.35
135	10.1	11.3	0.57	33718	11321	2.98	33718	0.34	1.34
135	10.1	11.3	1	33138	11853	2.80	33138	0.36	1.36
135	10.1	11.3	1.1	32175	11854	2.71	32175	0.37	1.37
135	10.3	11.9	0.57	29304	9947	2.95	29304	0.34	1.34
135	10.3	11.9	1	32371	12197	2.65	32371	0.38	1.38
135	10.3	11.9	1.1	34801	12822	2.71	34801	0.37	1.37
135	10.5	12.4	0.57	31596	10747	2.94	31596	0.34	1.34
135	10.5	12.4	1	33590	13080	2.57	33590	0.39	1.39
135	10.5	12.4	1.1	33037	13604	2.43	33037	0.41	1.41
135	10.7	13	0.57	32200	11709	2.75	32200	0.36	1.36
135	10.7	13	1	34005	14020	2.43	34005	0.41	1.41
135	10.7	13	1.1	33582	14692	2.29	33582	0.44	1.44
135	10.9	13.5	0.57	32016	12450	2.57	32016	0.39	1.39
135	10.9	13.5	1	34153	14941	2.29	34153	0.44	1.44
135	10.9	13.5	1.1	31048	15524	2.00	31048	0.50	1.50
135	11.8	16	0.57	33351	16675	2.00	33351	0.50	1.50
135	11.8	16	1	33676	19748	1.71	33676	0.59	1.59
135	11.8	16	1.1	32343	20581	1.57	32343	0.64	1.64
135	12.8	19	0.57	33560	22526	1.49	33560	0.67	1.67
135	12.8	19	1	34526	26852	1.29	34526	0.78	1.78
135	12.8	19	1.1	35700	27763	1.29	35700	0.78	1.78

(continued)

(continued)

Direction	Wave period (Sec)	Wave height (m)	Current (cm/s)	Base shear (KN)		RSR	Peak load (KN)	100 year/ peak load	System redundancy
				Collapse load (KN)	100 year load (KN)				
180	10	10.8	0.57	29680	8019	3.70	32101	0.25	1.25
180	10	10.8	1	29401	9798	3.00	32358	0.30	1.30
180	10	10.8	1.1	29888	10304	2.90	32991	0.31	1.31
180	10.1	11.3	0.57	30118	8602	3.50	31852	0.27	1.27
180	10.1	11.3	1	28269	10468	2.70	32472	0.32	1.32
180	10.1	11.3	1.1	28399	10920	2.60	32782	0.33	1.33
180	10.3	11.9	0.57	29773	9301	3.20	31644	0.29	1.29
180	10.3	11.9	1	28208	11281	2.50	32730	0.34	1.34
180	10.3	11.9	1.1	28393	11828	2.40	33132	0.36	1.36
180	10.5	12.4	0.57	29036	10010	2.90	32053	0.31	1.31
180	10.5	12.4	1	28471	12113	2.35	32113	0.38	1.38
180	10.5	12.4	1.1	28901	12563	2.30	32677	0.38	1.38
180	10.7	13	0.57	29522	10932	2.70	31727	0.34	1.34
180	10.7	13	1	28585	12991	2.20	32494	0.40	1.40
180	10.7	13	1.1	27934	13624	2.05	32711	0.42	1.42
180	10.9	13.5	0.57	28000	11665	2.40	31506	0.37	1.37
180	10.9	13.5	1	29312	13956	2.10	32110	0.43	1.43
180	10.9	13.5	1.1	28965	14480	2.00	33317	0.43	1.43
180	11.8	16	0.57	30102	15841	1.90	32490	0.49	1.49
180	11.8	16	1	29824	18638	1.60	32627	0.57	1.57
180	11.8	16	1.1	31083	19425	1.60	33031	0.59	1.59
180	12.8	19	0.57	30846	22031	1.40	32505	0.68	1.68
180	12.8	19	1	30655	25544	1.20	33219	0.77	1.77
180	12.8	19	1.1	31644	26369	1.20	34292	0.77	1.77
225	10	10.8	0.57	30055	8836	3.40	30055	0.29	1.29
225	10	10.8	1	32438	10808	3.00	32438	0.33	1.33
225	10	10.8	1.1	31846	11369	2.80	31846	0.36	1.36
225	10.1	11.3	0.57	30284	9459	3.20	30284	0.31	1.31
225	10.1	11.3	1	32272	11522	2.80	32272	0.36	1.36
225	10.1	11.3	1.1	31607	12038	2.63	31607	0.38	1.38
225	10.3	11.9	0.57	30123	10207	2.95	30123	0.34	1.34
225	10.3	11.9	1	32224	12391	2.60	32224	0.38	1.38
225	10.3	11.9	1.1	32517	13003	2.50	32517	0.40	1.40
225	10.5	12.4	0.57	31643	10907	2.90	31643	0.34	1.34
225	10.5	12.4	1	31860	13272	2.40	31860	0.42	1.42
225	10.5	12.4	1.1	31733	13793	2.30	31733	0.43	1.43
225	10.7	13	0.57	31271	11909	2.63	31271	0.38	1.38

(continued)

(continued)

Direction	Wave period (Sec)	Wave height (m)	Current (cm/s)	Base shear (KN)		RSR	Peak load (KN)	100 year/ peak load	System redundancy
				Collapse load (KN)	100 year load (KN)				
225	10.7	13	1	31618	14207	2.23	31618	0.45	1.45
225	10.7	13	1.1	31622	14878	2.13	31622	0.47	1.47
225	10.9	13.5	0.57	31619	12644	2.50	31619	0.40	1.40
225	10.9	13.5	1	31810	15144	2.10	31810	0.48	1.48
225	10.9	13.5	1.1	31851	15726	2.03	31851	0.49	1.49
225	11.8	16	0.57	32206	16946	1.90	32206	0.53	1.53
225	11.8	16	1	31991	19993	1.60	31991	0.62	1.62
225	11.8	16	1.1	32106	16675	1.93	32106	0.52	1.52
225	12.8	19	0.57	32565	23258	1.40	32565	0.71	1.71
225	12.8	19	1	32466	27053	1.20	32466	0.83	1.83
225	12.8	19	1.1	32857	27961	1.18	32857	0.85	1.85
270	10	10.8	0.57	26235	8743	3.00	27986	0.31	1.31
270	10	10.8	1	26747	10697	2.50	28887	0.37	1.37
270	10	10.8	1.1	27000	11248	2.40	28126	0.40	1.40
270	10.1	11.3	0.57	25586	9474	2.70	27483	0.34	1.34
270	10.1	11.3	1	26521	11529	2.30	28829	0.40	1.40
270	10.1	11.3	1.1	27671	12029	2.30	30078	0.40	1.40
270	10.3	11.9	0.57	26726	10277	2.60	27756	0.37	1.37
270	10.3	11.9	1	27443	12472	2.20	28692	0.43	1.43
270	10.3	11.9	1.1	27450	13070	2.10	28759	0.45	1.45
270	10.5	12.4	0.57	26683	11116	2.40	28908	0.38	1.38
270	10.5	12.4	1	26821	13409	2.00	29504	0.45	1.45
270	10.5	12.4	1.1	27811	13904	2.00	29204	0.48	1.48
270	10.7	13	0.57	26611	12095	2.20	29032	0.42	1.42
270	10.7	13	1	27247	14339	1.90	28682	0.50	1.50
270	10.7	13	1.1	26987	14991	1.80	28488	0.53	1.53
270	10.9	13.5	0.57	26941	12827	2.10	29509	0.43	1.43
270	10.9	13.5	1	27514	15284	1.80	29044	0.53	1.53
270	10.9	13.5	1.1	26946	15849	1.70	28533	0.56	1.56
270	11.8	16	0.57	27845	17402	1.60	29587	0.59	1.59
270	11.8	16	1	28600	20427	1.40	30643	0.67	1.67
270	11.8	16	1.1	27654	21271	1.30	29782	0.71	1.71
270	12.8	19	0.57	28919	24099	1.20	31330	0.77	1.77
270	12.8	19	1	30668	27879	1.10	30668	0.91	1.91
270	12.8	19	1.1	28766	28766	1.00	31645	0.91	1.91
315	10	10.8	0.57	22910	8480	2.70	22910	0.37	1.37
315	10	10.8	1	21941	10447	2.10	21941	0.48	1.48

(continued)

(continued)

Direction	Wave period (Sec)	Wave height (m)	Current (cm/s)	Base shear (KN)		RSR	Peak load (KN)	100 year/ peak load	System redundancy
				Collapse load (KN)	100 year load (KN)				
315	10	10.8	1.1	22021	11010	2.00	22021	0.50	1.50
315	10.1	11.3	0.57	22545	9017	2.50	22545	0.40	1.40
315	10.1	11.3	1	22293	11145	2.00	23421	0.48	1.48
315	10.1	11.3	1.1	22166	11665	1.90	23346	0.50	1.50
315	10.3	11.9	0.57	22519	9785	2.30	22519	0.43	1.43
315	10.3	11.9	1	21607	12003	1.80	22820	0.53	1.53
315	10.3	11.9	1.1	21472	12629	1.70	21472	0.59	1.59
315	10.5	12.4	0.57	22119	10531	2.10	23185	0.45	1.45
315	10.5	12.4	1	21902	12882	1.70	23203	0.56	1.56
315	10.5	12.4	1.1	22817	13413	1.70	22817	0.59	1.59
315	10.7	13	0.57	21787	11466	1.90	22947	0.50	1.50
315	10.7	13	1	22106	13815	1.60	23501	0.59	1.59
315	10.7	13	1.1	21742	14493	1.50	23204	0.62	1.62
315	10.9	13.5	0.57	21960	12199	1.80	23194	0.53	1.53
315	10.9	13.5	1	22118	14744	1.50	23605	0.62	1.62
315	10.9	13.5	1.1	21464	15330	1.40	23010	0.67	1.67
315	11.8	16	0.57	21354	16425	1.30	23009	0.71	1.71
315	11.8	16	1	21482	19527	1.10	23447	0.83	1.83
315	11.8	16	1.1	22424	20384	1.10	24476	0.83	1.83
315	12.8	19	0.57	22725	22725	1.00	22725	1.00	2.00
315	12.8	19	1	21236	21236	1.00	21236	1.00	2.00
315	12.8	19	1.1	24712	24712	1.00	24712	1.00	2.00

(b) SBO Jacket

Direction	Wave (m)	Wave Period (Sec)	Current (cm/s)	Base shear (KN)		RSR	Peak load base shear (KN)	100 year/ peak load	System redundancy
				Collapse load (KN)	100 year load (KN)				
0	7.7	9.6	0.68	43156	7993	5.40	79804	0.10	1.10
0	7.7	9.6	0.86	45096	8673	5.20	74514	0.12	1.12
0	7.7	9.6	0.94	45053	9011	5.00	89585	0.10	1.10
0	8.1	9.9	0.68	45135	8680	5.20	82968	0.10	1.10
0	8.1	9.9	0.86	43212	9394	4.60	89780	0.10	1.10
0	8.1	9.9	0.94	44511	9677	4.60	77304	0.13	1.13
0	8.5	10.1	0.68	43053	9360	4.60	89488	0.10	1.10
0	8.5	10.1	0.86	43950	9989	4.40	81870	0.12	1.12

(continued)

(continued)

Direction	Wave (m)	Wave Period (Sec)	Current (cm/s)	Base shear (KN)		RSR	Peak load base shear (KN)	100 year/ peak load	System redundancy
				Collapse load (KN)	100 year load (KN)				
0	8.5	10.1	0.94	43426	10340	4.20	86547	0.12	1.12
0	8.9	10.2	0.68	43480	9883	4.40	80949	0.12	1.12
0	8.9	10.2	0.86	44611	10622	4.20	88679	0.12	1.12
0	8.9	10.2	0.94	45738	10891	4.20	82579	0.13	1.13
0	9.2	10.3	0.68	43518	10362	4.20	86508	0.12	1.12
0	9.2	10.3	0.86	44372	11094	4.00	86046	0.13	1.13
0	9.2	10.3	0.94	45922	11481	4.00	73369	0.16	1.16
0	9.6	10.9	0.68	43233	11378	3.80	90719	0.13	1.13
0	9.6	10.9	0.86	46117	12137	3.80	82148	0.15	1.15
0	9.6	10.9	0.94	45247	12569	3.60	90249	0.14	1.14
0	11.6	11.4	0.68	42478	15171	2.80	75764	0.20	1.20
0	11.6	11.4	0.86	45431	16226	2.80	87717	0.18	1.18
0	11.6	11.4	0.94	43286	16649	2.60	92795	0.18	1.18
0	13.9	11.9	0.68	46103	20957	2.20	79574	0.26	1.26
0	13.9	11.9	0.86	44562	22282	2.00	88984	0.25	1.25
0	13.9	11.9	0.94	46022	23012	2.00	87160	0.26	1.26
0	16.2	13.3	0.68	48389	30244	1.60	90540	0.33	1.33
0	16.2	13.3	0.86	45336	32384	1.40	96932	0.33	1.33
0	16.2	13.3	0.94	46455	33183	1.40	99238	0.33	1.33
0	18.1	14.1	0.68	46953	39128	1.20	85988	0.46	1.46
0	18.1	14.1	0.86	49840	41535	1.20	91301	0.45	1.45
0	18.1	14.1	0.94	50795	42330	1.20	92916	0.46	1.46
61.59	7.7	9.6	0.68	43881	10971	4.00	92254	0.12	1.12
61.59	7.7	9.6	0.86	45003	11844	3.80	98998	0.12	1.12
61.59	7.7	9.6	0.94	44263	12297	3.60	98237	0.13	1.13
61.59	8.1	9.9	0.68	44331	11667	3.80	93425	0.12	1.12
61.59	8.1	9.9	0.86	45551	12654	3.60	98405	0.13	1.13
61.59	8.1	9.9	0.94	47042	13069	3.60	99135	0.13	1.13
61.59	8.5	10.1	0.68	45002	12502	3.60	87516	0.14	1.14
61.59	8.5	10.1	0.86	45516	13388	3.40	93601	0.14	1.14
61.59	8.5	10.1	0.94	47190	13881	3.40	99765	0.14	1.14
61.59	8.9	10.2	0.68	44632	13128	3.40	99613	0.13	1.13
61.59	8.9	10.2	0.86	45278	14151	3.20	98682	0.14	1.14
61.59	8.9	10.2	0.94	46516	14538	3.20	98787	0.15	1.15
61.59	9.2	10.3	0.68	46589	13704	3.40	98524	0.14	1.14
61.59	9.2	10.3	0.86	46915	14662	3.20	99596	0.15	1.15
61.59	9.2	10.3	0.94	48557	15175	3.20	96998	0.16	1.16
61.59	9.6	10.9	0.68	47056	14706	3.20	99614	0.15	1.15

(continued)

(continued)

Direction	Wave (m)	Wave Period (Sec)	Current (cm/s)	Base shear (KN)		RSR	Peak load base shear (KN)	100 year/ peak load	System redun-dancy
				Collapse load (KN)	100 year load (KN)				
61.59	9.6	10.9	0.86	47104	15703	3.00	94140	0.17	1.17
61.59	9.6	10.9	0.94	48772	16259	3.00	97440	0.17	1.17
61.59	11.6	11.4	0.68	49467	19027	2.60	98694	0.19	1.19
61.59	11.6	11.4	0.86	48894	20375	2.40	97703	0.21	1.21
61.59	11.6	11.4	0.94	46107	20959	2.20	96242	0.22	1.22
61.59	13.9	11.9	0.68	46468	25817	1.80	97984	0.26	1.26
61.59	13.9	11.9	0.86	49454	27477	1.80	98799	0.28	1.28
61.59	13.9	11.9	0.94	45406	28380	1.60	96433	0.29	1.29
61.59	16.2	13.3	0.68	51077	36488	1.40	94817	0.38	1.38
61.59	16.2	13.3	0.86	46946	39124	1.20	93862	0.42	1.42
61.59	16.2	13.3	0.94	47932	39946	1.20	95817	0.42	1.42
61.59	18.1	14.1	0.68	46784	46784	1.00	93540	0.50	1.50
61.59	18.1	14.1	0.86	49754	49754	1.00	99397	0.50	1.50
61.59	18.1	14.1	0.94	50829	50829	1.00	91469	0.56	1.56
90	7.7	9.6	0.68	45971	11494	4.00	93756	0.12	1.12
90	7.7	9.6	0.86	47306	12450	3.80	94316	0.13	1.13
90	7.7	9.6	0.94	49074	12915	3.80	92512	0.14	1.14
90	8.1	9.9	0.68	46772	12309	3.80	90558	0.14	1.14
90	8.1	9.9	0.86	47937	13317	3.60	87608	0.15	1.15
90	8.1	9.9	0.94	49424	13730	3.60	92997	0.15	1.15
90	8.5	10.1	0.68	47215	13116	3.60	86282	0.15	1.15
90	8.5	10.1	0.86	47699	14031	3.40	84047	0.17	1.17
90	8.5	10.1	0.94	49402	14531	3.40	92784	0.16	1.16
90	8.9	10.2	0.68	49595	13778	3.60	96755	0.14	1.14
90	8.9	10.2	0.86	50364	14814	3.40	91520	0.16	1.16
90	8.9	10.2	0.94	48695	15219	3.20	70229	0.22	1.22
90	9.2	10.3	0.68	48840	14366	3.40	91710	0.16	1.16
90	9.2	10.3	0.86	49138	15358	3.20	70822	0.22	1.22
90	9.2	10.3	0.94	50794	15874	3.20	70023	0.23	1.23
90	9.6	10.9	0.68	49139	15358	3.20	70617	0.22	1.22
90	9.6	10.9	0.86	49157	16388	3.00	72045	0.23	1.23
90	9.6	10.9	0.94	50860	16955	3.00	84944	0.20	1.20
90	11.6	11.4	0.68	51702	19887	2.60	91472	0.22	1.22
90	11.6	11.4	0.86	51023	21261	2.40	68493	0.31	1.31
90	11.6	11.4	0.94	52473	21866	2.40	95983	0.23	1.23
90	13.9	11.9	0.68	50254	27920	1.80	94795	0.29	1.29
90	13.9	11.9	0.86	53351	29641	1.80	88828	0.33	1.33

(continued)

(continued)

Direction	Wave (m)	Wave Period (Sec)	Current (cm/s)	Base shear (KN)		RSR	Peak load base shear (KN)	100 year/ peak load	System redundancy
				Collapse load (KN)	100 year load (KN)				
90	13.9	11.9	0.94	55022	30570	1.80	97676	0.31	1.31
90	16.2	13.3	0.68	48297	40249	1.20	96453	0.42	1.42
90	16.2	13.3	0.86	51688	43078	1.20	94556	0.46	1.46
90	16.2	13.3	0.94	52726	43943	1.20	96451	0.46	1.46
90	18.1	14.1	0.68	51277	51277	1.00	92157	0.56	1.56
90	18.1	14.1	0.86	54251	54251	1.00	97526	0.56	1.56
90	18.1	14.1	0.94	55486	55486	1.00	99665	0.56	1.56
118.41	7.7	9.6	0.68	38797	11412	3.40	93523	0.12	1.12
118.41	7.7	9.6	0.86	39259	12269	3.20	95435	0.13	1.13
118.41	7.7	9.6	0.94	40716	12725	3.20	96410	0.13	1.13
118.41	8.1	9.9	0.68	38818	12131	3.20	96634	0.13	1.13
118.41	8.1	9.9	0.86	41911	13098	3.20	96835	0.14	1.14
118.41	8.1	9.9	0.94	40506	13503	3.00	96796	0.14	1.14
118.41	8.5	10.1	0.68	41360	12926	3.20	98063	0.13	1.13
118.41	8.5	10.1	0.86	41373	13792	3.00	98992	0.14	1.14
118.41	8.5	10.1	0.94	42749	14251	3.00	99386	0.14	1.14
118.41	8.9	10.2	0.68	40546	13516	3.00	97195	0.14	1.14
118.41	8.9	10.2	0.86	43496	14500	3.00	98277	0.15	1.15
118.41	8.9	10.2	0.94	41712	14898	2.80	95331	0.16	1.16
118.41	9.2	10.3	0.68	42236	14080	3.00	98230	0.14	1.14
118.41	9.2	10.3	0.86	42033	15013	2.80	98768	0.15	1.15
118.41	9.2	10.3	0.94	43450	15519	2.80	98967	0.16	1.16
118.41	9.6	10.9	0.68	42162	15059	2.80	98996	0.15	1.15
118.41	9.6	10.9	0.86	44977	16065	2.80	99271	0.16	1.16
118.41	9.6	10.9	0.94	43204	16619	2.60	99626	0.17	1.17
118.41	11.6	11.4	0.68	46460	19360	2.40	96534	0.20	1.20
118.41	11.6	11.4	0.86	45406	20641	2.20	98852	0.21	1.21
118.41	11.6	11.4	0.94	46670	21218	2.20	97386	0.22	1.22
118.41	13.9	11.9	0.68	47254	26255	1.80	99513	0.26	1.26
118.41	13.9	11.9	0.86	50216	27902	1.80	94772	0.29	1.29
118.41	13.9	11.9	0.94	46064	28793	1.60	97686	0.29	1.29
118.41	16.2	13.3	0.68	44250	36877	1.20	95601	0.39	1.39
118.41	16.2	13.3	0.86	47331	39448	1.20	94516	0.42	1.42
118.41	16.2	13.3	0.94	48298	40251	1.20	88640	0.45	1.45
118.41	18.1	14.1	0.68	46984	46984	1.00	93811	0.50	1.50
118.41	18.1	14.1	0.86	49775	49775	1.00	99419	0.50	1.50
118.41	18.1	14.1	0.94	50882	50882	1.00	91530	0.56	1.56

(continued)

(continued)

Direction	Wave (m)	Wave Period (Sec)	Current (cm/s)	Base shear (KN)		RSR	Peak load base shear (KN)	100 year/ peak load	System redundancy
				Collapse load (KN)	100 year load (KN)				
180	7.7	9.6	0.68	41265	8253	5.00	70695	0.12	1.12
180	7.7	9.6	0.86	43081	8975	4.80	69846	0.13	1.13
180	7.7	9.6	0.94	42837	9313	4.60	70586	0.13	1.13
180	8.1	9.9	0.68	42793	8915	4.80	67621	0.13	1.13
180	8.1	9.9	0.86	42545	9670	4.40	71246	0.14	1.14
180	8.1	9.9	0.94	43882	9973	4.40	69603	0.14	1.14
180	8.5	10.1	0.68	42153	9580	4.40	72585	0.13	1.13
180	8.5	10.1	0.86	43052	10250	4.20	71494	0.14	1.14
180	8.5	10.1	0.94	44552	10608	4.20	74111	0.14	1.14
180	8.9	10.2	0.68	44248	10056	4.40	68210	0.15	1.15
180	8.9	10.2	0.86	45480	19829	2.29	75589	0.26	1.26
180	8.9	10.2	0.94	44414	11104	4.00	72956	0.15	1.15
180	9.2	10.3	0.68	44129	10507	4.20	73277	0.14	1.14
180	9.2	10.3	0.86	44196	11229	3.94	76130	0.15	1.15
180	9.2	10.3	0.94	46471	11618	4.00	78669	0.15	1.15
180	9.6	10.9	0.68	45907	11477	4.00	75590	0.15	1.15
180	9.6	10.9	0.86	46570	12256	3.80	75780	0.16	1.16
180	9.6	10.9	0.94	45737	12705	3.60	76007	0.17	1.17
180	11.6	11.4	0.68	48259	15082	3.20	75252	0.20	1.20
180	11.6	11.4	0.86	48579	16193	3.00	80790	0.20	1.20
180	11.6	11.4	0.94	49985	16662	3.00	89652	0.19	1.19
180	13.9	11.9	0.68	47268	21487	2.20	85719	0.25	1.25
180	13.9	11.9	0.86	50293	22862	2.20	82101	0.28	1.28
180	13.9	11.9	0.94	51938	23610	2.20	84729	0.28	1.28
180	16.2	13.3	0.68	48126	30081	1.60	84039	0.36	1.36
180	16.2	13.3	0.86	51367	32107	1.60	89669	0.36	1.36
180	16.2	13.3	0.94	52566	32856	1.60	98258	0.33	1.33
180	18.1	14.1	0.68	54033	38599	1.40	99923	0.39	1.39
180	18.1	14.1	0.86	49040	40870	1.20	89713	0.46	1.46
180	18.1	14.1	0.94	50120	41770	1.20	99947	0.42	1.42
241.59	7.7	9.6	0.68	32476	11599	2.80	95054	0.12	1.12
241.59	7.7	9.6	0.86	34964	12490	2.80	99770	0.13	1.13
241.59	7.7	9.6	0.94	33673	12952	2.60	98329	0.13	1.13
241.59	8.1	9.9	0.68	34484	12319	2.80	98371	0.13	1.13
241.59	8.1	9.9	0.86	34592	13308	2.60	90404	0.15	1.15
241.59	8.1	9.9	0.94	35615	13701	2.60	92951	0.15	1.15
241.59	8.5	10.1	0.68	33996	13077	2.60	91441	0.14	1.14

(continued)

(continued)

Direction	Wave (m)	Wave Period (Sec)	Current (cm/s)	Base shear (KN)		RSR	Peak load base shear (KN)	100 year/ peak load	System redun-dancy
				Collapse load (KN)	100 year load (KN)				
241.59	8.5	10.1	0.86	36337	13977	2.60	97703	0.14	1.14
241.59	8.5	10.1	0.94	34756	14482	2.40	75247	0.19	1.19
241.59	8.9	10.2	0.68	35521	13666	2.60	73724	0.19	1.19
241.59	8.9	10.2	0.86	35319	14720	2.40	79422	0.19	1.19
241.59	8.9	10.2	0.94	36219	15095	2.40	93679	0.16	1.16
241.59	9.2	10.3	0.68	36991	14230	2.60	99435	0.14	1.14
241.59	9.2	10.3	0.86	36456	15193	2.40	88003	0.17	1.17
241.59	9.2	10.3	0.94	37725	15721	2.40	78538	0.20	1.20
241.59	9.6	10.9	0.68	36595	15250	2.40	82256	0.19	1.19
241.59	9.6	10.9	0.86	39001	16253	2.40	97447	0.17	1.17
241.59	9.6	10.9	0.94	37009	16826	2.20	77324	0.22	1.22
241.59	11.6	11.4	0.68	39005	19506	2.00	97432	0.20	1.20
241.59	11.6	11.4	0.86	41743	20873	2.00	70911	0.29	1.29
241.59	11.6	11.4	0.94	38631	21467	1.80	94496	0.23	1.23
241.59	13.9	11.9	0.68	42404	26508	1.60	95399	0.28	1.28
241.59	13.9	11.9	0.86	39445	28178	1.40	95778	0.29	1.29
241.59	13.9	11.9	0.94	40725	29091	1.40	98874	0.29	1.29
241.59	16.2	13.3	0.68	44928	37446	1.20	97316	0.38	1.38
241.59	16.2	13.3	0.86	40062	40062	1.00	88089	0.45	1.45
241.59	16.2	13.3	0.94	40892	40892	1.00	98126	0.42	1.42
241.59	18.1	14.1	0.68	37906	47382	0.80	94691	0.50	1.50
241.59	18.1	14.1	0.86	40246	50309	0.80	90554	0.56	1.56
241.59	18.1	14.1	0.94	41110	51389	0.80	92489	0.56	1.56
270	7.7	9.6	0.68	32181	11494	2.80	73594	0.16	1.16
270	7.7	9.6	0.86	32350	12443	2.60	86600	0.14	1.14
270	7.7	9.6	0.94	33563	12909	2.60	87642	0.15	1.15
270	8.1	9.9	0.68	31987	12304	2.60	85932	0.14	1.14
270	8.1	9.9	0.86	34590	13305	2.60	87858	0.15	1.15
270	8.1	9.9	0.94	35665	13718	2.60	90577	0.15	1.15
270	8.5	10.1	0.68	34075	13106	2.60	78547	0.17	1.17
270	8.5	10.1	0.86	33645	14019	2.40	81191	0.17	1.17
270	8.5	10.1	0.94	34853	14523	2.40	87001	0.17	1.17
270	8.9	10.2	0.68	33044	13769	2.40	87971	0.16	1.16
270	8.9	10.2	0.86	35530	14805	2.40	88641	0.17	1.17
270	8.9	10.2	0.94	36507	15211	2.40	85069	0.18	1.18
270	9.2	10.3	0.68	34453	14356	2.40	83150	0.17	1.17
270	9.2	10.3	0.86	36837	15349	2.40	94689	0.16	1.16

(continued)

(continued)

Direction	Wave (m)	Wave Period (Sec)	Current (cm/s)	Base shear (KN)		RSR	Peak load base shear (KN)	100 year/ peak load	System redundancy
				Collapse load (KN)	100 year load (KN)				
270	9.2	10.3	0.94	34903	15866	2.20	85666	0.19	1.19
270	9.6	10.9	0.68	36828	15345	2.40	82759	0.19	1.19
270	9.6	10.9	0.86	36026	16375	2.20	87973	0.19	1.19
270	9.6	10.9	0.94	37274	16942	2.20	91317	0.19	1.19
270	11.6	11.4	0.68	35762	19869	1.80	83352	0.24	1.24
270	11.6	11.4	0.86	38261	21256	1.80	93418	0.23	1.23
270	11.6	11.4	0.94	39345	21860	1.80	91745	0.24	1.24
270	13.9	11.9	0.68	39013	27868	1.40	83628	0.33	1.33
270	13.9	11.9	0.86	41424	29590	1.40	95037	0.31	1.31
270	13.9	11.9	0.94	36621	30518	1.20	91427	0.33	1.33
270	16.2	13.3	0.68	40576	40576	1.00	81044	0.50	1.50
270	16.2	13.3	0.86	34649	43311	0.80	95153	0.46	1.46
270	16.2	13.3	0.94	35344	44181	0.98	88241	0.50	1.50
270	18.1	14.1	0.68	41039	51299	0.80	92228	0.56	1.56
270	18.1	14.1	0.86	43442	54304	0.80	97648	0.56	1.56
270	18.1	14.1	0.94	44405	55506	0.80	99816	0.56	1.56
298.41	7.7	9.6	0.68	32998	11786	2.80	98537	0.12	1.12
298.41	7.7	9.6	0.86	32898	12654	2.60	90845	0.14	1.14
298.41	7.7	9.6	0.94	34064	13105	2.60	93946	0.14	1.14
298.41	8.1	9.9	0.68	32518	12509	2.60	87314	0.14	1.14
298.41	8.1	9.9	0.86	35069	13488	2.60	94097	0.14	1.14
298.41	8.1	9.9	0.94	33359	13902	2.40	78078	0.18	1.18
298.41	8.5	10.1	0.68	34614	13315	2.60	81791	0.16	1.16
298.41	8.5	10.1	0.86	34092	14207	2.40	96224	0.15	1.15
298.41	8.5	10.1	0.94	35286	14704	2.40	96718	0.15	1.15
298.41	8.9	10.2	0.68	33500	13960	2.40	72680	0.19	1.19
298.41	8.9	10.2	0.86	35932	14973	2.40	98648	0.15	1.15
298.41	8.9	10.2	0.94	33783	15358	2.20	94872	0.16	1.16
298.41	9.2	10.3	0.68	34843	14519	2.40	92405	0.16	1.16
298.41	9.2	10.3	0.86	34089	15496	2.20	65021	0.24	1.24
298.41	9.2	10.3	0.94	35217	16009	2.20	89347	0.18	1.18
298.41	9.6	10.9	0.68	34148	15523	2.20	95904	0.16	1.16
298.41	9.6	10.9	0.86	36351	16524	2.20	82682	0.20	1.20
298.41	9.6	10.9	0.94	34168	17085	2.00	95231	0.18	1.18
298.41	11.6	11.4	0.68	35731	19852	1.80	90425	0.22	1.22
298.41	11.6	11.4	0.86	38155	21197	1.80	97231	0.22	1.22
298.41	11.6	11.4	0.94	34854	21785	1.60	99877	0.22	1.22

(continued)

(continued)

Direction	Wave (m)	Wave Period (Sec)	Current (cm/s)	Base shear (KN)		RSR	Peak load base shear (KN)	100 year/ peak load	System redun-dancy
				Collapse load (KN)	100 year load (KN)				
298.41	13.9	11.9	0.68	37323	26659	1.40	95747	0.28	1.28
298.41	13.9	11.9	0.86	39654	28324	1.40	62262	0.45	1.45
298.41	13.9	11.9	0.94	35071	29228	1.20	99102	0.29	1.29
298.41	16.2	13.3	0.68	37462	37462	1.00	97208	0.39	1.39
298.41	16.2	13.3	0.86	40089	40089	1.00	96024	0.42	1.42
298.41	16.2	13.3	0.94	40919	40919	1.00	98020	0.42	1.42
298.41	18.1	14.1	0.68	37999	47502	0.80	94846	0.50	1.50
298.41	18.1	14.1	0.86	50464	40371	1.25	90708	0.45	1.45
298.41	18.1	14.1	0.94	51534	41227	1.25	92613	0.45	1.45

(c) SKO1 Jacket

Direction	Wave (m)	Wave period (Sec)	Current (cm/s)	Base shear (KN)		RSR	Peak load base shear (KN)	100 year/ peak load	System redun-dancy
				Collapse load (KN)	100 year load (KN)				
0	9.9	10.2	0.68	21509	6935	3.10	47775	0.15	1.15
0	9.9	10.2	0.95	22237	8083	2.75	42212	0.19	1.19
0	9.9	10.2	1.05	23389	8500	2.75	46859	0.18	1.18
0	10.4	10.5	0.68	22221	7402	3.00	41360	0.18	1.18
0	10.4	10.5	0.95	23563	8564	2.75	35319	0.24	1.24
0	10.4	10.5	1.05	22636	9051	2.50	41304	0.22	1.22
0	10.9	10.7	0.68	21678	7880	2.75	40036	0.20	1.20
0	10.9	10.7	0.95	22853	9135	2.50	53785	0.17	1.17
0	10.9	10.7	1.05	24123	9644	2.50	41781	0.23	1.23
0	11.4	10.9	0.68	22987	8354	2.75	37111	0.23	1.23
0	11.4	10.9	0.95	24210	9680	2.50	39152	0.25	1.25
0	11.4	10.9	1.05	22822	10141	2.25	41098	0.25	1.25
0	11.9	11.1	0.68	22169	8865	2.50	38805	0.23	1.23
0	11.9	11.1	0.95	22875	10164	2.25	44497	0.23	1.23
0	11.9	11.1	1.05	24150	13411	1.80	42425	0.32	1.32
0	12.4	11.3	0.68	23489	9391	2.50	40986	0.23	1.23
0	12.4	11.3	0.95	24197	10749	2.25	42454	0.25	1.25
0	12.4	11.3	1.05	22667	11331	2.00	42101	0.27	1.27
0	15.0	12.3	0.68	24540	12267	2.00	48441	0.25	1.25
0	15.0	12.3	0.95	24506	13998	1.75	43525	0.32	1.32
0	15.0	12.3	1.05	25499	14568	1.75	46769	0.31	1.31

(continued)

(continued)

Direction	Wave (m)	Wave period (Sec)	Current (cm/s)	Base shear (KN)		RSR	Peak load base shear (KN)	100 year/ peak load	System redundancy
				Collapse load (KN)	100 year load (KN)				
0	17.5	13.2	0.68	23516	15670	1.50	43100	0.36	1.36
0	17.5	13.2	0.95	26406	17602	1.50	43480	0.40	1.40
0	17.5	13.2	1.05	22970	18374	1.25	46225	0.40	1.40
0	20.0	14.0	0.68	24382	19500	1.25	46692	0.42	1.42
0	20.0	14.0	0.95	27244	21793	1.25	48429	0.45	1.45
0	20.0	14.0	1.05	28252	22599	1.25	50345	0.45	1.45
0	22.5	14.7	0.68	27406	27406	1.00	49263	0.56	1.56
0	22.5	14.7	0.95	24252	30318	0.80	41824	0.72	1.72
0	22.5	14.7	1.05	25018	31278	0.80	52340	0.60	1.60
45	9.9	10.2	0.68	16025	9139	1.75	43518	0.21	1.21
45	9.9	10.2	0.95	16303	10832	1.51	45168	0.24	1.24
45	9.9	10.2	1.05	17211	11452	1.50	49285	0.23	1.23
45	10.4	10.5	0.68	17166	9788	1.75	41981	0.23	1.23
45	10.4	10.5	0.95	17282	11499	1.50	44731	0.26	1.26
45	10.4	10.5	1.05	18358	12215	1.50	44261	0.28	1.28
45	10.9	10.7	0.68	18351	10462	1.75	46023	0.23	1.23
45	10.9	10.7	0.95	18497	12307	1.50	48676	0.25	1.25
45	10.9	10.7	1.05	16367	13053	1.25	45198	0.29	1.29
45	11.4	10.9	0.68	16766	11153	1.50	51070	0.22	1.22
45	11.4	10.9	0.95	16420	13094	1.25	46665	0.28	1.28
45	11.4	10.9	1.05	17254	13776	1.25	49476	0.28	1.28
45	11.9	11.1	0.68	17848	11875	1.50	47257	0.25	1.25
45	11.9	11.1	0.95	17284	13783	1.25	49843	0.28	1.28
45	11.9	11.1	1.05	18293	14609	1.25	50615	0.29	1.29
45	12.4	11.3	0.68	18927	12611	1.50	49417	0.26	1.26
45	12.4	11.3	0.95	18283	14601	1.25	49018	0.30	1.30
45	12.4	11.3	1.05	19355	15452	1.25	46621	0.33	1.33
45	15.0	12.3	0.68	16671	16671	1.00	48394	0.34	1.34
45	15.0	12.3	0.95	19170	19170	1.00	51601	0.37	1.37
45	15.0	12.3	1.05	19988	19988	1.00	49207	0.41	1.41
45	17.5	13.2	0.68	17120	21402	0.80	44908	0.48	1.48
45	17.5	13.2	0.95	18132	24881	0.73	46192	0.54	1.54
45	17.5	13.2	1.05	18973	25332	0.75	45300	0.56	1.56
45	20.0	14.0	0.68	19983	26695	0.75	53650	0.50	1.50
45	20.0	14.0	0.95	17989	30065	0.60	49474	0.61	1.61
45	20.0	14.0	1.05	18686	31219	0.60	47488	0.66	1.66
45	22.5	14.7	0.68	17998	36061	0.50	49573	0.73	1.73

(continued)

(continued)

Direction	Wave (m)	Wave period (Sec)	Current (cm/s)	Base shear (KN)		RSR	Peak load base shear (KN)	100 year/ peak load	System redundancy
				Collapse load (KN)	100 year load (KN)				
45	22.5	14.7	0.95	19965	40011	0.50	53997	0.74	1.74
45	22.5	14.7	1.05	20656	41380	0.50	51528	0.80	1.80
90	9.9	10.2	0.68	23197	10294	2.25	42023	0.24	1.24
90	9.9	10.2	0.95	24145	12049	2.00	44982	0.27	1.27
90	9.9	10.2	1.05	22210	12686	1.75	49528	0.26	1.26
90	10.4	10.5	0.68	22060	10997	2.01	43420	0.25	1.25
90	10.4	10.5	0.95	22355	12769	1.75	48229	0.26	1.26
90	10.4	10.5	1.05	23689	13509	1.75	46287	0.29	1.29
90	10.9	10.7	0.68	23723	11838	2.00	51007	0.23	1.23
90	10.9	10.7	0.95	24101	13746	1.75	46923	0.29	1.29
90	10.9	10.7	1.05	21798	14521	1.50	53080	0.27	1.27
90	11.4	10.9	0.68	22055	12566	1.76	48326	0.26	1.26
90	11.4	10.9	0.95	21901	14590	1.50	49983	0.29	1.29
90	11.4	10.9	1.05	22982	15294	1.50	47676	0.32	1.32
90	11.9	11.1	0.68	23419	13359	1.75	50807	0.26	1.26
90	11.9	11.1	0.95	23055	15341	1.50	42749	0.36	1.36
90	11.9	11.1	1.05	24344	16201	1.50	46224	0.35	1.35
90	12.4	11.3	0.68	21492	14317	1.50	41518	0.34	1.34
90	12.4	11.3	0.95	24632	16396	1.50	51216	0.32	1.32
90	12.4	11.3	1.05	21676	17284	1.25	51922	0.33	1.33
90	15.0	12.3	0.68	23557	18818	1.25	48421	0.39	1.39
90	15.0	12.3	0.95	26846	21461	1.25	46156	0.46	1.46
90	15.0	12.3	1.05	22344	22344	1.00	53155	0.42	1.42
90	17.5	13.2	0.68	24133	24133	1.00	50153	0.48	1.48
90	17.5	13.2	0.95	27062	27062	1.00	47429	0.57	1.57
90	17.5	13.2	1.05	28242	28242	1.00	51653	0.55	1.55
90	20.0	14.0	0.68	22541	30091	0.75	54827	0.55	1.55
90	20.0	14.0	0.95	25183	33618	0.75	49499	0.68	1.68
90	20.0	14.0	1.05	26086	34811	0.75	55760	0.62	1.62
90	22.5	14.7	0.68	24805	41569	0.60	46733	0.89	1.89
90	22.5	14.7	0.95	27372	46121	0.59	50433	0.91	1.91
90	22.5	14.7	1.05	23554	49254	0.48	49254	1.00	2.00
135	9.9	10.2	0.68	20344	9026	2.25	42885	0.21	1.21
135	9.9	10.2	0.95	18804	10727	1.75	49880	0.22	1.22
135	9.9	10.2	1.05	19896	11351	1.75	46482	0.24	1.24
135	10.4	10.5	0.68	19458	9713	2.00	39854	0.24	1.24
135	10.4	10.5	0.95	19993	11406	1.75	47752	0.24	1.24

(continued)

(continued)

Direction	Wave (m)	Wave period (Sec)	Current (cm/s)	Base shear (KN)		RSR	Peak load base shear (KN)	100 year/ peak load	System redun-dancy
				Collapse load (KN)	100 year load (KN)				
135	10.4	10.5	1.05	21259	12125	1.75	49738	0.24	1.24
135	10.9	10.7	0.68	20747	10356	2.00	44110	0.23	1.23
135	10.9	10.7	0.95	19564	12208	1.60	41953	0.29	1.29
135	10.9	10.7	1.05	19466	12957	1.50	43639	0.30	1.30
135	11.4	10.9	0.68	19369	11050	1.75	42992	0.26	1.26
135	11.4	10.9	0.95	19529	12999	1.50	41778	0.31	1.31
135	11.4	10.9	1.05	20559	13684	1.50	48277	0.28	1.28
135	11.9	11.1	0.68	20641	11775	1.75	50003	0.24	1.24
135	11.9	11.1	0.95	20569	13691	1.50	37415	0.37	1.37
135	11.9	11.1	1.05	21792	14520	1.50	42959	0.34	1.34
135	12.4	11.3	0.68	18801	12515	1.50	48611	0.26	1.26
135	12.4	11.3	0.95	21780	14512	1.50	47592	0.30	1.30
135	12.4	11.3	1.05	19237	15367	1.25	51826	0.30	1.30
135	15.0	12.3	0.68	20709	16540	1.25	49532	0.33	1.33
135	15.0	12.3	0.95	19099	19099	1.00	51819	0.37	1.37
135	15.0	12.3	1.05	19941	19941	1.00	49903	0.40	1.40
135	17.5	13.2	0.68	21293	21293	1.00	54176	0.39	1.39
135	17.5	13.2	0.95	19308	24161	0.80	45647	0.53	1.53
135	17.5	13.2	1.05	20206	25265	0.80	47765	0.53	1.53
135	20.0	14.0	0.68	19975	26644	0.75	55610	0.48	1.48
135	20.0	14.0	0.95	22451	29957	0.75	44959	0.67	1.67
135	20.0	14.0	1.05	23335	31138	0.75	49110	0.63	1.63
135	22.5	14.7	0.68	21532	35981	0.60	53714	0.67	1.67
135	22.5	14.7	0.95	19995	39956	0.50	49045	0.81	1.81
135	22.5	14.7	1.05	20667	41355	0.50	45398	0.91	1.91
180	9.9	10.2	0.68	24271	6476	3.75	32370	0.20	1.20
180	9.9	10.2	0.95	24354	7479	3.26	37445	0.20	1.20
180	9.9	10.2	1.05	25600	7880	3.25	39295	0.20	1.20
180	10.4	10.5	0.68	24108	6892	3.50	34458	0.20	1.20
180	10.4	10.5	0.95	23804	7938	3.00	36819	0.22	1.22
180	10.4	10.5	1.05	25142	8384	3.00	41871	0.20	1.20
180	10.9	10.7	0.68	23747	7310	3.25	36572	0.20	1.20
180	10.9	10.7	0.95	25376	8461	3.00	48530	0.17	1.17
180	10.9	10.7	1.05	24539	8927	2.75	42408	0.21	1.21
180	11.4	10.9	0.68	23230	7746	3.00	40046	0.19	1.19
180	11.4	10.9	0.95	24632	8960	2.75	43873	0.20	1.20
180	11.4	10.9	1.05	25795	9382	2.75	40785	0.23	1.23

(continued)

(continued)

Direction	Wave (m)	Wave period (Sec)	Current (cm/s)	Base shear (KN)		RSR	Peak load base shear (KN)	100 year/ peak load	System redundancy
				Collapse load (KN)	100 year load (KN)				
180	11.9	11.1	0.68	24631	8214	3.00	44588	0.18	1.18
180	11.9	11.1	0.95	25856	9404	2.75	49885	0.19	1.19
180	11.9	11.1	1.05	24795	9921	2.50	42479	0.23	1.23
180	12.4	11.3	0.68	23907	8697	2.75	43308	0.20	1.20
180	12.4	11.3	0.95	24843	9940	2.50	49774	0.20	1.20
180	12.4	11.3	1.05	26180	10474	2.50	49428	0.21	1.21
180	15.0	12.3	0.68	25494	11333	2.25	45921	0.25	1.25
180	15.0	12.3	0.95	25835	12919	2.00	48650	0.27	1.27
180	15.0	12.3	1.05	26879	13440	2.00	42980	0.31	1.31
180	17.5	13.2	0.68	25289	14453	1.75	44879	0.32	1.32
180	17.5	13.2	0.95	28386	16220	1.75	45955	0.35	1.35
180	17.5	13.2	1.05	25389	16928	1.50	49076	0.34	1.34
180	20.0	14.0	0.68	26945	17963	1.50	44915	0.40	1.40
180	20.0	14.0	0.95	25075	20061	1.25	52487	0.38	1.38
180	20.0	14.0	1.05	25999	20798	1.25	49262	0.42	1.42
180	22.5	14.7	0.68	27637	25119	1.10	43331	0.58	1.58
180	22.5	14.7	0.95	27748	27748	1.00	46543	0.60	1.60
180	22.5	14.7	1.05	28637	28637	1.00	50049	0.57	1.57
225	9.9	10.2	0.68	18677	6783	2.75	34020	0.20	1.20
225	9.9	10.2	0.95	17985	7984	2.25	39954	0.20	1.20
225	9.9	10.2	1.05	18979	8423	2.25	42250	0.20	1.20
225	10.4	10.5	0.68	18151	7252	2.50	36326	0.20	1.20
225	10.4	10.5	0.95	19054	8456	2.25	42409	0.20	1.20
225	10.4	10.5	1.05	17952	8964	2.00	44913	0.20	1.20
225	10.9	10.7	0.68	17392	7720	2.25	38825	0.20	1.20
225	10.9	10.7	0.95	18082	9029	2.00	45032	0.20	1.20
225	10.9	10.7	1.05	19144	9558	2.00	50758	0.19	1.19
225	11.4	10.9	0.68	18497	8210	2.25	41265	0.20	1.20
225	11.4	10.9	0.95	19203	9586	2.00	47751	0.20	1.20
225	11.4	10.9	1.05	20139	10070	2.00	48987	0.21	1.21
225	11.9	11.1	0.68	17467	8722	2.00	43610	0.20	1.20
225	11.9	11.1	0.95	17645	10075	1.75	47220	0.21	1.21
225	11.9	11.1	1.05	18682	10661	1.75	51766	0.21	1.21
225	12.4	11.3	0.68	18514	9243	2.00	53695	0.17	1.17
225	12.4	11.3	0.95	18674	10655	1.75	49623	0.21	1.21
225	12.4	11.3	1.05	19736	11258	1.75	47273	0.24	1.24
225	15.0	12.3	0.68	18157	12085	1.50	49378	0.24	1.24

(continued)

(continued)

Direction	Wave (m)	Wave period (Sec)	Current (cm/s)	Base shear (KN)		RSR	Peak load base shear (KN)	100 year/ peak load	System redundancy
				Collapse load (KN)	100 year load (KN)				
225	15.0	12.3	0.95	20809	13870	1.50	47864	0.29	1.29
225	15.0	12.3	1.05	18100	14465	1.25	49934	0.29	1.29
225	17.5	13.2	0.68	19323	15430	1.25	53870	0.29	1.29
225	17.5	13.2	0.95	21794	17419	1.25	57378	0.30	1.30
225	17.5	13.2	1.05	18267	18267	1.00	49971	0.37	1.37
225	20.0	14.0	0.68	19219	19219	1.00	57947	0.33	1.33
225	20.0	14.0	0.95	21542	21542	1.00	57842	0.37	1.37
225	20.0	14.0	1.05	22383	22383	1.00	57041	0.39	1.39
225	22.5	14.7	0.68	19297	25737	0.75	50835	0.51	1.51
225	22.5	14.7	0.95	21436	28622	0.75	60259	0.47	1.47
225	22.5	14.7	1.05	22179	29633	0.75	57779	0.51	1.51
270	9.9	10.2	0.68	25781	7925	3.25	31892	0.25	1.25
270	9.9	10.2	0.95	24764	9166	2.70	36800	0.25	1.25
270	9.9	10.2	1.05	26477	9617	2.75	42722	0.23	1.23
270	10.4	10.5	0.68	25288	8421	3.00	34215	0.25	1.25
270	10.4	10.5	0.95	26639	9675	2.75	40002	0.24	1.24
270	10.4	10.5	1.05	25522	10199	2.50	43149	0.24	1.24
270	10.9	10.7	0.68	24798	9007	2.75	34495	0.26	1.26
270	10.9	10.7	0.95	25942	10365	2.50	31374	0.33	1.33
270	10.9	10.7	1.05	24595	10913	2.25	38447	0.28	1.28
270	11.4	10.9	0.68	26238	9529	2.75	41832	0.23	1.23
270	11.4	10.9	0.95	24671	10961	2.25	50704	0.22	1.22
270	11.4	10.9	1.05	25813	11459	2.25	39382	0.29	1.29
270	11.9	11.1	0.68	25251	10089	2.50	35445	0.28	1.28
270	11.9	11.1	0.95	25888	11492	2.25	41357	0.28	1.28
270	11.9	11.1	1.05	27264	12100	2.25	36721	0.33	1.33
270	12.4	11.3	0.68	24266	10767	2.25	38498	0.28	1.28
270	12.4	11.3	0.95	24514	12237	2.00	43159	0.28	1.28
270	12.4	11.3	1.05	24483	12866	1.90	40172	0.32	1.32
270	15.0	12.3	0.68	24450	13947	1.75	43328	0.32	1.32
270	15.0	12.3	0.95	27726	15818	1.75	51589	0.31	1.31
270	15.0	12.3	1.05	24692	16435	1.50	44187	0.37	1.37
270	17.5	13.2	0.68	26541	17681	1.50	49056	0.36	1.36
270	17.5	13.2	0.95	24746	19766	1.25	49496	0.40	1.40
270	17.5	13.2	1.05	25785	20597	1.25	52976	0.39	1.39
270	20.0	14.0	0.68	27398	21883	1.25	48175	0.45	1.45
270	20.0	14.0	0.95	26808	24350	1.10	47242	0.52	1.52

(continued)

(continued)

Direction	Wave (m)	Wave period (Sec)	Current (cm/s)	Base shear (KN)		RSR	Peak load base shear (KN)	100 year/ peak load	System redun-dancy
				Collapse load (KN)	100 year load (KN)				
270	20.0	14.0	1.05	25256	25256	1.00	50126	0.50	1.50
270	22.5	14.7	0.68	26901	29901	0.90	44886	0.67	1.67
270	22.5	14.7	0.95	26352	32994	0.80	45691	0.72	1.72
270	22.5	14.7	1.05	25485	34031	0.75	46958	0.72	1.72
315	9.9	10.2	0.68	18864	7252	2.60	31718	0.23	1.23
315	9.9	10.2	0.95	19290	8567	2.25	39418	0.22	1.22
315	9.9	10.2	1.05	20369	9047	2.25	41437	0.22	1.22
315	10.4	10.5	0.68	19429	7767	2.50	34564	0.22	1.22
315	10.4	10.5	0.95	20475	9094	2.25	34345	0.26	1.26
315	10.4	10.5	1.05	19310	9650	2.00	45768	0.21	1.21
315	10.9	10.7	0.68	19062	8281	2.30	47973	0.17	1.17
315	10.9	10.7	0.95	19444	9714	2.00	43645	0.22	1.22
315	10.9	10.7	1.05	20601	10294	2.00	44147	0.23	1.23
315	11.4	10.9	0.68	19851	8818	2.25	40973	0.22	1.22
315	11.4	10.9	0.95	20664	10325	2.00	41037	0.25	1.25
315	11.4	10.9	1.05	19011	10855	1.75	39429	0.28	1.28
315	11.9	11.1	0.68	18770	9377	2.00	33748	0.28	1.28
315	11.9	11.1	0.95	19019	10859	1.75	41412	0.26	1.26
315	11.9	11.1	1.05	20139	11501	1.75	45686	0.25	1.25
315	12.4	11.3	0.68	18918	9949	1.90	34569	0.29	1.29
315	12.4	11.3	0.95	19556	11494	1.70	39256	0.29	1.29
315	12.4	11.3	1.05	19481	12155	1.60	41261	0.29	1.29
315	15.0	12.3	0.68	19604	13059	1.50	49319	0.26	1.26
315	15.0	12.3	0.95	22544	15016	1.50	44292	0.34	1.34
315	15.0	12.3	1.05	20386	15668	1.30	44531	0.35	1.35
315	17.5	13.2	0.68	20917	16722	1.25	41588	0.40	1.40
315	17.5	13.2	0.95	20807	18903	1.10	40571	0.47	1.47
315	17.5	13.2	1.05	19791	19791	1.00	44582	0.44	1.44
315	20.0	14.0	0.68	20844	20844	1.00	45765	0.46	1.46
315	20.0	14.0	0.95	21076	23435	0.90	41996	0.56	1.56
315	20.0	14.0	1.05	21897	24345	0.90	43435	0.56	1.56
315	22.5	14.7	0.68	22517	28156	0.80	41898	0.67	1.67
315	22.5	14.7	0.95	21860	31273	0.70	40360	0.77	1.77
315	22.5	14.7	1.05	22624	32342	0.70	44195	0.73	1.73

(d) SKO2 Jacket

Direction	Wave (m)	Wave period (sec)	Current (cm/s)	Base shear (KN)		RSR	Peak load base shear (KN)	100 year/ peak load	System redun-dancy
				Collapse load (KN)	100 year load (KN)				
0	11.7	10.6	0.55	20870	8151	2.56	39946	0.20	1.20
0	11.7	10.6	0.95	22738	9592	2.37	47147	0.20	1.20
0	11.7	10.6	1.2	23332	10715	2.18	52713	0.20	1.20
0	12.3	11.0	0.55	22163	8649	2.56	42433	0.20	1.20
0	12.3	11.0	0.95	22213	10207	2.18	50222	0.20	1.20
0	12.3	11.0	1.2	24799	11382	2.18	53735	0.21	1.21
0	12.9	11.2	0.55	21859	9226	2.37	45317	0.20	1.20
0	12.9	11.2	0.95	23695	10880	2.18	53585	0.20	1.20
0	12.9	11.2	1.2	23978	12090	1.98	52459	0.23	1.23
0	13.5	11.4	0.55	21357	9818	2.18	48277	0.20	1.20
0	13.5	11.4	0.95	22893	11547	1.98	54639	0.21	1.21
0	13.5	11.4	1.2	25293	12747	1.98	52831	0.24	1.24
0	14.0	11.7	0.55	22438	10309	2.18	48726	0.21	1.21
0	14.0	11.7	0.95	23912	12057	1.98	52320	0.23	1.23
0	14.0	11.7	1.2	23898	13366	1.79	52813	0.25	1.25
0	14.6	11.9	0.55	23818	10937	2.18	53843	0.20	1.20
0	14.6	11.9	0.95	25309	12755	1.98	52868	0.24	1.24
0	14.6	11.9	1.2	25276	14132	1.79	55879	0.25	1.25
0	17.6	13.0	0.55	26607	14871	1.79	58779	0.25	1.25
0	17.6	13.0	0.95	27423	17215	1.59	54610	0.32	1.32
0	17.6	13.0	1.2	30159	18925	1.59	56352	0.34	1.34
0	20.5	14.0	0.55	26984	19332	1.40	61746	0.31	1.31
0	20.5	14.0	0.95	30873	22110	1.40	61480	0.36	1.36
0	20.5	14.0	1.2	28937	24148	1.20	62424	0.39	1.39
0	23.4	14.9	0.55	31391	26193	1.20	67509	0.39	1.39
0	23.4	14.9	0.95	35515	29630	1.20	64917	0.46	1.46
0	23.4	14.9	1.2	32009	32009	1.00	70071	0.46	1.46
45	11.7	10.6	0.55	32084	15121	2.12	45965	0.33	1.33
45	11.7	10.6	0.95	34157	17835	1.92	52289	0.34	1.34
45	11.7	10.6	1.2	36184	19968	1.81	60525	0.33	1.33
45	12.3	11.0	0.55	36436	16398	2.22	45871	0.36	1.36
45	12.3	11.0	0.95	36938	19299	1.91	56571	0.34	1.34
45	12.3	11.0	1.2	39032	21551	1.81	45925	0.47	1.47
45	12.9	11.2	0.55	37396	17650	2.12	52450	0.34	1.34
45	12.9	11.2	0.95	37594	20751	1.81	53971	0.38	1.38
45	12.9	11.2	1.2	39449	23081	1.71	53287	0.43	1.43

(continued)

(continued)

Direction	Wave (m)	Wave period (sec)	Current (cm/s)	Base shear (KN)		RSR	Peak load base shear (KN)	100 year/ peak load	System redun-dancy
				Collapse load (KN)	100 year load (KN)				
45	13.5	11.4	0.55	38192	18946	2.02	58146	0.33	1.33
45	13.5	11.4	0.95	40398	22298	1.81	53962	0.41	1.41
45	13.5	11.4	1.2	42051	24611	1.71	53933	0.46	1.46
45	14.0	11.7	0.55	40596	20147	2.01	49885	0.40	1.40
45	14.0	11.7	0.95	40066	23442	1.71	54434	0.43	1.43
45	14.0	11.7	1.2	41708	25955	1.61	41708	0.62	1.62
45	14.6	11.9	0.55	38760	21400	1.81	47517	0.45	1.45
45	14.6	11.9	0.95	42621	24948	1.71	55249	0.45	1.45
45	14.6	11.9	1.2	41590	27625	1.51	58323	0.47	1.47
45	17.6	13.0	0.55	42812	28440	1.51	57046	0.50	1.50
45	17.6	13.0	0.95	42849	32892	1.30	59452	0.55	1.55
45	17.6	13.0	1.2	43428	36138	1.20	54002	0.67	1.67
45	20.5	14.0	0.55	41791	37963	1.10	59644	0.64	1.64
45	20.5	14.0	0.95	43242	43242	1.00	56594	0.76	1.76
45	20.5	14.0	1.2	42612	47386	0.90	58709	0.81	1.81
45	23.4	14.9	0.55	43927	48845	0.90	63110	0.77	1.77
45	23.4	14.9	0.95	44129	55233	0.80	68883	0.80	1.80
45	23.4	14.9	1.2	47360	59274	0.80	77536	0.76	1.76
90	11.7	10.6	0.55	36066	7361	4.90	36066	0.20	1.20
90	11.7	10.6	0.95	38307	8849	4.33	43507	0.20	1.20
90	11.7	10.6	1.2	37348	9965	3.75	49075	0.20	1.20
90	12.3	11.0	0.55	36069	7986	4.52	39188	0.20	1.20
90	12.3	11.0	0.95	37536	9523	3.94	46870	0.20	1.20
90	12.3	11.0	1.2	38074	10710	3.55	53003	0.20	1.20
90	12.9	11.2	0.55	36875	8524	4.33	41878	0.20	1.20
90	12.9	11.2	0.95	38231	10197	3.75	50494	0.20	1.20
90	12.9	11.2	1.2	38385	11421	3.36	54231	0.21	1.21
90	13.5	11.4	0.55	37547	9082	4.13	44672	0.20	1.20
90	13.5	11.4	0.95	38650	10870	3.56	53646	0.20	1.20
90	13.5	11.4	1.2	38311	12100	3.17	50101	0.24	1.24
90	14.0	11.7	0.55	38190	9687	3.94	47692	0.20	1.20
90	14.0	11.7	0.95	38639	11495	3.36	52379	0.22	1.22
90	14.0	11.7	1.2	38107	12826	2.97	51792	0.25	1.25
90	14.6	11.9	0.55	38865	10365	3.75	47923	0.22	1.22
90	14.6	11.9	0.95	38673	12213	3.17	53851	0.23	1.23
90	14.6	11.9	1.2	37779	13612	2.78	56986	0.24	1.24
90	17.6	13.0	0.55	37866	14678	2.58	55245	0.27	1.27

(continued)

(continued)

Direction	Wave (m)	Wave period (sec)	Current (cm/s)	Base shear (KN)		RSR	Peak load base shear (KN)	100 year/ peak load	System redun-dancy
				Collapse load (KN)	100 year load (KN)				
90	17.6	13.0	0.95	40798	17108	2.38	61286	0.28	1.28
90	17.6	13.0	1.2	41282	18866	2.19	59999	0.31	1.31
90	20.5	14.0	0.55	38594	19390	1.99	61050	0.32	1.32
90	20.5	14.0	0.95	39926	22266	1.79	58064	0.38	1.38
90	20.5	14.0	1.2	38887	24374	1.60	63194	0.39	1.39
90	23.4	14.9	0.55	42861	26858	1.60	63998	0.42	1.42
90	23.4	14.9	0.95	42485	30402	1.40	66737	0.46	1.46
90	23.4	14.9	1.2	39388	32855	1.20	72155	0.46	1.46
135	11.7	10.6	0.55	30627	7875	3.89	38213	0.21	1.21
135	11.7	10.6	0.95	32366	9201	3.52	44844	0.21	1.21
135	11.7	10.6	1.2	34237	10275	3.33	50216	0.20	1.20
135	12.3	11.0	0.55	30936	8356	3.70	40618	0.21	1.21
135	12.3	11.0	0.95	32766	9843	3.33	48054	0.20	1.20
135	12.3	11.0	1.2	34451	10966	3.14	53675	0.20	1.20
135	12.9	11.2	0.55	31402	8933	3.52	43504	0.21	1.21
135	12.9	11.2	0.95	33019	10518	3.14	51435	0.20	1.20
135	12.9	11.2	1.2	34449	11677	2.95	57139	0.20	1.20
135	13.5	11.4	0.55	31726	9537	3.33	46525	0.20	1.20
135	13.5	11.4	0.95	33015	11199	2.95	54850	0.20	1.20
135	13.5	11.4	1.2	34050	12348	2.76	55638	0.22	1.22
135	14.0	11.7	0.55	33466	10048	3.33	49086	0.20	1.20
135	14.0	11.7	0.95	34589	11723	2.95	57462	0.20	1.20
135	14.0	11.7	1.2	35820	12980	2.76	58706	0.22	1.22
135	14.6	11.9	0.55	33463	10657	3.14	52142	0.20	1.20
135	14.6	11.9	0.95	34189	12398	2.76	58370	0.21	1.21
135	14.6	11.9	1.2	35201	13718	2.57	45942	0.30	1.30
135	17.6	13.0	0.55	37070	14437	2.57	54043	0.27	1.27
135	17.6	13.0	0.95	39652	16692	2.38	59389	0.28	1.28
135	17.6	13.0	1.2	39994	18338	2.18	61661	0.30	1.30
135	20.5	14.0	0.55	40962	18776	2.18	59587	0.32	1.32
135	20.5	14.0	0.95	42606	21448	1.99	72203	0.30	1.30
135	20.5	14.0	1.2	41912	23413	1.79	69680	0.34	1.34
135	23.4	14.9	0.55	40272	25279	1.59	65366	0.39	1.39
135	23.4	14.9	0.95	39837	28538	1.40	73755	0.39	1.39
135	23.4	14.9	1.2	43001	30798	1.40	79654	0.39	1.39
180	11.7	10.6	0.55	24913	7812	3.19	38904	0.20	1.20
180	11.7	10.6	0.95	27693	9257	2.99	46127	0.20	1.20

(continued)

(continued)

Direction	Wave (m)	Wave period (sec)	Current (cm/s)	Base shear (KN)		RSR	Peak load base shear (KN)	100 year/ peak load	System redundancy
				Collapse load (KN)	100 year load (KN)				
180	11.7	10.6	1.2	28999	10382	2.79	51752	0.20	1.20
180	12.3	11.0	0.55	26508	8310	3.19	41395	0.20	1.20
180	12.3	11.0	0.95	27475	9838	2.79	49029	0.20	1.20
180	12.3	11.0	1.2	28615	11030	2.59	54946	0.20	1.20
180	12.9	11.2	0.55	26651	8910	2.99	44390	0.20	1.20
180	12.9	11.2	0.95	27336	10538	2.59	52530	0.20	1.20
180	12.9	11.2	1.2	28185	11767	2.40	58660	0.20	1.20
180	13.5	11.4	0.55	26638	9539	2.79	45696	0.21	1.21
180	13.5	11.4	0.95	29276	11284	2.59	56254	0.20	1.20
180	13.5	11.4	1.2	29924	12491	2.40	50239	0.25	1.25
180	14.0	11.7	0.55	28056	10045	2.79	50067	0.20	1.20
180	14.0	11.7	0.95	28289	11810	2.40	58881	0.20	1.20
180	14.0	11.7	1.2	31454	13128	2.40	62816	0.21	1.21
180	14.6	11.9	0.55	27684	10672	2.59	53198	0.20	1.20
180	14.6	11.9	0.95	29965	12508	2.40	62290	0.20	1.20
180	14.6	11.9	1.2	30520	13894	2.20	58113	0.24	1.24
180	17.6	13.0	0.55	31971	14554	2.20	63836	0.23	1.23
180	17.6	13.0	0.95	33785	16912	2.00	64084	0.26	1.26
180	17.6	13.0	1.2	33502	18630	1.80	70569	0.26	1.26
180	20.5	14.0	0.55	34200	19017	1.80	68425	0.28	1.28
180	20.5	14.0	0.95	34879	21814	1.60	69598	0.31	1.31
180	20.5	14.0	1.2	38161	23865	1.60	76404	0.31	1.31
180	23.4	14.9	0.55	41590	26009	1.60	72775	0.36	1.36
180	23.4	14.9	0.95	41189	29432	1.40	82031	0.36	1.36
180	23.4	14.9	1.2	44509	31804	1.40	76218	0.42	1.42
225	11.7	10.6	0.55	30000	7716	3.89	37429	0.21	1.21
225	11.7	10.6	0.95	31819	9047	3.52	44083	0.21	1.21
225	11.7	10.6	1.2	31781	10130	3.14	50137	0.20	1.20
225	12.3	11.0	0.55	30383	8208	3.70	39889	0.21	1.21
225	12.3	11.0	0.95	32152	9660	3.33	47153	0.20	1.20
225	12.3	11.0	1.2	33896	10791	3.14	50318	0.21	1.21
225	12.9	11.2	0.55	30790	8761	3.51	42652	0.21	1.21
225	12.9	11.2	0.95	32347	10306	3.14	50432	0.20	1.20
225	12.9	11.2	1.2	33838	11471	2.95	51780	0.22	1.22
225	13.5	11.4	0.55	30903	9293	3.33	45316	0.21	1.21
225	13.5	11.4	0.95	32319	10965	2.95	49491	0.22	1.22
225	13.5	11.4	1.2	33418	12120	2.76	54103	0.22	1.22

(continued)

(continued)

Direction	Wave (m)	Wave period (sec)	Current (cm/s)	Base shear (KN)		RSR	Peak load base shear (KN)	100 year/ peak load	System redun-dancy
				Collapse load (KN)	100 year load (KN)				
225	14.0	11.7	0.55	30664	9780	3.14	47869	0.20	1.20
225	14.0	11.7	0.95	31595	11469	2.75	56275	0.20	1.20
225	14.0	11.7	1.2	35132	12732	2.76	57957	0.22	1.22
225	14.6	11.9	0.55	30588	10388	2.94	47514	0.22	1.22
225	14.6	11.9	0.95	33489	12145	2.76	52609	0.23	1.23
225	14.6	11.9	1.2	34580	13477	2.57	56813	0.24	1.24
225	17.6	13.0	0.55	33797	14251	2.37	56215	0.25	1.25
225	17.6	13.0	0.95	35798	16429	2.18	64356	0.26	1.26
225	17.6	13.0	1.2	35870	10879	3.30	64386	0.17	1.17
225	20.5	14.0	0.55	33058	18494	1.79	62548	0.30	1.30
225	20.5	14.0	0.95	33715	21180	1.59	65873	0.32	1.32
225	20.5	14.0	1.2	36872	23153	1.59	61930	0.37	1.37
225	23.4	14.9	0.55	34734	24892	1.40	62226	0.40	1.40
225	23.4	14.9	0.95	33742	28166	1.20	54856	0.51	1.51
225	23.4	14.9	1.2	36466	30436	1.20	72658	0.42	1.42
270	11.7	10.6	0.55	22518	7658	2.94	37440	0.20	1.20
270	11.7	10.6	0.95	23324	9111	2.56	44355	0.21	1.21
270	11.7	10.6	1.2	24272	10246	2.37	42289	0.24	1.24
270	12.3	11.0	0.55	22460	8168	2.75	39892	0.20	1.20
270	12.3	11.0	0.95	24962	9742	2.56	42226	0.23	1.23
270	12.3	11.0	1.2	25909	10928	2.37	45344	0.24	1.24
270	12.9	11.2	0.55	24020	8725	2.75	39595	0.22	1.22
270	12.9	11.2	0.95	24633	10397	2.37	43073	0.24	1.24
270	12.9	11.2	1.2	25285	11618	2.18	47211	0.25	1.25
270	13.5	11.4	0.55	23851	9314	2.56	40400	0.23	1.23
270	13.5	11.4	0.95	24066	11063	2.18	45501	0.24	1.24
270	13.5	11.4	1.2	26721	12270	2.18	45206	0.27	1.27
270	14.0	11.7	0.55	23259	9824	2.37	40012	0.25	1.25
270	14.0	11.7	0.95	25198	11578	2.18	44840	0.26	1.26
270	14.0	11.7	1.2	25614	12921	1.98	45902	0.28	1.28
270	14.6	11.9	0.55	24758	10449	2.37	41217	0.25	1.25
270	14.6	11.9	0.95	26841	12325	2.18	45968	0.27	1.27
270	14.6	11.9	1.2	27245	13736	1.98	49006	0.28	1.28
270	17.6	13.0	0.55	26632	14897	1.79	47368	0.31	1.31
270	17.6	13.0	0.95	27482	17262	1.59	47474	0.36	1.36
270	17.6	13.0	1.2	26562	19037	1.40	52972	0.36	1.36
270	20.5	14.0	0.55	27328	19585	1.40	50440	0.39	1.39

(continued)

(continued)

Direction	Wave (m)	Wave period (sec)	Current (cm/s)	Base shear (KN)		RSR	Peak load base shear (KN)	100 year/ peak load	System redun-dancy
				Collapse load (KN)	100 year load (KN)				
270	20.5	14.0	0.95	26898	22453	1.20	53694	0.42	1.42
270	20.5	14.0	1.2	29422	24556	1.20	58264	0.42	1.42
270	23.4	14.9	0.55	26915	26915	1.00	53635	0.50	1.50
270	23.4	14.9	0.95	30477	30477	1.00	58929	0.52	1.52
270	23.4	14.9	1.2	32941	32941	1.00	59242	0.56	1.56
315	11.7	10.6	0.55	22300	7625	2.92	36977	0.21	1.21
315	11.7	10.6	0.95	24565	8958	2.74	43643	0.21	1.21
315	11.7	10.6	1.2	25635	10037	2.55	49052	0.20	1.20
315	12.3	11.0	0.55	23738	8104	2.93	39374	0.21	1.21
315	12.3	11.0	0.95	24379	9553	2.55	46624	0.20	1.20
315	12.3	11.0	1.2	27303	10678	2.56	52250	0.20	1.20
315	12.9	11.2	0.55	23671	8639	2.74	42048	0.21	1.21
315	12.9	11.2	0.95	26028	10188	2.55	49812	0.20	1.20
315	12.9	11.2	1.2	26824	11344	2.36	52746	0.22	1.22
315	13.5	11.4	0.55	23411	9181	2.55	44767	0.21	1.21
315	13.5	11.4	0.95	25606	10837	2.36	50704	0.21	1.21
315	13.5	11.4	1.2	28357	11983	2.37	47072	0.25	1.25
315	14.0	11.7	0.55	24684	9671	2.55	47234	0.20	1.20
315	14.0	11.7	0.95	26820	11343	2.36	53486	0.21	1.21
315	14.0	11.7	1.2	27369	12597	2.17	54593	0.23	1.23
315	14.6	11.9	0.55	26258	10276	2.56	50257	0.20	1.20
315	14.6	11.9	0.95	26091	12016	2.17	54122	0.22	1.22
315	14.6	11.9	1.2	28994	13336	2.17	58380	0.23	1.23
315	17.6	13.0	0.55	27920	14104	1.98	52910	0.27	1.27
315	17.6	13.0	0.95	29209	16355	1.79	58718	0.28	1.28
315	17.6	13.0	1.2	32167	17998	1.79	60102	0.30	1.30
315	20.5	14.0	0.55	32965	18442	1.79	54704	0.34	1.34
315	20.5	14.0	0.95	33604	21110	1.59	62072	0.34	1.34
315	20.5	14.0	1.2	32186	20372	1.58	62696	0.32	1.32
315	23.4	14.9	0.55	34588	24788	1.40	63404	0.39	1.39
315	23.4	14.9	0.95	33632	28075	1.20	61557	0.46	1.46
315	23.4	14.9	1.2	36365	30352	1.20	66438	0.46	1.46

(e) SKO2a Jacket

Direction	Wave (m)	Wave period (Sec)	Current (cm/s)	Base shear (KN)		RSR	Peak load (KN)	100 year/ peak load	System redun-dancy
				Collapse load (KN)	100 year load (KN)				
0	11.7	10.6	0.55	20857	8140	2.56	39790	0.20	1.20
0	11.7	10.6	0.95	22723	9597	2.37	38571	0.25	1.25
0	11.7	10.6	1.2	23318	10694	2.18	38740	0.28	1.28
0	12.3	11.0	0.55	20808	8802	2.36	40736	0.22	1.22
0	12.3	11.0	0.95	22477	10325	2.18	40274	0.26	1.26
0	12.3	11.0	1.2	22601	11382	1.99	42670	0.27	1.27
0	12.9	11.2	0.55	20543	9466	2.17	40684	0.23	1.23
0	12.9	11.2	0.95	21791	11018	1.98	31697	0.35	1.35
0	12.9	11.2	1.2	24192	12218	1.98	36192	0.34	1.34
0	13.5	11.4	0.55	19989	10097	1.98	32829	0.31	1.31
0	13.5	11.4	0.95	20995	11771	1.78	41668	0.28	1.28
0	13.5	11.4	1.2	23071	12925	1.78	40418	0.32	1.32
0	14.0	11.7	0.55	21174	10709	1.98	41265	0.26	1.26
0	14.0	11.7	0.95	22034	12528	1.76	32034	0.39	1.39
0	14.0	11.7	1.2	24290	13602	1.79	42784	0.32	1.32
0	14.6	11.9	0.55	20285	11378	1.78	40183	0.28	1.28
0	14.6	11.9	0.95	20801	13091	1.59	40846	0.32	1.32
0	14.6	11.9	1.2	22819	14351	1.59	42323	0.34	1.34
0	17.6	13.0	0.55	22955	16459	1.39	39115	0.42	1.42
0	17.6	13.0	0.95	22326	18631	1.20	35600	0.52	1.52
0	17.6	13.0	1.2	24119	20118	1.20	39991	0.50	1.50
0	20.5	14.0	0.55	23633	19711	1.20	39096	0.50	1.50
0	20.5	14.0	0.95	26501	22126	1.20	39536	0.56	1.56
0	20.5	14.0	1.2	23785	23785	1.00	39000	0.61	1.61
0	23.4	14.9	0.55	28195	28195	1.00	39275	0.72	1.72
0	23.4	14.9	0.95	30687	30687	1.00	36750	0.84	1.84
0	23.4	14.9	1.2	26238	32726	0.80	39154	0.84	1.84
45	11.7	10.6	0.55	31418	8001	3.93	31878	0.25	1.25
45	11.7	10.6	0.95	31934	9360	3.41	34302	0.27	1.27
45	11.7	10.6	1.2	33130	10382	3.19	38053	0.27	1.27
45	12.3	11.0	0.55	31506	8640	3.65	31506	0.27	1.27
45	12.3	11.0	0.95	32048	10070	3.18	36801	0.27	1.27
45	12.3	11.0	1.2	35666	11208	3.18	38310	0.29	1.29
45	12.9	11.2	0.55	29976	9274	3.23	36037	0.26	1.26
45	12.9	11.2	0.95	31781	10751	2.96	36889	0.29	1.29
45	12.9	11.2	1.2	32353	11971	2.70	37827	0.32	1.32

(continued)

(continued)

Direction	Wave (m)	Wave period (Sec)	Current (cm/s)	Base shear (KN)		RSR	Peak load (KN)	100 year/ peak load	System redun-dancy
				Collapse load (KN)	100 year load (KN)				
45	13.5	11.4	0.55	31471	9900	3.18	36189	0.27	1.27
45	13.5	11.4	0.95	34084	11580	2.94	36825	0.31	1.31
45	13.5	11.4	1.2	34444	12732	2.71	37517	0.34	1.34
45	14.0	11.7	0.55	32741	11059	2.96	32741	0.34	1.34
45	14.0	11.7	0.95	32844	12150	2.70	37377	0.33	1.33
45	14.0	11.7	1.2	33022	13401	2.46	37991	0.35	1.35
45	14.6	11.9	0.55	28326	10453	2.71	29285	0.36	1.36
45	14.6	11.9	0.95	31766	12900	2.46	37885	0.34	1.34
45	14.6	11.9	1.2	31628	14235	2.22	38252	0.37	1.37
45	17.6	13.0	0.55	32535	14640	2.22	36098	0.41	1.41
45	17.6	13.0	0.95	31568	18165	1.74	32532	0.56	1.56
45	17.6	13.0	1.2	34083	19648	1.73	34083	0.58	1.58
45	20.5	14.0	0.55	34089	19679	1.73	34089	0.58	1.58
45	20.5	14.0	0.95	32772	21962	1.49	32772	0.67	1.67
45	20.5	14.0	1.2	35012	23468	1.49	35012	0.67	1.67
45	23.4	14.9	0.55	32654	26432	1.24	32654	0.81	1.81
45	23.4	14.9	0.95	35643	28633	1.24	35643	0.80	1.80
45	23.4	14.9	1.2	30500	30500	1.00	30500	1.00	2.00
90	11.7	10.6	0.55	28777	7296	3.94	35903	0.20	1.20
90	11.7	10.6	0.95	29536	8745	3.38	36432	0.24	1.24
90	11.7	10.6	1.2	29422	9869	2.98	29422	0.34	1.34
90	12.3	11.0	0.55	29829	7929	3.76	36031	0.22	1.22
90	12.3	11.0	0.95	30113	9472	3.18	39395	0.24	1.24
90	12.3	11.0	1.2	29399	10537	2.79	29399	0.36	1.36
90	12.9	11.2	0.55	28803	8543	3.37	35489	0.24	1.24
90	12.9	11.2	0.95	30116	10100	2.98	40045	0.25	1.25
90	12.9	11.2	1.2	29284	11252	2.60	38219	0.29	1.29
90	13.5	11.4	0.55	29058	9140	3.18	38078	0.24	1.24
90	13.5	11.4	0.95	30135	10790	2.79	40759	0.26	1.26
90	13.5	11.4	1.2	28649	12038	2.38	38089	0.32	1.32
90	14.0	11.7	0.55	28941	9712	2.98	33352	0.29	1.29
90	14.0	11.7	0.95	29396	11304	2.60	33873	0.33	1.33
90	14.0	11.7	1.2	30249	12562	2.41	40159	0.31	1.31
90	14.6	11.9	0.55	30702	10289	2.98	30702	0.34	1.34
90	14.6	11.9	0.95	28977	12172	2.38	38485	0.32	1.32
90	14.6	11.9	1.2	29337	13426	2.19	39228	0.34	1.34
90	17.6	13.0	0.55	31384	15771	1.99	37948	0.42	1.42

(continued)

(continued)

Direction	Wave (m)	Wave period (Sec)	Current (cm/s)	Base shear (KN)		RSR	Peak load (KN)	100 year/ peak load	System redun-dancy
				Collapse load (KN)	100 year load (KN)				
90	17.6	13.0	0.95	28808	18069	1.59	35941	0.50	1.50
90	17.6	13.0	1.2	31269	19597	1.60	35799	0.55	1.55
90	20.5	14.0	0.55	30598	19174	1.60	34353	0.56	1.56
90	20.5	14.0	0.95	30243	21629	1.40	34496	0.63	1.63
90	20.5	14.0	1.2	32697	23420	1.40	37337	0.63	1.63
90	23.4	14.9	0.55	33226	27725	1.20	38814	0.71	1.71
90	23.4	14.9	0.95	30327	30327	1.00	36199	0.84	1.84
90	23.4	14.9	1.2	32429	32429	1.00	32429	1.00	2.00
135	11.7	10.6	0.55	30452	7778	3.92	30452	0.26	1.26
135	11.7	10.6	0.95	32196	9045	3.56	35665	0.25	1.25
135	11.7	10.6	1.2	32069	10109	3.17	35954	0.28	1.28
135	12.3	11.0	0.55	31056	8313	3.74	32635	0.25	1.25
135	12.3	11.0	0.95	32815	9754	3.36	32815	0.30	1.30
135	12.3	11.0	1.2	32041	10787	2.97	36159	0.30	1.30
135	12.9	11.2	0.55	29955	8924	3.36	35147	0.25	1.25
135	12.9	11.2	0.95	32928	10462	3.15	32928	0.32	1.32
135	12.9	11.2	1.2	31973	11577	2.76	36326	0.32	1.32
135	13.5	11.4	0.55	30167	9539	3.16	33681	0.28	1.28
135	13.5	11.4	0.95	30884	11192	2.76	35233	0.32	1.32
135	13.5	11.4	1.2	31454	12262	2.57	36132	0.34	1.34
135	14.0	11.7	0.55	30003	10168	2.95	30003	0.34	1.34
135	14.0	11.7	0.95	32424	11743	2.76	33689	0.35	1.35
135	14.0	11.7	1.2	33258	12947	2.57	35767	0.36	1.36
135	14.6	11.9	0.55	29792	10801	2.76	36698	0.29	1.29
135	14.6	11.9	0.95	31929	12447	2.57	36568	0.34	1.34
135	14.6	11.9	1.2	32440	13658	2.38	35053	0.39	1.39
135	17.6	13.0	0.55	30814	15531	1.98	33719	0.46	1.46
135	17.6	13.0	0.95	31538	17625	1.79	34688	0.51	1.51
135	17.6	13.0	1.2	34114	19051	1.79	34114	0.56	1.56
135	20.5	14.0	0.55	29725	18656	1.59	33279	0.56	1.56
135	20.5	14.0	0.95	33390	20978	1.59	33390	0.63	1.63
135	20.5	14.0	1.2	31468	22560	1.39	35750	0.63	1.63
135	23.4	14.9	0.55	31741	26539	1.20	31741	0.84	1.84
135	23.4	14.9	0.95	31710	28875	1.10	33052	0.87	1.87
135	23.4	14.9	1.2	32352	30826	1.05	33863	0.91	1.91
180	11.7	10.6	0.55	24769	7717	3.21	38621	0.20	1.20
180	11.7	10.6	0.95	25708	9160	2.81	38511	0.24	1.24

(continued)

(continued)

Direction	Wave (m)	Wave period (Sec)	Current (cm/s)	Base shear (KN)		RSR	Peak load (KN)	100 year/ peak load	System redun-dancy
				Collapse load (KN)	100 year load (KN)				
180	11.7	10.6	1.2	26789	10251	2.61	37207	0.28	1.28
180	12.3	11.0	0.55	25094	8348	3.01	38418	0.22	1.22
180	12.3	11.0	0.95	25675	9862	2.60	41158	0.24	1.24
180	12.3	11.0	1.2	26309	10949	2.40	41597	0.26	1.26
180	12.9	11.2	0.55	25164	8976	2.80	37634	0.24	1.24
180	12.9	11.2	0.95	25358	10554	2.40	40077	0.26	1.26
180	12.9	11.2	1.2	28273	11767	2.40	39991	0.29	1.29
180	13.5	11.4	0.55	25036	9602	2.61	38450	0.25	1.25
180	13.5	11.4	0.95	27170	11308	2.40	38435	0.29	1.29
180	13.5	11.4	1.2	27487	12481	2.20	39917	0.31	1.31
180	14.0	11.7	0.55	24730	10293	2.40	39088	0.26	1.26
180	14.0	11.7	0.95	26307	11945	2.20	40558	0.29	1.29
180	14.0	11.7	1.2	26437	13205	2.00	36437	0.36	1.36
180	14.6	11.9	0.55	24133	10957	2.20	39414	0.28	1.28
180	14.6	11.9	0.95	25392	12683	2.00	40570	0.31	1.31
180	14.6	11.9	1.2	27927	13950	2.00	39059	0.36	1.36
180	17.6	13.0	0.55	25447	15888	1.60	38066	0.42	1.42
180	17.6	13.0	0.95	28792	17973	1.60	39517	0.45	1.45
180	17.6	13.0	1.2	27305	19500	1.40	38938	0.50	1.50
180	20.5	14.0	0.55	26895	19207	1.40	38331	0.50	1.50
180	20.5	14.0	0.95	30251	21603	1.40	38833	0.56	1.56
180	20.5	14.0	1.2	27913	23249	1.20	37181	0.63	1.63
180	23.4	14.9	0.55	33227	27692	1.20	33227	0.83	1.83
180	23.4	14.9	0.95	30158	30158	1.00	36161	0.83	1.83
180	23.4	14.9	1.2	32242	32242	1.00	38571	0.84	1.84
225	11.7	10.6	0.55	22393	7632	2.93	29516	0.26	1.26
225	11.7	10.6	0.95	22013	8957	2.46	30561	0.29	1.29
225	11.7	10.6	1.2	24722	10037	2.46	29586	0.34	1.34
225	12.3	11.0	0.55	22184	8220	2.70	28115	0.29	1.29
225	12.3	11.0	0.95	23745	9645	2.46	26085	0.37	1.37
225	12.3	11.0	1.2	23720	10674	2.22	28888	0.37	1.37
225	12.9	11.2	0.55	21714	8829	2.46	28098	0.31	1.31
225	12.9	11.2	0.95	22795	10263	2.22	30072	0.34	1.34
225	12.9	11.2	1.2	25377	11416	2.22	30799	0.37	1.37
225	13.5	11.4	0.55	23210	9431	2.46	30021	0.31	1.31
225	13.5	11.4	0.95	24389	10977	2.22	29715	0.37	1.37
225	13.5	11.4	1.2	23931	12083	1.98	29805	0.41	1.41

(continued)

(continued)

Direction	Wave (m)	Wave period (Sec)	Current (cm/s)	Base shear (KN)		RSR	Peak load (KN)	100 year/ peak load	System redun-dancy
				Collapse load (KN)	100 year load (KN)				
225	14.0	11.7	0.55	24586	9984	2.46	29258	0.34	1.34
225	14.0	11.7	0.95	22800	11516	1.98	28398	0.41	1.41
225	14.0	11.7	1.2	25202	12719	1.98	28302	0.45	1.45
225	14.6	11.9	0.55	23540	10598	2.22	28680	0.37	1.37
225	14.6	11.9	0.95	24158	12199	1.98	30071	0.41	1.41
225	14.6	11.9	1.2	23315	13414	1.74	29837	0.45	1.45
225	17.6	13.0	0.55	22903	15362	1.49	26641	0.58	1.58
225	17.6	13.0	0.95	26052	17470	1.49	31700	0.55	1.55
225	17.6	13.0	1.2	23559	18906	1.25	28191	0.67	1.67
225	20.5	14.0	0.55	23093	18535	1.25	27633	0.67	1.67
225	20.5	14.0	0.95	25837	20743	1.25	25837	0.80	1.80
225	20.5	14.0	1.2	27812	22333	1.25	27812	0.80	1.80
225	23.4	14.9	0.55	19408	25758	0.75	25758	1.00	2.00
225	23.4	14.9	0.95	21172	28099	0.75	28099	1.00	2.00
225	23.4	14.9	1.2	22636	29754	0.76	29754	1.00	2.00
270	11.7	10.6	0.55	24117	7616	3.17	30796	0.25	1.25
270	11.7	10.6	0.95	23221	9066	2.56	36697	0.25	1.25
270	11.7	10.6	1.2	22173	10198	2.17	32130	0.32	1.32
270	12.3	11.0	0.55	22562	8197	2.75	32021	0.26	1.26
270	12.3	11.0	0.95	23094	9750	2.37	32593	0.30	1.30
270	12.3	11.0	1.2	23565	10831	2.18	32035	0.34	1.34
270	12.9	11.2	0.55	22661	8849	2.56	32956	0.27	1.27
270	12.9	11.2	0.95	22523	10360	2.17	32619	0.32	1.32
270	12.9	11.2	1.2	22914	11570	1.98	31982	0.36	1.36
270	13.5	11.4	0.55	22337	9433	2.37	31533	0.30	1.30
270	13.5	11.4	0.95	24091	11070	2.18	32744	0.34	1.34
270	13.5	11.4	1.2	24240	12230	1.98	33878	0.36	1.36
270	14.0	11.7	0.55	21625	9949	2.17	31322	0.32	1.32
270	14.0	11.7	0.95	22999	11608	1.98	32074	0.36	1.36
270	14.0	11.7	1.2	22993	12875	1.79	32993	0.39	1.39
270	14.6	11.9	0.55	22990	10568	2.18	31236	0.34	1.34
270	14.6	11.9	0.95	24379	12299	1.98	32540	0.38	1.38
270	14.6	11.9	1.2	24262	13578	1.79	38070	0.36	1.36
270	17.6	13.0	0.55	22304	15995	1.39	31661	0.51	1.51
270	17.6	13.0	0.95	25550	18320	1.39	37172	0.49	1.49
270	17.6	13.0	1.2	23800	19873	1.20	31637	0.63	1.63
270	20.5	14.0	0.55	23404	19541	1.20	31094	0.63	1.63

(continued)

(continued)

Direction	Wave (m)	Wave period (Sec)	Current (cm/s)	Base shear (KN)		RSR	Peak load (KN)	100 year/ peak load	System redun-dancy
				Collapse load (KN)	100 year load (KN)				
270	20.5	14.0	0.95	22007	22007	1.00	30708	0.72	1.72
270	20.5	14.0	1.2	23717	23717	1.00	33111	0.72	1.72
270	23.4	14.9	0.55	22278	27778	0.80	32778	0.85	1.85
270	23.4	14.9	0.95	24322	30323	0.80	30323	1.00	2.00
270	23.4	14.9	1.2	25963	32398	0.80	32398	1.00	2.00
315	11.7	10.6	0.55	22236	7624	2.92	30951	0.25	1.25
315	11.7	10.6	0.95	22768	8954	2.54	31240	0.29	1.29
315	11.7	10.6	1.2	25563	10028	2.55	31282	0.32	1.32
315	12.3	11.0	0.55	22385	8199	2.73	30188	0.27	1.27
315	12.3	11.0	0.95	22650	9623	2.35	24542	0.39	1.39
315	12.3	11.0	1.2	25109	10647	2.36	31219	0.34	1.34
315	12.9	11.2	0.55	22359	8795	2.54	30695	0.29	1.29
315	12.9	11.2	0.95	24107	10232	2.36	26107	0.39	1.39
315	12.9	11.2	1.2	24652	11378	2.17	28366	0.40	1.40
315	13.5	11.4	0.55	22064	9379	2.35	30897	0.30	1.30
315	13.5	11.4	0.95	23684	10938	2.17	31987	0.34	1.34
315	13.5	11.4	1.2	23762	12039	1.97	33074	0.36	1.36
315	14.0	11.7	0.55	21413	9907	2.16	30937	0.32	1.32
315	14.0	11.7	0.95	22637	11478	1.97	31509	0.36	1.36
315	14.0	11.7	1.2	25039	12678	1.97	27486	0.46	1.46
315	14.6	11.9	0.55	22778	10527	2.16	30886	0.34	1.34
315	14.6	11.9	0.95	24019	12168	1.97	31002	0.39	1.39
315	14.6	11.9	1.2	23828	13376	1.78	31614	0.42	1.42
315	17.6	13.0	0.55	24518	15435	1.59	30514	0.51	1.51
315	17.6	13.0	0.95	24370	17502	1.39	31187	0.56	1.56
315	17.6	13.0	1.2	26307	18887	1.39	29976	0.63	1.63
315	20.5	14.0	0.55	25828	18544	1.39	29442	0.63	1.63
315	20.5	14.0	0.95	24853	20763	1.20	28922	0.72	1.72
315	20.5	14.0	1.2	26770	22365	1.20	31136	0.72	1.72
315	23.4	14.9	0.55	25868	25868	1.00	27709	0.93	1.93
315	23.4	14.9	0.95	28126	28126	1.00	28126	1.00	2.00
315	23.4	14.9	1.2	30072	30072	1.00	30072	1.00	2.00

Glossary of Useful Terms

Bias Mean value/nominal value

COV Coefficient of Variation (Standard deviation by Mean)

Factor of safety Ratio of resistance to stress (load)

Limit state Boundary between safe and unsafe region

Load factor Nominal load effects are multiplied by a γ factor to cater the uncertainties and excessive loads

Mean coefficient Mean of bias values

Nominal strength calculated from section properties like yield strength

Random variable It has no fixed value and it is evaluated by using the characteristic distribution and its parameters

Reliability ($1 - P_f$) Complement of failure probability. Probability that the Jacket will perform as desired for intended design life

RSR $\frac{\text{Ultimate Base Shear at Collapse}}{\text{Design Environmental Load (Base Shear)}}$

Resistance factor Nominal strength or resistance is multiplied by a φ factor to cater for uncertainties in strength

Return Period Return Period $= \frac{1}{p_f}$, Average period of time which is passed between occurrences of events at the site

Safety index Mean Safety Margin/Uncertainty Level

Significant wave height Mean of highest 1/3 of all waves present in wave train

Standard deviation (SD) Square root of variance

Standard normal space Space of normally distributed random variables with zero mean values and unit standard deviation and zero correlation coefficients

System redundancy $\left[\frac{\text{Design Collapse Load}}{\text{Peak Collapse Load}}\right] + 1$

Z. Nizamani, *Environmental Load Factors and System Strength Evaluation of Offshore Jacket Platforms*, Ocean Engineering & Oceanography 4,
DOI 10.1007/978-3-319-15051-2